

Thèse de doctorat de l'Université de Lille

Faculté des Sciences et technologies – Département biologie

Ecole doctorale **SMRE** – Sciences de la Matière, du Rayonnement et de l'Environnement

Dynamiques éco-évolutives des espèces exploitées en Mer du Nord en réponse à des variations biotiques et abiotiques de l'environnement

Présentée et défendue par **Alaia Morell**

Le 12 décembre 2022, à Boulogne-sur-Mer

Pour obtenir le grade de docteur en Biologie de l'environnement, des organismes, des populations,
écologie

Composition du jury :

Frida Ben Rais Lasram PR – Université du Littoral Côte d'Opale (ULCO), Wimereux (France)	Présidente du jury
Marie Savina-Rolland CR – IFREMER Lorient (France)	Rapportrice
Eric Edeline DR – INRAE Rennes (France)	Rapporteur
Martin Huret CR – IFREMER Brest (France)	Examineur
Paul Marchal DR – IFREMER Boulogne-sur-mer (France)	Directeur de thèse
Yunne-Jai Shin DR – IRD Montpellier (France)	Co-directrice de thèse
Bruno Ernande CR – IFREMER Montpellier (France)	Co-encadrant
Morgane Travers-Trolet CR – IFREMER Nantes (France)	Co-encadrante

Résumé

Les scénarios de changements globaux sont précieux pour guider les stratégies de gestion et de gouvernance, inciter à la prise de décision et augmenter la prise de conscience collective sur les tendances futures de la biodiversité. Le degré de réalisme et d'intégration des modèles écosystémiques utilisés à cet effet est en constante progression, mais ils négligent encore souvent l'évolution des populations marines dans les projections futures. Or, celles-ci s'adaptent aux changements globaux, que ce soit par la plasticité phénotypique ou l'évolution, au travers de modifications de leurs caractéristiques biologiques telles que les traits d'histoire de vie, physiologiques et bioénergétiques. L'enjeu de cette thèse est de développer un modèle écosystémique qui permette d'explorer des scénarios de biodiversité aux échelles intra- et inter-spécifiques en représentant explicitement la plasticité phénotypique des traits d'histoire de vie, leur variabilité génétique, leur sélection et leur évolution sous l'influence combinée de la pêche et du changement climatique, ainsi que la dérive génétique et la perte de diversité génétique qui en résultent. Appliqué à la mer du Nord, ce nouveau modèle est utilisé pour comprendre les processus responsables des changements de traits d'histoire de vie qu'ils soient d'origine plastique ou d'origine évolutive. D'une part, les processus bioénergétiques sous-jacents aux changements plastiques sont étudiés par une approche originale comparant les différences entre les courbes de réponses thermiques fondamentales et réalisées pour différentes espèces et stades du cycle de vie. D'autre part, les changements des traits d'histoire de vie sont explorés à travers le prisme de l'évolution grâce à la prise en compte de pressions de sélection multiples telles que la pêche, les interactions proies-prédateurs et le changement climatique.

L'intégration des processus plastiques et évolutifs dans les modèles écosystémiques permet de décrire la variabilité interindividuelle des traits biologiques et de comprendre leurs tendances temporelles observées dans le milieu marin. En cela, elle répond à l'enjeu crucial de crédibilité des projections de la biodiversité intra- et inter-spécifique sous scénarios combinant climat et pêche.

L'intégration de ces processus permettra également de quantifier plus précisément les effets synergiques et antagonistes de ces deux pressions et de prendre en compte la capacité d'adaptation des populations aux changements globaux pour estimer de manière plus fiable leur résilience.

Mots clés : Traits d'histoire de vie, Modèle écosystémique, Réponses physiologiques thermiques, Evolution induite par la pêche, Hypoxie

Abstract

Title: Eco-evolutionary dynamics of exploited species in the North Sea in response to biotic and abiotic variations of the environment.

Global change scenarios are valuable for guiding management and governance strategies, stimulating decision making, and increasing collective awareness of future biodiversity trends. The degree of realism and integration of ecosystem models used for this purpose is constantly improving, but they still often neglect the evolution of marine populations in future projections. However, marine populations adapt to global changes, either through phenotypic plasticity or evolution, through modifications of their biological characteristics such as life history traits, physiological and bioenergetic traits. The challenge of this thesis is to develop an ecosystem model that allows the exploration of biodiversity scenarios at intra- and inter-specific scales by explicitly representing the phenotypic plasticity of life history traits, their genetic variability, selection and evolution under the combined influence of fisheries and climate change, and the resulting genetic drift and loss of genetic diversity. Applied to the North Sea, this new model is used to understand the processes responsible for changes in life history traits, whether they are of plastic or evolutionary origin. On the one hand, the bioenergetic processes underlying plastic changes are studied by an original approach comparing the differences between the fundamental and realized thermal response curves for different species and life history stages. On the other hand, changes in life history traits are explored through an evolutionary lens by taking into account multiple selection pressures such as fishing, prey-predator interactions and climate change.

The integration of plastic and evolutionary processes in ecosystem models allows to describe the inter-individual variability of biological traits and to understand their temporal trends observed in the marine environment. In this way, it responds to the crucial issue of credibility of intra- and inter-specific biodiversity projections under scenarios combining climate and fisheries. The integration of these processes will also allow to quantify more precisely the synergistic and antagonistic effects of

these two pressures and to take into account the capacity of populations to adapt to global changes in order to estimate more reliably their resilience.

Keyword: Life history traits, Ecosystem modeling, Thermal physiological responses, Fisheries-induced evolution, Hypoxia

Remerciements

Un peu plus de quatre années se sont écoulées, pendant lesquelles j'ai réalisé ces travaux de thèse qui ont été accompagné d'une extraordinaire aventure humaine, sur le plan professionnel comme personnel. Je suis très émue quand je repense à toutes les personnes que j'ai eues la chance de croiser, à Boubou comme à Montpellier.

Je vais commencer par la personne avec qui j'ai eu énormément de chance de travailler : un immense merci à toi Bruno, pour tes innombrables qualités scientifiques comme humaines. Tu étais toujours très disponible pour toutes mes « petites » questions de cinq minutes qui se transformaient toujours en deux heures de discussions toujours passionnantes pour moi, aussi bien sur des considérations scientifiques ou que des conseils variés. Merci également pour ton précieux soutien pendant ces longues périodes de télétravail : tu m'as aidé à garder la motivation, même quand je travaillais seule à la maison. Bref, je n'ai pas les mots suffisants. Je n'aurais pas pu être mieux encadrée.

Merci Morgane pour m'avoir mis le pied à l'étrier « OSMOSE » lors de déplacements à Nantes dans la joie et la bonne humeur : tu m'as transmis le goût de voir la modélisation comme un cluedo et surtout, j'ai bien compris grâce à toi que dans OSMOSE comme dans la vie, le plus important c'est la bouffe. C'était toujours un plaisir de te croiser aussi dans les différentes conférences comme à Rouen ou à Brest. De façon générale, merci pour ta bonne humeur.

Et merci à ma troisième encadrante (et pas des moindres). Merci Yunne pour tes coups de pouce et tes remarques toujours très pertinentes avec ton tact légendaire. Ta manière de travailler et l'implication que tu as dans la science, notamment pour l'impliquer dans la gestion, sont une grande source d'inspiration pour moi. La voie à suivre. Ce paragraphe est ce que j'avais écrit dans un premier brouillon de remerciements avant que j'arrive à Montpellier. L'année complète en présentiel à Montpellier m'a permis de découvrir également tes grandes qualités humaines : un énorme merci

pour ta bienveillance, tes encouragements et ton regard pertinent dans des discussions diverses et variées. Et aussi merci aussi de m'avoir incité à reprendre la danse.

Enfin, je sais que tu n'étais pas mon encadrant, mais sans toi je n'aurais certainement pas fini ma thèse aujourd'hui : merci Nicolas pour avoir été si réactif, patient, efficace et pédagogue pour le développement du modèle. J'ai été marquée par ma venue à Sète d'une semaine, et au bout d'une heure le premier jour « bon bah ça marche ! ». C'était super. Trouver et télécharger « Hot shots 2 » était bien la moindre des choses que je pouvais faire pour te remercier.

Merci à Paul pour avoir été officiellement mon directeur de thèse, et pour tes conseils lors de mes comités de thèse. Merci à Philippe Gros, Luis-Miguel Chevin et David McKenzie d'avoir accepté de faire partie de mon comité de thèse. Merci à Marie Savina-Rolland, Eric Edeline, Frida Ben Rais Lasram et Martin Huret d'avoir accepté de corriger ce travail. J'ai beaucoup apprécié vos apports et retours respectifs sur mon travail, qui me seront très utiles pour le valoriser.

Merci à tous les gens avec qui j'ai bossé dans le projet SOMBEE, en particulier Ambre et Maité : vous êtes vraiment une super équipe de gens brillants, souriants, et motivés. Ça a été un plaisir de faire équipe avec vous pour commencer dans le monde de la recherche.

Jusqu'à là c'était clair dans ma tête pour les remerciements, et maintenant il y a tellement de monde que j'aimerais remercier que je ne sais pas par où commencer. Commençons à Boulogne. Merci aux amis indéfectibles et aux copains de vie qui ont rendus le temps dans le Nord beaucoup plus ensoleillé. La petite Maria tellement pétillante et toujours partante pour une petite digue. Blanchette qui m'apporte un soutien indéfectible. El Carlito, petit soleil de Noël et du bureau. La bonne vieille Julia qui m'entraîne à l'Almanac 226. La grande Kelly, sa joie de vivre et ses aventures rocambolesques. Michlak la morue alias le meilleur public du monde. Tibal le frimeur et le boss des mots-fléchés. Mon ptit coloc Julo et nos discussions interminables sur la vie. L'incroyable Maud et sa sagesse. Matthias et Francky, le trio toujours réuni pendant ma première année (alias Sparky 1 et Sparky 2). Julien (alias la dip) et son sacré caractère. Maupas le coincheur fou. Chloé et nos english

Monday dans le bureau. Enfin beaucoup d'autres personnes que j'ai eu le bonheur de rencontré Tata, Martinou et Martinou, Alizée, Sarah, Aurélie, Solène, Duduss, Geoffy geof, Sophie, Fabouch, Matthew, Marine, Inès, Eric, tous les gens des beach-apéro-volley, les kippers, les zadhocs... et encore beaucoup d'autres, merci, vous avez tous été une source de joie infinie.

Merci également aux collègues d'IFREMER, en commençant par ceux avec qui j'ai eu la chance de partager un bureau, Chloé, Alexandre, Léa, Charles et Alizée. Merci d'avoir supporté mes jeux de mots, et mes humeurs changeantes au fil de ma calibration (**** de Norway pout !). Merci également à Chef (margotte), Yfff, Franck, Clémence (super coloc d'une semaine), Solène, Thibaut, Geoffrey, Céline, Antoine pour l'étage du bas, et Pierre (le voisin du pays-basque et copain d'impro !), Ghassen (merci particulièrement à toi pour ton positivisme, toutes nos supers conversations et tes encouragements), Arnaud, Kélig, Raph, Caro, et Christophe pour l'étage du haut. Merci à ceux avec qui j'ai embarqué en particulier au hibou et à Michlack : avec vous j'ai réalisé mon rêve de partir en mer, avec vous c'était encore mieux que je l'imaginais.

Quitter tout ce petit monde de Boulogne a été un déchirement. L'arrivée à Montpellier a été difficile, seule dans un bureau dans un premier temps. Avec mes capacités physiologiques, les masques et les confinements, ça a été long... et puis... ça aurait pu être la fin des remerciements, et j'aurais dit « A job is a job ». Mais Nacho est arrivé : il a apporté plein de vie dans mon bureau qui est devenu notre bureau. Sacré Nacho, quelle sagesse toujours les bons mots dans les moments de panique, ce qui a été crucial dans la dernière année de thèse (« You live and you learn »). Un grand merci. Un grand merci aussi à Cléa (Cliaaaa ou « the dancing friend ») avec qui est la troisième pièce et dernière arrivée d'un trio très rigolo. Et puis, merci à tout Marbec Marvellous, notamment Camille la bienveillance incarnée, Raphaël le célèbre, Valentine la porteuse de robe bleue à herbe, Anaëlle la déterminée, Adèle la dynamique, Adriche le débateur têtu, Jeanne la ponctuelle des pauses, Antoine le Disneyphile, Fabrice le discret, Micka et c'est tchao, Ulysse le vendeur de chiens trop mignons et Loïc le critique. Gracias a Ricardo para los morochas y los Margikarpes. Enfin, le meilleur pour la fin,

merci à l'irremplaçable Gaël Mariani. Merci pour ta bienveillance, tes douces chansons de Patrick Coutin et ton enthousiasme. Maintenant j'attends que tu me dédies ta thèse.

Enfin, merci à mes petites pommes de pins d'être toujours là après les années, merci à Kiki et Yaya pour leur soutien moral indéfectible, et enfin bien le merci à mes petits loups de Rennes qui sont toujours là quoi qu'il arrive (en particulier Roucky, Lilou, Fannou, la thou, Clem, Céline, Nanou et Tico : merci pour tout).

La musique prend une place de premier ordre dans ma vie. Je ne pense pas que je tiendrai moralement sans certains albums clés qui ont tourné en boucle pendant ces quatre ans, merci à Julian pour tous ses projets qui sont autant des coups que des voix, ainsi qu'à la bande à Steen sans honte. Merci au roi gésier et au sorcier lézard de me faire voyager avec frénésie et merci à Adrienne de trouver les mélodies qui me vole mon stress en toute situation.

Ces remerciements touchent bientôt à leur fin, mais ne crois pas que j'allais t'oublier : un immense merci à la douce et gracieuse Léa Joly, une coloc, une thésarde de la même année, une collègue, un co-bureautaire mais surtout une amie hors pair. Avoir commencé en même temps a été la chance d'avoir quelqu'un qui vivait et comprenait les épreuves de la thèse aux mêmes moments. Pas besoin d'en dire plus, encore merci.

Je pense qu'un paragraphe entier ne suffirait pas à te remercier Adrien (alias Dadou) pour ton soutien et surtout ta bonne humeur contagieuse. Tous les malheurs du monde de la calibration, de la rédaction ou de l'administration ne suffiraient pas à m'abattre quand j'ai ton soutien et ta joie au quotidien. Mille mercis.

Et enfin, un immense merci à toute ma famille, qui a toujours été là pour moi, encore plus que d'habitude avec le télétravail. Merci tout particulier à ma mamie, à mon frère et par-dessus tout à ma maman. Vous avoir dans ma vie est le plus précieux des cadeaux.

Table des matières

Résumé.....	i
Abstract.....	iii
Remerciements.....	v
Table des matières.....	xi
Liste des figures.....	xv
Liste des tableaux.....	xvii
Liste des équations.....	xix
Liste des acronymes.....	xxi

Chapitre 1 : Introduction générale 1

1.1 Les impacts humains sur la biodiversité, de l'échelle génétique à l'échelle fonctionnelle et spécifique	1
1.1.1 Vision éco-centrée et éco- anthropocentrée de la biodiversité	1
1.1.2 Facteurs impactant la biodiversité marine : le changement climatique et la pêche	3
1.1.3 Importance de l'étude des dynamiques éco-évolutives : interactions entre les différents niveaux d'organisation de la biodiversité.....	6
1.2 Concepts théoriques expliquant la variation individuelle des traits d'histoire de vie	7
1.2.1 De Darwin à la théorie des traits d'histoire de vie.	7
1.2.2 La théorie des traits d'histoire de vie.....	8
1.3 Changements plastiques et évolutifs des traits d'histoire de vie chez les populations exploitées	15
1.3.1 Plasticité phénotypique en réponse à la pêche, à la température, et à l'oxygène	15
1.3.2 Evolution induite par les pressions anthropiques.....	17
1.4 Interactions des réponses écologiques et évolutives aux niveaux intra- et inter-spécifiques : modélisation des changements des traits d'histoire de vie dans un réseau trophique spatialisé. ..	20
1.4.1 Etat de l'art des modèles multi-spécifiques, outils d'étude de la diversité spécifique.	21
1.4.2 Etude des changements évolutifs induits par la pêche à l'échelle monospécifique à l'aide de modèles éco-génétiques.....	23
1.4.3 Vers des modèles multispécifiques évolutifs: apports des modèles théoriques et début des modèles appliqués.....	24
1.5 Le cas d'étude « mer du Nord » : une zone de laboratoire à taille de bassin.....	26
1.5.1 L'écosystème mer du Nord : description et délimitation de la zone d'étude.....	27
1.5.2 La mer du Nord : une zone fortement exploitée par l'homme	31

1.5.3	Fonctionnement des communautés de mer du Nord : travaux d'étude des communautés et de modélisation en mer du Nord	36
1.6	Objectifs et structure de la thèse	39
Chapter 2: Bioen-OSMOSE: A bioenergetic marine ecosystem model with physiological response to temperature and oxygen		43
2.1	Introduction.....	44
2.2	Method	46
2.2.1	Model description	46
2.2.2	Application to the North Sea ecosystem: Bioen-OSMOSE-NS	61
2.3	Results and discussion.....	64
2.3.1	Model evaluation	64
2.3.2	The physiological level: spatial pattern	73
2.4	Conclusion	75
Chapter 3: Trophic level determines the difference between fundamental and realized thermal performance curves realistic ...		77
3.1	Introduction.....	78
3.2	Materials and methods	82
3.2.1	Model Description	82
3.2.2	The North Sea-Eastern English Channel (NS) ecosystem	87
3.2.3	Application of Bioen-OSMOSE to the North Sea-Eastern English Channel ecosystem .	88
3.2.4	Simulations and processing of the outputs.....	89
3.3	Results	91
3.3.1	Comparison of fundamental and realized net energy TPCs.....	91
3.3.2	Seasonal variation in net energy rate.....	93
3.3.3	Disentangling the sources of difference between fundamental and realized net energy TPCs	95
3.3.4	Trophic level effect on the difference between fundamental and realized net energy TPCs	97
3.4	Discussion	98
3.4.1	Oxygen and food availability: two crucial physiological performances drivers	98
3.4.2	Omnivory degree and trophic level explain variation across life stages and species of the effect of food limitation on realized TPCs.....	99
3.4.3	Deoxygenation effect on realized TPCs remains weak in the absence of hypoxia	101
3.4.4	Early life stage realized TPCs differ most from fundamental TPCs due to trophic competition	102

3.4.5	Consequences for thermal studies.....	104
3.4.6	Projections under climate change scenario	105
Chapter 4: Ev-OSMOSE: An eco-genetic marine ecosystem model		
.....		107
4.1	Introduction.....	108
4.2	Materials and methods	109
4.2.1	Model description	110
4.2.2	The North Sea ecosystem application: Ev-OSMOSE-NS	128
4.3	Results	133
4.3.1	Emerging phenotypic variability	134
4.3.2	Genotypic value transmission	140
4.4	Discussion	142
4.4.1	Modeling phenotypic variance of life-history traits.....	142
4.4.2	Genotypic value transmission	145
4.5	Conclusion	148
Chapter 5: Fisheries-induced evolution in an evolving community		
.....		151
5.1	Introduction.....	152
5.2	Materials and methods	154
5.2.1	The multispecies Ev-OSMOSE model applied to the North Sea.....	154
5.2.2	Characteristics of the performed simulations.....	156
5.3	Results	158
5.3.1	Evolutionary trends in maturation and reproductive effort	158
5.3.2	Implication for species' fitness and community demographics.....	163
5.4	Discussion	166
5.4.1	Life-history evolutionary trends in a community	166
5.4.2	Evolutionary changes' impact on fitness and demography	172
Chapitre 6 : Discussion générale		175
6.1	Variations intraspécifique des traits d'histoire de vie dans un écosystème : une échelle nécessaire pour comprendre la diversité fonctionnelle et spécifique.....	176
6.1.1	Déterminants environnementaux des flux physiologiques.....	176
6.1.2	Variations génétiques des traits d'histoire de vie	178
6.2	Réalisme & limites du cadre de modélisation Bioen-OSMOSE et Ev-OSMOSE.....	179

6.2.1	Apports d'un modèle bioénergétique pour modéliser le cycle de vie individuel	179
6.2.2	Comment affiner la description de la réponse à la température ?	180
6.2.3	Structure des génotypes.....	183
6.3	Des modèles écosystémiques se complexifiant : éclairage du fonctionnement des écosystèmes ou simulations de données aussi complexes que l'observé ?	185
6.4	Perspectives.....	186
6.4.1	Projections de biodiversité sous scénarios climatiques futurs	187
6.4.2	Scénarios de gestion de pêche qui optimisent la diversité génétique et minimisent le changement de diversité fonctionnelle	190
6.5	Conclusion	192
Références		193
Annexes		223
8.1	Annexes du chapitre 2.....	223
8.1.1	Supporting Information S1: Process overview	223
8.1.2	Supporting Information S2: Parametrization of the new sub-model.....	227
8.1.3	Supporting Information S3: Mortality process description.....	235
8.1.4	Supporting Information S4: Input parameters and intermediate parameters of Bioen-OSMOSE-NS for the 16 species modeled explicitly.	238
8.1.5	Supporting Information S5: Parameters of the low trophic level (LTL) groups.....	242
8.1.6	Supporting Information S6: References for the life cycle parameters used in the North Sea model.....	243
8.1.7	Supporting Information S7: Species distribution relative to ontogenetic stages.	244
8.1.8	Supporting Information S8: Reproductive season.	249
8.1.9	Supporting Information S9: Monthly maps of LTL and temperature and oxygen variables from POLCOMS-ERSEM averaged on the 2010-2019 period.....	252
8.1.10	Supporting Information S10: Target values for the calibration.	259
8.1.11	Supporting Information S11: Fishing selectivity per species.....	260
8.2	Annexes du chapitre 4.....	260
8.2.1	Supporting Information S11 - Estimation procedure for the coefficient of variations of the traits under selection	261
8.2.2	Supporting Information S12 – Ecological validation of Ev-OSMOSE-NS: Simulated biomass and catches.	266
8.2.3	Supporting Information S13 – Genotype transmission validation	268
8.3	Références des annexes	270

Liste des figures

Figure 1 : Facteurs directs expliquant le déclin de la biodiversité dans les écosystèmes terrestres, d'eau douce et marins.....	4
Figure 2 : Schéma synthétisant la théorie des traits d'histoire de vie, adapté de Stearns (1992) (A) avec un schéma de <i>trade-off</i> (B) et de norme de réaction (C).....	10
Figure 3 : Norme de réaction de maturation linéaire et plasticité de l'âge et de la taille à maturité en fonction de la variation de l'environnement.....	14
Figure 4 : Résumé du cadre de modélisation éco-génétique.....	24
Figure 5 : Carte de la bathymétrie de la mer du Nord	27
Figure 6 : Aperçu de l'écorégion mer du Nord avec les principales pressions régionales, les activités humaines et l'état de l'écosystème.....	35
Figure 7 : Périodes sur lesquelles une évolution induite par la pêche a été mise en évidence par différentes études pour les stocks de mer du Nord.....	38
Figure 8: Graphical description of the Bioen-OSMOSE model	47
Figure 9: Thermal responses of the bioenergetic fluxes from ingestion to tissue growth in Bioen-OSMOSE.....	53
Figure 10: Case study area map.	61
Figure 11: Boxplot of size-at-age per species for observed and simulated individual data.....	65
Figure 12: Age (A) and size (B) maturity ogives per species for observed and simulated data	68
Figure 13: Fisheries catches (A) and biomasses (B), in thousand tons, per species for stock assessment estimates and simulated data	71
Figure 14: Diet in percent of biomass eaten of prey species per size class of the predator species in cm	72
Figure 15: Spatial variability of the mean adult mass-specific net energy rate available for new tissue production, per model cell for cod, herring and dab.	74
Figure 16: Thermal curves of the bioenergetic fluxes from ingestion to tissue growth as modeled in our framework.....	80
Figure 17: Graphical description of the Bioen-OSMOSE model.....	84
Figure 18: (A) Bioenergetic flux responses to oxygen. (B) Mobilization and maintenance responses to temperature. (C) Functional response in Bioen-OSMOSE, i.e., ingested energy as a function of accessible prey density. (D) The net energy available for tissue production response to temperature	86
Figure 19: Summary of the Bioen-OSMOSE-NS configuration	89
Figure 20: Sources of difference between fundamental and realized net energy TPCs and how to disentangle them.....	90
Figure 21: Fundamental and realized net energy TPCs per species and life stage	92
Figure 22: (A) Seasonal variation of the net energy rate per gram of individual at the energy acquisition power, per species, per life stage. (B) Temporal correlations between seasonal variations of realized and fundamental net energy rates at early stage (E), juvenile (J) stage and adult (Ad.) stage.	95
Figure 23: Percent difference between fundamental and realized net energy TPCs according to life stage and source of difference	96
Figure 24: Difference between fundamental and realized net energy rate TPCs due to food limitation, D ; P , per life stage as a function of trophic level.....	97

Figure 25: Graphical summary of the Ev-OSMOSE model.....	110
Figure 26: Ev-OSMOSE processes describing trait variations from loci to population level and the causes impacting trait values	115
Figure 27: Bioenergetic sub-model fluxes from the ingestion to the tissue growth, namely somatic and gonadic growth (A). Linear maturation reaction norm (B). Proportion of net energy ρ allocated to gonadic growth (C).	122
Figure 28: Representation of the Ev-OSMOSE-NS model applied to the North Sea and the Eastern Channel.....	128
Figure 29: Age- (A) and length-based (B) maturity ogives per species for observed, simulated without and simulated with phenotypic variance individual data for species for which empirical maturation data are available.	136
Figure 30: Boxplot of length-at-age per species for observed, simulated without and simulated with phenotypic variance individual data	138
Figure 31: Sum of squared errors between observed and simulated mean (A) and standard deviation (B) of length-at-age from Ev-OSMOSE-NS and Bioen-OSMOSE-NS per species	139
Figure 32: Transmission of genotypic values of the maturation reaction norm intercept m_0 (A) and of the gonado-somatic index r (B) from parental pools to the new spawned cohort.....	140
Figure 33: Fishing selectivity per species as parameterized in Ev-OSMOSE-NS.....	156
Figure 34: Evolution of the population mean genotypic values of m_0 (A) and r (B) over 50 years of simulation.....	162
Figure 35: Fitness trends without and with evolution over 205 simulated cohorts by species, averaged over 28 replicates	165
Figure 36: Trend in the sum of species' mean cohort fitness without and with evolution	166
Figure 37: Illustration schématique d'une réponse fondamentale thermique d'une performance (pouvant être l'acquisition d'énergie nette par exemple) et de trois exemples de réponses réalisées : (A) un cas de nourriture et d'oxygène saturés, (B) un cas de nourriture et d'oxygène non saturés et constants spatiotemporellement, et (C) un cas de nourriture et d'oxygène non saturés et non constants spatiotemporellement de sorte à covarier avec la température.	177
Figure 38: Plan de simulations avec sept scénarios testés en réponse au changement climatique en utilisant Bioen-OSMOSE-NS	188

Liste des tableaux

Tableau 1: Variables and functions of the bioenergetics and life-history sub-models.....	57
Tableau 2: Species- specific parameters of the bioenergetic and life-history sub-model.....	59
Tableau 3 : Fundamental optimal temperature T_{opt} per species (°C) and its realized counterpart per species and life stage.....	93
Tableau 4: Result of an ANCOVA model of the difference due to food limitation D . ; P explained by trophic level, life stage, and the interaction between the two variables	97
Tableau 5: Variables and functions used in the Ev-OSMOSE model.....	124
Tableau 6: Species-specific parameters in the Ev-OSMOSE model.....	127
Tableau 7: Micro-environmental noise and genotypic variances of process traits in Ev-OSOMOSE-NS.	131
Tableau 8: Calibrated species parameters for the 15 focus species in Ev-OSMOSE-NS.	133
Tableau 9: Calibrated coefficients of accessibility to fish of low trophic level (LTL) groups in Ev-OSMOSE-NS.....	133
Tableau 10: Mean adult predation and fishing mortality rate per year per species (first and second columns respectively) and correlations of the times series trends of m_0 mean genotypic value and an r mean genotypic value per species (last column).	160



Liste des équations

Biomasse accessible de proies :

$$P(i, t) = \frac{\sum_j \gamma(i, j) B(j, t)}{N(i, t)} \quad \text{with } j \in \left\{ j \mid (c(j, t) = c(i, t)) \cap \left(\frac{L(i, t)}{R_{max}} \leq L(j, t) \leq \frac{L(i, t)}{R_{min}} \right) \right\} \quad (1) \dots\dots\dots 50$$

Ingestion :

$$I(i, t) = f(P(i, t)) = \min(P(i, t); I_{max} \psi(i, t) w(i, t)^\beta) \quad (2) \dots\dots\dots 50$$

$$\psi(i, t) = \begin{cases} \theta & \text{if } a(i, t) < a_l \\ 1 & \text{otherwise} \end{cases} \quad (3) \dots\dots\dots 50$$

Energie mobilisée :

$$E_M(i, t) = \xi I(i, t) \lambda([O_2])(i, t) \varphi_M(T(i, t)) \quad (4) \dots\dots\dots 51$$

$$\lambda([O_2]) = c_{O,1} \frac{[O_2]}{[O_2] + c_{O,2}} \quad (5) \dots\dots\dots 51$$

$$\varphi_M(T) = \Phi \frac{e^{-\frac{\varepsilon_M}{k_B T}}}{1 + \frac{\varepsilon_M}{\varepsilon_D - \varepsilon_M} e^{\frac{\varepsilon_D}{k_B} \left(\frac{1}{T_p} - \frac{1}{T} \right)}} \quad (6) \dots\dots\dots 51$$

Maintenance :

$$E_m(i, t) = c_m w(i, t)^\beta \varphi_m(T(i, t)) \quad (7) \dots\dots\dots 52$$

$$\varphi_m(T) = e^{-\frac{\varepsilon_m}{k_B T}} \quad (8) \dots\dots\dots 52$$

Energie nette pour la production de tissu et flux en avals

$$E_P(i, t) = E_M(i, t) - E_m(i, t) \quad (9) \dots\dots\dots 52$$

$$\rho(i, t) = m(i, t) \frac{r}{\eta E_P(i)} w(i, t) \quad (10) \dots\dots\dots 54$$

$$\frac{dw}{dt}(i, t) = \begin{cases} (1 - \rho(i, t)) E_P(i, t) & \text{if } E_P(i, t) \geq 0 \\ 0 & \text{otherwise} \end{cases} \quad (11) \dots\dots\dots 54$$

$$\frac{dg}{dt}(i, t) = \begin{cases} \eta \rho(i, t) E_P(i, t) & \text{if } E_P(i, t) \geq 0 \\ \eta E_P(i, t) & \text{if } -g(i, t) \leq \eta E_P(i, t) < 0 \\ -g(i, t) & \text{if } \eta E_P(i, t) < -g(i, t) < 0 \end{cases} \quad (12) \dots\dots\dots 54$$

Maturation :

$$m(i, t) = \begin{cases} 0 & \text{if } L(i, t) < m_0 + m_1 a(i, t) \text{ (immature)} \\ 1 & \text{if } L(i, t) \geq m_0 + m_1 a(i, t) \text{ (mature)} \end{cases} \quad (13) \dots\dots\dots 55$$

Production de nouveaux individus :

$$N_{eggs}(i, t) = sp \left(t \bmod \frac{365}{\Delta t} \right) N(i, t) \frac{g(i, t)}{2w_{egg}} \quad (14) \dots\dots\dots 55$$

$$N(i', t) = \frac{\sum_{j|s(j)=s(i)} N_{eggs}(j, t)}{n_{s(i)}} \quad (15) \dots\dots\dots 56$$

Modèle éco-génétique :

$$G_z(i) = \overline{G_z}(0) + \sum_{l=1}^{l=l_z} (A_{z,l,1}(i) + A_{z,l,2}(i)) \quad (16) \dots\dots\dots 118$$

$$z(i) = G_z(i) + e_z(i) \quad (17) \dots\dots\dots 119$$

$$p_i(t) = \frac{N_{eggs}(i, t)}{\sum_{j|s(j)=s(i)} N_{eggs}(j, t)} \quad (18) \dots\dots\dots 119$$

Mortalité par *foraging* :

$$M_f(i) = k_1 \cdot e^{k_2 \cdot (I_{\max}(i) - \overline{I_{\max}}(0))} \quad (19) \dots\dots\dots 123$$

$$N(i, t + dt) = N(i, t) e^{-M_f(i) dt} \quad (20) \dots\dots\dots 123$$

Calcul de *Fitness* :

$$R_0 = \sum_{a=0}^{a=a_{\max}} s(a) N_{egg}(a) \quad (21) \dots\dots\dots 158$$

Liste des acronymes

AS : Aerobic Scope

ATP : Adénosine-Triphosphate

CIEM : Conseil International pour l'Exploration de la Mer

FIE : Fisheries-Induced Evolution

ICES : International Council for the Exploration of the Sea

IBTS : International Bottom Trawl Survey

IPBES : Intergovernmental science-policy Platform on Biodiversity and Ecosystem Services

LMRN : Linear Maturation Reaction Norm

HTL : High Trophic Level

LTL : Low Trophic Level

MEM : Marine Ecosystem Model

NS : North Sea

OCLTT : Oxygen- and Capacity-Limited Thermal Tolerance

OMZ : Oxygen Minimum Zone

PIE : Predation-Induced Evolution

SMALK : Size Maturity Age Length Key

SMS : Stochastic Multi-Species

SSE : Sum of Squared Errors

TL : Trophic Level

TPC : Thermal Performance Curve

TSR : Temperature Size Rule

UN : United Nation

Chapitre 1 : Introduction générale

1.1 Les impacts humains sur la biodiversité, de l'échelle génétique à l'échelle fonctionnelle et spécifique

Les impacts humains sur les écosystèmes atteignent de nos jours des niveaux inédits. Tous les écosystèmes marins à travers le monde sont touchés par les pressions anthropiques (Halpern et al., 2015). La globalité des composantes biologiques des écosystèmes marins est affectée : des compartiments bactériens impliqués dans les cycles biogéochimiques aux prédateurs supérieurs comme les oiseaux marins, les raies ou les requins (Halpern et al., 2007). En résumé, l'ensemble de la biodiversité, c'est-à-dire l'ensemble des composantes et des variations du monde vivant, est impactée. Cette biodiversité possède différents niveaux d'organisation au sein des écosystèmes et chacun subit des effets liés aux activités humaines : la diversité génétique (diversité intra-spécifique des gènes) (Exposito-Alonso et al., 2022), la diversité fonctionnelle (diversité des traits qui caractérisent la fonction d'un organisme dans un écosystème comme par exemple les traits morphologiques, physiologiques ou phénologiques) (Villéger et al., 2010) et la diversité spécifique (diversité d'espèces) (Pimm et al., 2014).

1.1.1 Vision éco-centrée et éco-anthropocentrée de la biodiversité

Pour définir l'importance de la biodiversité et les objectifs de sa conservation, il est nécessaire de définir dans quel cadre éthique et moral se positionne notre relation à cette biodiversité. Les différents cadres éthiques définissant la relation entre l'homme et la biodiversité ont été pertinemment résumés par les mots d'Axel Kahn lors d'un colloque sur la biodiversité (Axel Kahn, discours, 2020). La biodiversité dans son ensemble forme une grande partie du milieu naturel des humains et est en ce sens un bien commun à l'humanité. Nous avons quatre différentes conceptions de relation avec ce bien commun : (i) l'anthropocentrisme, (ii) l'anthropocentrisme écologique, (iii) l'éco-centrisme et (iv) le géocentrisme. La première est de considérer ce bien commun comme

quelque chose dont on fait un usage et ainsi vouloir optimiser cet usage dans un temps court. Cette vision n'intègre donc pas de conservation dans la relation de l'humanité avec la nature. L'anthropocentrisme devient l'anthropocentrisme écologique quand sont envisagés les services que nous rend notre environnement pour l'ensemble des humains, y compris ceux des générations futures. C'est à partir de cette conception de l'environnement que peut commencer la volonté de conservation pour préserver les usages de la nature pour tous les humains. L'éco-centrisme pose la valeur de la nature en tant que telle, nature à laquelle appartient la nature humaine. L'humain est alors une partie de la nature en équilibre et en coévolution avec son environnement et se trouve ainsi co-responsable de conserver l'environnement et donc la biodiversité pour préserver cet équilibre. Enfin, la quatrième conception, la géocentrique, considère la terre, son environnement et sa biodiversité comme la valeur supérieure à préserver, et implique de lutter contre ce qui les menace, y compris l'humain si nécessaire. Axel Kahn écarte cette conception car elle amène à une contestation de la place de l'humain par l'humain, et donc à un contresens philosophique.

Cette description des différentes visions de la relation homme-nature selon Axel Kahn dans cette introduction, a tout d'abord comme intérêt d'attirer l'attention sur la vision éco-centriste de la nature et donc de la biodiversité car partie de la nature. L'importance de la biodiversité et de sa conservation en tant que telle est encore trop rarement développée comme contexte et motif de travail justifiant la description de cette biodiversité, l'étude de son fonctionnement, de l'interaction de différents types de biodiversité. Dans ce cadre-là, l'importance de préserver les différents types de biodiversité peut se justifier pour le lien entre chaque type de biodiversité et le bénéfice que chaque niveau de biodiversité peut apporter à l'autre. Par exemple, le maintien de la diversité spécifique permet d'éviter un cercle vicieux de conséquences négatives sur la diversité spécifique elle-même comme un phénomène de cascade trophique (Ripple et al., 2016) ou une déstabilisation, voire une extinction, d'un prédateur suite à la disparition de sa proie (Taylor, 1990). Le maintien de la diversité génétique est aussi une condition à la résilience de la diversité spécifique (Ruegg and Turbek, 2022) car elle permet l'adaptation des espèces à des changements d'environnement par un

changement de traits et donc une modification de la diversité fonctionnelle. La redondance et la rareté de certains traits dans la diversité fonctionnelle permet aussi de favoriser la stabilité et la résilience du système et donc le maintien de la diversité spécifique (McLean et al., 2019a; Murgier et al., 2021). En résumé, le maintien de tous les types de la biodiversité garantit de donner les meilleures chances de maintien à la biodiversité pour elle-même.

La considération de la biodiversité pour elle-même n'exclut pas que la biodiversité ait une importance cruciale d'un point de vue anthropocentré. La diversité spécifique est source d'une grande variété de services pour l'humanité, appelés services écosystémiques (IPBES, 2019a). Parmi ces services, on peut notamment citer la sécurité alimentaire (Glamann et al., 2017; Tscharrntke et al., 2012), le stockage et la séquestration du carbone (Bianchi et al., 2021), les pratiques culturelles (Clark et al., 2014), la production d'oxygène (Corcoran and Boeing, 2012), l'inspiration pour la création et l'innovation (Bull et al., 1992), les molécules pharmaceutiques (Howes et al., 2020) ou encore l'émerveillement et le bien-être (Clark et al., 2014).

1.1.2 Facteurs impactant la biodiversité marine : le changement climatique et la pêche

Malgré la nécessité de préserver la biodiversité pour elle-même et pour ce qu'elle apporte à l'humanité, cette biodiversité connaît actuellement un fort déclin en lien avec les activités anthropiques (Figure 1, IPBES, 2019a). Le nombre d'espèces diminue, avec un taux d'extinction environ 1000 fois plus élevé que le taux d'extinction naturel des espèces (Pimm et al., 2014). Dans les écosystèmes marins, les trois principales causes de déclin sont en ordre d'importance : l'exploitation directe, le changement d'utilisation des terres/mers et le changement climatique.

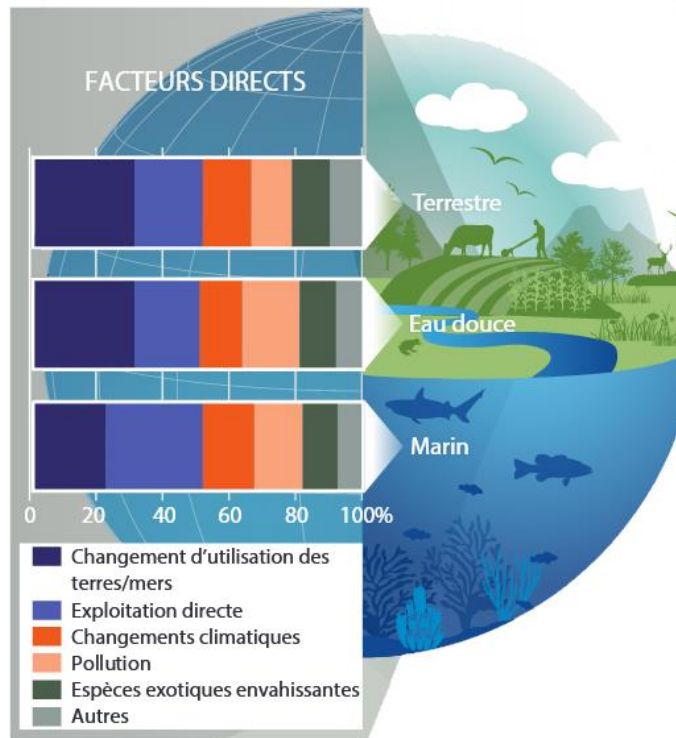


Figure 1 : Facteurs directs expliquant le déclin de la biodiversité dans les écosystèmes terrestres, d'eau douce et marins (selon IPBES (2019b)).

Les travaux présentés dans cette thèse s'intéressent en particulier aux impacts de la pêche et du changement climatique. Ces deux facteurs impactent les trois types de biodiversité décrits précédemment, et les écosystèmes marins dans leur ensemble (Coll et al., 2016; Halpern et al., 2008; Heino et al., 2015; Parmesan, 2006).

La pêche est le premier facteur qui impacte les écosystèmes marins (Figure 1, IPBES, 2019a). Sa principale conséquence est la diminution des biomasses : la déplétion de biomasse par la pêche est estimée à un tiers par rapport à une période antérieure à la pêche (Bianchi et al., 2021). On estime actuellement que 1% des espèces de poissons se sont éteintes depuis l'an 1500 (IPBES, 2019a). Par son caractère sélectif, la pêche impacte aussi la diversité fonctionnelle, par exemple en modifiant le fonctionnement trophique de l'écosystème (Pauly, 1998), en diminuant les espèces aux traits fonctionnellement rares (Murgier et al., 2021), ou encore en modifiant les traits des espèces (Heino et al., 2015). Enfin, la pêche érode la diversité génétique (Marty et al., 2015).

Le changement climatique impacte la biodiversité marine principalement par le réchauffement, la désoxygénation et l'acidification des océans.

Le réchauffement des océans est la facette du changement climatique la plus étudiée. Il entraîne des changements de diversité spécifique spatialement, avec des extinctions locales liées à des déplacements des aires de distribution des espèces vers les pôles ou en profondeur (Cheung et al., 2009; Dulvy et al., 2008; Perry et al., 2005). Ces déplacements peuvent entraîner des *mismatch* trophiques pouvant accentuer les extinctions locales (Doney et al., 2012) et provoquer des perturbations qui peuvent être amplifiées par des modifications de la productivité des écosystèmes (Doney et al., 2012; Du Pontavice et al., 2020; Lotze et al., 2019; Tittensor et al., 2021). Le réchauffement induit des changements de diversité fonctionnelle par la sélection d'espèces à cycle de vie court (McLean et al., 2019b), par des changements adaptatifs des traits individuels comme les traits d'histoire de vie (Gienapp et al., 2008; Waples and Audzijonyte, 2016) ou par des changements physiologiques (Angilletta, 2009; Audzijonyte et al., 2018; Pörtner, 2001; Pörtner et al., 2017). Enfin, tout comme la pêche, le changement climatique altère la diversité génétique (Pauls et al., 2013).

Aux effets du réchauffement s'ajoute les effets de la désoxygénation et de l'acidification. La désoxygénation diminue notamment les flux physiologiques (Thomas et al., 2019) et peut entraîner des extinctions locales avec la formation de zones hypoxiques ou anoxiques (Laffoley and Baxter, 2019). L'acidification peut également impacter la diversité spécifique par deux voies principales : (i) elle pose des problèmes de maintien des écosystèmes reposant sur un support calcifié, comme par exemple les écosystèmes coralliens (Brandl et al., 2020; Hoegh-Guldberg et al., 2017), et des problèmes de survie directe chez les espèces avec un squelette calcifié externe (Hendriks et al., 2010). Chez les poissons, l'acidification pourrait avoir des impacts sur le métabolisme et donc sur les traits des espèces, mais ces impacts restent encore débattus (Heuer and Grosell, 2014).

1.1.3 Importance de l'étude des dynamiques éco-évolutives : interactions entre les différents niveaux d'organisation de la biodiversité

Les impacts anthropogéniques sur la biodiversité au niveau des individus, des populations, des communautés et des écosystèmes et les interactions entre niveaux montrent la nécessité de travailler dans un cadre qui intègre les différents types de biodiversité et leurs réponses aux pressions multiples. Dans cette optique, l'étude des dynamiques éco-évolutives a reçu une attention croissante ces dernières années (Brunner et al., 2019; Hendry, 2016; Kinnison et al., 2015; Norberg et al., 2012; Pelletier et al., 2009).

L'étude des dynamiques éco-évolutives permet de prendre en compte le taux d'évolution génétique des populations et ses conséquences en termes de changements de traits fonctionnels (Hendry, 2016; Hendry et al., 2018). Expliciter les liens entre les traits d'histoire de vie, la dynamique de population et l'évolution permet d'aborder la notion de résilience face aux perturbations en identifiant par exemple des situations de sauvetages ou de pièges évolutifs (Yacine et al., 2021), les cas de coévolution (Cortez, 2018), les boucles de rétroactions éco-évolutives (Edeline and Loeuille, 2021; Perälä and Kuparinen, 2020), les points de basculement (Dakos et al., 2019), des dynamiques cryptiques (Brans et al., 2022; Kinnison et al., 2015) ou encore des conflits émergents entre adaptations et migrations (Thompson and Fronhofer, 2019).

En l'absence des dynamiques éco-évolutives dans les projections de biodiversité sous scénarios de gestion de pêche ou de changement climatique futur, ces projections peuvent ne pas représenter des changements abruptes pouvant avoir des conséquences négatives majeures pour les socio-écosystèmes (Chaparro-Pedraza and de Roos, 2020). Inversement, des projections surestimant les impacts humains en ne prenant pas en compte les potentiels sauvetages évolutifs peuvent entraîner une inadéquation entre les recommandations scientifiques sur la gestion d'une ressource et les constats empiriques des exploitants sur l'état de cette ressource. Le risque dans ce cas est la perte de

confiance des acteurs exploitant la ressource dans les avis scientifiques de gestion, voire leurs contestations. Ces deux possibilités montrent la nécessité d'intégrer les dynamiques éco-évolutives dans des outils de gestion et de projections futures.

Pour étudier les dynamiques éco-évolutives au niveau des écosystèmes marins, des outils de modélisation appliquée intégrant les dynamiques éco-évolutives sont nécessaires notamment au niveau multispécifique (Romero-Mujalli et al., 2019). Ces modèles, d'un type nouveau, doivent être développés en réunissant les théories de l'écologie évolutive notamment la théorie des traits d'histoire de vie (partie 1.2), des réponses plastiques et évolutives cohérentes avec celles observées empiriquement chez les populations de poissons exploitées (partie 1.3) et les outils de modélisation des écosystèmes marins déjà existants (partie 1.4). Les dynamiques éco-évolutives étant étudiées au niveau de l'écosystème mer du Nord dans ces travaux de thèse, l'état de l'art des travaux sur le système mer du Nord, ses communautés de poissons exploités et les pressions auxquelles elles font face sera présenté en partie 1.5. L'introduction se terminera par une partie décrivant les chapitres de ce manuscrit et les questions de recherche et objectifs associés à chaque chapitre.

1.2 Concepts théoriques expliquant la variation individuelle des traits d'histoire de vie

1.2.1 De Darwin à la théorie des traits d'histoire de vie.

La sélection naturelle, initialement décrite par Darwin dans l'origine des espèces (Darwin, 1859), est le mécanisme qui implique que les individus les mieux adaptés à un environnement, c'est-à-dire ceux avec une meilleure *fitness*, ont le meilleur succès reproducteur et la meilleure survie. Une condition à l'évolution en réponse à la sélection naturelle est la présence d'un mécanisme de transmission et d'hérédité des variations avantageuses d'une génération à la suivante. Les lois régissant le mécanisme d'hérédité ont été découvertes par Mendel (1866) et mises en lumière au début du XX^e siècle. Le support de l'hérédité, la molécule d'ADN (dont une portion est nommée gène) n'est découverte que bien plus tard, en 1953 par Watson et Crick (Watson and Crick, 1953).

D'autre part, une distinction est également rapidement faite entre la part héritable d'un caractère d'un individu, le génotype, et la valeur observable du caractère sur laquelle la sélection naturelle agit, le phénotype (Johansen, 1909).

Durant le début du XX^e siècle, de l'association de la théorie Darwinienne et des lois mendéliennes émerge la génétique des populations. Cette discipline a pour but d'étudier les changements de fréquences de gènes dans une population et leur vitesse de changement. Elle s'intéresse aussi aux états d'équilibres évolutifs et à leurs perturbations liées à la variation en *fitness*, qui peut émerger de la sélection, la mutation, la dérive génétique, les flux de gènes et l'assortiment non aléatoire lors de la reproduction. La génétique des populations ne dit alors rien de la vitesse de changement des phénotypes et des causes expliquant la meilleure *fitness* de certains individus par rapport à d'autres.

La volonté de comprendre en quoi des individus variables en termes de traits d'histoire de vie ont des *fitness* différentes dans un environnement donné et de pouvoir prédire les phénotypes émergents dans un environnement donné a mené à la théorie des traits d'histoire de vie.

1.2.2 La théorie des traits d'histoire de vie

1.2.2.1 Synthèse de la théorie des traits d'histoire de vie

La théorie des traits d'histoire de vie a été synthétisée et promue par Stearns (Stearns, 1992) et Roff (Roff, 1993). Elle s'intéresse aux traits définissant les histoires de vie, à leur variabilité génétique et à leur évolution sous l'effet de la sélection naturelle. Elle souligne aussi le caractère central de la plasticité et de l'évolution des traits d'histoire de vie pour comprendre la dynamique de populations. Les différents types d'organisations biologiques (gène, trait d'histoire de vie, population et communauté) sont liés dans cette théorie qui réunit des concepts de biologie évolutive, de dynamique de population, de génétique quantitative et de physiologie. Cette théorie a été développée dans le but de comprendre l'action de la sélection naturelle sur le phénotype observé dans des populations naturelles, ainsi que sur le génotype sous-jacent.

Un trait d'histoire de vie est un trait déterminant pour la reproduction et la survie (Stearns, 1992) : dans cette théorie, un individu est défini uniquement par ses traits démographiques (par exemple, la taille à la naissance, le taux de croissance, l'âge et la taille à maturité ou encore l'investissement reproductif).

La valeur phénotypique d'un trait d'histoire de vie est en partie dépendante de la démographie par des processus de densité dépendance de la population et du génotype (Figure 2). Le génotype est lui-même régi par la génétique quantitative.

La différence entre génotype et phénotype s'explique par des *trade-offs*, qui traduisent le partage de ressources au niveau physiologique entre différents traits d'histoire de vie (Figure 2B) et par l'influence de l'environnement sur l'expression du génotype, aussi appelé plasticité phénotypique. La plasticité phénotypique est communément modélisée par des normes de réactions qui représentent la transformation d'une variation environnementale en variation phénotypique (Figure 2C).

A chaque phénotype est associé une *fitness* dans un environnement donné. La sélection naturelle est appliquée sur le phénotype et impacte le génotype à l'échelle de la population. Une part de la variabilité génotypique des traits d'histoire de vie s'explique par la phylogénie et le résultat de la macroévolution. Cette partie ne sera pas traitée dans la suite de cette thèse. L'autre partie de la variance des traits est au niveau intra-spécifique : cette variance génotypique varie sous les pressions contemporaines telles que le changement climatique ou la pêche. Le changement de variance génétique ou de moyenne génotypique au fil des générations est appelé microévolution. La suite des travaux présentés dans ce manuscrit sera centrée sur la microévolution.

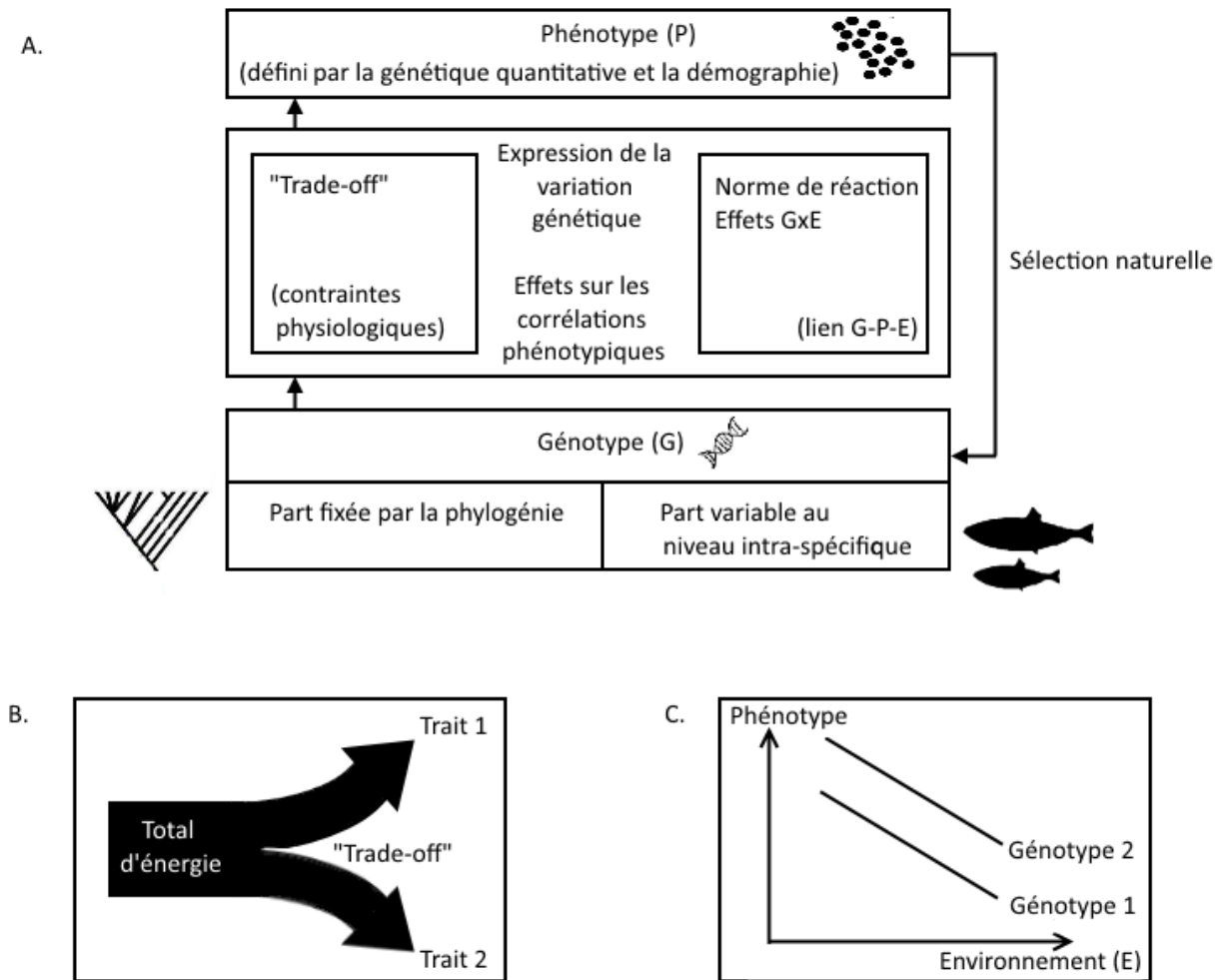


Figure 2 : Schéma synthétisant la théorie des traits d'histoire de vie, adapté de Stearns (1992) (A) avec une définition schématique de la notion de *trade-off* (B) et de norme de réaction (C). P représente le phénotype, G représente le génotype, E représente l'environnement.

1.2.2.2 L'héritabilité, une condition à l'évolution

Un trait peut évoluer si ce trait a une héritabilité significativement non nulle. L'héritabilité est la proportion de la variation totale d'un trait qui est d'origine génétique. Une héritabilité non nulle indique qu'un trait est au moins en partie génétiquement variable dans la population et qu'un changement de trait peut donc être transmis entre générations. Pour qu'un changement de trait transmis soit une réponse à la sélection, la variation du trait doit se traduire par une variation de *fitness* dans la population et le changement transmis doit se faire dans le sens d'une augmentation de la *fitness*. Par définition, les traits d'histoire de vie ont une forte influence sur la *fitness*. Dès que l'héritabilité d'un trait d'histoire de vie est significativement non nulle, il y a une réponse évolutive à

la sélection naturelle. Un trait avec une héritabilité plus forte répondra plus vite à la sélection qu'un trait avec une héritabilité plus faible.

En dépit de leur forte influence sur la *fitness*, les traits d'histoire de vie ont une faible héritabilité dans les populations animales (Houle, 1992; Mousseau and Roff, 1987; Price and Schluter, 1991) : il a été estimé qu'ils possédaient une héritabilité moyenne d'environ 0.26 (Mousseau and Roff, 1987). Cette basse héritabilité pourrait s'expliquer par l'architecture génétique des traits d'histoire de vie (Merilä and Sheldon, 1999) ou par la forte interaction entre l'environnement (Price and Schluter, 1991) et le génotype, ou par la corrélation entre traits d'histoire de vie (Price and Schluter, 1991) ou enfin par une forte sélection stabilisante érodant leur variabilité génétique, précisément du fait de leur forte influence sur la *fitness* (Stearns 1992).

1.2.2.3 Corrélations des traits d'histoire de vie issues de *trade-offs* physiologiques

Au niveau individuel, la valeur d'un trait d'histoire de vie est contrainte par la valeur des autres traits d'histoire de vie pour des raisons physiologiques. L'individu possède une quantité finie d'énergie acquise via son alimentation. L'augmentation de l'allocation de l'énergie disponible à une fonction métabolique se fait donc au détriment d'une autre (Figure 2B). Par exemple, l'allocation d'énergie à la reproduction peut augmenter au détriment de la croissance (Boukal et al., 2014).

Des compromis physiologiques émergent les phénotypes à un niveau plus intégré tels que la fécondité relative, les tailles aux âges ou encore la taille et l'âge à maturité.

Les traits d'histoire de vie sont déterminés par des traits physiologiques sous-jacents. L'évolution de ces traits de processus change les valeurs des *trade-offs*. En étant modifiés, ces *trade-offs* modifient les traits d'histoire de vie de façon corrélée.

1.2.2.4 Plasticité phénotypique en réponse à l'environnement et concept de norme de réaction

1.2.2.4.1 La plasticité phénotypique : une adaptation à la variabilité de l'environnement

Un changement de génotype n'entraîne pas une unique réponse possible du phénotype : il existe un découplage partiel entre les variations phénotypiques et génotypiques. L'environnement et ses interactions avec le génotype peuvent expliquer la diversité des phénotypes observés pour un même génotype (voir Figure 2A). Les variations du phénotype générées par un unique génotype en réponse aux variations de l'environnement sont appelées plasticité phénotypique.

Cette capacité peut être une adaptation à un environnement variable (Bradshaw, 1965; Murren et al., 2015; Pigliucci et al., 2006). Un génotype qui permet une plasticité phénotypique importante peut être une adaptation car il peut être un avantage par rapport à un génotype produisant un phénotype fixe, notamment dans un environnement variable, où il permet d'être compétitif en termes de *fitness* même si l'environnement varie contrairement à un génotype à phénotype fixe qui est optimal pour un environnement donné. Le degré de plasticité phénotypique est une propriété déterminée par le génotype pouvant évoluer car elle est génétiquement variable dans une population.

1.2.2.4.2 Représentation de la plasticité phénotypique

La plasticité phénotypique peut être représentée par une norme de réaction : une norme de réaction est la courbe qui associe, pour le génotype d'un trait continu donné, les différentes valeurs de son phénotype aux variations environnementales. Pour une norme de réaction linéaire, la plasticité phénotypique est représentée par la pente (Angilletta, 2009).

Le concept de norme de réaction est particulièrement utilisé dans le domaine de l'adaptation thermique (Angilletta, 2009) et dans le domaine de l'évolution induite par la pêche (Stearns and Koella, 1986).

1.2.2.4.3 En réponse à la variabilité d'une variable environnementale: l'exemple de la plasticité phénotypique thermique

Les traits d'histoire de vie peuvent répondre plastiquement à des changements des variables environnementales abiotiques telles que la température (Angilletta, 2009) ou l'oxygène (Thomas et al., 2019). La norme de réaction thermique est un cas particulier des normes de réaction où le trait étudié répond à la température. Le trait en question peut être n'importe quel trait répondant à la température (Angilletta, 2009). La norme de réaction thermique est notamment utilisée pour décrire la réponse de la performance à la température, alors appelée courbe de performances thermiques (*Thermal performance curves* (TPC) en anglais) (Huey and Stevenson, 1979).

Les TPC déterminent les températures critiques de vie d'un organisme ainsi que la température qui optimise la performance de l'organisme : elles ont donc une forme de réponse en cloche. Angilletta (2009) énonce trois théories expliquant les mécanismes de cette réponse en cloche, ou fenêtre thermique : (i) les effets de la température sur les enzymes (Hochachka and Somero, 2002), (ii) sur la membrane cellulaire (Hazel and Eugene Williams, 1990), et (iii) une limitation de la capacité d'apport en oxygène à certaines températures (Pörtner, 2001). L'hypothèse de la limitation de la capacité d'apport en oxygène est couramment utilisée pour étudier les réponses thermiques des poissons.

La plasticité du phénotype en réponse à la température a aussi la capacité d'évoluer entraînant la modification des températures optimales ou critiques des organismes (Angilletta, 2009). L'étude de l'évolution de cette plasticité nécessite l'estimation de la variabilité des réponses à la température intra-populationnelle à l'aide par exemple de données expérimentales. Compte tenu de la disponibilité des données chez un nombre restreint d'espèces, cette évolution potentielle en réponse au changement climatique ne sera pas traitée dans ce travail. La réponse évolutive au changement climatique considérée sera uniquement une réponse des traits d'histoire de vie.

1.2.2.4.4 En réponse à la variabilité des conditions environnementales : l'exemple de la norme de réaction de maturation.

L'âge et la taille à maturation présentent une forte variabilité dans une population. Cette variabilité est d'origine plastique et génétique. Les variations de la taille et de l'âge à maturité sont fortement corrélées. Pour étudier les variations plastiques de l'âge et de la taille à maturité, Stearns and Koella

(1986) ont défini les normes de réaction de maturation. Ces dernières sont définies comme l'ensemble des combinaisons taille-âge auxquelles un individu peut devenir mature. La plasticité de la maturation en réponse à l'environnement est donc décrite par une norme de réaction bi-variée. En effet, dans l'approche proposée par Stearns and Koella (1986), la norme de réaction de maturation est représentée en deux dimensions (la taille en fonction de l'âge). La réponse à l'environnement est prise en compte dans la variabilité des taux de croissance juvénile jusqu'à la maturation (Figure 3) qui est censée représenter la variabilité des conditions environnementales affectant la maturation. Dans cette approche, un individu est considéré mature quand sa courbe de croissance rencontre la norme de réaction : à ce point d'intersection émergent son âge et sa taille à maturité.

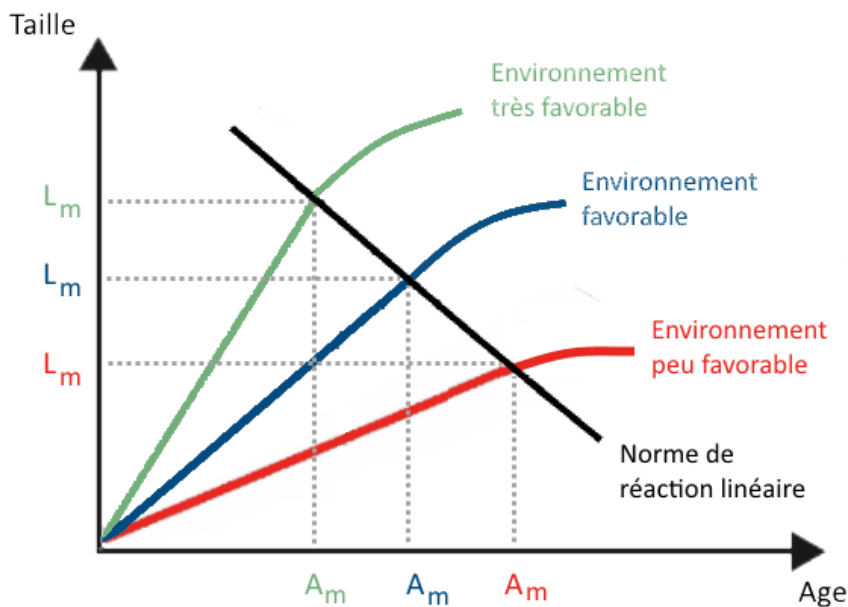


Figure 3 : Norme de réaction de maturation linéaire (droite noire) et plasticité de l'âge et de la taille à maturité en fonction de la variation de l'environnement (courbes de croissance individuelles en couleur).

Les déterminants de la norme de réaction de maturation peuvent être sous contrôle génétique. Dans le cas d'une norme de réaction linéaire (Figure 3), les déterminants pouvant varier génétiquement sont son ordonnée à l'origine et sa pente. Le changement de la norme de réaction entraîne une variation de l'âge et de la taille à maturité et donc du début de la période ontogénique de reproduction. Ce changement impacte la *fitness* et peut donc évoluer. Il existe un compromis évolutif

qui régit l'évolution de la norme de réaction. Une évolution vers une maturation plus précoce peut être un avantage car elle permet de se reproduire plus tôt à l'échelle de la vie d'un organisme. Au contraire, une évolution vers une maturation plus tardive permet une taille plus importante, et ainsi une survie et une fécondité plus importantes (Stearns, 1992).

1.3 Changements plastiques et évolutifs des traits d'histoire de vie chez les populations exploitées

Le prélèvement de ressources halieutiques a drastiquement accéléré les changements phénotypiques des traits observables (Darimont et al., 2009). Ces derniers sont également induits par l'augmentation de la température de l'eau (Audzijonyte et al., 2020, 2018).

1.3.1 Plasticité phénotypique en réponse à la pêche, à la température, et à l'oxygène

1.3.1.1 Plasticité phénotypique thermique des poissons

La littérature autour des réponses plastiques thermiques des traits décrit principalement des changements de taille avec l'augmentation des températures : la diminution en taille des ectothermes (Daufresne et al., 2009) et plus particulièrement des poissons (van Rijn et al., 2017) est la principale réponse à l'augmentation des températures. Elle a été nommée règle taille-température, en anglais la *temperature size rule* (TSR) (Audzijonyte et al., 2018). Des études ont aussi montré empiriquement et par la modélisation que la réponse à la température n'est pas unilatérale : la taille peut parfois aussi augmenter avec la température (Audzijonyte et al., 2020; Uszko et al., 2022).

De nombreux mécanismes ont été proposés pour expliquer cette réponse plastique. Le plus répandu est la théorie de la limitation de la capacité d'apport en oxygène (abrégée OCLTT pour *Oxygen-and Capacity-limited thermal tolerance*) (Pörtner, 2001; Pörtner et al., 2017). Pörtner et ses collègues expliquent la diminution en taille avec la température par une diminution des capacités aérobiques

nettes quand la température augmente au-delà d'une température optimale : la capacité d'extraire de l'oxygène du milieu (offre) augmente plus lentement que les besoins métaboliques basaux en oxygène (demande) avec la température. La différence entre les deux diminue donc avec l'augmentation de la température, ce qui entraîne une diminution des capacités aérobiques pour d'autres processus, dont la croissance. De façon similaire, cette théorie prévoit également une diminution plastique de la reproduction avec la température.

D'autres mécanismes sont proposés pour expliquer la TSR (Audzijonyte et al., 2018). Parmi eux, Audzijonyte et al., (2018) émettent l'hypothèse que la diminution de taille pourrait émerger de la modification plastique du *trade-off* entre reproduction et croissance somatique. Cette hypothèse induirait, contrairement au cadre proposé par l'OCLTT, une augmentation plastique de l'allocation de l'énergie à la reproduction.

Comme vu précédemment (voir partie 1.2.2.4), un changement d'environnement entraîne un changement de croissance et peut donc impacter l'âge et la taille à maturité. La température peut ainsi modifier ces traits d'histoire de vie. Il a également été montré expérimentalement que l'augmentation de la température pouvait impacter la norme de réaction de maturation en la décalant vers des tailles plus basses et des âges plus jeunes, indépendamment de la croissance (Kuparinen et al., 2011; Tobin and Wright, 2011).

1.3.1.2 Plasticité phénotypique des traits de vie induite par la pêche

Les changements de traits induits par la pêche peuvent avoir une origine plastique : la diminution de biomasse d'une population entraîne la diminution de la pression de compétition intra-populationnelle pour les survivants. Ce phénomène densité-dépendant entraîne au niveau individuel un taux d'énergie d'acquisition plus élevé et ainsi une augmentation de la croissance somatique et de la reproduction (Verhulst, 1838). L'augmentation des taux de croissance implique des individus plus grands suite à la diminution de la densité de la population (Bouffet-Halle et al., 2021), et en

conséquence une maturation plus précoce (Gobin et al., 2018). L'effet plastique de la pêche peut interagir avec son impact évolutif (voir partie 1.3.2) : la présence d'un fort effet de densité-dépendance peut modifier la direction et la vitesse des changements évolutifs de la pêche sur les traits d'histoire de vie en changeant par exemple l'âge auquel les individus recrute dans la pêcherie (Gobin et al., 2018).

1.3.2 Evolution induite par les pressions anthropiques

1.3.2.1 Acceptation de l'évolution contemporaine des traits

L'échelle de temps de l'évolution (au sens de Darwin) a longtemps été considérée comme considérablement supérieure au temps de réponse écologique, et en ce sens ignorée de la gestion des ressources halieutiques et de l'étude des écosystèmes marins. L'idée qu'une pression anthropique, comme la pêche, puisse entraîner une modification au niveau génétique d'une population exploitée a émergé dans les années 70 (Hutchings and Kuparinen, 2019) d'abord avec une étude sur une espèce d'eau douce (Handford et al., 1977) puis des espèces anadromes (Ricker, 1981) et enfin des espèces marines (Law and Grey, 1989). Une très vaste littérature existe depuis sur les changements évolutifs contemporains observés chez les populations marines pour des traits divers tels que les traits d'histoire de vie, le comportement ou la physiologie en réponse à la pêche (Heino et al., 2015; Hollins et al., 2018; Uusi-Heikkilä et al., 2008). Il existe aussi une réponse adaptative au changement climatique (Bradshaw, 2006; Parmesan, 2006). Les études empiriques identifiant les changements de traits liés au changement climatique comme étant évolutifs sont encore rares (Crozier and Hutchings, 2014; Merilä and Hendry, 2014). La pêche et le changement climatique sont deux pressions qui augmentent la mortalité totale subie par les populations halieutiques : en ce sens, le changement climatique pourrait entraîner des conséquences similaires à la pêche dans l'accélération des cycles de vie (voir partie 1.3.3.2). Dans cette introduction, l'accent est mis sur l'impact évolutif sur les traits d'histoire de vie car ce sont les impacts évolutifs les plus décrits. De plus, ces traits ont un effet direct sur les taux démographiques des populations et par conséquent sur

la communauté. L'évolution induite par la pêche sera ici abordée sous l'angle écologique, bien qu'elle ait aussi des conséquences pour la gestion des ressources halieutiques (Heino et al., 2013; Hutchings, 2009) et pour l'économie (Eikeset et al., 2013).

1.3.2.2 Accélération des cycles de vie

La pêche modifie les traits d'histoire de vie par deux pressions majeures : l'augmentation de la mortalité totale et la sélectivité par la taille. Ces deux caractéristiques de la pêche ont un impact similaire sur les cycles de vie : l'évolution induite par la pêche accélèrent les cycles de vie (Heino et al., 2015). L'accélération des cycles de vie a d'abord et de nombreuses fois été décrite en mer du Nord chez la plie (Rijnsdorp, 1993; Rijnsdorp et al., 2005; van Walraven et al., 2010) et la morue (Enberg et al., 2009; Holt and Jorgensen, 2015; Pardoe et al., 2019; Poulsen et al., 2006) et puis plus largement chez de nombreuses espèces démersales (Marty et al., 2014; Wright et al., 2011a), benthiques (Mollet et al., 2007), certains pélagiques comme le hareng (Claireaux et al., 2021; Enberg and Heino, 2007; Engelhard and Heino, 2004), des espèces anadromes (Young et al., 2020) et certains invertébrés (exemple d'un crabe (Hjelset, 2014)).

Les principaux traits d'histoire de vie impactés par l'évolution induite par la pêche sont la croissance juvénile, la taille et l'âge à maturation, et l'effort reproducteur.

La réponse évolutive de la maturation à la pêche est la réponse la plus fréquemment décrite et qui entraîne le changement phénotypique le plus évident (Heino et al., 2015). La réponse observée est une diminution de la taille et de l'âge à la maturation. La diminution de la taille à maturation est une adaptation principalement à la sélection par la taille : elle permet de se reproduire à des tailles pas ou peu pêchées. La diminution de l'âge de reproduction est aussi la contrepartie de l'augmentation globale de mortalité : la stratégie d'atteindre des âges avancés est dévaluée et l'avantage est donné à l'accélération de l'histoire de vie. Ces deux traits sont sélectionnés directement la sélection taille-dépendant et l'augmentation de la mortalité, et de façon indirecte par la forte corrélation existante entre taille et âge à maturité. La plasticité phénotypique de la maturation aussi diminue en réponse à

la pêche, ce qui se traduit par des translations ou par des changements de forme de la norme de réaction de maturation (Marty et al., 2011).

L'augmentation de l'effort reproducteur en réponse à la pêche a aussi été décrite à plusieurs reprises (Heino et al., 2015). Pour les individus adultes, il existe un *trade-off* entre allocation d'énergie à la reproduction et à la croissance somatique. Ainsi, l'augmentation de l'effort reproducteur se fait au détriment de la croissance à l'âge adulte et donc la taille à l'âge adulte diminue. Ces modifications sont des avantages en réponse à la pêche sélectionnant des grands individus. De plus, l'allocation supérieure à la reproduction est une réponse adaptative à l'augmentation de la mortalité totale : les individus vivant moins longtemps ont plus d'avantage à allouer plus d'énergie à la reproduction avant d'être pêchés.

Le troisième trait répondant de manière évolutive à la pêche est le taux d'acquisition d'énergie qui peut être approximé par la croissance juvénile (Enberg et al., 2012; Heino et al., 2015). L'effet de la pêche sur ce trait est encore débattu : la sélection semble agir dans deux directions simultanément et faire émerger une augmentation ou une diminution du taux d'acquisition d'énergie selon les cas (Enberg et al., 2012) : l'effet taille-sélectif de la pêche tend à privilégier des individus plus petits avec un taux d'acquisition d'énergie plus bas (Favro et al., 1979) alors que l'effet de mortalité additionnelle tend à favoriser un cycle de vie plus court et donc avec un taux d'acquisition d'énergie plus élevé (Enberg et al., 2009; Jørgensen and Fiksen, 2010).

1.3.2.3 Importance de la stratégie de pêche

Les effets évolutifs induits par la pêche vont également être dépendants de la stratégie de pêche notamment de deux points clés : la sélectivité en taille de l'engin de pêche utilisé et le stade ontogénique ciblé.

Une sélectivité en taille de la pêche de forme sigmoïde (telle qu'engendrée par les chaluts) peut avoir des effets opposés à ceux d'une sélectivité en cloche (engendrée par les filets dérivants) pour le taux d'acquisition d'énergie (Boukal et al., 2008) et pour la maturation (Boukal et al., 2008; Jørgensen et

al., 2009). La sélectivité en cloche peut aussi entraîner un état de bi-stabilité évolutive pour les traits (Boukal et al., 2008).

Selon le stade ontogénique ciblé par la pêche, des tendances évolutives différentes de celles observées empiriquement peuvent être prédites d'un point de vue théorique. Le prélèvement d'individus matures uniquement n'a pas les mêmes conséquences évolutives que le prélèvement d'individus à la fois matures et immatures, notamment sur la maturation et plus particulièrement sur la norme de réaction (Ernande et al., 2004).

1.3.2.4 Erosion génétique

La pêche entraîne de l'érosion génétique par la sélection d'une partie seulement de la variabilité génétique des traits d'histoire de vie. Cela peut également entraîner la disparition d'allèles sous-jacents à certains phénotypes ou une dérive génétique en diminuant les effectifs reproducteurs (Marty et al., 2015). Les conséquences de l'érosion génétique peuvent être la réduction de *fitness* d'une espèce à cause de l'augmentation de la consanguinité, de l'augmentation en fréquence d'allèles délétères, de mal adaptation et de perte d'adaptabilité (Leroy et al., 2018).

L'érosion de la diversité génétique est un enjeu de conservation majeur. Elle implique une potentielle impossibilité de retour à l'état initial du système suite à une diminution de la pression sélective (Kuparinen and Uusi-Heikkilä, 2019). La diminution de la diversité génétique en réponse à la pêche peut aussi impliquer la perte d'adaptabilité à d'autres pressions comme le changement climatique (Exposito-Alonso et al., 2022).

1.4 Interactions des réponses écologiques et évolutives aux niveaux intra- et inter-spécifiques : modélisation des changements des traits d'histoire de vie dans un réseau trophique spatialisé.

1.4.1 Etat de l'art des modèles multi-spécifiques, outils d'étude de la diversité spécifique

Les modèles écosystémiques sont des outils permettant la description d'au moins une composante d'un système biologique (par exemple les espèces) et au moins un processus en lien avec cette composante (par exemple la compétition) (Geary et al., 2020). Le modèle devient un modèle dit *end-to-end* quand il décrit l'ensemble des composantes d'un écosystème, allant de la description de la physique et de la biogéochimie jusqu'aux espèces de haut-niveau trophique, en incluant l'impact humain sur le système. Le succès actuel de ce type de modèle montre la volonté de comprendre des mécanismes complexes intégrant l'ensemble des composantes d'un système (Geary et al., 2020; Grimm et al., 2017; Rose et al., 2010).

Les modèles écosystémiques marins sont développés dans différentes équipes de recherches depuis environ 30 ans (Christensen and Pauly, 1992; Walters et al., 1997), et 15 ans pour les modèles end-to-end (Travers et al., 2009, 2007) avec certains objectifs communs, notamment (i) étudier la structure et le fonctionnement actuels des différentes composantes des socio-écosystèmes marins en prenant en compte les cascades de conséquences et les boucles de rétroactions entre les composantes multiples du système (ii) avoir un outil intégratif des effets directs et indirects des activités humaines pour informer les gestionnaires de manière systémique, (iii) comprendre mécaniquement les changements passés des socio-écosystèmes et (iv) anticiper l'évolution potentielle de la biodiversité sous scénarios, principalement scénarios de gestion et scénarios de changement climatique.

Les modèles utilisés le plus fréquemment pour l'étude des communautés de poissons diffèrent selon des critères variés : déterministe vs stochastique, individu centré vs résolu en équations différentielles, espèce-explicite vs spectre de taille, régional vs global... Ces modèles diffèrent également sur le nombre de processus représentés, explicitement ou non. Ces modèles permettent d'explorer des questions différentes (écologiques, économiques, ou encore impacts humains) et/ou à

des différentes échelles (individu, population, espèce, communauté, pêche, marché...) au sein de l'écosystème.

Parmi les modèles les plus utilisés, on pourrait citer Ecopath with Ecosim (EwE) (Christensen and Walters, 2004), Atlantis (Audzijonyte et al., 2019), OSMOSE (Shin and Cury, 2004, 2001; Travers et al., 2009), le modèle CaN (Planque and Mullan, 2020) ou encore le modèle SMS (Lewy, 2004) pour les modèles explicitant les espèces ou groupes fonctionnels et APECOSM (Maury, 2010) ou les modèles multi-espèces en spectre de taille (*multispecies size spectrum model* (Andersen, 2019; Blanchard et al., 2014)).

Le modèle EwE est le modèle le plus largement utilisé au monde : en août 2020, l'équipe de développement du modèle déclarait avoir environ 8000 utilisateurs dans 170 pays pour un total de 900 publications. Le succès de ce modèle et son accessibilité ont facilité la diffusion de l'approche écosystémique, ainsi que l'accumulation de connaissances des impacts humains sur les écosystèmes marins (Colléter et al., 2015).

Le modèle OSMOSE est un des seuls modèles écosystémiques marins de type individu centré (mais voir Giacomini et al., 2009). OSMOSE est un modèle de réseau trophique explicitant la dynamique des hauts niveaux trophiques. Couplé à des modèles biogéochimiques (par exemple, ROMS-N₂P₂Z₂D₂ (Travers et al., 2009), Eco3M (Diaz et al., 2019), ROMS-PISCES (Oliveros-Ramos et al., 2017), CROCO-BioEBUS (Hill Cruz et al., 2022), POLCOMS-ERSEM (Travers-Trolet et al., 2020)), il est possible de représenter l'ensemble de l'écosystème. Les propriétés trophiques de la communauté émergent des traits individuels et par espèce, de la prédation explicite et de la cooccurrence spatiale entre proie et prédateur. La description des traits d'histoire de vie au niveau individuel rend ce modèle particulièrement adapté à l'étude de leur variabilité intra-populationnelle, ainsi qu'à l'incorporation de la variabilité interindividuelle génotypique ou phénotypique issue de réponses physiologiques à un environnement variable (Romero-Mujalli et al., 2019).

1.4.2 Etude des changements évolutifs induits par la pêche à l'échelle monospécifique à l'aide de modèles éco-génétiques

Le modèle éco-génétique (Figure 4) est un cadre de modélisation qui a été développé pour suivre l'évolution d'un ou plusieurs traits d'histoire de vie dans les populations naturelles (Dunlop et al., 2009b). Les éléments décrits dans la théorie d'histoire de vie (Stearns, 1992) sont réunis dans un cadre de modélisation décrivant la structure démographique de la population, le phénotype des traits d'histoire de vie basé en partie sur le génotype, la densité-dépendance ainsi que l'impact de l'environnement. L'ensemble de ces éléments clés permet de modéliser l'évolution des histoires de vie dans les populations naturelles (Figure 4). Ce cadre de modélisation est principalement individu-centré et permet la représentation de la variation phénotypique et génotypique entre individus d'une même population. Le cycle de vie est modélisé par un modèle de croissance ou modèle bioénergétique (par exemple Boukal et al., 2014; Kooijman, 2010; Lester et al., 2004; Quince et al., 2008; West et al., 2001) décrivant a minima les compromis entre la croissance, la reproduction et la maturation liés à des allocations énergétiques. Le choix de ce modèle de cycle de vie est assez flexible : des réponses à l'environnement (température, oxygène...) peuvent être incorporées pour représenter mécaniquement une partie de la variabilité phénotypique mais cette possibilité n'a encore jamais été explorée à ma connaissance.

Les valeurs phénotypiques des traits d'histoire de vie modélisées dans un modèle éco-génétique sont en partie définies par une base génotypique. La transmission du génotype est représentée par un modèle représentant explicitement les loci (ex. Marty et al., 2015) ou par un modèle infinitésimal de génétique quantitative qui fait l'hypothèse d'une infinité de loci à effets infinitésimaux codant pour un trait (Dunlop et al., 2009a) . Ce dernier modélise la valeur des traits transmis aux descendants en la tirant aléatoirement dans une loi normale qui a pour moyenne la moyenne des traits des parents. De plus, les modèles éco-génétiques représentent aussi la sélection de deux parents pour la transmission de leur génotype à leur descendant.

Grâce à la flexibilité de ce cadre de modélisation, il a été très utilisé depuis sa publication pour étudier l'évolution des traits d'histoire de vie (Dunlop et al., 2009a, 2015; Hrycik et al., 2019; Kuparinen and Uusi-Heikkilä, 2019; Marty et al., 2015; Pardoe et al., 2019). Les modèles éco-génétiques associés à des réponses environnementales intégrées dans un modèle de bioénergétique semblent particulièrement adaptés pour étudier la variabilité génétique et environnementale des traits d'histoire de vie. Compatible avec un modèle écosystémique individu centré, son intégration dans ce dernier permettrait d'avoir un cadre de modélisation multispécifique permettant d'étudier les variations contemporaines des traits d'histoire de vie d'ordre plastiques en réponse à l'environnement et d'ordre évolutif en réponse à la sélection et leur impact sur la communauté d'espèces en interaction.

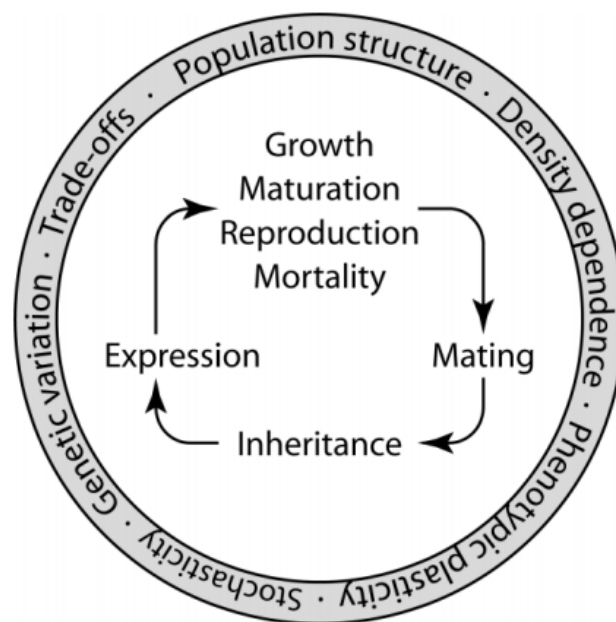


Figure 4 : Résumé du cadre de modélisation éco-génétique (selon Dunlop et al., 2009a). Les processus clés dans la description d'un individu sont au centre de la figure. Le cercle extérieur contient d'autres caractéristiques importantes d'un modèle éco-génétique.

1.4.3 Vers des modèles multispécifiques évolutifs: apports des modèles théoriques et début des modèles appliqués

Les changements évolutifs et leurs impacts écosystémiques ont longtemps été ignorés dans la gestion des pêches. Compte tenu des changements de traits dus à l'évolution ou à la plasticité

phénotypique et de leurs impacts sur les dynamiques écologiques, de la coévolution ou encore de l'éco-évolution au sein de la communauté, les conséquences des changements évolutifs doivent être considérés au niveau multispécifique (Edeline and Loeuille, 2021; Loeuille, 2019). Les dynamiques éco-évolutives commencent à être étudiées par plusieurs approches.

Une première famille de modèles théoriques explore la diversité des réponses éco-évolutives pouvant être attendue dans les écosystèmes marins exploités. Les changements évolutifs et écologiques conjoints peuvent avoir des conséquences positives sur la biodiversité de l'écosystème en évitant la disparition d'espèces par le biais de sauvetage évolutif (Yacine et al., 2021) ou grâce à la coévolution d'un prédateur et de sa proie (Prosnier et al., 2020). Les études théoriques montrent aussi qu'en ne prenant pas en compte les réponses évolutives à la pression de pêche ou climatique, les prédictions peuvent être erronées en n'identifiant pas de point de basculement du système (Ardichvili et al., 2022; Dakos et al., 2019; Tromeur and Loeuille, 2022). Par exemple, une modification adaptative de la taille peut entraîner la modification des interactions entre espèces, plus particulièrement la relation proie-prédateur (Edeline and Loeuille, 2021). Ces études identifient aussi des problèmes de réversibilité liés aux basculements du fonctionnement du système et à l'érosion génétique (Ardichvili et al., 2022; Edeline and Loeuille, 2021; Tromeur and Loeuille, 2022). L'érosion de la diversité génétique rend les populations moins susceptibles de s'adapter aux pressions supplémentaires par le biais de sauvetage évolutif.

L'ensemble de ces études éclaire les réponses possibles des communautés à des pressions quand les dynamiques éco-évolutives sont prises en compte. Le développement de modèles appliqués à des écosystèmes réels peut permettre de comprendre les réponses les plus plausibles face à des pressions grâce à la formulation de processus réalistes ajustés sur des données observées. Quelques études commencent à s'intéresser à certains aspects des dynamiques éco-évolutives avec des modèles écosystémiques appliqués. Les impacts écologiques des changements des traits d'histoire de vie sur une communauté en interaction ont récemment été explorés avec le modèle Atlantis dans

une approche où le changement de la taille corporelle est contraint à diminuer de manière implicite à chaque génération (Audzijonyte et al., 2013; Audzijonyte et al., 2014). Ces études soulignent que les changements de traits qui peuvent être d'origine évolutive ne peuvent pas être ignorés car ils modifient la dynamique des populations et des communautés. Les changements de traits évolutifs dans les communautés aquatiques de haut niveau trophique ont été aussi explorés au niveau d'une seule espèce au sein d'une communauté non évolutive en eau douce uniquement (Perälä and Kuparinen, 2020). Elle met en évidence le potentiel de sauvetage évolutif lorsqu'une espèce exploitée peut évoluer. La prédation et la pêche peuvent agir comme des forces sélectives synergiques ou additionnelles (Forestier et al., 2020a). Les modèles appliqués mis en œuvre jusqu'à présent soulignent l'impact que peuvent avoir des changements évolutifs sur une communauté d'espèces mais ne permettent pas de prendre en compte la complexité des dynamiques évolutives en négligeant les phénomènes de coévolution et les boucles de rétroactions mises en lumière par les modèles théoriques. Partant de ce constat, un des objectifs de cette thèse est de développer un modèle évolutif de communauté appliqué aux communautés de haut niveau trophique des milieux marins, qui puisse modéliser la variabilité génétique codant pour des variations de traits, l'évolution de ces traits, ainsi que les phénomènes de coévolution entre espèces, les impacts écologiques de ces changements et les boucles de rétroactions entre les changements observés (voir partie 1.6 pour le détail des objectifs de cette thèse).

1.5 Le cas d'étude « mer du Nord » : une zone de laboratoire à taille de bassin

Pour étudier les dynamiques éco-évolutives, ce travail prend comme cas d'étude l'écosystème Manche-Est – mer du Nord, (zone de pêche définie par le CIEM 7d et 4) qui sera abrégé mer du Nord dans la suite de cette introduction. La zone d'étude est incluse dans l'écorégion *Greater North Sea* définie par le CIEM (ICES, 2018a). Les caractéristiques principales de l'écorégion sont détaillées dans le document *Greater North Sea Ecoregion – Ecosystem overview* (ICES, 2018a).

Cette partie a pour but d'introduire les principales caractéristiques de la zone qui peuvent influencer sur la communauté ichthyologique, c'est-à-dire ses caractéristiques bathymétriques, thermiques et biogéochimiques (principalement oxygène et production primaire), de présenter les communautés biologiques actuelles de l'écosystème ainsi que les principales pressions humaines existant sur la zone pouvant impacter les communautés biologiques, et enfin de décrire les études s'intéressant au fonctionnement des communautés biologiques de cet écosystème, en mettant l'accent sur les travaux de modélisation écosystémique déjà existants dans la zone.

1.5.1 L'écosystème mer du Nord : description et délimitation de la zone d'étude

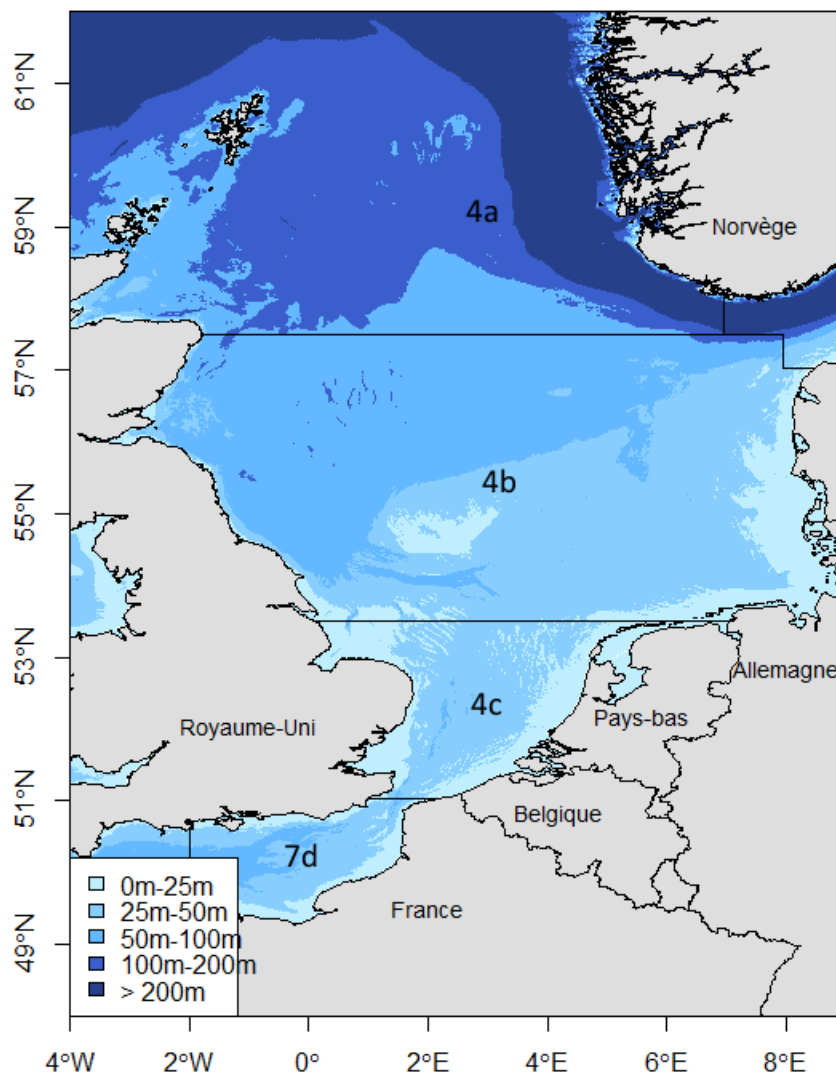


Figure 5 : Carte de la bathymétrie de la mer du Nord.

La mer du Nord se situe entre les pays suivants : le Royaume-Uni, la France, la Belgique, les Pays-Bas, l'Allemagne, le Danemark et la Norvège (Figure 5). L'ensemble de la zone est composé de quatre sous-zones caractérisées par des profondeurs différentes impliquant des différences écosystémiques majeures au niveau biogéochimique : le nord de la mer du Nord, le sud de la mer du Nord, la Manche-Est et la fosse norvégienne. La limite Nord-Sud dans la zone est l'isobathe des 50 mètres. Le cas d'étude se restreint aux zones entre 0 et 200 mètres de profondeur. La fosse norvégienne, qui est la zone la plus profonde du système mer du Nord (jusqu'à 500 mètres), a une communauté ichthyologique différente du reste de la mer du Nord, et est donc exclue de la zone d'étude. De plus, la partie de la zone située au nord des îles Shetland, qui présente des profondeurs supérieures à 200 mètres et soumise à une importante influence océanique, est aussi exclue. Ainsi, la zone d'étude sur laquelle se focalise ces travaux se compose de la Manche-Est et de la mer du Nord depuis le détroit du Pas-de-Calais jusqu'à l'isobathe 200m au nord de la zone. L'ensemble de la zone d'étude a une surface totale de 578 000 km².

La zone d'étude est peu profonde et caractérisée comme mer semi-continentale. L'ensemble de la zone subit le deuxième régime de marée le plus important au monde. Le courant majoritaire va du sud-ouest au nord-est de la zone, avec un hydrodynamisme particulièrement fort dans le détroit du Pas-de-Calais, entre la Manche-Est et la mer du Nord. La Manche-Est et la partie sud de la mer du Nord sont deux zones de faible profondeur (sud mer du Nord : 0-50 mètres ; Manche-Est : 0-70 mètres), mais la Manche-Est est caractérisée par des sédiments assez grossiers comparativement aux sables et sables vaseux de mer du Nord.

1.5.1.1 Variables environnementales en mer du Nord

1.5.1.1.1 Régime thermique

La mer du Nord se situe dans une zone de régime thermique tempéré. Au niveau décennal, le régime thermique est influencé par les oscillations nord atlantiques. L'ensemble de la zone présente des variations saisonnières de la température (Butenschön et al., 2016; Janssen et al., 1999). La Manche-

Est et le sud de la mer du Nord sont deux zones avec une colonne d'eau mixée ne présentant donc pas ou peu de stratification en été. La variation saisonnière des températures est importante du fait de la faible profondeur : cela implique un réchauffement important des eaux en été et les eaux les plus froides de la zone en hiver. Cette zone est la partie subissant les plus forts contrastes de température, de 6°C à 19°C en moyenne (Chen et al., 2022). La température de la partie nord varie moins selon la saison. Cette zone est stratifiée en été (ICES, 2018a; Janssen et al., 1999; Wakelin et al., 2020). La partie la plus profonde de la colonne d'eau a une température froide et une très faible variation de la température au cours de l'année contrairement à la partie plus en surface qui se réchauffe fortement en été.

1.5.1.1.2 Salinité

La salinité moyenne de la mer du Nord se situe autour de 34 g.L⁻¹. La partie de la zone d'étude avec le niveau de salinité le plus bas est sous l'influence de fleuves et se situe dans l'est et le sud-est de la zone d'étude avec des niveaux minimaux de l'ordre de 31 g.L⁻¹ (Janssen et al., 1999; Jones and Howarth, 1995).

1.5.1.1.3 Oxygène

La majorité de l'écosystème mer du Nord est actuellement considérée comme une zone sans problème d'hypoxie (Skogen et al., 2014). L'écosystème n'est pas répertorié dans les zones d'oxygène minimal (connues sous l'acronymes *OMZ* pour *oxygen minimum zone*), qui sont des zones d'hypoxie ou d'anoxie permanentes (Altieri and Diaz, 2019). Les problèmes d'hypoxie dans la zone (concentration d'oxygène dissout inférieure à 2 mg.L⁻¹) sont répertoriés localement et parfois saisonnièrement dans les zones côtières (Altieri and Diaz, 2019; Skogen et al., 2014) qui sont caractérisées par une forte production primaire (Holt et al., 2012; Wakelin et al., 2020). Dans une autre étude, uniquement la partie sud-est est répertoriée comme hypoxique un à deux mois dans l'année (Wakelin et al., 2020).

1.5.1.2 Description des espèces et des communautés de la mer du Nord

Les communautés biologiques de la mer du Nord sont très richement documentées grâce à des données issues de nombreux suivis de long terme pour la communauté benthique (Frid et al., 2000), la communauté ichtyologique (NS-IBTS-Q1, DATRAS), le phytoplancton et le zooplancton (Colebrook, 1985; Krause et al., 2003). Le fonctionnement des communautés ichtyologiques de mer du Nord a été décrit dans de nombreux travaux de modélisation écosystémique (Blanchard et al., 2014; Cormon et al., 2016; Heath, 2012; Lewy, 2004, 2004; Mackinson and Daskalov, 2007) et d'analyses fonctionnelles des communautés (McLean et al., 2018a, 2019c, 2019b; Murgier et al., 2021). Les conclusions de ces travaux seront présentées dans la partie 1.5.3.

Cette partie-ci s'attachera à décrire les caractéristiques et la composition spécifique actuelle de la communauté ichtyologique de la mer du Nord. Il existe d'autres communautés de hauts niveaux trophiques présentes dans l'écosystème, qui peuvent être des prédateurs ou compétiteurs des principales espèces de poissons de mer du Nord. On peut par exemple citer les raies, les requins, les oiseaux marins et les mammifères marins. Enfin, il est nécessaire de signaler l'importance de la communauté benthique pour le régime alimentaire des poissons démersaux et benthiques de mer du Nord principalement et partiellement pour les espèces pélagiques (DATRAS, 2010; Giraldo et al., 2017).

La partie haute du réseau trophique centrée sur les poissons est documentée notamment grâce aux campagnes de suivi océanographique de longue date en mer du Nord, aux données de captures de pêche, aux données de contenus stomacaux et aux études d'isotopes stables.

Le groupe majoritaire de l'écosystème en biomasse est le groupe des espèces pélagiques de petite taille (principalement hareng, lançon, maquereau, sprat, chinchard, et merlan bleu). Ces espèces sont présentes dans tout l'écosystème. Leur biomasse varie fortement en lien avec des migrations hors zone (notamment le chinchard et le merlan bleu) et en lien avec des cycles de vie courts et des

recrutements variables selon les années. Ces espèces ont un rôle clé dans le réseau trophique car ce sont des espèces fourrages (Daan, 1973; Hislop et al., 1991) (principalement le sprat, le lançon et les autres espèces au stade juvénile). Leurs proies sont principalement du plancton pélagique et leurs prédateurs des espèces démersales : les petits pélagiques assurent en ce sens un couplage pélagobenthique dans l'écosystème. Le hareng, considéré parfois comme benthopélagique, et le lançon qui s'enfouit à une période de l'année dans le sable, contribuent également au couplage dans le sens benthopélagique. Le lançon est une espèce particulièrement essentielle de l'écosystème mer du Nord en tant que proie de l'ensemble des groupes de l'écosystème (poissons, oiseaux marins et mammifères principalement).

Le groupe des démersaux est dominé par les gadidés (morue, merlan, tacaud, lieu noir et jaune, aiglefin...) et des espèces de la famille des gadiformes (merlu et congre principalement). Ce sont les espèces de plus haut niveau trophique parmi les poissons de la mer du Nord, principalement le merlan, la morue et le lieu noir : ces espèces proches du fond se nourrissent principalement sur des invertébrés benthiques et sur des petits poissons.

Grâce à son régime tempéré et à sa faible profondeur, la mer du Nord se caractérise par un groupe de poissons plats important et divers principalement dans le sud (Pauly, 1994; Piet et al., 1998). Ce groupe se nourrit principalement d'invertébrés benthiques et est peu prédaté par les démersaux une fois adulte.

1.5.2 La mer du Nord : une zone fortement exploitée par l'homme

La communauté de poissons actuelle est la résultante de l'histoire des activités humaines qui se sont développées dans la zone et des changements environnementaux passés. Cette partie a pour but de synthétiser les activités humaines pouvant impacter les communautés biologiques de mer du Nord (pêche, transport, industrialisation des estuaires...) ainsi que leurs conséquences qui constituent des changements majeurs de l'écosystème (changement climatique, invasion d'espèces...). La présentation des pressions se veut exhaustive dans leur mention. Cependant, plus de détails seront

donnés sur les deux pressions qui seront l'objet d'étude dans cette thèse : la pêche et le changement climatique.

1.5.2.1 La mer du Nord : une zone de pêche historique et majeure encore aujourd'hui

L'histoire de la pêche en mer du Nord commence à une époque très ancienne : on estime qu'elle remonte à la sédentarisation de l'Homme en Europe à la préhistoire (Gascuel, 2019) et aurait donc commencé il y a 7 500 ans (Lotze, 2007). Bien que cette exploitation soit uniquement côtière à l'époque, cette longue histoire implique que l'histoire évolutive des pêches puisse s'être déroulée sur une très longue période et ait pu modeler la diversité génétique et spécifique depuis des millénaires avant d'obtenir le résultat actuel. En d'autres termes, l'état vierge (qui est censé être l'état de référence en écologie évolutive) de l'écosystème mer du Nord a disparu depuis bien longtemps.

L'exploitation des ressources halieutiques de la mer du Nord s'intensifie dans la 2^{ème} moitié du XIX^e siècle avec l'invention du moteur à combustion : la pêche n'est véritablement plus uniquement côtière. La puissance de pêche augmente considérablement ainsi que les captures (Gascuel, 2019). La mer du Nord, qui est une zone très productive et très exploitée, devient alors la première zone de pêche au monde. Les captures en mer du Nord (écorégion *Greater North Sea*) augmentent jusqu'à culminer à 4 000 000 tonnes par an à la fin des années 60 et au début des années 70. Les captures ont depuis décliné jusqu'à se stabiliser autour de 2 000 000 de tonnes depuis une quinzaine d'années. Aujourd'hui, cette zone reste la première zone de pêche en Europe (ICES, 2018b).

La totalité de la mer du Nord et de la Manche-Est se trouve dans les zones économiques exclusives des pays qui la bordent (Angleterre, France, Belgique, Pays-Bas, Allemagne, Danemark et Norvège) et la grande majorité des captures est réalisée par ces sept pays.

La majorité des débarquements provient du nord de la zone (4a) et de la zone centrale (4b) (Figure 5). La composition en biomasse des espèces pêchées est dominée par les pélagiques, dont le groupe

est composé des quatre espèces les plus pêchées de la zone (hareng, lançon, maquereau, et sprat) puis les démersaux, les benthiques et enfin les crustacés et les élasmobranches (ICES, 2018b).

La pêche est le principal facteur de perte de diversité dans les écosystèmes marins (IPBES, 2019). L'impact principal est la diminution de la biomasse totale des espèces exploitées (Gislason, 1994). L'écosystème en période antérieure à la pêche industrielle était l'un des plus productifs au monde : au moment du pic d'exploitation de la mer du Nord, on estime qu'il restait environ 20% de la biomasse initiale de poissons dans l'écosystème mer du Nord (Bianchi et al., 2021). L'exploitation industrielle a entraîné l'effondrement de plusieurs stocks de poissons de la mer du Nord (Cook et al., 1997; Dickey-Collas et al., 2010; Lotze, 2007), notamment des deux espèces emblématiques de l'écosystème : le hareng (Dickey-Collas et al., 2010) et la morue (Cook et al., 1997). La pêche a plus récemment entraîné l'effondrement du lançon, l'espèce fourrage centrale de l'écosystème (Lindgren et al., 2018). En plus de ses impacts écologiques, la pêche a des conséquences évolutives qui ont été décrites chez de nombreuses espèces exploitées de mer du Nord (Marty et al., 2014; Mollet et al., 2007; Rijnsdorp, 1993) principalement sur des séries de données contenant le pic d'exploitation de l'écosystème aux alentours des années 60/70.

Enfin, une autre conséquence indirecte de la pêche est l'abrasion des substrats benthiques qui est considérée comme l'une des cinq pressions majeures auxquelles fait face l'écosystème (ICES, 2018a).

1.5.2.2 La mer du Nord : une zone de cumul d'activités humaines et de pressions sur la biodiversité marine

Une particularité de la mer du Nord est le cumul d'activités imposant une forte pression anthropique sur l'écosystème : le CIEM répertorie dix activités qui entraînent des pressions directes sur l'écosystème (Figure 6) (ICES, 2018a). Ces pressions ne sont pas directement l'objet de cette thèse mais sont énumérées car elles permettent de comprendre le contexte multi-pressions auquel font face les communautés biologiques de mer du Nord. Ce travail étant centré sur la pêche, la possibilité de conflits d'usage rend également intéressant l'exposé de ces activités.

Le changement d'usage des habitats est considéré comme l'un des trois facteurs impactant le plus la biodiversité marine avec le changement climatique et la pêche (IPBES, 2019). Ce changement d'usage peut survenir dans le cas d'installations *offshores* (plateformes pétrolières et/ou les installations d'énergies marines renouvelables), qui sont en augmentation (Xu et al., 2020) et qui ont été identifiées comme pouvant modifier les communautés marines et avoir un impact sur les captures (Fujii, 2015; Halouani et al., 2016; Nogues et al., 2022; Stenberg et al., 2015). L'extraction de sable ou de gravats dégrade la structure benthique de l'habitat et change temporairement son usage. Ces activités impactent les communautés marines, en particulier les communautés benthiques (de Groot, 1986; van Dalssen et al., 2000). Enfin les communautés marines de mer du Nord subissent aussi un autre changement d'usage qui est l'artificialisation des estuaires, zones de nurseries pour de nombreuses espèces (Le Pape et al., 2007).

Dans la zone se trouve également l'un des couloirs de circulation maritime les plus importants au monde, ce qui peut entraîner des problèmes de collisions (ICES, 2018a) ou des problèmes de pollution sonore pour les mammifères marins notamment (Hildebrand, 2009; Middel and Verones, 2017).

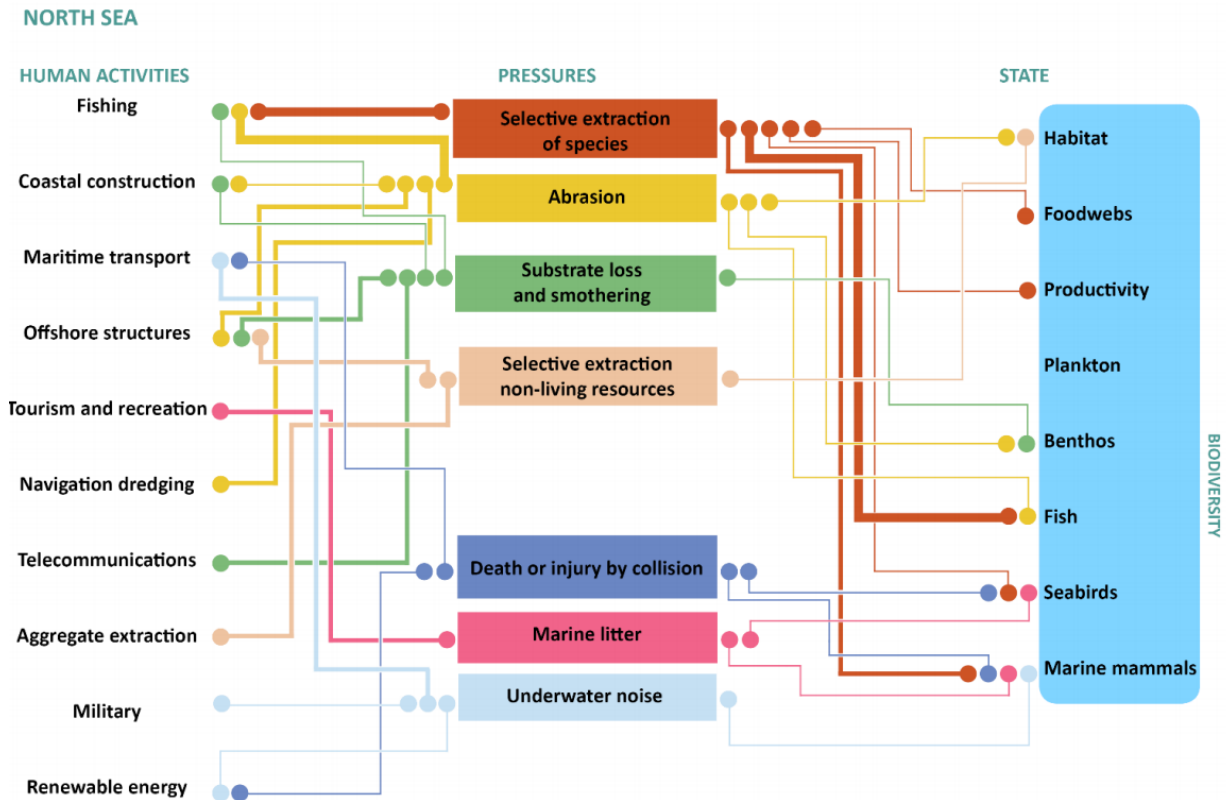


Figure 6 : Aperçu de l'écorégion mer du Nord avec les principales pressions régionales, les activités humaines et l'état de l'écosystème. La largeur des lignes indique l'importance relative des liens entre la pression et l'activité humaine ou avec la biodiversité (selon ICES, 2018).

1.5.2.3 Conséquences d'activités humaines hors zone qui impactent la biodiversité de la mer du Nord

L'écosystème mer du Nord subit également des conséquences indirectes d'activités humaines comme la pollution issue d'activités terrestres (par exemple plastique (Rummel, 2014) ou métaux (Kakuschke and Prange, 2007; Van Alsenoy et al., 1993)), l'invasion d'espèces (hors déplacements climatiques, Reise et al., 1998), l'eutrophisation côtière en lien avec les rejets agricoles (Boesch and Brinsfield, 2000) et le changement climatique.

Les changements physiques ou biogéochimiques liés au changement climatique en mer du Nord ont déjà impacté la biodiversité notamment sur les cinquante dernières années et vont encore l'impacter dans un future proche (voir la partie suivante sur les changements de communauté). La mer du Nord est considérée comme l'un des points chauds du réchauffement sur la période récente (Hobday and Pecl, 2014) avec un réchauffement particulièrement rapide sur les 30 dernières années : sa

température de surface a augmenté de 1.3°C sur cette période (Sherman et al., 2009). Les prédictions anticipent un réchauffement additionnel de 1.8°C dans les cinquante ans à venir (Rutterford et al., 2015). Les projections futures prévoient également une accentuation de la désoxygénation de la mer du Nord principalement à horizon 2100, notamment dans la zone sud-est qui présente déjà les concentrations en oxygène les plus faibles (Wakelin et al., 2020). Une zone anoxique est projetée comme étant présente jusqu'à 4 mois par an à l'est de la zone en 2100 contre 1 mois actuellement (Wakelin et al., 2020). Les projections futures de production primaire montrent des changements contrastés avec une augmentation de la production primaire à l'est de la zone et en Manche (principalement de 25% et parfois jusqu'à 75% d'augmentation) et une diminution de l'ordre de 25 à 50% dans l'ouest et dans le centre de la mer du Nord à horizon 2100 (Wakelin et al., 2020).

1.5.3 Fonctionnement des communautés de mer du Nord : travaux d'étude des communautés et de modélisation

La communauté ichthyologique de mer du Nord a été étudiée à travers des approches de traits fonctionnels, de modèles plurispécifiques et de modèles écosystémiques. Il n'existe actuellement pas de travaux qui étudient cette communauté comme une communauté en évolution (au sens de Darwin) : les études traitant de l'évolution des traits d'histoire de vie en mer du Nord sont des études mono-spécifiques. Cette partie a pour but d'exposer les principales études de changements des communautés passés chez les poissons, des changements évolutifs passés ainsi que les travaux de modélisation existants.

1.5.3.1 Changements de communauté passés

En réponse aux pressions de pêche et climatique, la communauté de mer du Nord est impactée aux trois niveaux d'organisation de la biodiversité : spécifique (Dencker et al., 2017; McLean et al., 2019c), fonctionnel (Beukhof et al., 2019; Dencker et al., 2017; McLean et al., 2019c; Murgier et al., 2021), et génétique (Marty et al., 2015).

Le changement climatique a entraîné en mer du Nord un changement de distribution des espèces vers le nord et en profondeur (Dulvy et al., 2008; Perry et al., 2005), avec un différentiel entre des espèces à cycle de vie court dont la distribution se déplace plus vite vers le nord que pour les autres. Les changements environnementaux ont également entraîné des changements de structure de l'écosystème (Beaugrand, 2004; Heath, 2012) avec un impact *bottom-up* important des changements planctoniques sur les communautés pélagique et démersale comme par exemple sur la morue (Beaugrand et al., 2003). Le réchauffement entraîne des changements d'espèces mais les traits fonctionnels des espèces favorisées par le réchauffement convergent vers des espèces à stratégie r, c'est-à-dire ayant un cycle de vie rapide (McLean et al., 2018b, 2018a, 2019c).

La pêche impacte également les communautés en favorisant des espèces à cycle de vie court (Jennings et al., 1999). Une diminution récente de la pression de pêche a été associée à une ré-augmentation des espèces rares fonctionnellement. Dans le cas de la mer du Nord, ce sont des espèces à stratégie K avec un cycle de vie plus long (Murgier et al., 2021).

1.5.3.2 Changements plastiques et évolutifs des traits

Le réchauffement des eaux en mer du Nord entraîne aussi des changements au niveau des traits à l'échelle intra spécifique en lien avec des réponses plastiques et des réponses évolutives.

Des études mettent en lumière des réponses physiologiques à la température variables spatialement (Harrald et al., 2010; Teal et al., 2012) impliquant un possible changement de trait avec la température. Des diminutions de taille synchrones pour plusieurs espèces ont été associées à une augmentation de la température (Baudron et al., 2014). Des changements de traits évolutifs induits par le changement climatique n'ont actuellement pas été reportés en mer du Nord, mais on estime que leurs conséquences seront similaires à la pêche c'est-à-dire une accélération du cycle de vie (Waples and Audzijonyte, 2016).

Des réponses plastiques à la pêche n'ont pas été particulièrement étudiées en mer du Nord à ma connaissance bien qu'étant une réponse à la pêche décrite de façon plus générale (voir partie

1.3.1.2). La réponse évolutive en réponse à la pêche a été étudiée chez de nombreuses espèces de mer du Nord, notamment les espèces démersales et benthiques, ainsi que chez le hareng de mer du Nord (Figure 7) (Enberg and Heino, 2007). Au niveau intra-populationnel, la pêche induit des cycles de vie plus courts (maturation plus rapide et plus d'allocation à la croissance juvénile et à la reproduction), avec des réponses plus marquées chez les espèces à cycle de vie long (morue ou aiglefin par exemple) que celles à cycle de vie plus court (hareng ou tacaud norvégien). Il est intéressant de constater que la pêche entraîne à la fois une sélection des espèces à cycle de vie court et induit en plus un cycle de vie plus court pour toutes les espèces.

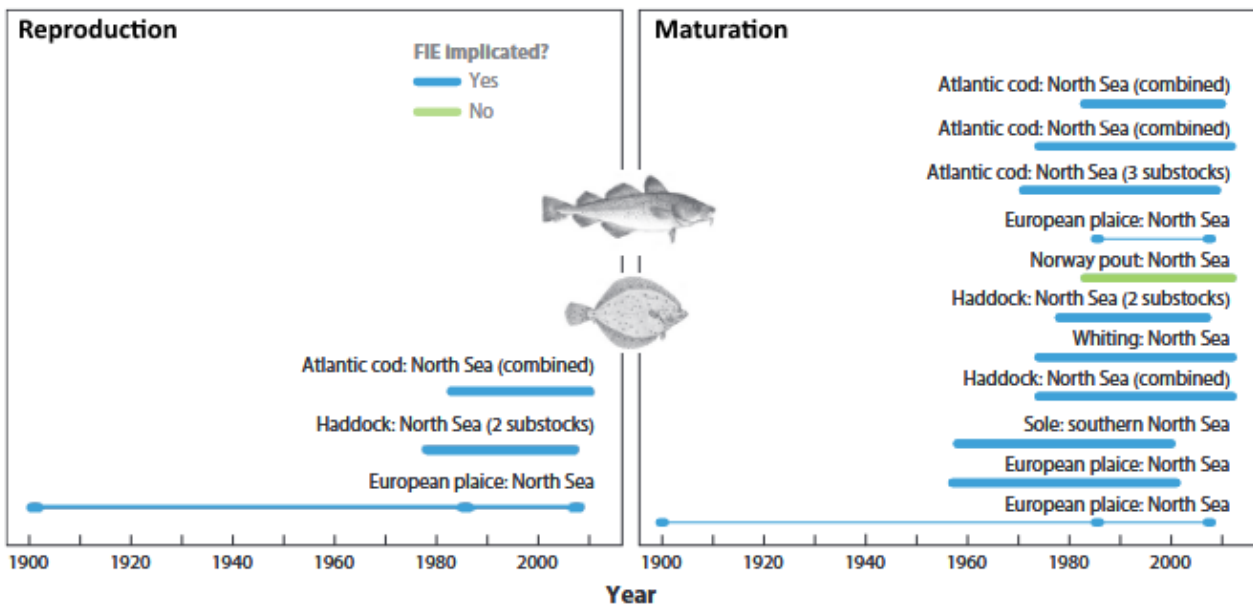


Figure 7 : Périodes sur lesquelles une évolution induite par la pêche (FIE sur la figure pour Fisheries induced evolution) a été mise en évidence par différentes études pour les stocks de mer du Nord. Figure adaptée de Heino et al. (2015) classant les études par traits pour la mer du Nord uniquement (reproduction : morue (Yoneda and Wright, 2004), aiglefin (Wright et al., 2011a), plie (Rijnsdorp et al., 2005) ; maturation : morue (Marty et al., 2014; Neuheimer and GrønkJær, 2012; Wright et al., 2011b) , plie (Grift et al., 2003; van Walraven et al., 2010), tacaud norvégien (Marty et al., 2014), aiglefin (Marty et al., 2014; Wright et al., 2011a), merlan (Marty et al., 2014), sole (Mollet et al., 2007)).

1.5.3.3 Modèles écosystémiques

Le réseau trophique de la mer du Nord a été intensivement étudié et modélisé, en considérant l'ensemble de l'écosystème (Blanchard et al., 2014; Cormon et al., 2016; Heath, 2012; Lewy, 2004,

2004; Mackinson and Daskalov, 2007; van de Wolfshaar et al., 2021) ou une partie (Manche-Est inclus) (Girardin et al., 2018; Stäbler et al., 2016; Travers-Trolet et al., 2019).

Ces travaux visaient en partie à décrire les espèces principales, la structure trophique et le fonctionnement actuel de l'écosystème (Girardin et al., 2018; Mackinson and Daskalov, 2007; Travers-Trolet et al., 2019). Certains modèles étudient l'impact de différents scénarios de pêche sur la zone d'étude (Blanchard et al., 2014) ou l'effet de scénarios de changements climatiques sur la pêche (Travers-Trolet et al., 2020). Actuellement ces modèles écosystémiques régionaux incluant le compartiment ichthyologique n'ont pas été utilisés pour faire des prédictions futures de biodiversité (comme par exemple celle existante en méditerranée (Moullec et al., 2019)).

1.6 Objectifs et structure de la thèse

La variabilité phénotypique des traits d'histoire de vie sera le fil conducteur de cette thèse. Cette variabilité phénotypique observée à l'échelle de la population est le reflet de la plasticité phénotypique en réponse au macro-environnement (environnement général de vie d'un organisme à grande échelle), la variabilité phénotypique interindividuelle liée au microenvironnement (environnement immédiat de l'organisme à petite échelle) ou la variabilité des traits émergeant de la variabilité génotypique sous-jacente.

L'objectif principal de cette thèse est d'étudier les **variations plastiques** et **évolutives** des **traits d'histoire de vie** d'organismes marins et leurs conséquences écosystémiques en réponse à trois facteurs de changements principaux : (i) l'environnement **abiotique**, (ii) l'environnement **biotique**, c'est-à-dire les variations en proies, compétiteurs et prédateurs, et (iii) à la **pêche**. La réalisation de ce premier objectif nécessite l'atteinte d'un objectif méthodologique en amont : le **développement d'un modèle écosystémique marin qui est individu-centré, éco-évolutif et multispécifique** et qui inclut la **variabilité phénotypique** issue de la **physiologie** et du **génotype**.

Cette thèse se découpe en six chapitres, dont les chapitres d'introduction et de discussion générale qui sont respectivement les chapitres 1 et 6 de cette thèse. Ces quatre autres chapitres sont rédigés sous format d'article scientifique et écrit en anglais.

- **Chapitre 2** : *Bioen-OSMOSE: A bioenergetic marine ecosystem model with physiological response to temperature and oxygen*

Le développement dans OSMOSE d'un nouveau module **bioénergétique**, décrivant mécaniquement l'émergence des traits d'histoire de vie avec des réponses **physiologiques à la température et à l'oxygène** est la première étape de développement du modèle réalisé durant cette thèse. Le modèle OSMOSE incluant ce nouveau développement a été appelé **Bioen-OSMOSE**. Il est décrit dans le chapitre 2.

Ce chapitre vise à présenter les équations du modèle Bioen-OSMOSE, les méthodes de paramétrisation du module bioénergétique, son application à la mer du Nord, sa validation sur des données observées et les variations physiologiques spatiales obtenues pour quelques espèces de mer du Nord.

- **Chapitre 3**: *Are fundamental thermal performance curves a good indicator of realized ones? A first answer with an individual-based bioenergetics marine food web model applied to the North Sea ecosystem*

Dans le chapitre 3, Bioen-OSMOSE appliqué à la mer du Nord est utilisé pour explorer comment la **variabilité** de la **température**, de **l'oxygène** et de la **nourriture** font varier **l'acquisition d'énergie nette**. Cette question est étudiée par une approche originale de comparaison de niche thermique fondamentale et réalisée. La variation d'énergie nette correspond au mécanisme **physiologique sous-jacent** à la **variation plastique** des traits d'histoire de vie.

- **Chapitre 4** : *Ev-OSMOSE: An eco-genetic marine ecosystem model*

Le développement d'un module **génétique** au sein du modèle Bioen-OSMOSE permet d'ajouter la **variabilité génétique** et les **dynamiques évolutives** des traits d'histoire de vie dans un modèle d'écosystème marin. Le modèle **éco-évolutif** résultant est nommé **Ev-OSMOSE** et est présenté au chapitre 4.

Ce chapitre vise à présenter les équations du modèle Ev-OSMOSE, les méthodes de paramétrisation du module génétique, son application à la mer du Nord, et sa validation sur des données observées et les attendus évolutifs théoriques.

- **Chapitre 5: Fisheries induced evolution in an evolving community**

Dans ce chapitre, le modèle Ev-OSMOSE est appliqué à la mer du Nord pour étudier l'impact de l'**évolution** induite par la pêche sur **les traits d'histoire de vie d'espèces qui évoluent et qui interagissent**, et les conséquences écologiques sur la **communauté**.

L'apport de ces travaux de thèse à la littérature existante sera discuté enfin dans un dernier chapitre de discussion générale. Cette partie sera l'occasion de proposer des travaux futurs qui pourraient être réalisés à la suite de cette thèse à court et à moyen terme. Elle sera aussi l'occasion de discuter de l'avancée des compréhensions mécanistes de la plasticité des traits d'histoires de vie et de leur inclusion potentielle dans des modèles éco-évolutifs. Enfin, comme chaque travail de recherche soulève toujours de nouvelles questions, ces dernières seront discutées en ouverture de la discussion.

Chapter 2: Bioen-OSMOSE: A bioenergetic marine ecosystem model with physiological response to temperature and oxygen

Alaia Morell, Yunne-Jai Shin, Nicolas Barrier, Morgane Travers-Trolet, Ghassen Halouani, Bruno Ernande

ABSTRACT

Marine ecosystem models have been used to project the impacts of climate-induced changes in temperature and oxygen on biodiversity mainly through changes in species spatial distributions and primary production. However, fish populations may also respond to climatic pressures via physiological changes, leading to modifications in their life history that could either mitigate or worsen the consequences of climate change.

Building on the individual-based multispecies ecosystem model OSMOSE, Bioen-OSMOSE has been developed to account for high trophic levels' physiological responses to temperature and oxygen in future climate projections. This paper presents an overview of the Bioen-OSMOSE model, mainly detailing the new developments. These consist in the implementation of a bioenergetic sub-model that mechanistically describes somatic growth, sexual maturation and reproduction as they emerge from the energy fluxes sustained by food intake under the hypotheses of a biphasic growth model and plastic maturation age and size represented by a maturation reaction norm. These fluxes depend on temperature and oxygen concentration, thus allowing plastic physiological responses to climate change.

To illustrate the capabilities of Bioen-OSMOSE to represent realistic ecosystem dynamics, the model is applied to the North Sea ecosystem. The model outputs are confronted with population biomass, catch, maturity ogive, mean size-at-age and diet data of each species of the fish community. A first

exploration of current species spatial variability in response to temperature or oxygen is presented in this paper. The model succeeds in reproducing observations, with good performances for all indicators.

This new model development opens the scope for new fields of research such as the exploration of seasonal or spatial variation in life history in response to biotic and abiotic factors at the individual, population and community levels. Understanding such variability is crucial to improve our knowledge on potential climate change impacts on marine ecosystems and to make more reliable projections under climate change scenarios.

2.1 Introduction

The development of increasingly realistic marine ecosystem models (MEMs) is needed to improve understanding and knowledge about marine ecosystems, which is one of the main challenges of the UN Decade of the Oceans (Heymans et al., 2020). MEMs are end-to-end models representing ecosystems from primary production to top predators, linking the species and/or functional groups via trophic interactions. These models also account for abiotic and human activity impacts on ecosystem dynamics (Rose et al., 2010; Steenbeek et al., 2021; Travers et al., 2007). MEMs are still being improved through the development of sub-models that increase their reliability in supporting ecosystem-based management (Pikitch et al., 2004; Rose et al., 2010).

The rates of ocean temperature rise and deoxygenation make urgent the development of mechanistic tools to forecast realistically their impacts from the physiology of marine organisms, to the population demographic impacts and to the consequence on marine trophic webs (Breitburg et al., 2018; Urban et al., 2016). Efforts to model the temperature impacts on marine biodiversity at the ecosystem level has so far focused mainly on the bottom-up effect of temperature on the ecosystem via changes in primary production (Lefort et al., 2015; Moullec et al., 2019) and on the distribution shift of species according to their preferred temperature (Albouy et al., 2014; Fernandes et al., 2013; Moullec et al., 2019; Serpetti et al., 2017). Mechanistic physiological response to temperature in

MEM is modeled in size spectrum models and to our knowledge is not currently incorporated into an explicit multispecies model (Lefort et al., 2015; Maury, 2010). Although oxygen concentration is considered as a main pressure on marine biodiversity (Laffoley & Baxter, 2019), the oxygen physiological impact on marine ecosystems is still not explicitly modeled in MEMs.

The core of recent model developments linking environmental conditions and physiological response is primarily on single-species models. These frameworks mechanistically describe life history cycles and metabolic fluxes. The response of metabolic rates to temperature is used in several frameworks (Gillooly et al., 2002; Kooijman, 2010) which are applied to project future population dynamics and spatial distribution under climate change scenarios. The response of metabolic rates to oxygen through its impact on ingestion (Thomas et al., 2019) has been recently introduced in the Dynamic Energy Budget framework to study the impact of hypoxia on population dynamics (Lavaud et al., 2019).

The model Bioen-OSMOSE is a new framework that mechanistically describes the emergence of life history traits through an explicit description of the underlying bioenergetic fluxes and their response to food, temperature and oxygen variation in a multispecies food web model. It has been developed from the OSMOSE framework (Shin & Cury, 2004; www.osmose-model.org), which is an individual-based, spatially and temporally explicit, multispecies model for regional marine ecosystems. Designed to be possibly coupled to ocean and biogeochemical models, it includes the components of the entire ecosystem, from primary production to fish populations and human fishing activity, but the core of the model describes the dynamics of fish and macroinvertebrate species. In this paper, we provide a detailed description of the principles and equations of the Bioen-OSMOSE framework, as well as parameterization guidelines (detailed in Supporting Information). An application to the North Sea ecosystem is provided as a case study example. We then confront simulation outputs from the North Sea example to observed data to assess the consistency of the new model development and explore spatial variability in fish metabolic fluxes in response to temperature and oxygen.

2.2 Method

2.2.1 Model description

The Bioen-OSMOSE model (Figure 8) represents fish individual physiological responses to temperature and oxygen variations and their consequences on fish communities in marine ecosystems. It is an individual-based, spatially and temporally explicit multispecies model accounting for trophic interactions. The main characteristics of the model are opportunistic predation based on size adequacy and spatiotemporal co-occurrence of predators and prey, the mechanistic description of individuals' life-history traits emerging from bioenergetics. The aims of the model are to explore the functioning of marine trophic webs, the ecosystem impacts of individual physiological modifications due to temperature and oxygen, and the consequences of fishing pressure or climate change, from individual phenotype, to the population and to the community scale. The Bioen-OSMOSE model extends the existing OSMOSE model by (i) explicitly accounting for the mechanistic dependence of life-history traits on bioenergetics and (ii) describing intra- and inter-specific phenotypic variability originating from plastic responses to spatio-temporal biotic and abiotic factor variations. A process overview is given in Supporting Information S1.

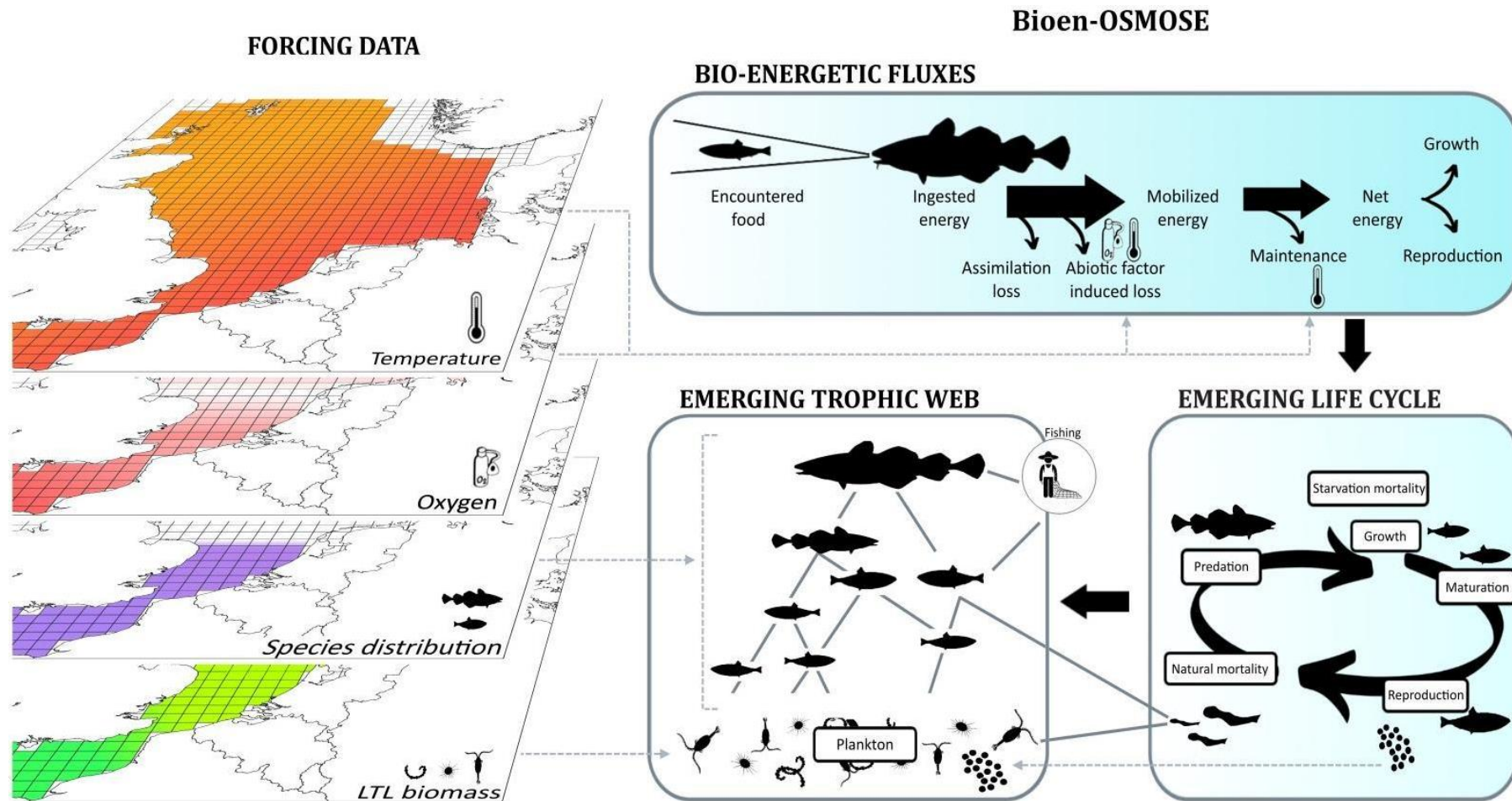


Figure 8: Graphical description of the Bioen-OSMOSE model. In the Bioen-OSMOSE model trophic relationships emerge from spatio-temporal co-occurrence and size adequacy between predators and prey, the former resulting from ontogenic spatial distributions and possibly LTL biomass distribution. The life cycle emerges from the underlying bioenergetic fluxes that describe the internal processes from energy ingestion (which relies on the encountered prey) to growth, maturation and reproduction. The internal fluxes are partly driven by environmental conditions, i.e, temperature and oxygen.

2.2.1.1 Biological unit, state variables and spatial characteristics

The biological unit of the model is a school (a super-individual in individual-based modeling terminology). It is formed by individuals from the same species that are biologically identical. The state variables characterizing a school i at time step t belong to four categories (see Table 1 for state variable definitions and their units):

- Ontogenic state of individuals described by their age $a(i, t)$, somatic mass $w(i, t)$ and gonadic mass $g(i, t)$;
- Abundance, namely the number of individuals in the school $N(i, t)$;
- Spatial location, i.e., the grid cell $c(i, t)$ where the school is located; and
- Taxonomic identity, i.e., the species $s(i)$ to which the school belongs.

Fish schools are distributed on a horizontal spatial grid that is composed of regular cells and that covers the geographical range of the ecosystem represented. A cell c is characterized by its spatial coordinates, longitude $x(c)$ and latitude $y(c)$, and several other variables: (i) the vertically-distributed values (z vertical layers) of k physico-chemical factors $pc_k(c, t, z)$ (such as temperature $T(c, t, z)$ or the level of oxygen saturation (%) $[O_2](c, t, z)$) and (ii) the biomass of all low trophic level (LTL) groups (indexed by j) $B_{LTL}(c, j, t)$ that are not explicitly modeled in Bioen-OSMOSE but provided as input from coupled hydrodynamic and biogeochemical models.

Below we describe the bioenergetic sub-model that we developed to describe individual life-history and its responses to environmental variations. The individuals described with this level of detail belong to high trophic level (HTL) species, mainly fish and macroinvertebrate species.

2.2.1.2 Individual life history description

Individual life history emerges from underlying bioenergetic fluxes which are described according to a biphasic growth model (Andersen, 2019; Boukal et al., 2014; Quince et al., 2008). The body mass-dependent energy fluxes are allocated according to physiological tradeoffs between competing

processes: maintenance, somatic growth and gonadic growth. The sexual maturation of individuals relies on the concept of maturation reaction norms that depicts how the process of maturation responds plastically to variation in body growth (Heino et al., 2002; Stearns & Koella, 1986). This combination of processes mechanistically describes how somatic growth, sexual maturation and reproduction emerge from energy fluxes sustained by food intake resulting from opportunistic size-based predator-prey interactions.

On top of the biphasic growth model, individuals' energy mobilization and maintenance energetic costs depend on dissolved oxygen concentration and temperature so that the resulting metabolic rate (the net energy available for new tissue production) and thus somatic and gonadic growth vary with these abiotic parameters in a way that conforms to the oxygen- and capacity-limited thermal tolerance theory (OCLTT; Pörtner, 2001) and more generally to thermal performance curves (TPC; Angilletta, 2009).

In the following description, energetic fluxes are expressed in somatic mass unit equivalents under the assumption that the ratio of energy density between somatic and gonadic tissues η is independent of size. All the parameters of the bioenergetic and life-history sub-model are species-specific parameters except one parameter is constant across species, namely the Boltzmann constant (Table 2).

2.2.1.2.1 Ingestion, assimilation and mobilization

For an individual in school i , the ingested food $I(i, t)$ at time step t is described by a Holling's type 1 functional response (Holling, 1959) that depends on its somatic mass $w(i, t)$ (Christensen & Walters, 2004; Holt & Jorgensen, 2014; Shin & Cury, 2004) in two ways. First, it determines the prey biomass $P(i, t)$ available to an individual of school i . All other fish schools and LTL organisms (from the forcing biogeochemical model) that are present in the same grid cell $c(i, t)$ are potential prey if their body size is compatible with a minimum R_{min} (Shin & Cury, 2004) and a maximum R_{max} predator to prey size ratio based on individual total length $L(i, t) = \left(\frac{w(i, t)}{k}\right)^{\frac{1}{\alpha}}$ (Travers et al., 2009) so that:

$$P(i, t) = \frac{\sum_j \gamma(i, j) B(j, t)}{N(i, t)}$$

$$\text{with } j \in \left\{ j \mid (c(j, t) = c(i, t)) \cap \left(\frac{L(i, t)}{R_{max}} \leq L(j, t) \leq \frac{L(i, t)}{R_{min}} \right) \right\} \quad (1)$$

where k and α are the allometric length-somatic mass relationship coefficient and exponent, respectively, $\gamma(i, j)$ is the accessibility coefficient of potential prey school j to school i that is essentially determined by the position in the water column of species $s(j)$ relative to species $s(i)$ according to their life stage, and $B(j, t) = N(j, t) w(j, t)$ is the biomass of prey school j at time step t . The maximum possible food ingestion rate scales with the mass with a scaling exponent β . The ingested food can then be written as:

$$I(i, t) = f(P(i, t)) = \min(P(i, t); I_{max} \psi(i, t) w(i, t)^\beta) \quad (2)$$

with I_{max} the maximum ingestion rate per mass unit at exponent β (or mass-specific maximum ingestion rate) of individuals in school i and $\psi(i, t)$ a multiplicative factor that depends on their life stage such that:

$$\psi(i, t) = \begin{cases} \theta & \text{if } a(i, t) < a_l \\ 1 & \text{otherwise} \end{cases} \quad (3)$$

where a_l is the age at the end of an early-life fast-growth period (e.g., larval period or the larval and post-larval period, defined according to data availability, see Supporting Information S2) and θ a multiplicative factor accounting for higher mass-specific ingestion rate at this stage. A portion ξ of the ingested food $I(i, t)$ is assimilated, $(1 - \xi)$ being lost due to excretion and feces egestion.

Reserves are not modeled in Bioen-OSMOSE: the assimilated energy is directly mobilized. The difference between assimilated and mobilized energy depends on oxygen and temperature conditions (Figure 9). Mobilized energy E_M , referred to as active metabolic rate in the ecophysiology literature, fuels all metabolic processes such as maintenance, digestion, foraging, somatic growth, gonadic growth, etc... The mobilization of energy relies on the use of oxygen to transform the energy held in the chemical bonds of nutrients into a usable form, namely ATP (Clarke, 2019). In

consequence, the maximum possible energy mobilized depends (i) directly on dissolved oxygen saturation that sets up an upper limit to mobilization at a given temperature and (ii) as temperature increases, on the capacity of individuals to sustain oxygen uptake and delivery for ATP production.

The mobilized energy rate E_M is thus described by:

$$E_M(i, t) = \xi I(i, t) \lambda([O_2](i, t)) \varphi_M(T(i, t)) \quad (4)$$

with $\lambda([O_2](i, t))$ and $\varphi_M(T(i, t))$ being the mobilization responses to dissolved oxygen saturation $[O_2](i, t) = [O_2](c(i, t))$ and temperature $T(i, t) = T(c(i, t))$, respectively, encountered by school i in the grid cell $c(i, t)$. These are scaled between 0 and 1 such that, in optimal oxygen saturation and temperature conditions, all assimilated energy $E_M(i, t) = \xi I(i, t)$ can be mobilized and, in suboptimal conditions, only a fraction of assimilated energy can be mobilized $E_M(i, t) < \xi I(i, t)$.

More precisely, the effect of dissolved oxygen is described by a dose-response function $\lambda(\cdot)$ (Thomas et al., 2019) which increases with the saturation of dissolved oxygen:

$$\lambda([O_2]) = c_{O,1} \frac{[O_2]}{[O_2] + c_{O,2}} \quad (5)$$

with parameters $c_{O,1}$ and $c_{O,2}$ the asymptote and the slope of the dose-response function. The effect of temperature $\varphi_M(\cdot)$ is such that first, energy mobilization increases with temperature according to an Arrhenius-like law due to chemical reaction rate acceleration until reaching limitation in individuals' ventilation and circulation capacity. Hence, oxygen uptake and delivery for energy mobilization saturates or even decreases at high temperatures, potentially due to temperature dependence of the rate of enzyme-catalyzed chemical reactions (Arcus et al., 2016) or enzyme denaturation (Pawar et al., 2015). This effect is described according to the Johnson & Lewin (1946) model (Pawar et al., 2015):

$$\varphi_M(T) = \Phi \frac{e^{-\frac{\varepsilon_M}{k_B T}}}{1 + \frac{\varepsilon_M}{\varepsilon_D - \varepsilon_M} e^{-\frac{\varepsilon_D}{k_B} (\frac{1}{T_p} - \frac{1}{T})}} \quad (6)$$

with k_B the Boltzmann constant, ε_M the activation energy for the Arrhenius-like increase in mobilized energy with temperature T before reaching its peak value at T_p , ε_D the activation energy when the

energy mobilization declines with T above T_p , and $\Phi = \left(1 + \frac{\varepsilon_M}{\varepsilon_D - \varepsilon_M}\right) e^{\frac{\varepsilon_M}{k_B T_p}}$ a standardizing constant ensuring that $\varphi_M(T_p) = 1$.

2.2.1.2.2 Maintenance

The mobilized energy E_M fuels all metabolic processes starting in priority with the costs of maintenance of existing tissues E_m which is often referred to as the standard metabolic rate in the ecophysiology literature. Here, we also include in the maintenance costs, the routine activities of individuals, including foraging and digestion, so that they are actually best compared to the routine metabolic rate in the ecophysiology literature. The maintenance costs are explicitly modeled to describe the share of mobilized energy between maintenance and the production of new tissues (Charnov et al., 2001; Holt & Jorgensen, 2014), with precedence of the former over the latter, as well as to link mechanistically starvation mortality to energetic starvation when neither mobilized energy nor gonad energy reserves can cover the costs of maintenance (see next section on new tissue production for more details). The maintenance energy rate E_m scales with the individual's somatic mass $w(i, t)$ with the same exponent β as the maximum ingestion rate. The maintenance rate also increases with the temperature $T(i, t)$ experienced by individuals according to the Arrhenius law (Brown et al., 2004; Gillooly et al., 2002; Kooijman, 2010) and can be described as:

$$E_m(i, t) = c_m w(i, t)^\beta \varphi_m(T(i, t)) \quad (7)$$

with C_m the mass-specific maintenance rate and $\varphi_m(\cdot)$ the Arrhenius function m defined as:

$$\varphi_m(T) = e^{-\frac{\varepsilon_m}{k_B T}} \quad (8)$$

with ε_m the activation energy for the increase of the maintenance rate with temperature.

2.2.1.2.3 Net energy available for new tissue production

The net energy available for new tissues production E_p is the difference between the mobilized energy E_M and the maintenance costs E_m defined as follows:

$$E_p(i, t) = E_M(i, t) - E_m(i, t) \quad (9)$$

Given that the mobilized energy rate E_M increases at a lower rate than the maintenance rate E_m close to the species preferred temperature, it results that, all other things being equal, the emerging relationship between the net energy rate E_P (and thus somatic and gonadic growth, see next section) and temperature is dome-shaped and conforms to the OCLTT theory and the principle of TPC (red curve in Figure 9).

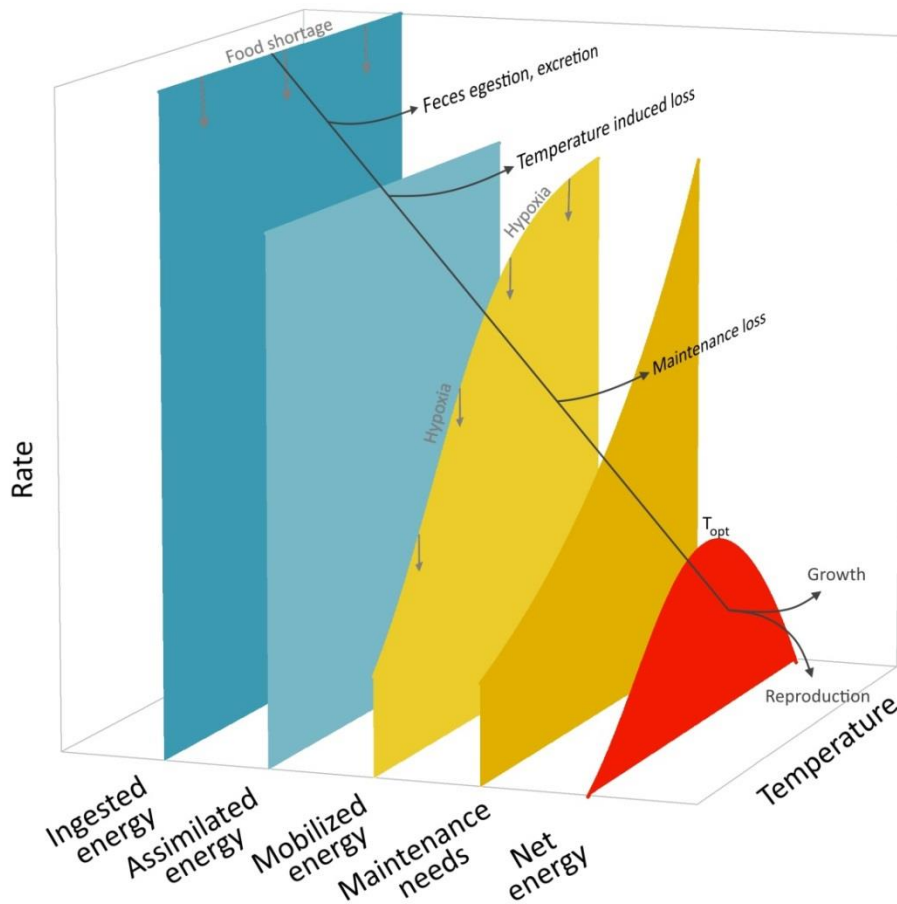


Figure 9: Thermal responses of the bioenergetic fluxes from ingestion to tissue growth in Bioen-OSMOSE. The net energy rate dome-shaped curve (in red) conforms to the OCLTT theory and the principle of TPC. Food shortage impacts ingested energy and downstream fluxes. Hypoxia impacts mobilized energy and downstream fluxes. The maximum of the net energy rate (red curve) is called T_{opt} hereafter.

2.2.1.2.4 New tissue production: somatic and gonadic growth

The net energy E_P contributes to the production of new tissues with a proportion ρ being allocated to the gonadic compartment $g(i, t)$ and a proportion $(1 - \rho)$ to the somatic one $w(i, t)$. This proportion depends on the sexual maturity status $m(i, t)$ of the schools' individuals and their somatic mass $w(i, t)$. Before sexual maturation, i.e., when the maturity status $m(i, t) = 0$, ρ is equal

to 0 and, after maturation, i.e., when $m(i, t) = 1$, ρ is determined such that the annual mean gonado-somatic index of individuals $\frac{g(i, t)}{w(i, t)}$ is constant throughout their adult life-stage and equal to r

(Boukal et al., 2014; Lester et al., 2004; Quince et al., 2008):

$$\rho(i, t) = m(i, t) \frac{r}{\eta \overline{E_P}(i)} w(i, t) \quad (10)$$

where, η is the ratio of energy density between somatic and gonadic tissues,

$$\overline{E_P}(i) = \frac{\Delta t}{a(i, t)} \sum_{t'=0}^{t'=a(i, t)/\Delta t} E_P(i, t')$$

is the average net energy available per time step to individuals of school i since their birth, with Δt being the duration of a time step. Eq. 10 differs from a deterministic continuous time version of the same model (Boukal et al., 2014; Lester et al., 2004; Quince et al., 2008) where the current net energy $E_P(i, t)$ would be used instead of the average $\overline{E_P}(i)$. The averaging in a stochastic discrete time individual-based model such as Bioen-OSMOSE ensures a smooth increase of the proportion ρ as individuals grow by dampening strong variations in $E_P(i, t)$ and thus in $\rho(i, t)$ due to the stochasticity of prey encounters and hence of the ingested energy $I(i, t)$.

According to the definition of ρ , all net energy E_P is allocated to somatic growth before maturation and it is shared between somatic and gonadic growth after, with the proportion ρ allocated to gonads increasing with somatic mass (Boukal et al., 2014), which limits somatic growth as individuals become bigger. In case the mobilized energy E_M cannot cover the maintenance costs E_m , i.e., when $E_P < 0$, new tissue production is not possible and the gonadic compartment $g(i, t)$ is resorbed to provide energy for sustaining maintenance. Somatic growth is then defined as follows:

$$\frac{dw}{dt}(i, t) = \begin{cases} (1 - \rho(i, t)) E_P(i, t) & \text{if } E_P(i, t) \geq 0 \\ 0 & \text{otherwise} \end{cases} \quad (11)$$

and gonadic growth as:

$$\frac{dg}{dt}(i, t) = \begin{cases} \eta \rho(i, t) E_P(i, t) & \text{if } E_P(i, t) \geq 0 \\ \eta E_P(i, t) & \text{if } -g(i, t) \leq \eta E_P(i, t) < 0 \\ -g(i, t) & \text{if } \eta E_P(i, t) < -g(i, t) < 0 \end{cases} \quad (12)$$

where the second and third conditional formulas account for maintenance coverage by energy reserves contained in gonads. In the former case, gonads' energy can fully cover maintenance costs but in the latter it cannot, so that individuals undergo energetic starvation and incur additional starvation mortality (see Supporting Information S3).

2.2.1.2.5 Maturation

Age and size at maturation vary strongly between individuals due to phenotypic plasticity. This plasticity in maturation is modeled by a deterministic linear maturation reaction norm (LMRN) that represents all the age-length combinations at which an individual can become mature (Stearns, 1992; Stearns & Koella, 1986). In this framework, individuals become sexually mature when their growth trajectory in terms of body length intersects the LMRN. The maturity status $m(i, t)$ of individuals of school i at time step t is thus described as:

$$m(i, t) = \begin{cases} 0 & \text{if } L(i, t) < m_0 + m_1 a(i, t) \text{ (immature)} \\ 1 & \text{if } L(i, t) \geq m_0 + m_1 a(i, t) \text{ (mature)} \end{cases} \quad (13)$$

with m_0 and m_1 the intercept and slope of the LMRN, respectively.

2.2.1.2.6 Reproduction

Mature individuals spawn during the breeding season, then a gonad portion is used to release eggs, what is represented by a gonad portion released $sp(t')$ above 0. The sex-ratio is assumed to be 1:1 for all species and the number of eggs produced by school i at time t is defined as follows:

$$N_{eggs}(i, t) = sp \left(t \bmod \frac{365}{\Delta t} \right) N(i, t) \frac{g(i, t)}{2w_{egg}} \quad (14)$$

with $t \bmod \frac{365}{\Delta t}$ giving the time of the year at time step t for a time step size of Δt , and w_{egg} the mass of an egg.

At each time step t of the breeding season (i.e., t for which $sp \left(i, t \bmod \frac{365}{\Delta t} \right) > 0$), $n_{s(i)}$ new schools are produced by species $s(i)$, with the number of eggs, and thus individuals, per new school i' calculated as follows:

$$N(i', t) = \frac{\sum_{j|s(j)=s(i)} N_{eggs}(j, t)}{n_{s(i)}} \quad (15)$$

with $\sum_{j|s(j)=s(i)} N_{eggs}(j, t)$ the total number of eggs produced by schools of species $s(i)$ at time step t , age of offspring set to 0, $a(i', t) = 0$, their somatic mass to the mass of an egg, $w(i', t) = w_{egg}$, and their gonadic mass to 0, $g(i', t) = 0$. The new schools are released randomly depending on the specific larvae habitat map.

2.2.1.2.7 Mortality

At each time step, a school experiences several mortality sources. The total mortality of a school i is the sum of predation mortality caused by other schools, starvation mortality, fishing mortality, and additional mortalities (i.e. larval, senescence, diseases, and non-explicitly modeled predators). For a school i , the starvation mortality results from the encountered food, the environmental abiotic variables and its maintenance rate. If the mobilized energy E_M covers the maintenance costs E_m , there is no starvation. However, if the mobilized energy E_M is lower than the maintenance costs, the school i has an energetic deficit. In this case, the gonad $g(i, t)$ is used as a reserve. In case the gonad content does not cover the exceeding maintenance costs, the school i faces starvation mortality proportionally to the remaining energetic deficit. The equations and details about all mortality processes are in Supporting Information S3.

Table 1: Variables and functions of the bioenergetics and life-history sub-models. (Δt :time step duration)

Symbol	Description	Units	Equations
Entities: Fish schools			
Ontogenic state			
<i>State variables</i>			
$a(i, t)$	Age of school i 's individuals at time step t	y	3, 13
$w(i, t)$	Somatic mass of school i 's individuals at time step t	g	2, 7, 10,11
$g(i, t)$	Gonadic mass of school i 's individuals at time step t	g	12, 14
<i>Emerging individual variables</i>			
$L(i, t)$	Total length of school i 's individuals at time step t	cm	1,13
$m(i, t)$	Maturity state of school i 's individuals at time step t	–	10, 13
$a_m(i)$	Maturation age of school i 's individuals	y	
$w_m(i)$	Maturation somatic mass of school i 's individuals	g	
$L_m(i)$	Maturation length of school i 's individuals	cm	
$N_{eggs}(i, t)$	Total fecundity of school i at first time step t of the breeding season	#	14, 15
<i>Abundance: State variable</i>			
$N(i, t)$	Number of individuals in school i at time step t	#	1, 14,15
$B(i, t)$	Biomass of school i at time step t	g	1
<i>Spatial Location: State variable</i>			
$c(i, t)$	Grid cell of school i at time step t	–	1
<i>Taxonomic identity: State variable</i>			
$s(i)$	Species to which school i belongs	–	
Bioenergetics			
<i>Emerging individual variables</i>			
$P(i, t)$	Available prey biomass to an individual of school i at time step t	g	1, 2
$\psi(i, t)$	Life-stage dependent multiplicative factor of maximum mass-specific ingestion rate of school i at time step t	–	2, 3

$I(i, t)$	Ingestion rate of individuals in school i at time step t	g $\cdot \Delta t^{-1}$	2, 4
$E_M(i, t)$	Mobilized energy rate of individuals of school i at time step t	g $\cdot \Delta t^{-1}$	4, 9
$E_m(i, t)$	Maintenance cost rate of individuals of school i at time step t	g $\cdot \Delta t^{-1}$	7, 9
$E_p(i, t)$	Net energy available for new tissue production	g $\cdot \Delta t^{-1}$	9, 10, 11, 12
$\rho(i, t)$	Proportion of net energy allocated to gonadic growth	–	10, 11, 12
$\frac{dw}{dt}(i, t)$	Somatic growth rate	g $\cdot \Delta t^{-1}$	11
$\frac{dg}{dt}(i, t)$	Gonadic growth rate	g $\cdot \Delta t^{-1}$	12
<i>Functional responses</i>			
$f(P)$	Holling's type 1 functional response to prey biomass P	–	2
$\lambda([O_2])$	Dose-response function of energy mobilization to dissolved oxygen concentration $[O_2]$	–	4, 5
$\varphi_M(T)$	Response of energy mobilization to temperature T	–	4, 6
$\varphi_m(T)$	Response of maintenance rate to temperature T	–	7, 8
Spatial scales and units: grid cells			
Spatial coordinates: <i>State variables</i>			
$x(c)$	Longitude of grid cell c		
$y(c)$	Latitude of grid cell c		
Physico-chemical factors: <i>State variables</i>			
$pc_k(c, t, z)$	Value of physico-chemical factor k of grid cell c at time step t of layer z		
$T(c, t)$	Temperature of grid cell c at time step t	K	4, 6, 7, 8
$[O_2](c, t)$	Dissolved O_2 concentration of grid cell c at time step t	%	4, 5
Biomass of LTL: <i>State variables</i>			
$B_{LTL}(c, j, t)$	Biomass of <i>LTL</i> group j of grid cell c at time step t	g	

Table 2: Species- specific parameters of the bioenergetic and life-history sub-model. (Δt : time step duration). One parameter is constant across species, namely the Boltzmann constant ($k_B = 8.62 \cdot 10^{-5} \text{ eV} \cdot \text{K}^{-1}$).

Symbol	Description	Units	Equations	Source
Ingestion, assimilation and mobilization				
R_{min}, R_{max}	Minimum and maximum predator to prey size ratio	–	1	Literature
$\gamma(i, j)$	Accessibility coefficient of prey species $s(j)$ to predator species $s(i)$ according to life stage	–	1	Literature
I_{max}	Maximum mass-specific ingestion rate	$g \cdot g^{-\beta} \cdot \Delta t^{-1}$	2	Calibrated
β	Scaling exponent of maximum ingestion rate and maintenance rate with body mass	–	2, 7	Assumed
θ	Multiplicative factor of maximum mass-specific ingestion rate at larval stage	–	3	Estimated ¹
a_l	Age at the end of the fast growth period	y	3	Literature
ξ	Assimilation efficiency	–	4	Literature
$c_{O,1}$	Asymptote of energy mobilization dose-response function to dissolved oxygen saturation	–	5	Estimated ²
$c_{O,2}$	Slope of energy mobilization dose-response function to dissolved oxygen saturation	%	5	Estimated ²
ε_M	Increasing activation energy of the energy mobilization temperature function	eV	6	Estimated ³
ε_D	Declining activation energy of the energy mobilization temperature function	eV	6	Estimated ³
T_p	Temperature of peak value in energy mobilization	K	6	Estimated ³
Φ	Normalization constant of the energy mobilization temperature function	–	6	Estimated ³
Maintenance				
c_m	Mass-specific maintenance rate	$g \cdot \Delta t^{-1}$	7	Literature
ε_m	Activation energy of the maintenance temperature function	eV	8	Estimated ³
Maturation				
m_0	Intercept of the maturity reaction norm	cm	13	Estimated ¹
m_1	Slope of the maturity reaction norm	cm · y ⁻¹	13	Estimated ¹
New tissue production				
η	Energy density ratio between somatic and gonadic tissue	–	10, 12	Literature

k	Allometric length-somatic mass relationship coefficient	$g \cdot cm^{-\alpha}$		Estimated ⁴
α	Allometric length-somatic mass relationship exponent	–		Estimated ⁴
Reproduction				
r	Gonado-somatic index	–	10	Estimated ¹
w_{egg}	Egg mass	g		Estimated ⁵
$sp(t)$	Spawning seasonality expressed as a fraction of the gonad energy available at the time step t	–	14	Literature
$n_{s(i)}$	Number of new schools produced at each time step of the breeding season for the species s of school i	#	15	Arbitrary

¹ from Size Maturity Age Length Key (SMALK) data (see Supporting Information S2.1)

² from ecophysiological data (see Supporting Information S2.4)

³ from a combination of SMALK and thermal tolerance data (see Supporting Information S2.3)

⁴ from length-mass data

⁵ from fecundity data (see Supporting Information S2.5)

2.2.2 Application to the North Sea ecosystem: Bioen-OSMOSE-NS

2.2.2.1 Area and explicit species

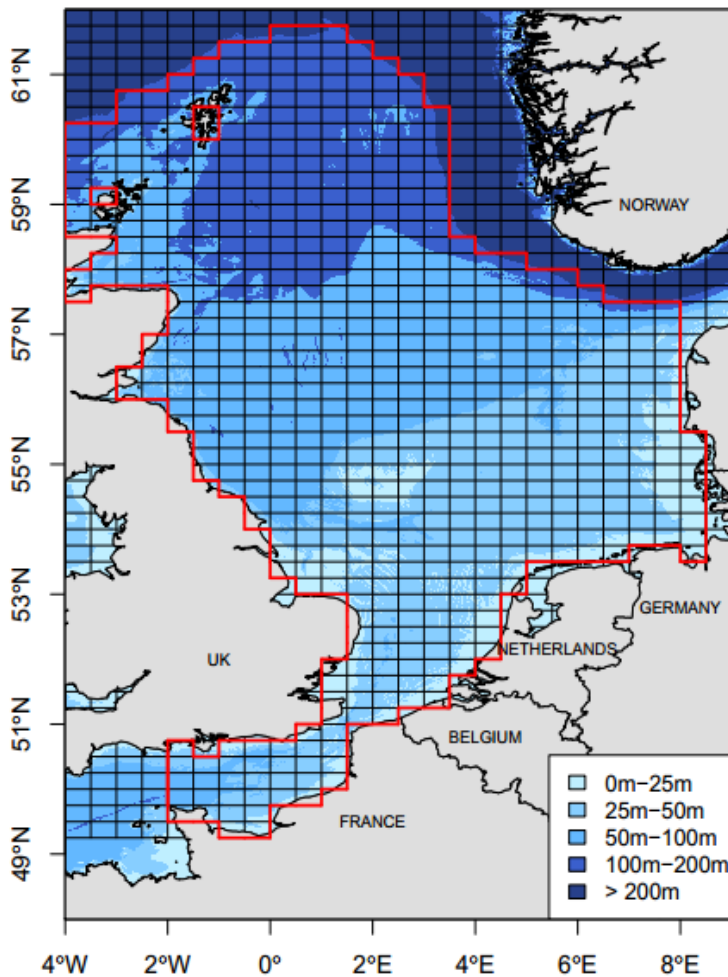


Figure 10: Case study area map. The Bioen-OSMOSE-NS area is delimited with the red line. The area is divided in 632 regular cells of 0.25° x 0.5° delimited with black lines.

The Bioen-OSMOSE-NS area includes the North Sea (ICES area 4) and the eastern English Channel (ICES area 7d), excluding the area deeper than 200m (notably the Norwegian Trench), and extends from 49° N to 62° N and from 4° W to 8.5° E (red delimitation in Figure 10). The model covers the area by 632 regular cells of 0.25° x 0.5°. 16 HTL species are modeled explicitly, accounting for 89% of the total

fisheries landings in the area over the period 2010-2017 (ICES 4abc and 7d) and more than 90% of the scientific North Sea International Bottom Trawl Survey (NS-IBTS-Q1, DATRAS) catches. There are five pelagic species, seven demersal species, three benthic flatfish and one shrimp functional group. The species and their input parameters are listed in Supporting Information S4, Table S3, and the data sources, references, and/or methodology to estimate these parameters are presented in the Supporting Information S6. The species spatial distributions are described by presence/absence maps, and informed per life stages (egg-larvae, juvenile, and adult) whenever information was available (Supporting Information S7). As individuals are represented in a 2D horizontal environment,

a predator-prey accessibility matrix Γ , used to determine the accessibility coefficient $\gamma(i, j)$ (see Eq. 1 and Table 2), is defined according to the vertical distribution overlap between potential predator and prey species possibly per life stage (Supporting Information S4, Table S5). The gonad portion released $sp(t)$ is estimated from the seasonality of eggs' release (see Supporting Information S2.5). The seasonality of eggs' release data are taken from the literature and presented in Supporting Information S8. The fishing mortality rates are size-dependent due to fisheries size-selectivity. The calibrated maximum fishing mortality rates F_{max} are in Supporting Information S4, Table S3. The species-specific fishing selectivity curves are in Supporting Information S11. The larval and additional mortality are in Supporting Information S4, Table S3.

2.2.2.2 Forcing variables: low trophic levels and physical variables

The Bioen-OSMOSE model is forced by temperature and oxygen variables and by LTL biomass fields. The forcing data come from the regional biogeochemical model POLCOMS-ERSEM applied to the North Sea ecosystem (Butenschön et al., 2016). The modeled period is 2010-2019. There are five pelagic (micro-phytoplankton, diatoms, heterotrophic flagellates, micro-zooplankton, meso-zooplankton) and three benthic (suspension feeders, deposit feeders and meiobenthos) LTL groups (Supporting Information S5): the biomass of the former is available in three dimensions and therefore integrated vertically, while the biomass of the latter is available in two-dimensions. Two other groups of large and very large benthos are set as homogeneous prey fields in space and time due to the absence of data and model output for these LTL groups. For the temperature and oxygen variables, their values are integrated over the 43 vertical layers of POLCOMS-ERSEM to force pelagic and demersal HTL species. Only the values in the deepest layer are used for benthic species. Monthly maps for each LTL group and temperature and oxygen variables are shown in Supporting Information S9.

2.2.2.3 Calibration

The model is calibrated, i.e., parameters for which an independent estimator is unavailable are estimated, using maximum likelihood estimation based on an optimization method adapted to high-dimensional parameter space, namely an evolutionary algorithm available in the package *calibraR* in R (Oliveros-Ramos & Shin, 2016). The algorithm explores the space of unknown parameters (referred to as “calibrated” in Supporting Information S4, Table S3) so as to maximize the likelihood obtained by comparing model outputs to observed data. Data used to calibrate Bioen-OSMOSE-NS are fisheries landings (ICES, 2019a), size-at-age from scientific surveys (NS-IBTS-Q1, North Sea International Bottom Trawl Survey (2010-2019), available online at <http://datras.ices.dk>) and estimated biomasses for assessed species (ICES, 2019b, 2018c, 2018d, 2018e, 2016). The discard rate of assessed species is low except for dab and plaice: the data used as landings and biomass for these species includes estimated discards from stock assessments. The biomasses estimated for stocks entirely located within the study area are directly used (herring, sandeel, sprat, sole, and whiting). For stock with a wider distribution than the study area, the biomass data is taken proportional to total stock biomass according to the ratio between landings in the study area and total landings (mackerel, norway pout, plaice, saithe, cod, haddock, dab, hake). There is no biomass target value for unassessed species (horse mackerel, grey gurnard, hake, shrimp). The calibration is performed for an average state of the ecosystem for the period 2010-2019 by using observed data averaged over the period as target values (Supporting Information S10). The calibration is run using four phases with a new set of parameters to be estimated added at each phase for better convergence of the optimization: the first phase calibrates the LTL group accessibility coefficients only (Supporting Information S5), the larval mortalities are added for the second phase (Supporting Information S4, Table S3), the maximum ingestion I_{max} rates are added on phase three (Supporting Information S4, Table S3), and the maximum fishing mortality rates and the additional mortality rates are added in the last phase (Supporting Information S4, Table S3).

The calibrated configuration is run for 80 years. The first 70 years is the spin-up period, a period during which the system stabilizes. The results presented hereafter are the years after the spin-up

period. 28 replicates of the model are run with the same parameterization to account for Bioen-OSMOSE stochasticity.

2.3 Results and discussion

In this paper, we present the Bioen-OSMOSE framework with its first application to the North Sea ecosystem, involving the coupling of the POLCOMS-ERSEM model for the physical and LTLs model with the HTLs Bioen-OSMOSE model. The North Sea trophic network has been intensively studied and modeled, either considering the whole ecosystem (Blanchard et al., 2014; Cormon et al., 2016; Heath, 2012; Lewy, 2004; Mackinson & Daskalov, 2007) or part of it (including the English Channel) (Girardin et al., 2018; Stähler et al., 2016; Travers-Trolet et al., 2019).

This is the first time that the Bioen-OSMOSE model is used, i.e the OSMOSE model (Shin & Cury, 2004) augmented with a mechanistic description of the emergence of life history from underlying bioenergetics and its response to temperature and oxygen seasonal and spatial variations. It is also, to our knowledge, the first application of a marine ecosystem model considering the impacts of physiologically-induced trait changes in response to food, oxygen, and temperature at the individual, population, and community levels.

2.3.1 Model evaluation

The calibration procedure allowed us to estimate unknown parameters to obtain a model configuration that fairly accurately represents the North Sea ecosystem. Particular attention was paid to obtaining satisfactory results for indicators at different biological levels, the final result being a compromise between indicators used as target (size-at-age, catch and biomass) and emerging variables (maturation and diet).

2.3.1.1 The individual level: size structure and maturity ogives

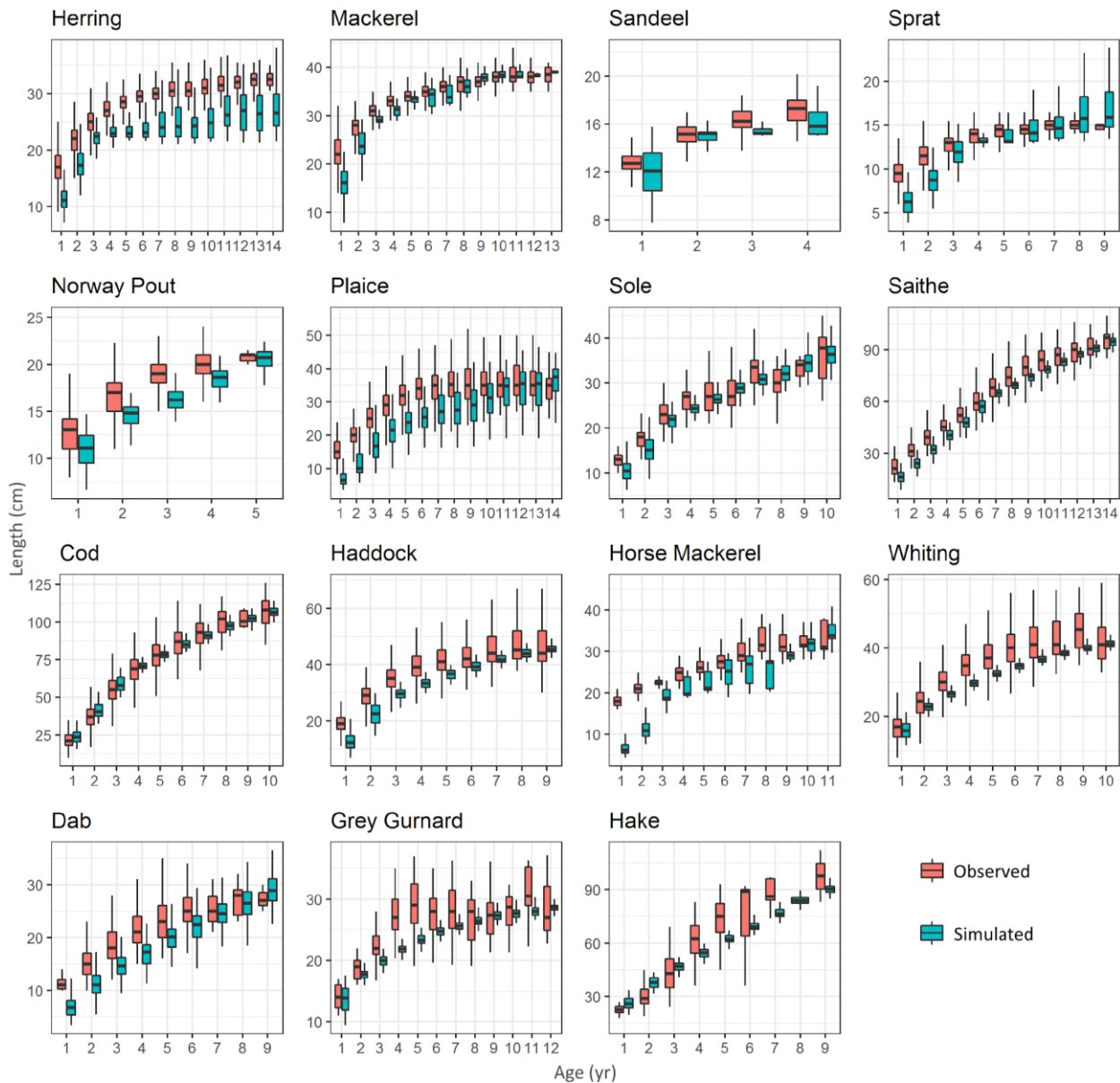


Figure 11: Boxplot of size-at-age per species for observed (pink) and simulated (blue) individual data. Horizontal bars represent the first, second and third quartiles. The whiskers' extremities represent 1.5 times the interquartile space (the distance between the first and third quartile). The shrimp group was not represented in this graph, as available observed data are not sufficiently taxonomically resolved to be relevant for this functional group.

The simulated mean sizes-at-age correctly reproduce the observed ones (Figure 11), supporting the credibility of the growth process described by the new bioenergetic sub-model. The Von-Bertalanffy-like shape and the indefinite growth are two realistic properties reproduced with our model. As observed in the data, it can be noted that growth is faster during the first years of life and the sizes at older ages slowly tend to an infinite size. The simulated and observed sizes-at-age interquartile

ranges overlap for almost all age classes of the species. The simulated size hierarchy between species is consistent with the observed one, which is a key expected property for a size-based model.

The simulated sizes-at-age 1 have generally the poorest fit to observed data. Size-at-age class 1 partly inherits uncertainties linked to size at hatching and to the growth rate at very early stages, notably the larval one, that is imperfectly accounted for by the multiplicative factor of maximum mass-specific ingestion rate for the larvae at larval stage θ . In addition, growth during the first year is mainly driven by food limitation implying that the size-at-age class 1 is the result of a complex model adjustment between growth rate, competition and prey accessibility.

The variance in size-at-age differs between observed and simulated data, mainly for demersal species. The observed variance in sizes-at-age is the result of macro-environmental variations, i.e. in the abiotic environment (Brown et al., 2004; Gislason et al., 2010; Thomas et al., 2019) and food availability (Brosset et al., 2016), micro-environmental variations, i.e., in undetectable or unaccounted for environmental conditions, and genetic variability in energy allocation inducing variability in size-at-age (Enberg et al., 2012). In contrast, the variance of simulated size-at-age only results from macro-environmental variations. Thus, the species with observed variance higher than the simulated variance is because genetic and micro-environmental variances are not modeled here.

Comparison of observed and simulated age and size maturity ogives demonstrate the ability of Bioen-OSMOSE to correctly reproduce maturation patterns (Figure 12). The simulated mean age at first maturation perfectly matches that observed for three species (cod, norway pout, and whiting). In observed data, age is given with yearly resolution. Therefore, we consider that a correct pattern is obtained for seven additional species for which the difference between simulated and observed age at maturity is less than one year (grey gurnard, haddock, hake, herring, mackerel, plaice and sole). The worst deviation is obtained for sprat and saithe with simulated maturation occurring at later ages and larger sizes than that observed. Saithe and sprat have lower mean sizes at early ages than observed ones (Figure 11) which can explain the late simulated maturation. However, both species

have simulated maturation ages that stand within observed ranges, being lower than the upper bounds of observed maturation ages, namely 9 years for saithe in the North Sea (Cohen et al., 1990) and 4 years for sprat (Ojaveer and Aps, 2003) in the Baltic Sea (only mean values were reported for the North Sea population).

The use of LMRNs improves the description of the variability in the maturation process compared to the use of fixed age or size at maturity, as is most commonly done in marine ecosystem models, such as previously in the OSMOSE framework (Shin & Cury, 2004) or in other models (Audzijonyte et al., 2019). Consequently, individuals from the same size or age class do not necessarily have the same maturity state (Figure 12), which increases the realism of the life cycle description. For the majority of the species, the slope of simulated age and size maturity ogives is higher than the observed one, meaning that the observed maturation process is more variable than in simulations. As for size-at-age, part of the observed variability in maturation is determined by genetic and/or micro-environmental variability (Law, 2000, p. 200; van Wijk et al., 2013) and is not modeled here.

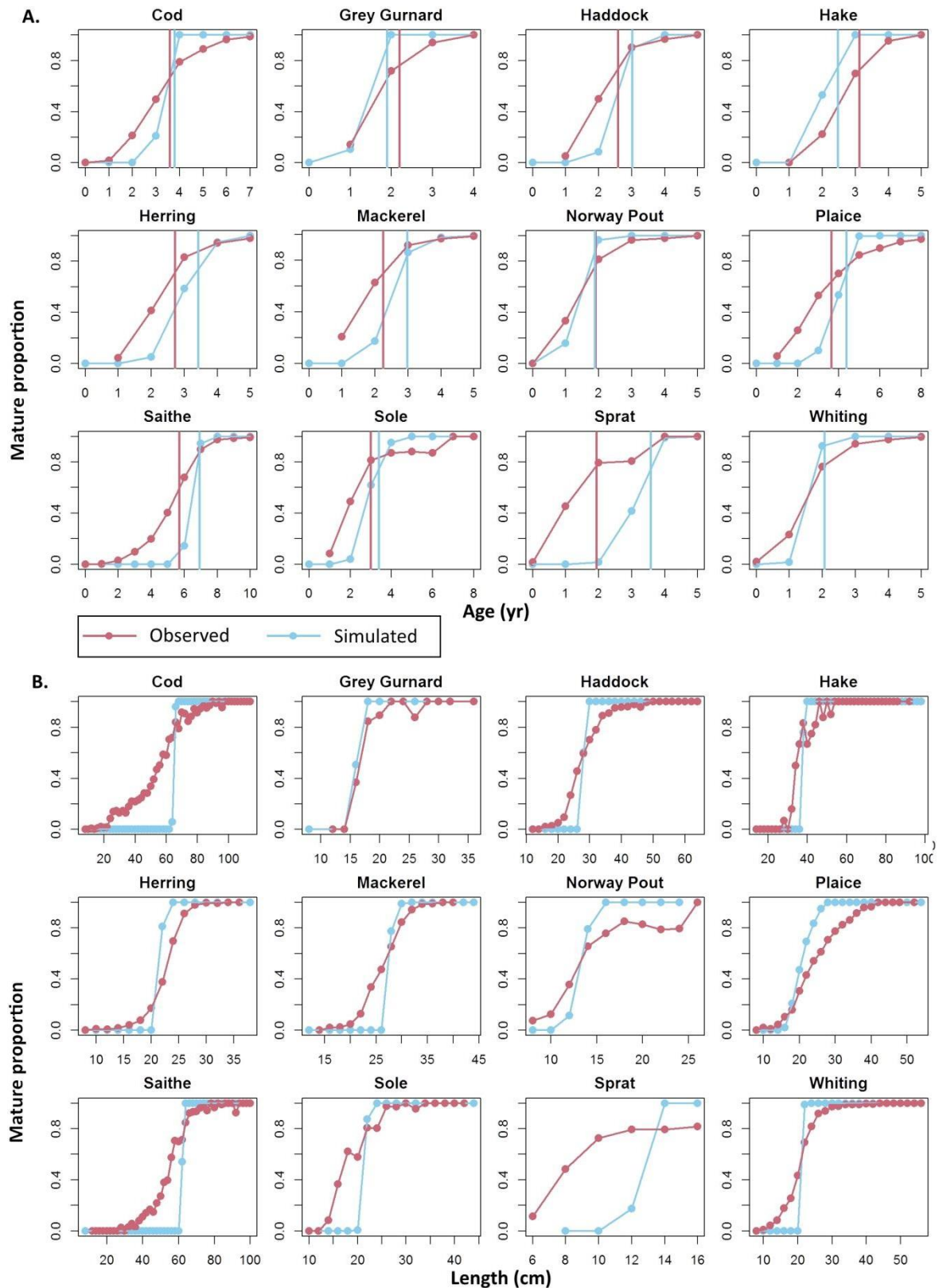


Figure 12: Age (A) and size (B) maturity ogives per species for observed (pink) and simulated (blue) data. Results are shown for species for which there is enough data to estimate and plot the observed age and size maturity ogives. Age data have a yearly resolution and size data a 2-centimeter resolution. The simulated (blue) and observed (pink) mean age at maturity are represented by vertical lines (A). The mean size at maturity is not represented. The observed size maturity ogive is not strictly increasing and does not allow a reliable estimation of the maturation size.

2.3.1.2 The population level: fisheries catches and species biomass

Given the high statistical confidence in catch data, a greater weight was given to the corresponding likelihood component in the calibration process which resulted in reaching targets, i.e., simulated catches were within the range of observed values, for the majority of species (Figure 13A). Plaice and dab are the two species for which the simulated catches were the farthest from their targets. Plaice and dab are two by-catch species that are largely discarded. These discards are estimated to be up to 40% for plaice and 90% for dab (ICES, 2018e). The catch data used as target here is reconstructed from the landings and discards estimates, which, in case of overestimation of discards, could explain the discrepancy between the target and the simulated values. The poor fit of plaice could also be partially explained because the migrations between the Eastern and Western English Channel stocks are not taken into account in Bioen-OSMOSE-NS (ICES, 2021).

The simulated biomasses are within acceptable ranges (Figure 13B) and the resulting dominance ranking between species groups respects the ranking based on stock assessment estimations: small pelagic fish are the dominant group with herring as the main species. Demersal species have lower biomasses with saithe and haddock as the most abundant ones. Flatfish are the minority group in the system, which is dominated by plaice.

The simulated biomasses of mackerel and sandeel are underestimated compared to the stock assessment biomass estimates (Figure 13B). Mackerel is a widely distributed stock in the North East Atlantic area and our biomass estimate in the North Sea (proportional to the total biomass in the North East Atlantic according to the ratio between North Sea landings and total landings) relies on the assumption of a uniform fishing effort in the assessed area. A higher fishing effort within the North Sea would lead to an overestimation of the target biomass for the area, which is credible since the North Sea is a historically heavily fished area. An ecopath model of the North Sea (Mackinson & Daskalov, 2007) also estimated a lower biomass for this species (980 400 t). Underestimation for sandeel is more troublesome as it is a key forage species in the North Sea (Engelhard et al., 2014), for

which the stock assessment is considered to be very detailed with 7 stocks in the area (ICES, 2016). The fact that the Bioen-OSMOSE-NS model does not describe the peculiar overwintering behavior of this species, which buries itself in sand and thus is less vulnerable to fishing and predation in winter (Henriksen et al., 2021), may explain the underestimation of its biomass. The sandeel may also be over-consumed by higher trophic level species in our model, indicating a missing forage species or an over-consumption of sandeel over LTL forced prey.

In Bioen-OSMOSE-NS, flatfish are represented by only the three main species of the North Sea ecosystem. However, there are other flatfish species each with low biomass levels (*Scophthalmus maximus*, *Microstomus kitt*, *Scophthalmus rhombus*, *Platichthys flesus*...) (NS-IBTS-Q1, DATRAS, Piet et al., 1998) but whose total biomass is not negligible (NS-IBTS-Q1, DATRAS, Mackinson & Daskalov, 2007). Thus, the overestimation of plaice biomass may compensate for the absence of these other flatfish in the model that may leave an empty trophic niche.

The high biomass of the shrimp functional group, dominated in the ecosystem by the species *Crangon crangon* and *Pandalus borealis*, may seem surprising. However, as the micro- and meso-zooplankton groups described by the biogeochemical model POLCOMS-ERSEM represent pelagic prey of sizes smaller than 0.5 cm only, we suggest that the shrimp functional group has a broader ecological role in the Bioen-OSMOSE-NS model by actually representing all LTL prey larger than 0.5 cm in the water column, whose biomass is critical to sustain the food web. These prey include demersal crustaceans with diel vertical migration such as *Crangon crangon* or *Pandalus borealis* as well as more pelagic species such as large amphipods (large *Bathyporeia elegans*) or euphausiids (*Thysanoessa sp.*, *Meganyctiphanes norvegica*).

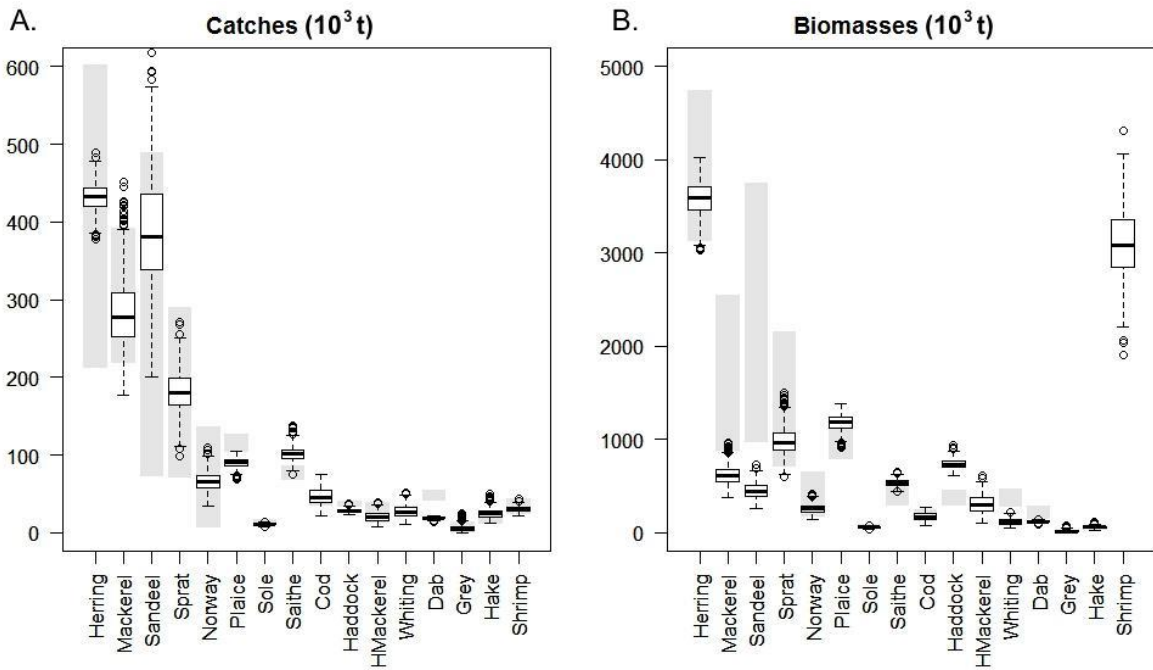


Figure 13: Fisheries catches (A) and biomasses (B), in thousand tons, per species for stock assessment estimates and simulated data. The boxplots represent the simulated data for 28 replicated simulations (stochastic model) for the catches and biomasses per species, with the first, second and third quartiles represented horizontally in each plot. The gray bars show the minimal and maximum values observed for catch and biomass estimates from stock assessment for the 2010-2019 period. The species without gray bars for biomasses are not assessed in the area.

2.3.1.3 The community level: trophic diets

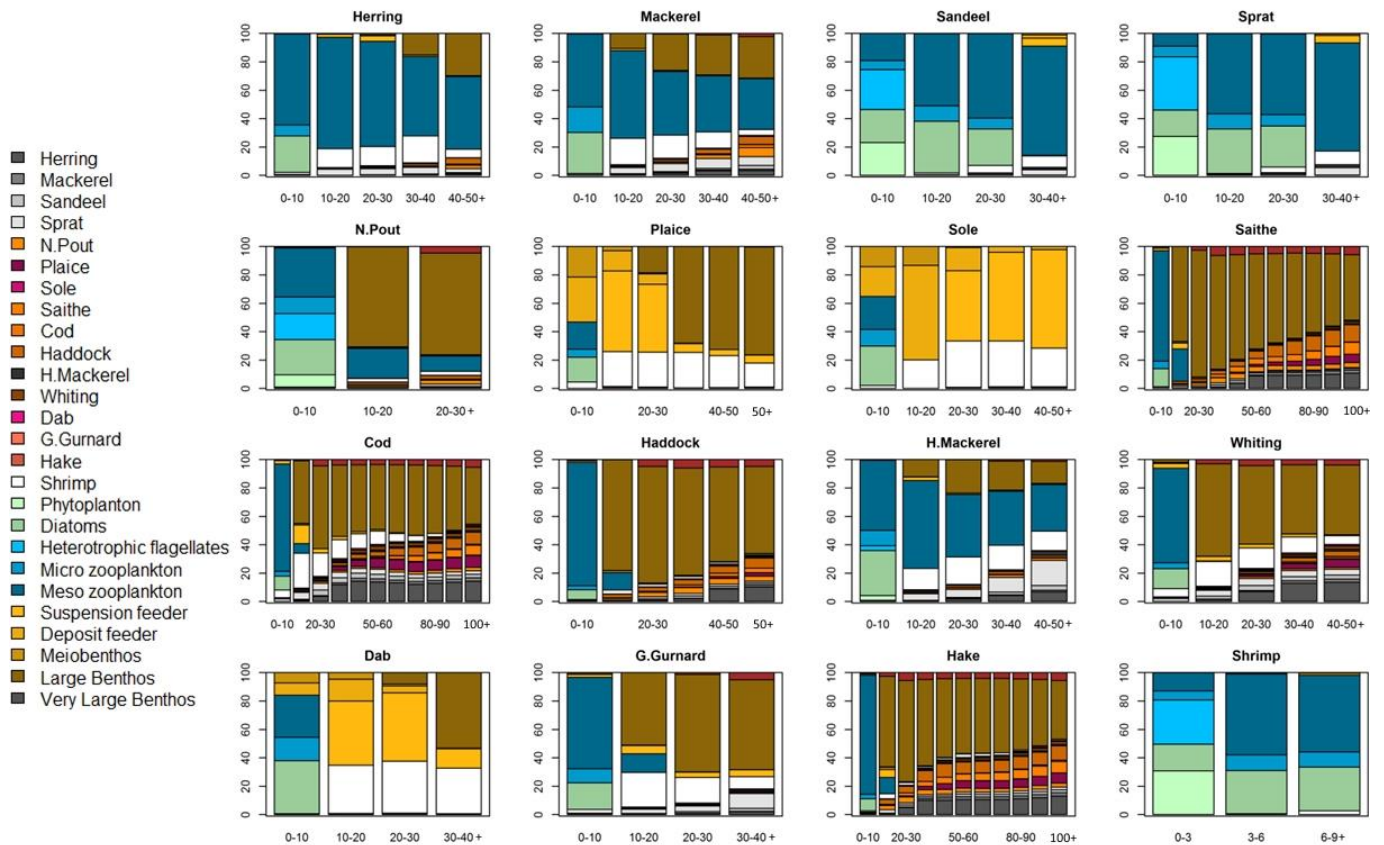


Figure 14: Diet in percent of biomass eaten of prey species per size class of the predator species in cm. For each predator species, the last size class (x-axis) includes all the larger individuals.

In Bioen-OSMOSE, the diet emerging from opportunistic predation reflects the species' relative abundances, their sizes and their spatio-temporal overlap. There are no pre-established predator-prey diet matrix in the parameterization of the model so confronting the output diets to observed ones, especially in terms of species composition, is a way to validate the model properties.

The simulated diets show patterns that are consistent with observations (Figure 14). The model reproduces correctly observed ontogenetic diet shifts (Timmerman et al., 2020). The prey composition shifts between pelagic early-life stages (size class 0-10 cm for fish species and 0-3 cm for the shrimp group) and the older life stages for all species. There are different emerging diet patterns depending on the predator's position in the water column. The pelagic species diet is dominated by phyto- and especially zoo-planktonic prey, which is consistent with studies on sprat and herring (De Silva, 1973; Last, 1989; Raab et al., 2012). The benthic species diet is composed of benthic LTL groups and the shrimp functional group, similarly to results obtained by an isotopic study (Timmerman et al.,

2021), by plaice and sole stomach content studies for adults (Rijnsdorp & Vingerhoed, 2001) and for juveniles (Amara et al., 2001) with smaller prey for sole than for plaice and dab of the same size (Amara et al., 2001). The demersal species have an intermediate diet composition with a high degree of piscivory for the larger fish. There is a steady increase in piscivory with size, mainly for demersal species, as shown empirically for whiting, cod, saithe and haddock in the area (Robb & Hislop, 1980; Timmerman et al., 2020) but not for Norway pout (Robb & Hislop, 1980). In addition, there is a significant part of benthic prey in the pelagic species diet, which correctly represents the strong pelagic-benthic coupling in this area (Giraldo et al., 2017; Timmerman et al., 2021): the pelagic piscivorous fish (mackerel and horse mackerel) also feed on benthic prey which represents half of their diet (Giraldo et al., 2017).

2.3.2 The physiological level: spatial pattern

New outputs and original questions emerge from the physiological responses of metabolic rates to biotic and abiotic variables and can be explored with the Bioen-OSMOSE model. The representation of emergent spatially and seasonally varying bioenergetic fluxes is an example of the new features brought by Bioen-OSMOSE that can help improve our understanding of the relationship between temperature and ecosystem dynamics, which is crucial in the context of global warming (Lindmark et al., 2022). This spatial and seasonal variability of metabolism in relation to temperature variation is often under-studied.

The simulated adult mean mass-specific net energy rate for new tissue production $\overline{e_p}$, is the ratio between the population mean mass-specific net energy rate (see Eq. 9) and the weight at the exponent β and it drives the energy allocated to growth and reproduction. It is spatially represented as an output example (Figure 15). This spatial representation of emerging bioenergetic fluxes highlights the high variability of mean mass-specific net energy rate for three widely distributed species in the North Sea ecosystem with contrasted thermal preferences: cod, herring and dab (quoted by increasing physiological optimum temperature T_{opt} , defined in Figure 9). The spatial

pattern of mean mass-specific net energy is mainly explained by species thermal preferences. The species with the lowest thermal preference (cod) has a greater net energy acquisition in the northern part of the area where the water is colder on average. The opposite pattern emerges for the species with the highest thermal preference (dab). There is a better energy acquisition in the south where the average temperature is higher than in the north. A similar spatial pattern for growth rate was predicted as outputs of a single-species bioenergetic model for two thermophilic flatfish in the North Sea (Teal et al., 2012). Herring, which has an intermediate thermal preference, exhibits a more spatially homogeneous emerging mean mass-specific net energy rate. During the period described by our model (2010-2019), temperature is the main driver of spatial variability in bioenergetic fluxes for these three species. The spatial distribution of food has little or no impact on adult energy acquisition for these examples as we observe that simulated food ingestion frequently reaches the maximum at the adult stage (results not shown). Likewise, oxygen saturation has no impact on the emerging spatial pattern because oxygen saturation is not low enough to become a primary driver of bioenergetic fluxes (Vaquer-Sunyer & Duarte, 2008, Supporting Information S10).

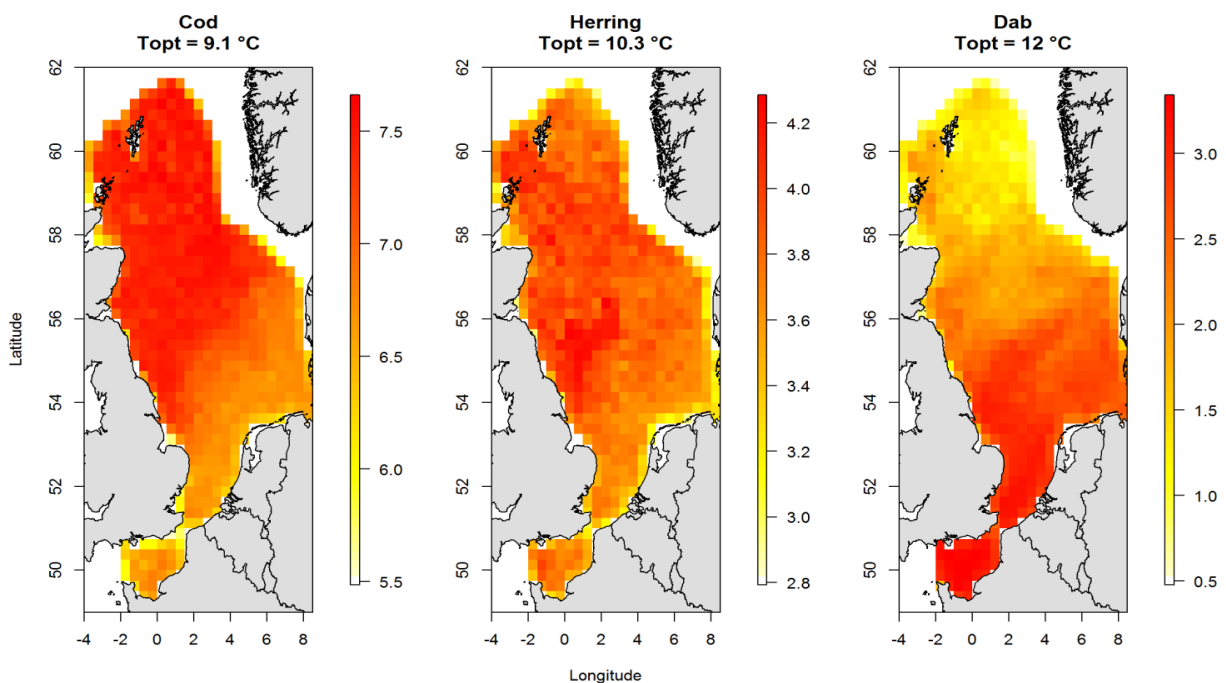


Figure 15: Spatial variability of the mean adult mass-specific net energy rate available for new tissue production, per model cell for cod, herring and dab. These three species are distributed over the whole modeled area although they have different optimum temperatures T_{opt} . Cod, herring and dab mean adult mass-specific net energy available rate for new tissue production averaged over the area

are 7.4, 3.3, and 2.7 $g \cdot g^{-\beta}$, respectively. Spatial variations of this bioenergetic flux can be driven by temperature, oxygen and food variation.

2.4 Conclusion

Applying Bioen-OSMOSE to the North Sea allows demonstrating the feasibility of its parameterization for several species with different levels of available knowledge and allows evaluating the framework capabilities. Bioen-OSMOSE-NS simulates many different outcomes that convincingly reproduce observations such as biomasses, catches, sizes at age, maturation ogives, and diets. The model also produces compelling spatial responses of the bioenergetic fluxes to temperature variations.

The Bioen-OSMOSE framework is also intended to be used for hindcast or forecast simulations. Hindcasting could help disentangling the effects of temperature increase and/or oxygen depletion on the historical trends in life-history traits. Hindcasting with Bioen-OSMOSE could also be useful to understand the contribution of temperature- and oxygen-induced physiological changes in population and community dynamic alterations that were observed in past periods. Given the increasing need to reliably forecast biodiversity under future climate change scenarios, we believe that Bioen-OSMOSE will also allow improving projections of regional ecosystem dynamics by taking into account future individual-level physiological changes and their consequences at the population and community levels.

Chapter 3: Trophic level determines the difference between fundamental and realized thermal performance curves.

Alaia Morell, Yunne-Jai Shin, Nicolas Barrier, Morgane Travers-Trolet, Bruno Ernande

ABSTRACT

Understanding how temperature affects fish populations is important for predicting the effects of climate change. Fundamental physiological thermal performance curves (TPCs) determined in controlled conditions are commonly used to project future species spatial distributions or physiological performances. However, realized physiological performances in the wild may differ as they result from both direct and indirect effects of temperature, the latter channeled through other extrinsic factors that covary with temperature, such as food or oxygen availability.

The Bioen-OSMOSE model is an individual-based marine ecosystem model, notably developed to account for plastic trait variations in response to biotic and abiotic environmental changes and their impacts on food-web dynamics. It mechanistically describes the emergence of net energy for new tissue production at the individual level from energy fluxes sustained by food intake through explicit opportunistic size-based predation. These fluxes depend directly on temperature, oxygen concentration and food availability. The available food biomass is composed of explicitly modeled prey species as well as plankton and benthos forcing the model, the biomass levels of which vary with temperature. This model is applied to the North Sea ecosystem to compare species' fundamental physiological TPCs with their realized ones. We explore the results for fifteen fish species at different life stages. The small pelagics and early life stages have the most different realized TPCs, mainly due to food limitation, whereas the realized TPCs of demersal higher trophic level species are similar to fundamental ones. This results from an increasing bottom-up effect of

spatio-temporal variability in low-trophic level prey availability and intraspecific competition for these on realized physiological TPCs as the trophic level and omnivory degree of fish diminishes across life-stages and species. In contrast, deoxygenation has a weak effect on realized physiological TPCs in the absence of hypoxic events in the area. These results complement previous analyses solely based on fundamental physiological thermal preferences and tolerances, and are crucial to better determine future thermal vulnerability and the persistence of populations in the context of climate warming.

3.1 Introduction

Temperature has pervasive effects on biological systems, from the cell (Koch et al., 2021) to the ecosystem scale (Parmesan, 2006), that are currently of great concern in the context of climate change. Temperature impacts marine ectotherms directly as a key driver of their physiological rates (Gillooly et al., 2002), ecology (Clarke, 2019) and biogeography (Deutsch et al., 2020). Modifications of individuals' physiology and bioenergetics affect all levels of organization of the ecosystem as they imply direct consequences on individual growth, reproduction and survival (Audzijonyte et al., 2018), and indirect ones on demographic rates, species interactions and more generally the entire community structure (Beaugrand and Kirby, 2018; Payne et al., 2021). Understanding individual physiological responses to temperature is receiving growing attention as it is key to reliable projections of future population and community dynamics under climate change (Audzijonyte et al., 2018; Lefevre, 2016; Lefevre et al., 2017).

The oxygen- and capacity-limited thermal tolerance (OCLTT) concept has been developed to link thermal physiological constraints to individual metabolism, performances and thermal niche (Pörtner, 2001; Pörtner et al., 2010). In this framework, the aerobic scope (AS) is the indicator for physiological performance. Defined as the difference between maximum oxygen supply and minimum (at rest) oxygen demand, it represents the maximum oxygen budget available to an individual to cover its energetic costs beyond maintenance such as locomotion, growth, and

reproduction. The temperature response of the AS is dome-shaped as a result of the exponential increase of minimum oxygen demand with temperature and a slower increase of maximum supply, that may even plateau or decrease above a preferred range of temperatures (Holt and Jorgensen, 2015; Pörtner, 2001) (Figure 16A). This response, namely the thermal performance curve (TPC; Angilletta, 2009) of the AS, is often used as a proxy of the TPCs of individual biological rates such as bioenergetic fluxes, growth, reproduction, or immune capacity, and more generally fitness (Pörtner and Peck, 2010). In this context, the temperature maximizing the AS is considered as an indicator of the optimal temperature for individual performances and/or fitness.

The use of the AS as a predictive framework of ectotherms' performance and fitness responses to temperature is still highly debated (Clark et al., 2013; Jutfelt et al., 2018; Lefevre et al., 2021, 2017). Conceptually, discrepancies between the temperature response of the AS and that of physiological performances, traits or fitness are indeed expected. First, these may stem from intrinsic causes. The share of an individual's net aerobic energy between downstream physiological processes is constrained by trade-offs. These trade-offs may be temperature-dependent themselves and generate a mismatch between the temperature response of the AS and that of downstream physiological performances, traits or fitness (Holt and Jorgensen, 2015). Second, the mismatch may also result from extrinsic factors that determine the amount of available energy. The AS is only a permissive factor among other upstream constraints, such as food intake or oxygen saturation, that together determine the amount of energy available for physiological processes (Jutfelt et al., 2018). Predicting the thermal niche and fitness response of individuals to temperature using AS alone is thus potentially misleading, as extrinsic factors may also vary with temperature (Figure 16B).

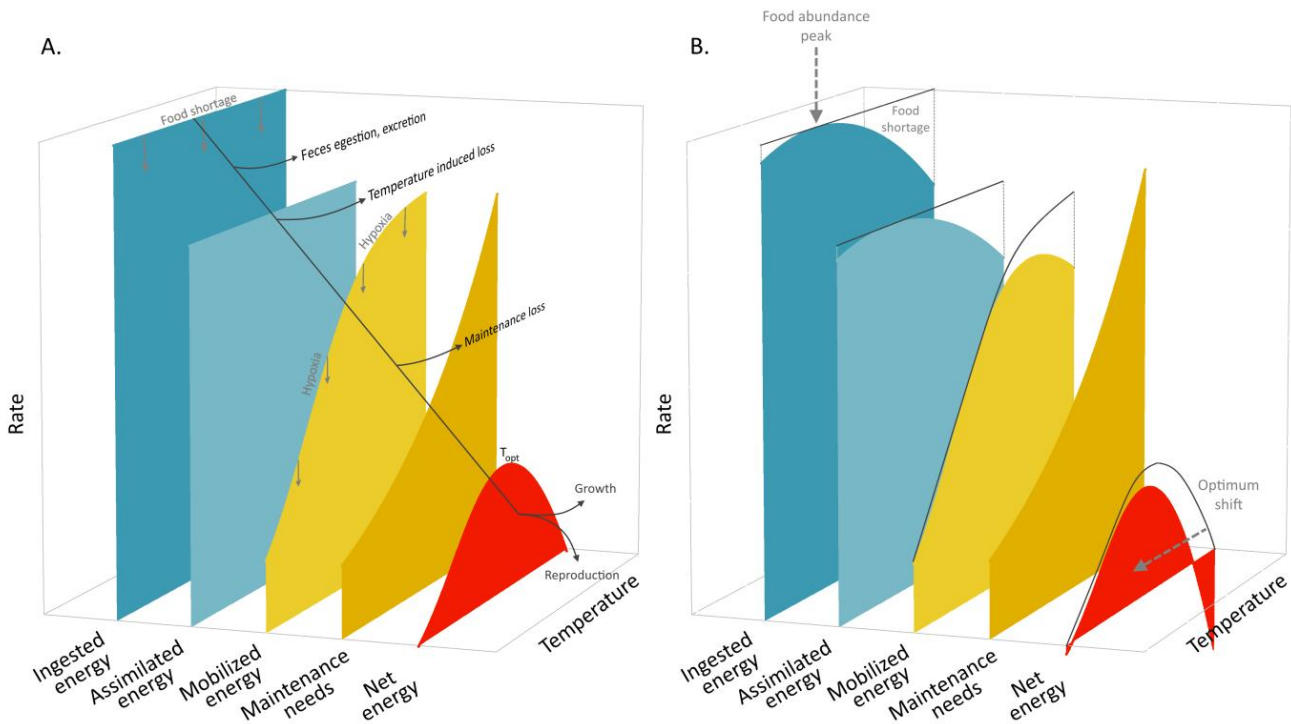


Figure 16: Thermal curves of the bioenergetic fluxes from ingestion to tissue growth as modeled in our framework. (A) The fundamental net energy thermal performance curve (the red dome-shaped curve) conforms to the OCLTT theory. Hypoxia impacts mobilized energy (yellow curve) and downstream fluxes. Food shortage impacts ingested energy (dark blue curve) and downstream fluxes. (B) The modification of extrinsic factors with temperature, such as food abundance, impacts the downstream bioenergetic fluxes in response to temperature. The red curve here is an example of a realized net energy TPC when food abundance varies with temperature. In this example, the *realized* net energy TPC is shifted to lower values compared to the *fundamental* one.

In other terms, extrinsic factors explain the differences between a species' fundamental thermal niche (*sensu* Hutchinson) or TPC, defined as the temperature range within which physiological functioning allows resting conditions independently from biotic interactions (i.e, the temperature range with positive AS, Figure 16A), and its realized one, defined as the temperature range bringing positive fitness while accounting for both physiology and species interactions (Pörtner et al., 2017, Figure 16B). Indirect temperature effects via extrinsic factors have been little investigated. We hypothesize that these are channeled through three main aspects: (i) the biogeographic distribution of species that induces co-variation between encountered temperature and co-occurrence/encounter rates between predators and prey, (ii) predators (top-down effect) and prey (bottom-up effect) abundances that are temperature-dependent and (iii) co-variation between temperature and other abiotic factors that affect metabolism such as oxygen saturation. All three

elements determine an individual's available energy for physiological processes, by affecting food intake (or more generally trophic interactions) for the two former and energy mobilization through respiration for the latter (Clarke, 2017), and may lead to high differences between fundamental and realized thermal niches.

Comparing fundamental and realized thermal niches and understanding how their differences depend on extrinsic factors are thus key for the informed use of AS to predict species response to temperature in the context of global warming. This requires ecosystem modeling tools that simultaneously encompass the explicit effect of temperature on several components of the ecosystem, namely the direct temperature response of individuals' AS and the indirect effects of temperature on energy availability through species spatial distributions, predators and prey abundances, and co-varying abiotic factors. In this paper, we use a recently developed ecosystem modeling framework, called Bioen-OSMOSE (Morell et al. submitted; Chap. 2), to investigate how trophic interactions, affected by predators and prey spatial distributions and abundances, and oxygen saturation determine differences between fundamental and realized TPCs of the net energy available to individuals for metabolic processes. Using the OSMOSE model (Shin and Cury, 2004, 2001) as a core base, Bioen-OSMOSE is an individual-based model representing the spatiotemporal dynamics and bioenergetics of multiple high-trophic level (HTL) species in regional marine ecosystems. It is unidirectionally forced by temperature, oxygen and low-trophic level (LTL) prey fields outputs from hydrodynamical and biogeochemical models. Trophic interactions emerge from opportunistic size-based predation between spatiotemporally co-occurring individuals. In this new framework, growth, sexual maturation and reproduction are explicitly modeled as emerging mechanistically from bioenergetics and vary with temperature and oxygen in a consistent way with the OCLTT framework. Applying Bioen-OSMOSE (described in Figure 17) to the North Sea-Eastern English Channel ecosystem (NS ecosystem hereafter) taken as a case study, we tackled the following questions: (i) what is the difference between the individual-level fundamental net energy TPC and the realized net energy TPC that emerges at the population level; (ii) does this difference depend on

species and/or life-stage and which of their characteristics explain the emerging pattern (spatial distribution, life-history, trophic ecology); and (iii) what are the main ecological determinants (prey abundance, competition, predation, oxygen saturation) of this difference. The NS is a temperate shallow continental sea characterized by contrasted temperature regimes, with very large seasonal variations. In addition, fish species inhabiting the NS are well-studied, with many laboratory physiological experiments. The NS therefore appears particularly well suited for a study on the comparison between fundamental and realized TPCs.

3.2 Materials and methods

3.2.1 Model Description

3.2.1.1 General description of Bioen-OSMOSE

To understand the direct and indirect effects of temperature on the net energy of HTL species, we use the multispecies model Bioen-OSMOSE applied to the NS ecosystem as a case study (Morell et al. submitted; Chap. 2). In Bioen-OSMOSE, the HTL species dynamics are spatialized, size- and age-structured and emerge from the mechanisms describing individuals' life cycle (Figure 17) (Morell et al. submitted; Chap. 2). The structure of the food web arises from opportunistic size-based predation and spatiotemporal co-occurrence of individual predators and prey. The Bioen-OSMOSE model also explicitly describes individuals' bioenergetics from food ingestion to the production of new somatic and gonadic tissues and their responses to oxygen, temperature and food variations. The bioenergetic mechanisms underlie the emergence of the life history traits of HTL species: somatic growth rate, maturation age and size, absolute fecundity, starvation mortality and, in conjunction with opportunistic size-based predation, predation mortality. Population and community dynamics result from the mechanistic individual-level life cycle modeling and species' spatial distribution (Figure 17).

Individuals' bioenergetics are described according to a biphasic growth model (Andersen, 2019; Boukal et al., 2014; Quince et al., 2008) in which body mass-dependent energy fluxes are allocated

between competing processes —namely maintenance, somatic growth and gonadic growth— thus accounting for physiological trade-offs (Roff, 1993; Stearns, 1992). The sexual maturation of individuals relies on the concept of maturation reaction norms that depicts how the process of maturation responds plastically to variation in body growth (Heino et al., 2002; Stearns and Koella, 1986). This combination mechanistically describes the processes of somatic growth, sexual maturation and reproduction as they emerge from the energy fluxes sustained by food intake resulting from size-based opportunistic predation. On top of the biphasic growth model, individuals' energy mobilization and maintenance energetic costs depend on oxygen and temperature such that the resulting net energy available for new tissue production conforms to the OCLTT theory and more generally to TPCs.

The biological unit of the model is a school (which is a super-individual in individual-based modeling terms). It is formed of individuals from the same species, born at the same time, and that are biologically identical, i.e., with the same individual-level state variables. More particularly, the state variables characterizing a school i at time step t belong to four categories in the Bioen-OSMOSE model:

- Ontogenic state of individuals described by their age $a(i, t)$, somatic mass $w(i, t)$ and gonadic mass $g(i, t)$;
- Abundance, namely the number of individuals in the school $N(i, t)$;
- Spatial location, i.e. the grid cell $c(i, t)$ where the school is located
- Taxonomic identity, i.e. the species $s(i)$ to which the school belongs.

3.2.1.2 Details of some key bioenergetic processes in Bioen-OSMOSE

A complete description of the model and its underlying assumptions are available in Morell et al. (submitted; Chap. 2) and are summarized in Figure 17. The bioenergetic processes that are necessary to understand the results from this study are presented hereafter and mentioned in Figure 16 and Figure 18.

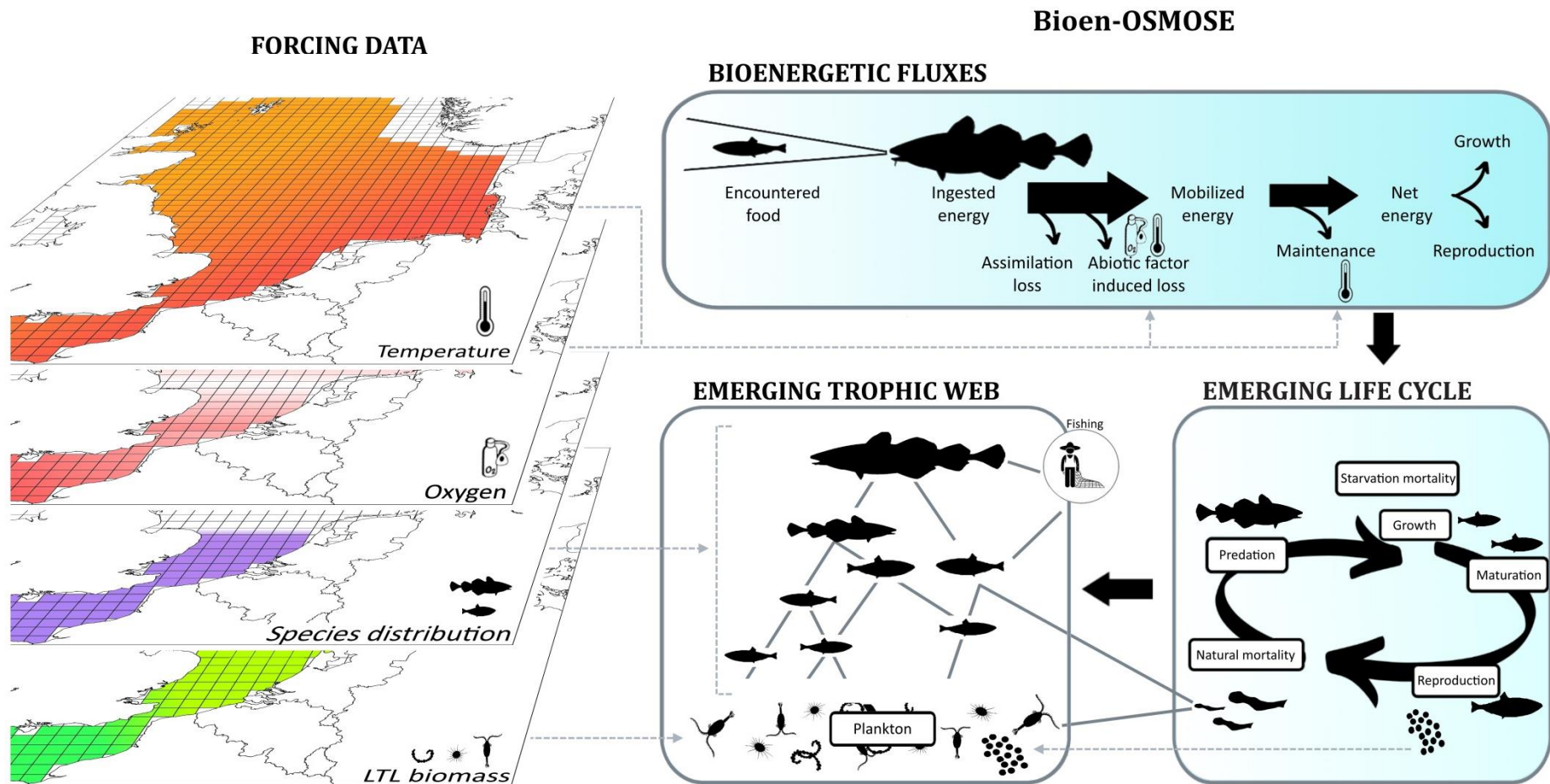


Figure 17: Graphical description of the Bioen-OSMOSE model. The simulated trophic web emerges from species distribution maps per ontogenetic stage, spatiotemporal co-occurrence between predators and prey, prey-predator size ratio, species life cycle and LTL biomass maps. The life cycle emerges from the underlying bioenergetic fluxes. These describe the internal processes from the ingestion of energy (which relies on the encountered prey) to growth and reproduction processes. The internal fluxes are driven by environmental conditions, i.e., temperature, oxygen and prey availability.

The ingested energy rate $I(i, t)$ is defined as a Holling's type 1 functional response, i.e., it increases linearly with the amount of prey biomass that is spatiotemporally co-occurring with the school i and in the relevant size range relative to individual weight $w(i, t)$, until it reaches a maximum corresponding to the satiety state level that also depends allometrically on $w(i, t)$ (Figure 18C). The predator-prey co-occurrence depends on the spatial distributions of the prey (other HTL schools and forcing LTL prey fields) and of the predator water column position. The maximum ingested energy rate per weight unit (I_{max}) is higher during the early-life stage, which is consistent with the faster growth observed in fish during this period of life.

A portion of the ingested energy is assimilated, the rest being lost due to excretion and feces egestion. A portion of assimilated energy is then mobilized. The mobilized energy $E_M(i, t)$ covers energetic costs of internal processes, i.e, growth of the somatic and gonadic tissues and maintenance. The portion of assimilated energy that is mobilized depends on temperature and oxygen. The effect of dissolved oxygen on mobilized energy is described by a dose-response function which increases with the saturation of dissolved oxygen (yellow curve, Figure 18A). The effect of temperature is described according to the Johnson and Lewin (1946) model (Pawar et al., 2015) : the response is an Arrhenius-like increasing curve until a temperature threshold above which the mobilized energy plateaus or decreases (yellow curve, Figure 18B). The mobilized energy rate fuels all metabolic processes starting in priority with the costs of maintenance of existing tissues $E_m(i, t)$ that increase with temperature according to an Arrhenius law (Gillooly et al., 2002; Kooijman, 2010) (grey curve, Figure 18B). The net energy rate available for new tissues production $E_P(i, t)$ is then the difference between mobilized energy $E_M(i, t)$ and maintenance $E_m(i, t)$ (red curve Figure 18D).

Given that the mobilized energy rate E_M increases with temperature more slowly than the maintenance rate E_m does, it results that, all other things being equal, the relationship between net energy rate E_P and temperature is dome-shaped and conforms to OCLTT theory and the expected shape of the *fundamental* TPC (red curve Figure 18D). However, the net energy rate E_P also depends

on the ingested energy I , which in turn depends on available prey biomass F , and on dissolved oxygen saturation $[O_2]$ through mobilized energy rate E_M , so that as soon as one of these covary with experienced temperature conditions, the *realized* TPC of net energy rate E_P will differ from the *fundamental* one.

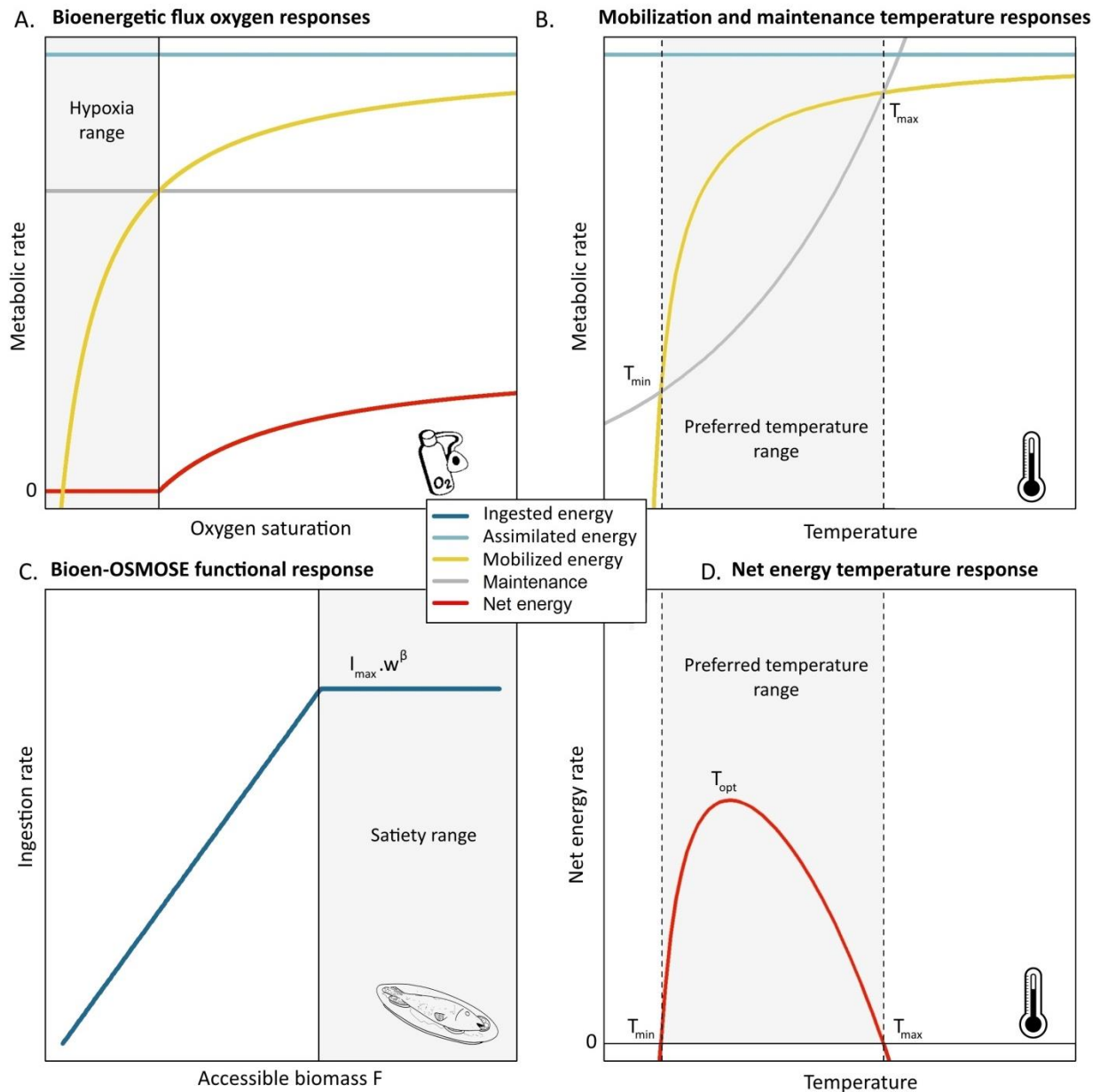


Figure 18: (A) Bioenergetic flux responses to oxygen. The range of values where maintenance needs are greater than mobilization supply is the hypoxic range, shown in gray. (B) Mobilization and maintenance responses to temperature. Values in the range where maintenance needs are lower than mobilization supply is the preferred temperature range, in gray. (C) Functional response in Bioen-OSMOSE, i.e., ingested energy as a function of accessible prey density. When accessible prey is above the satiety threshold (vertical line), ingestion is constant (gray area) and determined by the

mass-specific maximum ingestion I_{max} . (D) The net energy available for tissue production responds to temperature. This response and the preferred temperature range emerge from differences in mobilization and maintenance response, described in B. It is the net energy TPC.

Without entering into unnecessary details for this study, the net energy $E_p(i, t)$ is then fully allocated to the growth of the somatic compartment $w(i, t)$ before maturation and it is shared between growth of the somatic and gonadic $g(i, t)$ compartments after maturation. The share of energy between the two compartments is defined such that the gonado-somatic index of individuals $\frac{g(i, t)}{w(i, t)}$ is constant throughout their adult life-stage (Boukal et al., 2014; Lester et al., 2004; Quince et al., 2008), which results in a fraction of net energy allocated to the gonadic compartment that increases with their somatic mass. Age and size at maturation vary strongly between individuals due to phenotypic plasticity. This plasticity in maturation is modeled by a deterministic linear maturation reaction norm (LMRN) that represents all the age-length combinations at which an individual can become mature (Stearns, 1992; Stearns and Koella, 1986). In this framework, individuals become sexually mature when their growth trajectory in terms of body length intersects the LMRN. Finally, during the breeding season, all the energy contained in the gonadic compartment $g(i, t)$ of individuals in school i is used to produce eggs.

3.2.2 The North Sea-Eastern English Channel (NS) ecosystem

In this study, the Bioen-OSMOSE model is applied to the NS ecosystem to simulate the dynamics of the HTL species food web under the forcing of low trophic level (LTL) dynamics, temperature and oxygen provided by the regional coupled physical-biogeochemical POLCOMS-ERSEM model (Butenschön et al., 2016). The study area comprises the North Sea (except the Norwegian trench, i.e., restricted to depth shallower than 200m) and the Eastern English Channel. The study area is an epicontinental sea of the north-west of Europe of approximately 570 000 km². The northern part is the deepest area of the ecosystem: half of the seabed is between 50 and 100 meters deep and the other half between 100 and 200 meter deep. The southern part is shallower with a vast majority of the seabed less than 50 meters deep. The area covers a large latitudinal range from 49° N to 62° N.

In response to a high seasonal variation in temperature, the biological compartments of the ecosystem are organized seasonally. The abundance of primary and secondary production displays strong seasonal variations in conjunction with temperature. The abundance of fish eggs and larvae also vary seasonally and thus with temperature. Finally, seasonal migrations, for example for herring (*Clupea harengus*) or horse mackerel (*Trachurus trachurus*), are reported in this ecosystem, which also leads to seasonal species composition variation at later life stages.

3.2.3 Application of Bioen-OSMOSE to the North Sea-Eastern English Channel ecosystem

A complete description of the North Sea configuration (i.e., the application of the Bioen-OSMOSE model to the NS ecosystem referred to as Bioen-OSMOSE-NS hereafter), its parameterization and its calibration is available in Morell et al. (submitted; Chap. 2) and summarized in Figure 19. The configuration covers the NS ecosystem with a regular grid of 30 km×30 km cells on average for a total of 632 cells and has a temporal resolution of 15 days. It is parameterized and calibrated to represent a steady-state of the NS ecosystem corresponding to the average fisheries landings (ICES database) (ICES, 2019a), biomass (for assessed species) (ICES, 2016, 2018a, 2018b, 2018c, 2019b) and length-at-age of the HTL species over the period 2010-2019. Bioen-OSMOSE-NS is forced by a 15-day climatology representing the spatial and seasonal variability of LTL species biomass, temperature and dissolved oxygen saturation for an average year over the period 2010-2019 based on the POLCOMS-ERSEM model outputs. At each time step and in each cell, the biomass of 2 phytoplankton, 3 zooplankton and 3 benthos groups from POLCOMS-ERSEM and 2 homogeneous benthos groups is provided as potential LTL prey for the HTL species. Biomass is vertically integrated for the plankton groups while benthic groups are found only at the bottom. Likewise, vertically integrated average temperature and dissolved oxygen saturation are used to force pelagic and demersal HTL species bioenergetics while bottom values are used for benthic HTL species. 16 HTL species were modeled in Bioen-OSMOSE-NS: 1 shrimp functional group and 15 teleost fish species including 5 small pelagics, 7

demersal species and 3 flatfish species (Figure 19). For this study, results focus on the 15 teleost fish species.

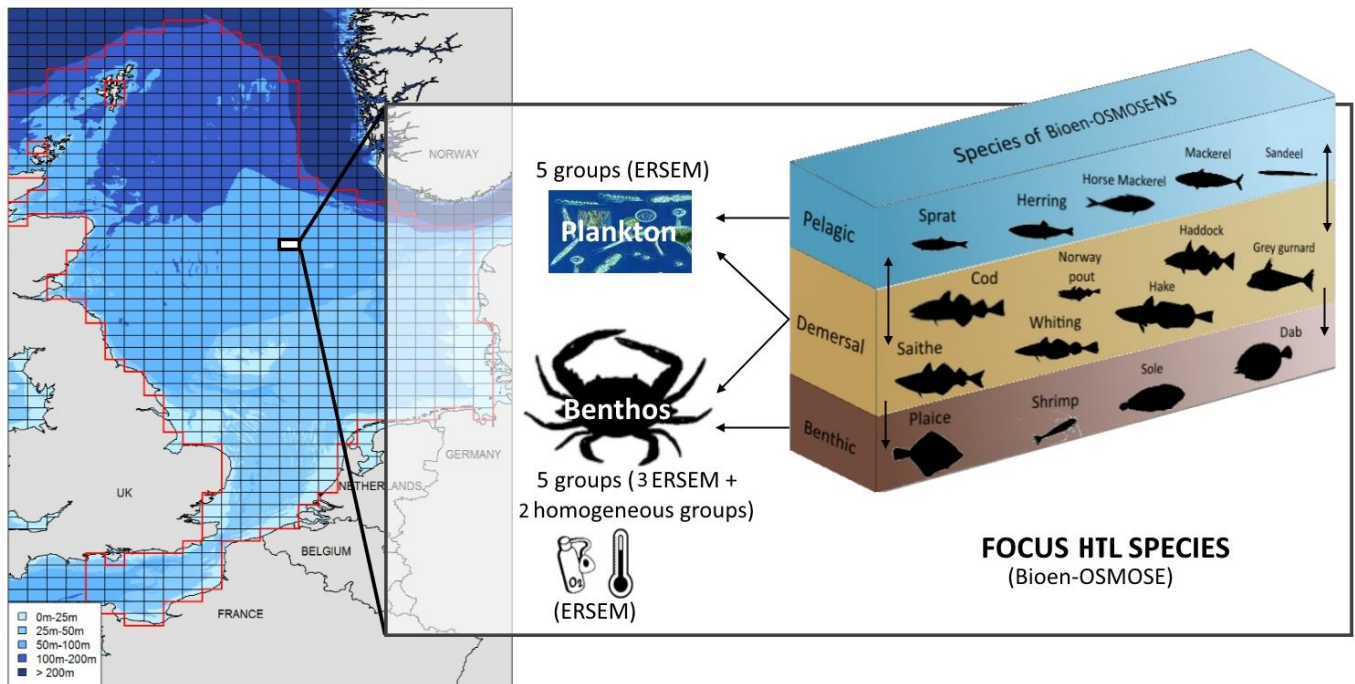


Figure 19: Summary of the Bioen-OSMOSE-NS configuration, i.e., the Bioen-OSMOSE model applied to the North Sea and the Eastern Channel. Sixteen focus HTL species are explicitly modeled in Bioen-OSMOSE-NS. Outputs from the coupled POLCOMS-ERSEM model force Bioen-OSMOSE-NS: temperature, oxygen, and the biomass of 8 LTL plankton and benthic groups. Two homogeneous benthic groups are added to represent large benthic prey.

3.2.4 Simulations and processing of the outputs

The outputs were obtained by running the calibrated configuration for 80 years. The first 70 years were used as a spin-up period to insure reaching a steady-state and only the last 10 years were considered for the results. The realized TPCs of net energy rate E_p for each life-stage of each species were constructed in the following way. Within each cell and at each time step, the average value of realized net energy rate E_p across all schools of the same species and the same life-stage was computed and recorded with the corresponding temperature in the cell. The resulting dataset of spatiotemporally varying combinations of average realized net energy rate E_p and temperature was then used to construct the realized net energy TPC per species and life-stage. Three life stages were considered: the early-life stage, i.e., the larval and post-larval fast growth stage (before 1 year-old),

the juvenile stage, i.e., between 1 year-old and sexual maturation, and the adult stage after sexual maturation. The realized net energy TPC depends on varying available food biomass F and dissolved oxygen saturation $[O_2]$ across temperature values. We denote it as $E_{O_2,F}(T)$ to account for this dependency. In contrast, the fundamental TPC is independent from food and oxygen conditions and we denote it as $E_{:,}(T)$. It was constructed as the response of net energy for tissue production E_P to temperature under optimal food and oxygen conditions, i.e., with ingestion I at its maximum and dissolved oxygen saturation at 100%.

The relative difference between the fundamental $E_{:,}(T)$ and realized $E_{O_2,F}(T)$ TPCs, denoted $D_{O_2,F}$, was estimated as the mean relative difference between fundamental and realized TPCs across all the

n data points per life stage: $D_{O_2,F} = \frac{1}{n} \sum_{j=1}^n \frac{E_{:,}(T_j) - E_{O_2,F}(T_j)}{E_{:,}(T_j)}$. The two sources of this difference, food

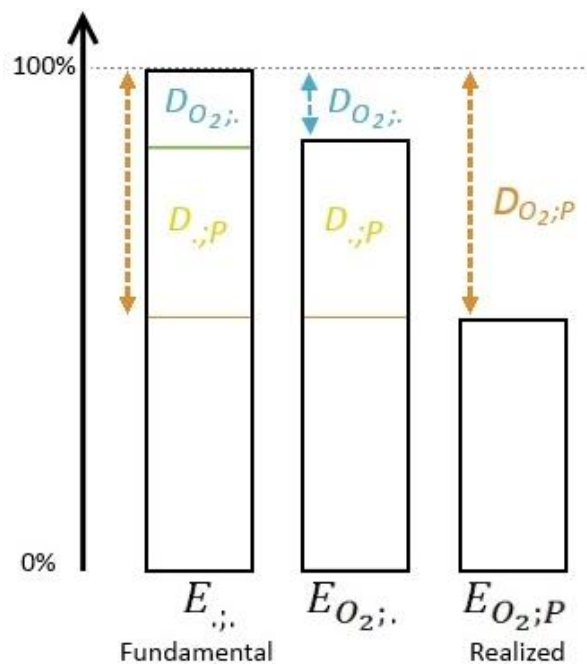
limitation and unsaturated O_2 conditions, were further disentangled (see Figure 20). First, we

estimated the realized net energy TPCs under optimal food conditions only $E_{O_2,:}(T)$ using species

habitat map per life stage and spatiotemporal variation of temperature and oxygen in the

corresponding habitat given by the POLCOMS-ERSEM model. Second, the relative difference between

$E_{O_2,:}(T)$ and the fundamental TPC $E_{:,}(T)$ allowed estimating the difference due to oxygen limitation



$D_{O_2,:}$ (see Figure 20). Third, the remaining

difference to reach $D_{O_2,F}$ was then the

consequences of food limitation and allowed

estimating directly $D_{:,F}$ without the need to

estimate the realized net energy TPC under

optimal oxygen conditions only $E_{:,F}(T)$.

Figure 20: Sources of difference between fundamental and realized net energy TPCs and how to disentangle them. The fundamental net energy TPC is the reference level considered as 100% of possible net energy across temperatures.

3.3 Results

3.3.1 Comparison of fundamental and realized net energy TPCs

The realized net energy TPCs differed from the fundamental ones for all life stages for all species with the early stage being the most different (Figure 21). The realized early stage TPC differed both in shape (e.g., a 'V-shape' instead of a dome-shape for haddock, norway pout and saithe) and absolute level from the fundamental one for all species. In contrast, the realized adult TPC shape was similar to the fundamental one, the main difference between realized and fundamental TPC being the absolute level of net energy rate. This difference increased when temperature got closer to the fundamental optimal temperature T_{opt} . For a majority of species, the realized juvenile TPC was similar to the adult one, except for herring, sandeel sprat, and plaice.

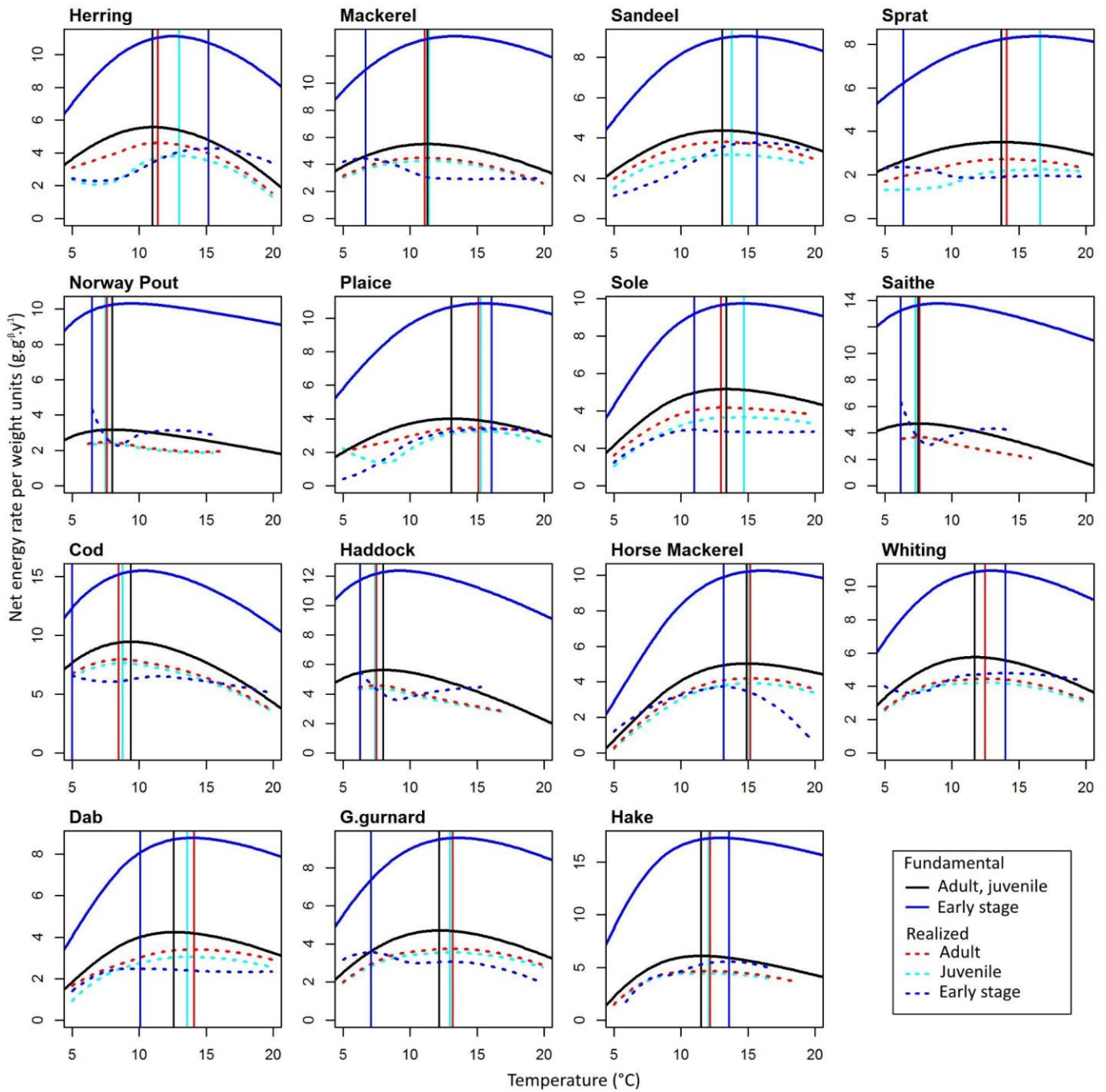


Figure 21: Fundamental and realized net energy TPCs per species and life stage. The fundamental TPC is calculated for a maximal ingestion rate, i.e., under optimal food, and oxygen conditions and depicted by the black continuous curves for juvenile and adult stages and the dark blue ones for the early stage. The red, the light blue and the dark blue dashed curves are the realized TPCs for the adult, juvenile and early stage, respectively. Vertical lines indicate temperatures at which the net energy rate is highest (T_{opt}). G. gurnard stands for Grey gurnard hereafter.

Table 3 : Fundamental optimal temperature T_{opt} per species (°C) and its realized counterpart per species and life stage. The last column is the standardized sum of squared differences between the fundamental and the realized T_{opt} for all three stages. The value in bold indicates the life stage for which the realized T_{opt} is the most distant from the fundamental one.

Species	T_{opt} early stage	T_{opt} juveniles	T_{opt} adult	Fundamental T_{opt}	Standardized sum square
Herring	15.2	13	11.4	11	2
Mackerel	6.7	11.4	11.1	11.3	1.9
Sandeel	15.7	13.8	13.1	13.1	0.6
Sprat	6.4	16.6	14.1	13.7	4.5
N. Pout	6.5	7.5	7.6	8	0.3
Plaice	16.1	15.3	15.1	13.1	1.4
Sole	11	14.7	13	13.4	0.6
Saithe	6.2	7.3	7.6	7.5	0.2
Cod	4	8.8	8.5	9.4	3.2
Haddock	6.3	7.4	7.5	8	0.4
H. Mackerel	13.2	15.1	15.2	14.9	0.2
Whiting	14	12.5	12.5	11.7	0.6
Dab	10.1	13.6	14.1	12.6	0.8
G. gurnard	7.1	13	13.2	12.2	2.3
Hake	13.6	12.1	12.2	11.5	0.5

For all species, the temperature T_{opt} at which the net energy rate is highest along the fundamental TPC was in the range of temperature values faced in the NS (Table 3). However, there were differences between fundamental and realized T_{opt} that varied across species and life stages (Table 3; Figure 21). Five species had the most similar fundamental and realized T_{opt} across life stages: Norway pout, saithe, haddock, horse mackerel, and hake (sum of squared differences in Table 3). In contrast, herring, mackerel, sprat, cod and grey gurnard were the species with the most different realized and fundamental T_{opt} . Across all species, the early stage was the stage for which realized T_{opt} differed most from the fundamental one for all the species (bolds values in Table 3).

3.3.2 Seasonal variation in net energy rate

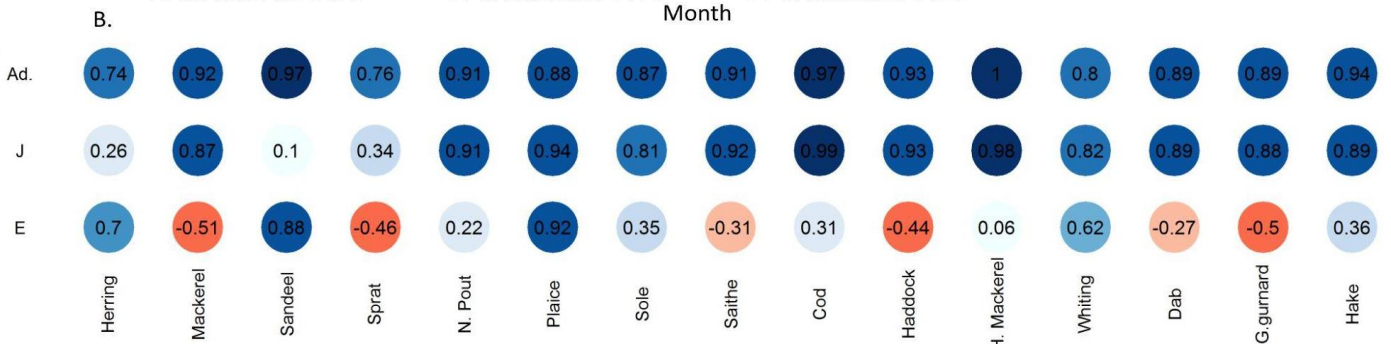
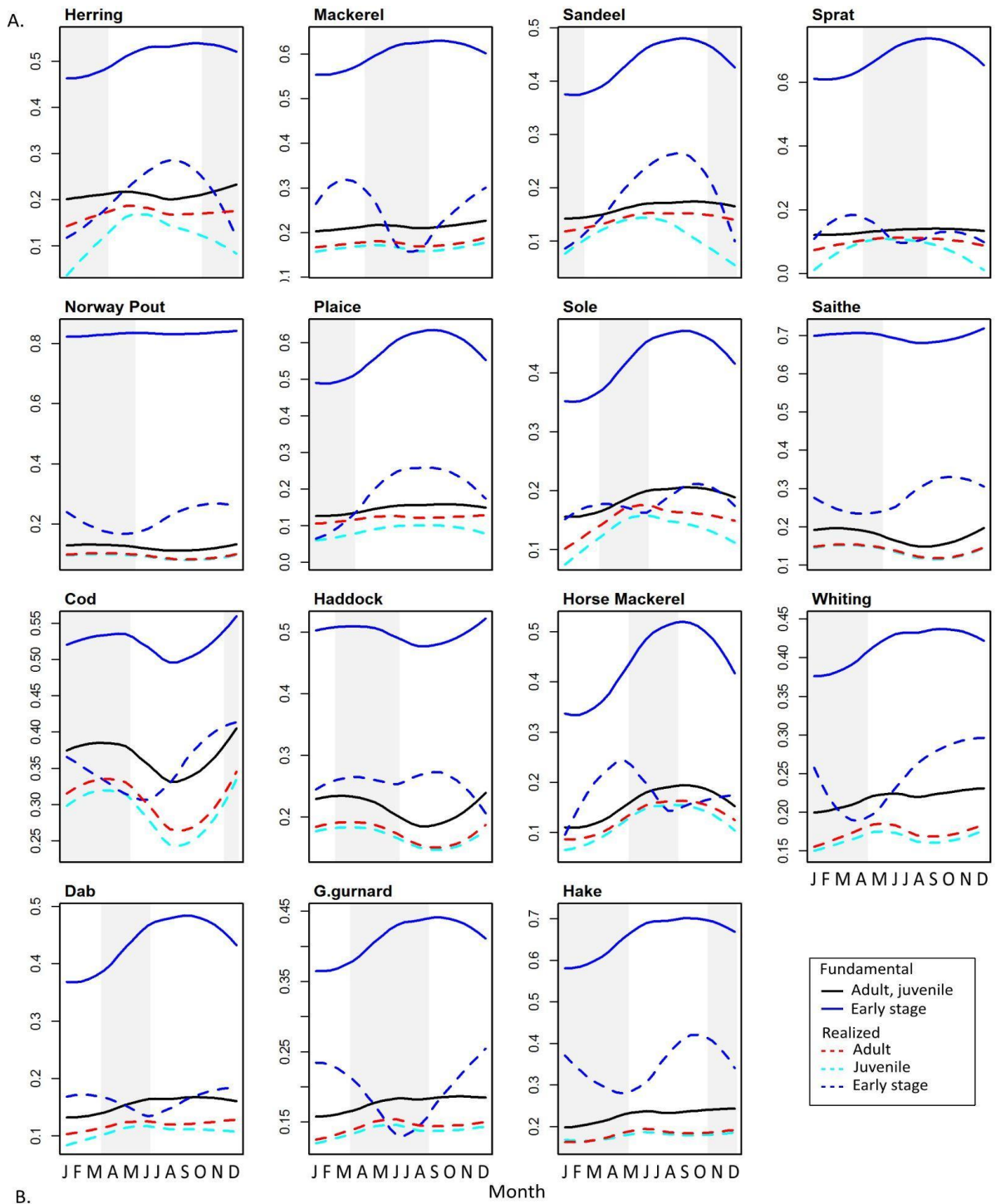


Figure 22: (A) Seasonal variation of the net energy rate per gram of individual at the energy acquisition power, per species, per life stage. The grey areas are the species' reproductive seasons. (B) Temporal correlations between seasonal variations of realized and fundamental net energy rates at early stage (E), juvenile (J) stage and adult (Ad.) stage.

The fundamental and realized net energy rates varied during the year (Figure 22A). The variation of the fundamental net energy was only due to temperature here. For adults, the almost constant difference between fundamental and realized net energy rate throughout the year indicated that seasonal variations of realized net energy rate were mainly driven by temperature as shown by the high correlations between the two rates (Figure 22B). The difference in absolute value was driven by other factors (see next subsection and Figure 23). For a majority of species, results were similar for juveniles, with absolute values of net energy rate inferior or equal to that of adults. However, for herring, sandeel, and sprat, seasonal variations of the realized net energy rate did not follow the same pattern as those of fundamental net energy rate (Figure 22A) which resulted in low correlations between the two rates (Figure 22B).

For early stages, the dominant pattern was a strong decrease of realized net energy rate during the reproductive season (grey areas in Figure 22A). For 11 species out of 15, this resulted in weak or even negative correlations between seasonal variations of realized net energy rate and fundamental net energy rate response to temperature (Figure 22B). In contrast, for the four other species (herring, sandeel, plaice and whiting), the correlations were strongly positive (Figure 22B).

3.3.3 Disentangling the sources of difference between fundamental and realized net energy TPCs

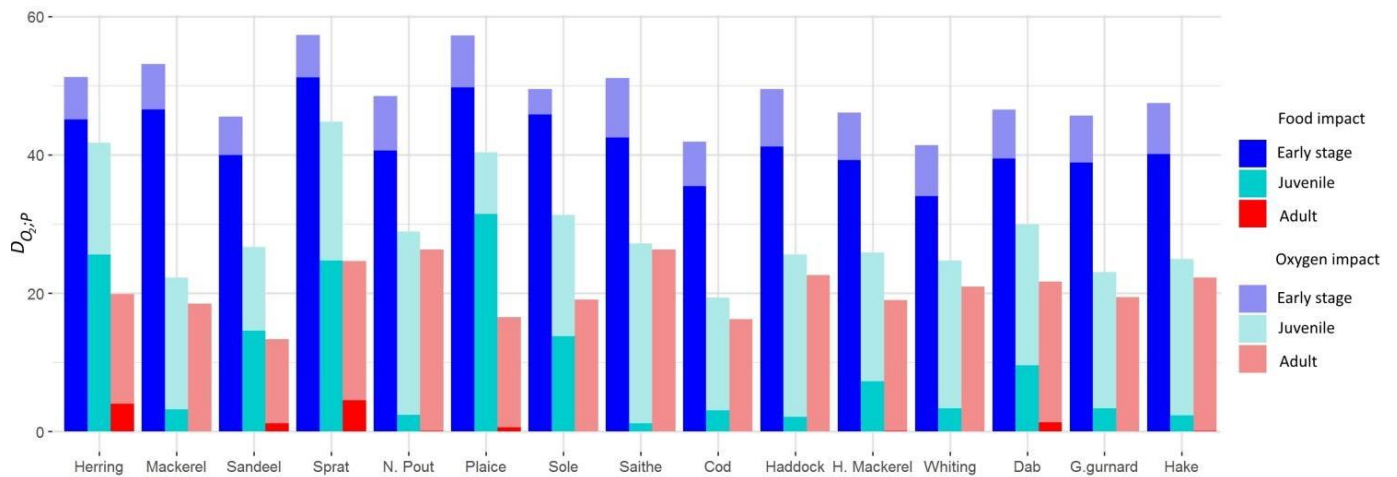


Figure 23: Percent difference between fundamental and realized net energy TPCs according to life stage and source of difference. For each species, the 3 stacked bars represent the relative difference between the fundamental and the realized TPC $D_{O_2,P}$ for the 3 life stages. Limited food and limited oxygen conditions can both contribute to this difference. Therefore, each stacked bar is subdivided into two parts: the light color part corresponds to the difference due to oxygen limitation D_{O_2} , and the dark color part is the difference explained by food limitation $D_{,P}$.

In our model, the difference between fundamental and realized net energy TPCs is the consequence of a non-saturated environment in oxygen and/or limited food availability. These sources of difference can be disentangled for each species and life stage (Figure 23). The pattern of change between life stages in the difference between fundamental and realized TPCs and in the relative contribution of O_2 and food limitations was relatively similar across species. Early stages exhibited the largest differences between fundamental and realized TPCs with differences ranging from 41.3% to 57.3%. Juvenile stages displayed intermediate differences ranging from 19.4% to 44.8%. Adult stages presented the smallest differences, which ranged from 13.3% to 26.3%. In addition to the decrease in differences between TPCs for the older life stages, the model results showed that the main source of the differences switches from food limitation to oxygen limitation with aging. The relative contribution of food limitation $D_{,P}$ ranged from 82.3% to 92.8% of $D_{O_2,P}$. (7.2% to 17.7% for the contribution of oxygen limitation D_{O_2} .) of the total difference between TPCs at the early stage, from 4.4% to 78% (22% to 95.6% for D_{O_2} .) at the juvenile stage, and from 0 to 20.2% (79.8% to 100% for D_{O_2} .) at the adult stage. Whereas the relative contribution of the two sources could vary a lot between species and life stages, the difference between TPCs due to oxygen limitation D_{O_2} was

relatively moderate, ranging from 5.5% to 25.2% of the fundamental net energy TPC, whereas the part of the difference due to food limitation exhibited more extreme values that ranged from 0% to 51.9%.

3.3.4 Trophic level effect on the difference between fundamental and realized net energy TPCs

Table 4: Result of an ANCOVA model of the difference due to food limitation $D_{:,p}$ explained by trophic level, life stage, and the interaction between the two variables. ($R^2 = 0.93$). Type II F tests for the significance of explanatory variables are presented together with estimated coefficients, their standard error (SE) and significance level (F tests). The residual df is 39. Trophic level was centered around a value of 2 and the coefficients are presented per life stage to facilitate interpretation.

Explanatory variable	df	F value	Variable P (>F)	Coefficient	Estimate	SE	t values	Coefficient P (> t)
Trophic level	1	22.5	<0.001	Early stage slope	-12.5	5.8	-2.2	0.05
				Juvenile slope	-21.7	3.9	-5.5	<0.001
				Adult slope	-2.5	1	-2.5	0.03
Stage	2	129.1	<0.001	Early stage intercept	55.4	17.8	4.5	<0.001
				Juvenile intercept	40.8	13.6	6.2	<0.001
				Adult intercept	4.9	19.8	-3.7	0.01
Trophic level:Stage	2	5.9	0.006					

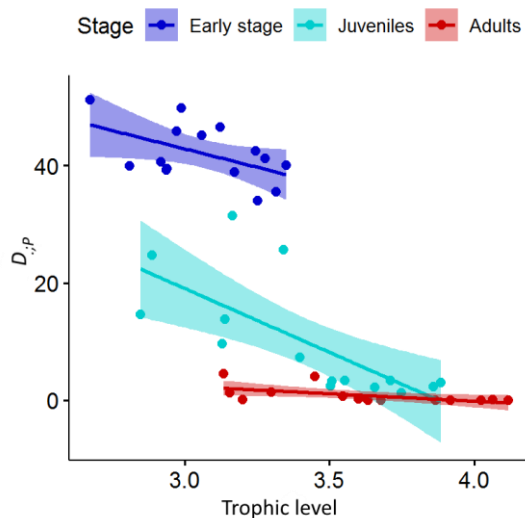


Figure 24: Difference between fundamental and realized net energy rate TPCs due to food limitation, $D_{:,p}$, per life stage as a function of trophic level. The trophic level was estimated per species per life stage from the outputs of the model. The regression line coefficients are estimated with an ANCOVA model explaining the difference $D_{:,p}$ by trophic level as the continuous covariable and life-stage as a categorical factor (see Table 4).

The difference between fundamental and realized net energy TPCs due to food limitation $D_{:,p}$ decreased significantly with species trophic level (Table 4, negative slope for the various life stages) and tended towards zero for the highest trophic levels (trophic level around 4) (Figure 24). The interaction between trophic level and life stage was significant overall (Table 4) indicating varying responses to trophic level across life-stages although always in the direction of a decrease. Trophic level had a significant effect on $D_{:,p}$ for the three stages (Table 4): $D_{:,p}$ decreased by 21.7%, 12.53% and 2.5% per trophic level TL for juveniles, early stage and adults, respectively. The intercept values decreased with older life stages: early stage intercept was higher than the juvenile one that was higher than the adult one (Figure 24 and Table 4), which confirmed that the difference between TPCs due to food limitation decreased with ageing and ontogeny (see previous subsection and Figure 23).

3.4 Discussion

3.4.1 Oxygen and food availability: two crucial physiological performances drivers

The estimation of fundamental TPCs of the AS has been developed to understand the response of individuals' performances or fitness to temperature (Pörtner et al., 2017) and to project future population dynamics under climate change scenarios (Pörtner, 2021; Pörtner and Farrell, 2008). However, the missing link between the estimation of aerobic scope TPCs in controlled conditions in the laboratory and their potential applications is to understand how the physiological response to *in situ* conditions impacts the realized TPC (Jutfelt et al., 2018). Using an individual-based spatialized trophic web model accounting for individual-level bioenergetics, this study develops and applies a method to estimate the differences between fundamental and realized TPCs. The originality of our study is that we model not only the direct effect of temperature on individuals' physiological performances, but also the effect of oxygen saturation and food spatiotemporal dynamics. Therefore, our study can both account for the indirect effects of temperature due to oxygen

saturation and food abundance that covary with temperature and disentangle the effect of each component on the realized TPC.

Whatever the driver, the realized net energy TPC is always lower than the fundamental one, which corroborates the idea raised by Jutfelt et al. (2018) that the temperature is only a permissive factor of the realized performances. The drivers of the difference between the fundamental and realized TPCs, $D_{O_2;F}$, are oxygen unsaturation and food limitation for all the species for at least one life stage (Figure 23). At the early life stage, the main driver of $D_{O_2;F}$ is food limitation whereas, at the adult stage, it is oxygen unsaturation.

3.4.2 Omnivory degree and trophic level explain variation across life stages and species of the effect of food limitation on realized TPCs

A previous study using the same model configuration has shown that the diet at early life and adult stages is not composed of the same prey (Morell et al. submitted; Chap. 2), consistently with field data in the same area (Pinnegar, 2014; Timmerman et al., 2020). Switches in diet between ontogenetic life stages could explain the significant effect of life stage on the difference between fundamental and realized TPCs due to food limitation. Early life stages feed mainly on phytoplankton and zooplankton which are highly variable in terms of abundance: there is an indirect bottom-up effect of temperature on realized TPC through co-variation of plankton production with temperature. In contrast, adults feed on macro-zooplankton mainly for pelagic species and on benthic prey or small fish for demersal and benthic species (Morell et al. submitted; Chap. 2). The abundance of these prey is relatively stable over the year compared to phytoplankton, so that the indirect effect of temperature on physiology due to food availability is low or null for adults. In addition, $D_{.,p}$ is lower for demersal and benthic species (e.g., hake, grey gurnard, dab, whiting in Figure 23) that have higher prey diversity and thus are highly omnivorous: the spatio-temporal mismatch with a prey can be

compensated with another one. The difference between fundamental and realized TPCs due to food limitation $D_{:,p}$ can thus be considered as a physiological consequence of the interaction between the match/mismatch hypothesis and the degree of omnivory of predators (Cushing, 1990). Species or early life stages that are specialist feeders potentially face a high rate of mismatch with their prey and thus have a high $D_{:,p}$ whereas species and adult life stage that are more omnivorous have a high encounter rate with prey and thus a low or null $D_{:,p}$.

A similar reasoning applies to the interpretation of the effect of trophic level: $D_{:,p}$ decreases with trophic level, across species, life stages and within life stages (Figure 24), until a threshold of TL=3.6. Above this value, $D_{:,p}$ is very close or equal to 0. The species diets emerging from opportunistic size-based predation in the model show that large benthos, which has a TL of 2.6, is a major prey of demersal and benthic adult individuals (Morell et al. submitted; Chap. 2). Large benthos is temporally and spatially homogeneous in the model, and likely not limiting, which results in a null or low $D_{:,p}$. The simplified description of the benthic groups limits the generalization of this result. Nevertheless, it is interesting to highlight that a species and/or life stage that has a spatiotemporally stable food source has little or no difference between its fundamental and realized TPC unless oxygen is limiting.

Our predictions about the food impact on realized TPCs are useful to consider in predictive studies. First, the fact that $D_{:,p}$ decreases with older stages and with TL are key outcomes in this sense. Second, to refine the effect of food limitation on realized TPC, our results suggest to take into account not only the level of food production in a system (primary production is often taken as a proxy but it could be misleading here), but also the level of match-mismatch between predators and prey (and therefore their spatio-temporal dynamics), and the degree of omnivory of predators. More generally, to identify the applicability of fundamental TPCs in predictive study, it would be interesting to apply this framework to other systems (such as upwelling, tropical or deep ecosystems) to emphasize the TL range and/or systems and/or species for which the fundamental TPCs is reliable.

3.4.3 Deoxygenation effect on realized TPCs remains weak in the absence of hypoxia

Our results indicate that oxygen saturation is the main contributor of $D_{O_2;P}$ at juvenile and adult stages (Figure 23), except for the juveniles of herring, sandeel, sprat and plaice. For these groups, the realized TPC has the same shape as the fundamental TPC, shifted to lower absolute rate values (Figure 21). Our results on seasonal variations in net energy rates suggest that oxygen limitation drives a constant difference between fundamental and realized net energy rate over the year, and thus with temperature variation (see Figure 22 for the adult and juvenile phases for which oxygen appears as the main driver of $D_{O_2;P}$ in Figure 23). These results are consistent with the current oxygen conditions in the NS ecosystem reported by several modeling studies, including the POLCOMS-ERSEM model used to force Bioen-OSMOSE-NS (Butenschön et al., 2016; Wakelin et al., 2020): the oxygen saturation is outside all species' hypoxic range (grey area Figure 18A) whatever the season and the location considered. In addition, the shape of the response of energy mobilization to oxygen saturation (yellow curve Figure 18A) implies a slow decrease of physiological performances with oxygen saturation reduction until a threshold corresponding to the upper limit of the hypoxia range (Thomas et al., 2019). The relative spatiotemporal stability of oxygen conditions in the North Sea, with oxygen saturation values ranging between 58% and 100%, combined with the weak mobilization rate response for this range of values (plateauing part of yellow curve Figure 18A) explain the homogeneous impact of oxygen between species and over the year. More generally, deoxygenation is expected to increase globally with (i) warming temperatures, (ii) increased stratification and (iii) eutrophication-induced hypoxia due to increased microbial activity in continental shelf regions (Laffoley and Baxter, 2019). The consequences on TPCs could respectively imply (i) a shift of realized TPCs towards lower values of net energy rate than the fundamental ones without modification of its dome-shaped curve, (ii) a differential impact on marine organisms according to their water column position with benthic species facing an increase of the difference

between fundamental and realized TPCs due to stratification and (iii) a modification of realized TPC shape at temperatures observed within hypoxic areas due to eutrophication. The future presence of hypoxic areas is one of the main events that will impact realized T_{opt} and more generally realized TPCs in future conditions.

3.4.4 Early life stage realized TPCs differ most from fundamental TPCs due to trophic competition

The early life stages are the most experimentally studied life stages in fisheries sciences (Catalán et al., 2019) and have been identified as pivotal (Hjort, 1914; Houde, 2008) due to multiple factors such as ontogenic critical stages (Joly et al., 2021), physiological limiting trade-offs (Di Pane et al., 2019), and their impact on recruitment (Olsen et al., 2011; Payne et al., 2009). Our results suggest that the early life stages are also critical regarding the difference between fundamental and realized TPCs due to extrinsic factors, mainly food limitation (Figure 23). This is consistent with the food limitation hypothesis that would drive recruitment success (Le Pape and Bonhommeau, 2015). Food limitation at the individual scale for early life stages is mainly driven by two mechanisms: planktonic prey biomass and competitors' abundance. Prey biomass limits the thermal performance of early life stages throughout the year, as their net energy rate never reaches the fundamental performance curve. However, the dynamics of prey biomass is not the only driver of the realized net energy dynamics. If this was the case, we would have expected the same variation of net energy rate over the year for all species, contrary to what the model's outputs show (Figure 22A). However, our results show that realized net energy seasonal variations are species dependent and linked to the reproductive season. The realized net energy rate decreases and reaches a minimum during the reproductive season for all species (Figure 22A). The first reason for this is a high intraspecific competition at this stage, which is maximum at the end of the reproductive season as the early stage abundance of the species peaks. The decrease in net energy rate at the time of each species' abundance peak highlights the high intraspecific density dependence caused by competition for food

resources at this stage. Symmetrically, intraspecific competition is relaxed and the net energy rate increases after the reproductive period because (i) individuals are larger than during the reproductive season and therefore have access to a diet which is more diverse and that fluctuates less over the year and (ii) early stage abundance strongly decreases because of high mortality during this stage.

The high competition and density dependence at this stage are commonly observed in the NS ecosystem, due to the spatialized life cycle of the majority of the species for which the early life stages are concentrated in nurseries (Bastrikin et al., 2014; Bolle et al., 1994; MacKenzie, 1985). In the NS ecosystem, the majority of the species spawn in late winter and spring. As we do not observe a decrease of realized net energy rate during spring for non-spring spawner species (e.g., horse mackerel), we hypothesize that our result is mainly explained by intraspecific competition. In the study area, nurseries do not overlap between species (Cariou et al., 2021) and the larvae assemblages vary over the year (Di Pane et al., 2020), which limits possibilities for interspecific competition during the early life stage. Contextualized in a temperate ecosystem with a high spatial specialization of the reproductive event per species, our results underline mainly a high intraspecific competition. Similar studies in tropical ecosystems where the majority of species are income breeders with continuous productivity could shed light on the impact of interspecific competition at the early stage on realized TPCs.

Our model uses a unique fundamental TPC shape across life stages per species denoting similar thermal tolerance throughout ontogeny (but notice that the fundamental TPC of the early life stage is homogeneously shifted towards higher values relative to older stages due to higher ingestion rate; Figure 20). Experimental data have shown changes in thermal tolerance between life stages (F. T. Dahlke et al., 2020; Pörtner and Peck, 2010). Early stages are actually expected to have a narrower thermal tolerance window than older ones (Pörtner and Peck, 2010). A narrower thermal niche for the early stage would modify quantitatively the value of $D_{O_2;P}$ but the qualitative results would remain identical as suggested in Figure 21: the early life stage realized TPC is lower than the

fundamental one for all species, for any temperature. In consequence, a more realistic narrower fundamental TPC for the early stage would imply a narrower but still lower realized TPC due to trophic and oxygen drivers.

3.4.5 Consequences for thermal studies

Our results underline qualitative considerations necessary to correctly use thermal preferences in studies projecting populations or communities responses to future climate scenarios. The fundamental TPC constrains the realized one: the latter is different and lower than the former for all species, all life stages and all temperatures (Figure 21). This suggests that using fundamental TPCs would tend to globally overestimate energy acquisition, and thus net energy rate and fitness, at the individual level. As individual properties determine population demographic rates (Stearns, 1992), energy acquisition overestimation at the individual level would lead to overestimation of population productivity. At the population level, a poor prediction of individual traits with an erroneous use of fundamental TPCs will propagate errors to the estimation of the population fitness and demographic rate of increase (Metz et al., 1992; Stearns, 1992). Lastly, the over-estimation of physiological performances implies an underestimation and an overestimation of the lower (T_{min}) and upper (T_{max}) temperature of species thermal tolerance range, respectively. Notably, the overestimation of T_{max} involves mis-predicting species local persistence with warming temperature and implies an overestimation of the resilience of populations and consequently the resilience of communities.

Our results also indicate the limits of laboratory studies to estimate the realized T_{opt} . In situ conditions, such as oxygen saturation and prey availability, modify the optimal temperature at which the realized TPC is at maximum (Table 3). The fundamental T_{opt} is life-stage dependent due to intrinsic factors (Dahlke et al., 2020). It appears that the realized T_{opt} is also life-stage dependent due to extrinsic factors (Table 3). The early stages have their T_{opt} farthest from the fundamental ones. The fundamental T_{opt} is a better approximation of realized T_{opt} for adults and juveniles. Likewise,

the realized T_{opt} for highest trophic level species is well approximated by the fundamental ones. These results indicate that the fundamental T_{opt} can be a good measure of the realized one when extrinsic factors such as oxygen and food are not limiting or when extrinsic factor limitations are constant with temperature. Reversely, the estimation of T_{opt} from species occurrence data should be used carefully: the T_{opt} obtained with this method would be valid to extrapolate species persistence under modified temperatures only if all other environmental conditions remain unchanged. Our results reinforce the need to include trophic relationships in climate niche models in addition to abiotic factors as temperature and oxygen. In addition, obtaining physiological realized performance data could help improve the modeling of species future spatial distributions and of their demographic responses to climate change (Talluto et al., 2016).

3.4.6 Projections under climate change scenario

Understanding how realized TPCs emerge from fundamental ones is necessary to improve the accuracy of future projections of rising temperature impacts on marine biodiversity. As individual performances are determined by abiotic and biotic factors, an integrative framework is needed to understand the direct and indirect effects of temperature on marine species performances. The estimation of the realized TPC could be a first step to understand the indirect effect of temperature as a consequence of its direct effect on interacting species. Rubalcaba et al. (2020) have shown that oxygen and temperature are crucial to estimate metabolic performances and then ecological niches to understand climate change impacts. Our results indicate that trophic relationships are also key to understanding physiological performance variation with temperature and thus climate change impacts. Albouy et al. (2014) showed that trophic interactions are crucial to project future species distribution and persistence. As our framework mechanistically accounts for temperature, oxygen and trophic effects on physiological performances, the next step would be to understand the link between current realized physiological performances, population dynamics and future species persistence.

In order to identify the link between realized physiological performances and future species persistence, our modeling framework is potentially usable in forecast simulations under climate change scenarios. Hypoxic areas in the NS are expected (Wakelin et al., 2020) and are one of the factors that will impact future realized TPCs for all species in the area. Modification in primary production in the future (Holt et al., 2012; Skogen et al., 2014) and potential regime shift in secondary production in the NS, as observed in the past (Beaugrand, 2004), are susceptible to modify the realized T_{opt} and TPCs. Finally, the shrinking of nursery areas with coastal artificialization and earlier reproductive period (Pankhurst et al., 2011) should increase intraspecific competition or introduce interspecific competition even though it is not observed in the current state of the system. All these future modifications of the ecosystem will increase the difference between fundamental and realized T_{opt} for marine organisms. As climate change and land use are two of the main anthropogenic drivers of the loss of marine biodiversity (IPBES, 2019), it is of foremost importance to understand how realized physiological performances change in response to these pressures to be able to anticipate future ecosystem changes. Rising temperatures combined with other multiple anthropogenic pressures are expected to shift realized TPCs to lower values and to modify realized T_{opt} . The forecast of realized TPCs under future climatic scenarios is a necessary step to improve the projections of future physiological performances, the emerging traits and their consequences on system dynamics.

Chapter 4: Ev-OSMOSE: An eco-genetic marine ecosystem model

Alaia Morell, Yunne-Jai Shin, Nicolas Barrier, Morgane Travers-Trolet, Bruno Ernande

ABSTRACT

In the last decade, marine ecosystem models have been increasingly used to project interspecific biodiversity under various global change and management scenarios, considering ecological dynamics only. However, fish populations may also adapt to climate and fishing pressures, via evolutionary changes, leading to modifications in their life-history that could either mitigate or worsen, or even make irreversible, the impacts of these pressures. Building on the individual-based ecosystem model Bioen-OSMOSE, a multi-species eco-evolutionary model, Ev-Osmose, has been developed to account for evolutionary dynamics in biodiversity projections. A gametic inheritance module describing the individuals' genetic structure has been implemented. The genetic structure is defined by finite numbers of loci and alleles per locus that determine the genetic variability of growth, maturation and reproductive effort. Climate change and fishing activities will generate selection pressures on fish life-history traits that will respond through microevolution. This paper is an overview of the Ev-OSMOSE model. To illustrate the abilities of the Ev-OSMOSE model in representing realistic ecosystem dynamics, genotypic and phenotypic trait variability and consistent evolutionary patterns, we applied the model to the North Sea ecosystem. The ecosystem dynamics result from the confrontation of simulated and observed data of biomass, catch, maturation ogives and length at age. The emerging trait variability is confronted to length-at-age and maturation data. To verify the consistency of resulting evolutionary patterns, we follow the evolution of a fitness indicator. Overall, a convincing state of the system has been checked at these different biological

levels, that opens perspectives for using Ev-OSMOSE in different marine regions under global change and management scenarios impacts on different biological levels.

4.1 Introduction

Anthropogenic activities alter the ecological and evolutionary dynamics of marine ecosystems. In addition to inducing direct mortality, selective pressures such as fishing exploitation and climate change trigger changes in the life history traits of marine organisms due to evolutionary processes (Crozier and Hutchings, 2014; Heino et al., 2015). Knowledge about genetic diversity, its erosion, and its impact on organisms' traits has been identified as a gap in current knowledge (IPBES, 2019), while existing studies have shown that small changes in traits, which may be evolutionary in nature, can imply large demographic and whole-community and ecosystem changes, with potential consequences for human activities (Audzijonyte et al., 2013; Audzijonyte et al., 2014). Incorporating genetic diversity and the resulting potential for adaptation into marine ecosystem models (MEMs) is thus considered as a key future development (Heymans et al., 2020; Rose et al., 2010). New modelling frameworks are needed to properly account for evolutionary changes and their impacts at the ecosystem scale to improve the reliability of predictions (Naish and Hard, 2008).

The existing marine modeling studies for addressing human-induced evolution have primarily focused on fisheries-induced evolution. The main modeling framework in this field is the eco-genetic model (Dunlop et al., 2009b; Heino et al., 2015). Eco-genetic models are single species models that describe the individual's life history, genetic variability using a quantitative genetic approach, density dependence and fishing as a selection pressure. More generally, this modelling framework allows the study of any pressure that induces evolutionary changes in life history traits (e.g, climate change, see Waples and Audzijonyte, 2016). However, eco-genetic models generally apply to single species, rendering difficult the upscale to the community and ecosystem levels, for example by accounting for the multiple interspecies interactions and the potential selective pressures those interactions may induce.

OSMOSE is a spatially explicit, multi-species and individual-based modeling framework for regional marine ecosystems (Shin and Cury, 2004). It includes the marine high trophic level components (fish and macro invertebrate) and fishing pressure explicitly and it is forced by coupled physical-biogeochemical models to represent the entire ecosystem. In this paper, we describe Ev-OSMOSE, a new modelling framework that incorporates an eco-genetic sub-model into OSMOSE. The eco-genetic sub-model describes individual life history by expliciting genetic and phenotypic variability in life history traits for multiple species interacting in a food web. A bio-energetic sub-model, the Bioen-OSMOSE model (Morell et al. submitted; Chap. 2), describing the life history in response to biotic and abiotic conditions has already been integrated in the OSMOSE model resulting in a multispecies framework with a mechanistic modeling of life history. Our new framework Ev-OSMOSE includes the genetic and phenotypic variances of life history traits described by the bio-energetic sub-model and thus allows the description of life history micro-evolution and adaptation in response to pressures. To our knowledge, this new model is the first marine ecosystem model to take into account micro-evolution and adaptation. This framework allows the study of evolutionary and ecological dynamics and their interactions at the multi-species level. It also allows to address the impacts of predation, fishing and climate-induced evolution. Featuring genetic variability, life history evolution, and multispecies interactions in a single framework make the model suitable for projecting future genetic, functional, and species diversity under fisheries and climate change scenarios, with consistent mechanisms linking these three organizational levels of biodiversity.

In this paper, we provide a detailed description of the principles and equations of the Ev-OSMOSE framework. Parameterization guidelines are provided with an application to the North Sea ecosystem as a case study example. Results from the North Sea application are also provided to verify the consistency of the new model developments.

4.2 Materials and methods

4.2.1 Model description

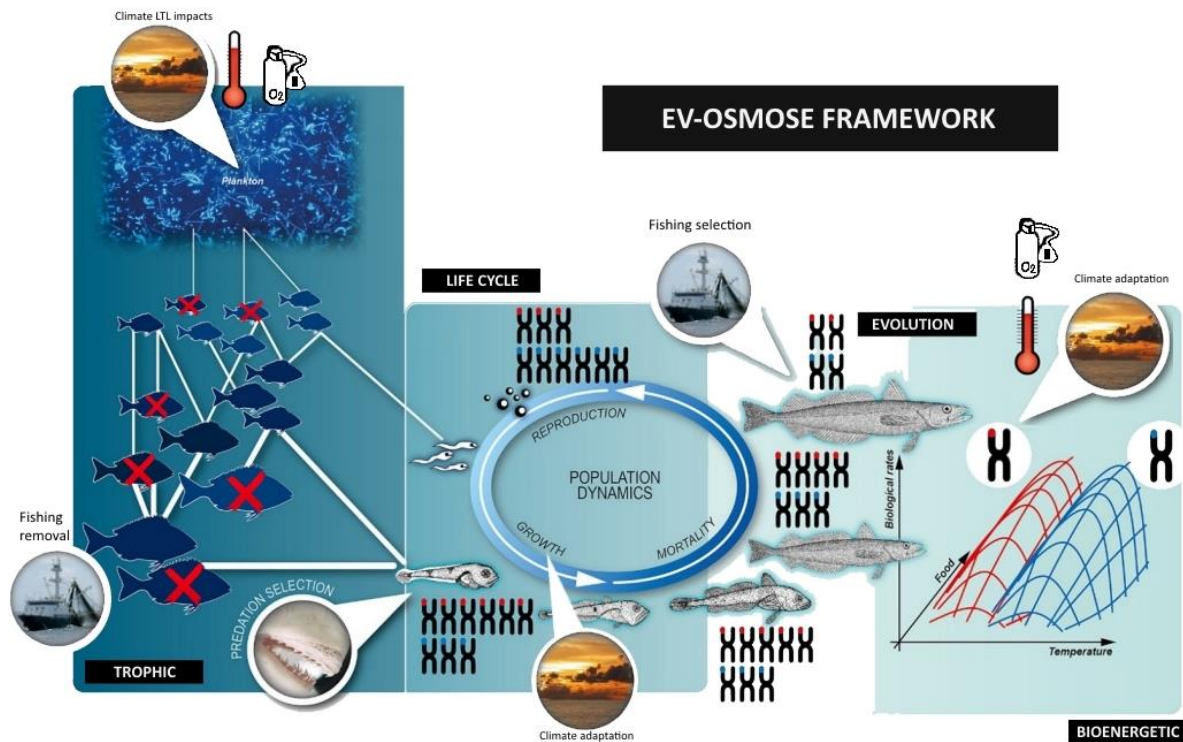


Figure 25: Graphical summary of the Ev-OSMOSE model. The Ev-OSMOSE model is a marine trophic web model where the trophic relationships emerge from species distributions per ontogenetic stage, spatiotemporal prey-predator co-occurrence and lengths adequacy, low trophic level (phytoplankton and zooplankton) biomass and species life cycle which is genetically determined and varies with temperature and oxygen.

The Ev-OSMOSE model represents the eco-evolutionary dynamics of fish communities in marine ecosystems (Figure 25). It is an individual-based, spatially-explicit multispecies model accounting for trophic interactions. The main characteristics of the model are opportunistic predation based on length and spatial co-occurrence of predators and prey, the mechanistic description of individuals' life-history traits emerging from genetics and bioenergetics, the consideration of inter-individual phenotypic variability due to both genotypic variability and plastic response to spatiotemporal variations in biotic and abiotic factors. The aim of the model is to explore the functioning and the eco-evolutionary dynamics of marine trophic webs, notably in response to perturbations such as fishing or climate change. The consequences of perturbations can be tracked from the individual genotype to the phenotype, to the population and to the community scale. The Ev-OSMOSE model

extends the existing OSMOSE model by (i) explicitly accounting for the dependence of life-history traits on bioenergetics that, in turn, are determined by individual's genotype, (ii) describing intra- and inter-specific genetic and abiotic phenotypic variability.

4.2.1.1 Biological unit, state variables and spatial characteristics

The biological unit of the model is a school (a super-individual in individual-based modeling terms). It is formed of individuals from the same species that are biologically identical, i.e., whose state variables have the same values. Individuals are all diploid hermaphrodites, i.e., males and females are not distinguished except, although the model is based on female life history. The state variables characterizing a school i at time step t belong to five categories (see Table 5Table 6 for definitions and units):

- Trait genetic determinism and expression that include individuals' genotype, composed of 2 alleles $A_{z,l,1}(i)$ and $A_{z,l,2}(i)$ at each of the l_z functional locus coding for each evolving trait z and 2 alleles $b_{l,1}(i)$ and $b_{l,2}(i)$ at each of l_b neutral locus, and the phenotypic expression noise $e_z(i)$ for each evolving trait z ;
- Ontogenic state of individuals described by their age $a(i, t)$, somatic mass $w(i, t)$ and gonadic mass $g(i, t)$;
- Abundance, namely the number of individuals in the school $N(i, t)$;
- Spatial location, i.e., the grid cell $c(i, t)$ where the school is located; and
- Taxonomic identity, i.e., the species $s(i)$ to which the school belongs.

A number of variables further characterizing the individuals of each school emerge from the three first categories of state variables (and thus are not strictly speaking state variables themselves). In terms of trait genetic determinism and expression, the effects of functional loci translate into a genotypic value $G_z(i)$ for each evolving trait z . Trait phenotypic values result from the influence of both the genotypic value $G_z(i)$ and the phenotypic expression noise $e_z(i)$. There are four evolving

traits in the model, and hence phenotypic values, namely maximum mass-specific ingestion rate $I_{\max}(i)$ that determines individuals' maximum energy uptake from predation, gonado-somatic index $r(i)$ that determines their energy allocation to somatic growth and reproduction, and two traits that specify their maturation schedule, that is the intercept $m_0(i)$ and the slope $m_1(i)$ of a deterministic linear maturation reaction norm (Stearns and Koella, 1986). Their evolution allows us to model the evolution of the three life history traits most described in response to fishing-induced evolution (Heino et al., 2015). Schools are also further described by emerging variables such as individuals' total body length $L(i, t)$ and their sexual maturity status $m(i, t)$ that allows distinguishing between juveniles and adults.

Fish schools are distributed on a horizontal spatial grid that is composed of regular cells and that covers the geographical range of the ecosystem represented. A cell c is characterized by its spatial coordinates, longitude $x(c)$ and latitude $y(c)$, and (i) physical and (ii) biogeochemical variables respectively: (i) the vertically-integrated value of physico-chemical factors $pc_k(c, t)$ (such as temperature $T(c, t)$ or the level of oxygen saturation (%) $[O_2](c, t)$; see the North Sea configuration in this paper as an example) and (ii) the biomass of each lower trophic level group (indexed by j) $B_{LTL}(c, t, j)$ that are not explicitly modeled but provided as input to Ev-OSMOSE from coupled hydrodynamic and biogeochemical models.

All schools belonging to the same species form a population and populations of different species form the fish community. Several aggregated population-based metrics can be tracked at the population level such as abundance $N(t)$, biomass $B(t)$, fishing catches $C(t)$ but also the genotypic and phenotypic means $\bar{G}_z(t)$ and $\bar{z}(t)$ and variances $\sigma_{A,z}^2(t)$ and $\sigma_z^2(t)$ of trait z (with $z \in \{I_{\max}, m_0, m_1, r\}$).

4.2.1.2 Design concepts

Ev-OSMOSE relies on a number of well-established concepts and theories and combines them in an original way to describe marine fish biodiversity and its dynamics from the intra-specific - genetic and phenotypic variability - to the inter-specific - taxonomic and trait-based - level. Previous multi-species models of fish communities have been designed to project interspecific biodiversity trajectories under various scenarios considering only ecological dynamics. However, fish populations may also adapt to natural and anthropogenic pressures via phenotypic plasticity and/or evolutionary changes, leading to modifications in their physiology and life-history that could either mitigate or worsen the consequences of these pressures. Ev-OSMOSE has been precisely developed to account for plastic and evolutionary dynamics in fish biodiversity projections by introducing the following elements to the existing OSMOSE model.

Ev-OSMOSE explicitly describes mendelian inheritance of quantitative traits determined by polygenic genotypes according to quantitative genetic principles. The genotypes are composed of a finite number of loci and alleles per locus with effects of heterogeneous amplitude (Soularue and Kremer, 2012), which allows accounting for realistic adaptive and neutral (genetic drift) evolutionary changes and genetic erosion induced by natural and anthropogenic selective pressures. Genetically determined quantitative traits affect individuals' bioenergetics and sexual maturation processes, which are described with a bioenergetic sub-model. The parameters names and units of the evolutionary sub-model are in Table 6.

Individuals' bioenergetics are described according to a biphasic growth model (Andersen, 2019; Boukal et al., 2014; Quince et al., 2008) in which body mass-dependent energy fluxes are allocated between competing processes —namely maintenance, somatic growth and gonadic growth— thus accounting for physiological trade-offs that constrain both phenotypically plastic and evolutionary responses of life-history traits to selective pressures (Roff, 1992; Stearns, 1992). Moreover, energy fluxes depend on temperature and dissolved oxygen so that metabolic rates follow the oxygen- and capacity-limited thermal tolerance theory (OCLTT; Pörtner, 2001). The details on the bioenergetic

sub-model are published in the description of the Bioen-OSMOSE model (Morell et al. submitted; Chap. 2).

4.2.1.3 Emerging properties: fitness, evolution and adaptation

Emergence of most phenomena or characteristics at higher organization levels than the individual one (e.g. population and community spatio-temporal dynamics, population and community age and length structures, species diet) are the same as in the original OSMOSE model.

Phenotypic values of schools' evolving traits— maximum ingestion rate $I_{\max}(i)$, gonado-somatic index $r(i)$, intercept $m_0(i)$ and slope $m_1(i)$ of the maturation reaction norm—are entirely determined by their genotype and a randomly drawn expression noise. In contrast, other individual variables or traits at higher integrative levels of organization (hereafter named “emerging variables”: somatic mass $w(i, t)$, length $L(i, t)$, gonadic mass $g(i, t)$ and thus fecundity $N_{eggs}(i, t)$, maturation age $a_m(i)$ and somatic mass $w_m(i)$ or length $L_m(i)$ at maturation) emerge from the combination of evolving traits' values, energy intake from length-based opportunistic predation and physiological or plastic responses of bioenergetics to ambient sea water temperature and dissolved oxygen concentration (Figure 26).

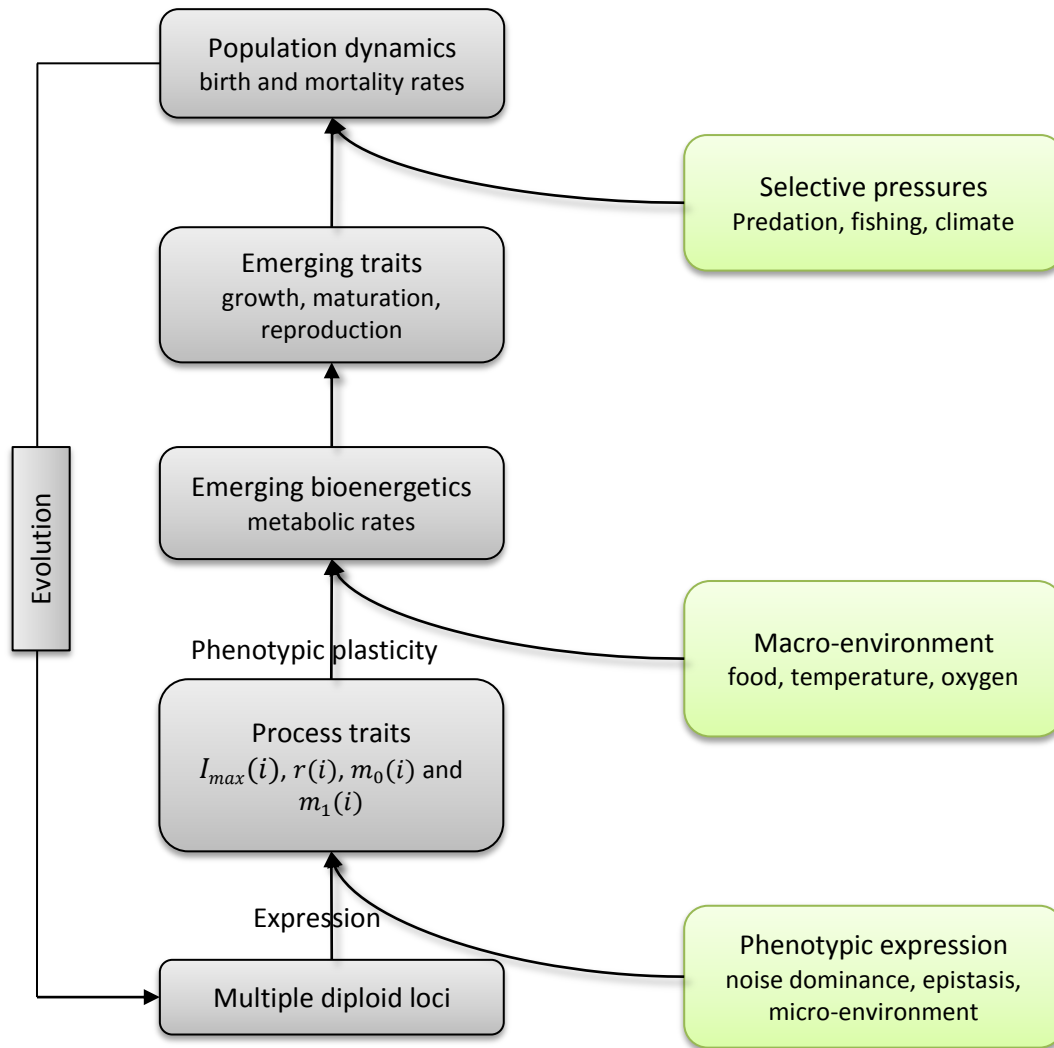


Figure 26: Ev-OSMOSE processes describing trait variations from loci to population level (grey) and the causes impacting trait values (green). The process traits are the traits underlying the physiological processes and trade-offs.

The distribution of genotypic and phenotypic values of evolving traits at the population level are fully prescribed initially by the values of the parameters describing genetic variability, namely the initial genotypic mean value $\overline{G}_z(0)$ and the initial additive genetic variance $\sigma_{A,z}^2(0)$, and the expression noise distribution, namely the expression variance $\sigma_{e,z}^2$, for a given trait z . As the simulation progresses, these distributions are affected by the processes of natural, fishing-induced and climate-induced selection and genetic drift so that their changes through time describe emerging evolutionary trajectories. Temporal changes in the phenotypic distribution of emerging variables

result from both the trajectories of the underlying evolving traits and phenotypically plastic responses to available food and ambient physico-chemical conditions.

The evolving trait values are variable in the populations and confer advantages or disadvantages in terms of survival and reproductive success relative to different pressures, notably predation, fishing, and climate changes. Therefore, Darwinian fitness, that governs the above-mentioned evolutionary trajectories together with genetic variability, emerges naturally from the modelled processes of mortality and reproduction. In consequence, populations may adapt to predation, fishing and climate change through evolution.

4.2.1.4 Initialization

For each species, the initial pool of allele values present in the population for each functional or neutral locus is randomly drawn from a prescribed distribution (see section 4.2.1.6.1 Genetic structure for details). The system starts with no school in the domain and is initialized by releasing eggs for every species during specific reproductive season time steps. For a given species, this seeding process stops when there is at least one mature individual in the population. The eggs are grouped in super-individuals, representing schools that are distributed spatially according to their habitat maps. During the spin-up period (until the system reaches an equilibrium), for each new school of eggs, a diploid genotype is randomly drawn from the functional and neutral pools of alleles at each locus. The mendelian transmission of genotype from parents to offspring starts at the end of the spin-up period.

4.2.1.5 Input

Ev-OSMOSE does not model oceanographic physical and chemical processes, but it is forced by spatially and temporally varying fields of temperature (°C) and oxygen (% of saturation) from coupled regional physical and biogeochemical models, data time series or from the regional downscaling of

earth system model outputs. As for the OSMOSE model, biomass prey fields are also used as input to provide LTL.

4.2.1.6 Genetic sub-model

The genetic sub-model introduces a source of intra-specific variability of the quantitative traits describing the individual life history, through additive genetic variance $\sigma_{A,z}^2$ and expression variance $\sigma_{e,z}^2$, and parental gene inheritance. The individuals are considered diploid hermaphrodites, i.e. without differentiation between males and females, the model being based on female life history. The genotypic values of the four heritable traits—maximum mass-specific ingestion rate I_{\max} , gonado-somatic index r , intercept m_0 and slope m_1 of linear maturation reaction norm—result from the expression of the corresponding functional loci. Neutral loci have no effect on individuals' phenotype: their evolution is the result of random drift. Hereafter, the genetic sub-model is described for any of the four evolving traits, generically denoted z .

4.2.1.6.1 Genetic structure

The genetic structure is described by a polygenic multi-allelic model with finite numbers of loci and alleles for both the functional and neutral parts of the genome. The value of trait z thus results from the expression of l_z functional loci, each of which has a pool of $n_{z,l}$ (with $l \in \{1, 2, \dots, l_z\}$) possible alleles in the initial population characterized by $n_{z,l}$ allelic values. Following classical quantitative genetics (Lynch and Walsh, 1998), we assume that the genotypic values $G_z(i)$ of trait z in the population initially follow a normal distribution $N(\overline{G_z}(0), \sigma_{A,z}^2(0))$ with $\overline{G_z}(0)$ the initial genotypic mean and $\sigma_{A,z}^2(0)$ the initial additive genetic variance. It follows (see justification in the next section) that the $n_{z,l}$ allelic values of locus l initially present in the population are randomly drawn from a normal distribution $N(0, \frac{\sigma_{A,z}^2(0)}{2.l_z})$ (Soularue and Kremer, 2012). This allelic model defines allelic values as deviations around the initial genotypic mean $\overline{G_z}(0)$ of the population and allows for

heterogeneous allelic values across loci coding for the same trait, many of them with minor effects and a few ones with major effects.

Similarly, the neutral part of the genome is described by l_b neutral loci, each of which has a pool of $n_{b,l}$ (with $l \in \{1,2,\dots,l_b\}$) possible alleles in the initial population characterized by their allelic values with no effect on evolving traits. The $n_{b,l}$ allelic identities of locus l initially present in the population are randomly drawn from a discrete uniform distribution with probability mass function $1/n_{b,l}$.

4.2.1.6.2 Traits' genetic determinism and expression

The two additive effect allele values $A_{z,l,1}(i)$ and $A_{z,l,2}(i)$ at a functional locus l ($l \in \{1,2,\dots,l_z\}$) coding for trait $z(i)$ of diploid individual i can each take one allelic value among the $n_{z,l}$ possible versions in the population. Alleles act additively at and between loci. Since allelic values describe deviations around the mean genotypic value of trait z , the genotype value $G_z(i)$ for trait $z(i)$ in school i is thus the sum of the initial genotypic mean $\overline{G_z}(0)$ of the trait for the population and of the two allelic values $A_{z,l,k}(i)$ at each locus l coding for the trait of interest.

$$G_z(i) = \overline{G_z}(0) + \sum_{l=1}^{l_z} (A_{z,l,1}(i) + A_{z,l,2}(i)) \quad (16)$$

Given the normal distribution additive property and that the initial distributions $N(0, \frac{\sigma_{A,z}^2(0)}{2.l_z})$ of allelic values in the population are independent between loci, the initial distribution of genotypic values $G_z(i)$ in the population thus follows a normal distribution $N(\overline{G_z}(0), \sigma_{A,z}^2(0))$. At later time steps t , the processes of selection, drift and inheritance will modify this distribution in terms of its mean $\overline{G_z}(t)$ and its variance $\sigma_{A,z}^2(t)$ but also potentially in terms of its shape as it is not constrained to remain normally distributed.

In Ev-OSMOSE, part of the phenotypic expression of emerging variables (e.g., somatic mass $w(i, t)$, gonadic mass $g(i, t)$, length $L_m(i)$ at maturation) is due to the bioenergetic responses to conditions faced by an individual: the available food, the temperature and the oxygen concentration in the

environment during the entire individual life cycle. In contrast, the four evolving traits (maximum mass-specific ingestion rate I_{\max} , gonado-somatic index r , intercept m_0 and slope m_1 of linear maturation reaction norm) describe underlying individual characteristics whose phenotypic expression does not depend on these “macro-environmental” conditions. Yet, the phenotypic expression of evolving traits will also be affected by dominance and recessivity of alleles at the same locus and epistasis between loci, which are not modeled explicitly in the present genetic model, as well as by “micro-environmental” variations capturing the potentially unaccounted effects of individuals’ internal environment or external micro-environment (Lynch and Walsh, 1998). These sources of phenotypic variability for evolving trait z are implicitly represented by an expression noise $e_z(i)$ randomly drawn from a normal distribution $N(0, \sigma_{e,z}^2)$ at the individual’s birth and added to the genotypic value of its trait z . The phenotypic value of evolving trait $z(i)$ for the school i is then

$$z(i) = G_z(i) + e_z(i) \quad (17)$$

4.2.1.6.3 Genetic inheritance

Both functional and neutral loci follow Mendelian inheritance under sexual reproduction. Reproduction is panmictic, which means that all sexually mature individuals can contribute to mating pairs of parents irrespective of their location and phenotype. If a new school is created at time step t , its two parents are randomly drawn from a multinomial distribution $M(2, p(t))$ for 2 trials with a probability vector $p(t)$ composed of as many elements $p_i(t)$ as there are schools in the population. The i th element $p_i(t)$ is defined as the relative fecundity of school i in the population at time step t ,

$$p_i(t) = \frac{N_{\text{eggs}}(i, t)}{\sum_{j|s(j)=s(i)} N_{\text{eggs}}(j, t)} \quad (18)$$

with $N_{\text{eggs}}(i, t)$ the fecundity of school i and $\sum_{j|s(j)=s(i)} N_{\text{eggs}}(j, t)$ the total fecundity of the species $s(i)$ population at time step t .

For each selected parental school, haploid gametes are assembled by randomly drawing one of the two alleles at each locus to represent allelic segregation during meiosis. This is done under the assumption of independence between loci, so that alleles recombine freely. New schools receive at

each functional and neutral locus one allele from both chosen parents by randomly picking a haploid gamete for each of them.

4.2.1.7 Bioenergetics and life-history sub-model

The four evolving traits of a school i — I_{\max} , r , m_0 and m_1 —together with its age $a(i, t)$ and somatic mass $w(i, t)$ determine its bioenergetics and life-history processes, namely somatic and gonadic growth, maturation, reproduction and mortality. The detailed description of the bioenergetics fluxes is provided in Morell et al. (submitted; Chap. 2). A general description of the bioenergetic fluxes is presented hereafter as well as their linkages with the four evolving parameters (Figure 27).

4.2.1.7.1 General principles

Individual life history emerges from underlying bioenergetic fluxes which are described according to a biphasic growth model (Figure 27) (Andersen, 2019; Boukal et al., 2014; Quince et al., 2008). The body mass-dependent energy fluxes are allocated according to physiological tradeoffs between competing processes: maintenance, somatic growth and gonadic growth. The sexual maturation of individuals relies on the concept of maturation reaction norms that depicts how the process of maturation responds plastically to variation in body growth (Heino et al., 2002; Stearns and Koella, 1986). This combination of processes mechanistically describes how somatic growth, sexual maturation and reproduction emerge from energy fluxes sustained by food intake resulting from opportunistic length-based predator-prey interactions.

On top of the biphasic growth model, individuals' energy mobilization and maintenance energetic costs depend on dissolved oxygen saturation and temperature so that the resulting metabolic rate (the net energy available for new tissue production) and thus somatic and gonadic growth vary with these abiotic parameters in a way that conforms to the oxygen- and capacity-limited thermal tolerance theory (OCLTT; Pörtner, 2001) and more generally to thermal performance curves (TPC; Angilletta, 2009). The equations underlying the bioenergetic sub-model and especially the plastic responses to dissolved oxygen saturation and temperature are not developed hereafter as they are

fully described in a previous paper (Morell et al. submitted; Chap. 2). As Ev-OSMOSE models the evolution of bio-energetic process traits underlying the life history, we propose a simplified description of the bioenergetic processes that are essential to understand the role of the traits, also illustrated with Figure 27.

4.2.1.7.2 Fluxes description: from the ingestion of energy to tissue growth

The bioenergetic fluxes are summed up in Figure 27A. The most upstream flux is the ingestion of energy. The ingested energy follows a Type 1 functional response to prey biomass: it increases linearly with the amount of prey biomass that is spatiotemporally co-occurring with the feeding school, until it reaches a maximum that increases with individual somatic mass, corresponding to the satiety state level. The predator-prey co-occurrence depends on the spatial distributions of the prey (other HTL schools and forcing LTL prey fields) and of the feeding schools.

A constant portion of the ingested energy is assimilated. The portion which is not assimilated is lost due to excretion and feces egestion. A portion of assimilated energy is then mobilized. The mobilized energy pays internal processes, i.e, growth of the somatic and gonadic tissues and maintenance in our framework.

The portion of assimilated energy that is mobilized depends on temperature and oxygen. The mobilized energy rate fuels all metabolic processes starting in priority with the costs of maintenance of existing tissues. The maintenance rate increases with temperature and with somatic mass. The difference between mobilized energy and maintenance is called net energy for new tissue production. The net energy is then fully allocated to the growth of the somatic compartment before maturation and it is shared between growth of the somatic and gonadic compartments after maturation. The increase of the somatic compartment implies growth in length and mass. The energy allocated to the gonadic compartment is used during the breeding season to produce eggs.

The maturation process is modeled by a deterministic linear maturation reaction norm (LMRN) that represents all the age-length combinations at which an individual can become mature (Stearns and Koella, 1986 ; Stearns, 1992) (Figure 27B). In this framework, individuals become sexually mature when their growth trajectory in terms of body length intersects the LMRN. The mature state $m(i, t)$ is 0 for immature individuals and 1 for mature individuals.

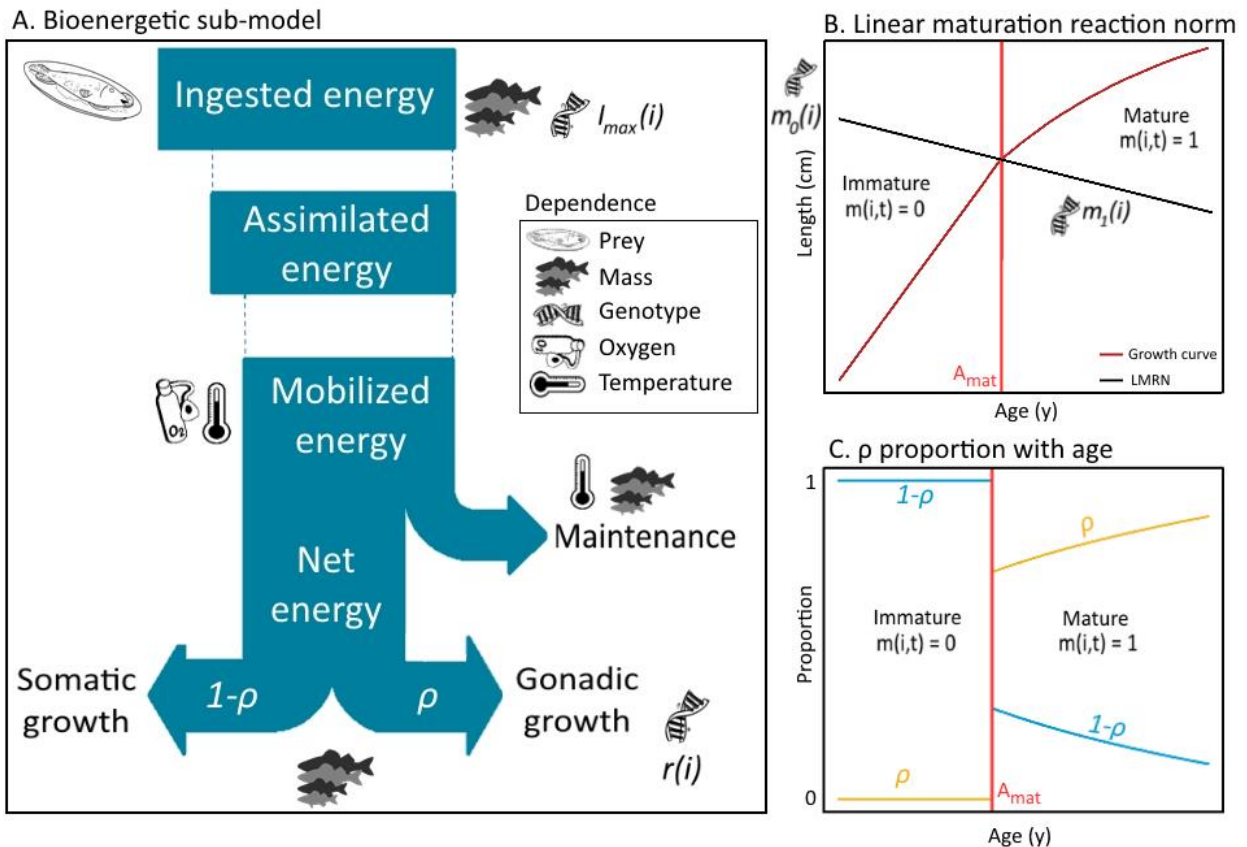


Figure 27: Bioenergetic sub-model fluxes from the ingestion to the tissue growth, namely somatic and gonadic growth (A). The flux dependences to biotic (individual genotype, available prey and somatic mass) and abiotic (temperature and oxygen) variables are specified with pictograms. Four parameters are prone to evolve: the maximum mass-specific ingestion rate I_{max} whose evolution impacts the ingested energy and downstream fluxes, the intercept m_0 and the slope m_1 of the linear maturation reaction norm (LMRN) (B) whose evolutions impact the maturation process, and the gonado-somatic index r whose evolution impacts the slope of the proportion of net energy ρ allocated to gonadic growth after maturity (C) and thus impacts the growth-reproduction tradeoff. The LMRN (B) models all the age-length combinations at which an individual can become mature.

4.2.1.8 Mortality

The mortality sub-model is described in the Supporting Information S3. To sum up the mortality process, a school i faces different sources of mortalities at each time step, namely predation

mortality caused by other schools (emerging), starvation mortality (emerging), fishing mortality $F(i)$, larval mortality $\mu_l(i)$ and diverse other natural mortalities $\mu(i)$ (i.e. senescence, diseases, and non-explicitly modeled predators). An additional foraging mortality is modeled in Ev-OSMOSE. This mortality describes the additional mortality due to foraging for prey. Each time step t is subdivided into multiple sub-time dt steps within which the different mortality sources impact a school i in a random order so as to simulate the simultaneous nature of these processes (see <http://documentation.osmose-model.org/> for more details). Hereafter, we detail the mortality that represents the main selective pressures and/or important evolutionary tradeoffs in our framework.

Organisms face a trade-off between foraging activity and mortality (Mangel, 2003) because more active foraging implies a higher exposure to predation, unfavorable conditions (e.g., triggering diseases) and/or increased oxidative stress. Assuming that variation in mass-specific maximum ingestion rate I_{\max} results from variation in foraging activity, this trade-off is modeled by including a foraging mortality that increases with the mass-specific maximum ingestion rate I_{\max} and thus when foraging activity is more intense. The instantaneous foraging mortality rate experienced by school i is defined as follows:

$$M_f(i) = k_1 \cdot e^{k_2 \cdot (I_{\max}(i) - \overline{I_{\max}}(0))} \quad (19)$$

with k_1 the foraging mortality that would face an individual i if it had an $I_{\max}(i)$ value equal to the initial mean genotypic value of the trait $\overline{I_{\max}}(0)$ in the population and k_2 the exponential slope translating the change of foraging activity linked to a deviation of $I_{\max}(i)$ from $\overline{I_{\max}}(0)$ into an multiplicative factor of the trade-off's strength. Change in the number of individuals in school i due to foraging mortality during sub-time step dt is then obtained as:

$$N(i, t + dt) = N(i, t) e^{-M_f(i) dt} \quad (20)$$

Fishing mortality is a major evolutionary pressure on marine populations due to total mortality increase and length selectivity. In the model, fishing mortality can be discretized per length class, i.e.,

a parameter of fishing mortality per species per length class can be used to realistically model the fishing process. The highest fishing mortality across length classes of a species is called F_{max} .

Predation-induced mortality is an explicit stochastic length-dependent process that emerges from the spatial co-occurrence between predators and prey, and the predators' ingestion process. The predation mortality applied to school i is simply the sum of the biomass losses due to the ingestion of all predator schools j with suitable body length, and present in the same grid cell $c(i, t)$ at sub-time step dt . From length-dependent interactions emerge a realistic selective predation pressure that decreases with fish length.

Starvation mortality occurs when an individual cannot cover its energetic maintenance needs, i.e. when net energy is negative. If the energy reserve, provided by gonads, is not sufficient to cover the maintenance needs, the school undergoes an energetic deficit and faces starvation mortality proportionally to its energy deficit. In our model, starvation mortality increases in response to climate change due to rising temperature, deoxygenation or decrease in food availability. The increase of total mortality through increased starvation mortality is expected to accelerate life cycle similarly to what is expected under fishing pressure (Waples and Audzijonyte, 2016).

Table 5: Variables and functions used in the Ev-OSMOSE model.

Symbol	Description	Units	Equations
Entities: Fish schools			
Genetic determinism and expression			
<i>State variables</i>			
$A_{z,l,k}(i)$	Additive effect of allele k ($k \in \{1,2\}$ as individuals are diploid) at locus l ($l \in \{1,2, \dots, l_z\}$) for trait z ($z \in \{I_{max}, m_0, m_1, r\}$) of school i	Trait unit	16
$e_z(i)$	Phenotypic expression noise for trait z ($z \in \{I_{max}, m_0, m_1, r\}$) of school i	Trait unit	17
$b_{l,k}(i)$	Identity of neutral allele k ($k \in \{1,2\}$ as individuals are diploid) at locus l ($l \in \{1,2, \dots, l_b\}$) of school i	–	
<i>Emerging individual variables: Traits</i>			

$G_z(i)$	Genotypic value of trait z ($z \in \{I_{\max}, m_0, m_1, r\}$) for school i	Trait unit	16,17
$z(i)$	Phenotypic value of trait z ($z \in \{I_{\max}, m_0, m_1, r\}$) for school i	Trait unit	17
$I_{\max}(i)$	Maximum mass-specific ingestion rate of school i	$g \cdot g^{-\beta} \cdot \text{timestep}^{-1*}$	
$r(i)$	Gonado-somatic index of school i	–	
$m_0(i)$	Intercept of the maturation reaction norm of school i	cm	
$m_1(i)$	Slope of the maturation reaction norm of school i	$\text{cm} \cdot \text{y}^{-1}$	
Genetic inheritance: <i>Emerging individual variables</i>			
$p_i(t)$	Probability of school i to be one of the 2 parents of a given new school produced during the breeding season starting at time step t	–	18
Ontogenic state			
<i>State variables</i>			
$a(i, t)$	Age of school i 's individuals at time step t	y	
$w(i, t)$	Somatic mass of school i 's individuals at time step t	g	
$g(i, t)$	Gonadic mass of school i 's individuals at time step t	g	
<i>Emerging individual variables</i>			
$L(i, t)$	Total length of school i 's individuals at time step t	cm	
$m(i, t)$	Maturity state of school i 's individuals at time step t	–	
$a_m(i)$	Maturation age of school i 's individuals	y	
$w_m(i)$	Maturation somatic mass of school i 's individuals	g	
$L_m(i)$	Maturation length of school i 's individuals	cm	
$N_{\text{eggs}}(i, t)$	Total fecundity of school i at first time step t of the breeding season	#	18
Abundance: <i>State variable</i>			
$N(i, t)$	Number of individuals in school i at time step t	#	20
Spatial Location: <i>State variable</i>			
$c(i, t)$	Grid cell of school i at time step t	–	
Taxonomic identity: <i>State variable</i>			
$s(i)$	Species to which school i belongs	–	18
Mortality: <i>Emerging variables</i>			
$B(i, t)$	Biomass of school i at time step t	g	
$M_f(i)$	Instantaneous foraging mortality rate of school i	timestep^{-1}	19,20
$F(i)$	Instantaneous fishing mortality rate of school i	timestep^{-1}	
$\mu_l(i)$	Instantaneous larval mortality rate of school i	timestep^{-1}	
$\mu(i)$	Instantaneous diverse mortality rate of school i	timestep^{-1}	
Entities: Fish populations			
<i>Abundance: Emerging population variables</i>			
$N(t)$	Population census size at time step t	#	
$B(t)$	Population biomass at time step t	ton	

$C(t)$	Fishing catches at time step t	ton
Trait distribution: <i>Emerging population variables</i>		
$\bar{G}_z(t)$	Population genotypic mean of trait z ($z \in \{I_{\max}, m_0, m_1, r\}$) at time step t	Trait unit
$\bar{z}(t)$	Population phenotypic mean of trait z ($z \in \{I_{\max}, m_0, m_1, r\}$) at time step t	Trait unit
$\sigma_{A,z}^2(t)$	Population additive genetic variance of trait z ($z \in \{I_{\max}, m_0, m_1, r\}$) at time step t	Trait unit
$\sigma_z^2(t)$	Population phenotypic variance of trait z ($z \in \{I_{\max}, m_0, m_1, r\}$) at time step t	Trait unit
Spatial scales and units: grid cells		
Spatial coordinates: <i>State variables</i>		
$x(c)$	Longitude of grid cell c	
$y(c)$	Latitude of grid cell c	
Physico-chemical factors: <i>State variables</i>		
$pc_k(c, t)$	Value of physico-chemical factor k of grid cell c at time step t	
$T(c, t)$	Temperature of grid cell c at time step t	K
$[O_2](c, t)$	Dissolved O_2 saturation of grid cell c at time step t	%
Abundance of lower trophic levels: <i>State variables</i>		
$B_{LTL}(c, t, j)$	Biomass of trophic level $LTL j$ of grid cell c at time step t	

* β is the scaling exponent of maximum ingestion rate and maintenance rate with body mass.

Table 6: Species-specific parameters in the Ev-OSMOSE model

Symbol	Description	Units	Equations	Source
Genome structure				
l_z	Number of functional loci for trait z ($z \in \{I_{\max}, m_0, m_1, r\}$)	–	16	Assumed
$n_{z,l}$	Number of possible allelic values at functional locus l ($l \in \{1, 2, \dots, l_z\}$) for trait z ($z \in \{I_{\max}, m_0, m_1, r\}$) in the initial population	–		Assumed
l_b	Number of neutral loci	–		Assumed
$n_{b,l}$	Number of possible allelic identities at neutral locus l ($l \in \{1, 2, \dots, l_b\}$) in the initial population	–		Assumed
$\bar{G}_z(0)$	Initial mean genotypic value of trait z ($z \in \{I_{\max}, m_0, m_1, r\}$) in the population	Trait unit	16	Estimated ¹ (m_0, m_1, r) or calibrated (I_{\max})
$\sigma_{A,z}^2(0)$	Initial additive genetic variance of trait z ($z \in \{I_{\max}, m_0, m_1, r\}$) in the population	Trait unit		Calibrated or assumed
Trait expression				
\bar{e}_z	Mean expression noise for trait z ($z \in \{I_{\max}, m_0, m_1, r\}$)	Trait unit		Randomly drawn
$\sigma_{e,z}^2$	Expression noise variance for trait z ($z \in \{I_{\max}, m_0, m_1, r\}$)	Trait unit		Calibrated or assumed
Mortality				
F_{\max}	Maximum instantaneous fishing mortality rate	timestep ⁻¹		Calibrated
k_1	Instantaneous foraging mortality rate for an individual with an I_{\max} value equal to the initial mean genotypic value of the trait in the population	timestep ⁻¹	4	Calibrated
k_2	Exponential slope of the instantaneous foraging mortality	cm ⁻¹	4	Calibrated

¹ from SMALK data (sex–maturity–age–length key)

4.2.2 The North Sea ecosystem application: Ev-OSMOSE-NS

4.2.2.1 Application presentation

The Bioen-OSMOSE model, i.e. the Ev-OSMOSE model without the evolutionary sub-model, was applied to the North Sea ecosystem and published in Morell et al. (submitted; Chap. 2) and summed up in Figure 28. The model domain is delimited by the Norwegian Trench in the north east and includes the eastern English Channel. The grid is regular with cells of $0.25^\circ \times 0.5^\circ$ (632 cells). It models sixteen marine species, i.e. 15 fish and a crustacean functional group. The Ev-OSMOSE-NS, i.e. including the evolutionary sub-model, models only the 15 fish species. The crustacean group was withdrawn because of the lack of data to model this group explicitly. The configuration represents a mean steady state of the ecosystem for the period 2010-2019. The full description of the parameterization of the 15 fish species is provided in Morell et al. (submitted; Chap. 2). Hereafter, we detail the parameterization of the new evolutionary sub-model and the calibration that was performed with this new sub-model.

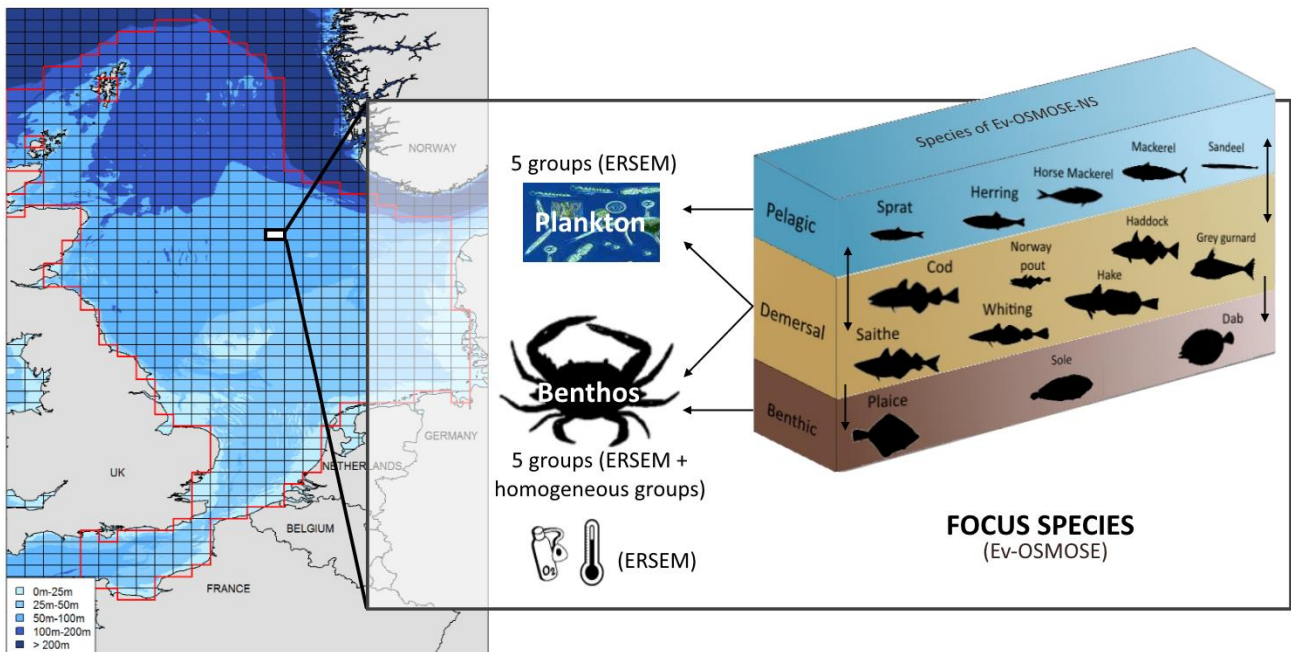


Figure 28: Representation of the Ev-OSMOSE-NS model applied to the North Sea and the Eastern English Channel. Fifteen focus species are explicitly modeled. Outputs from the coupled POLCOMS-ERSEM model force Ev-OSMOSE: temperature, oxygen, and the biomass of 8 LTL plankton and benthic groups. Two homogeneous benthic groups are added to model large benthic prey.

4.2.2.2 Parameterization of the evolutionary sub-model

Parameterizing the evolutionary sub-model requires, for each species and each evolving trait, fixing or estimating the following parameters: the initial mean genotypic value $\overline{G}_z(0)$, the initial additive genetic variance $\sigma_{A,z}^2(0)$, the expression noise variance $\sigma_{e,z}^2$, the number of functional loci l_z and the number of allelic values $n_{z,l}$ for each of them. It necessitates in addition determining values for the foraging mortality coefficients k_1 and k_2 . In this first application of the Ev-OSMOSE modelling framework, neutral loci were not activated, but values for the number of neutral loci l_b and the number of allelic identities $n_{b,l}$ for each of them are also required otherwise.

The mean initial genotypic value $\overline{G}_z(0)$ of a trait is, by definition, equal to the mean phenotypic value of the trait in the population as expression noise and allelic values are centered around 0. The initial mean genotypic/phenotypic values of the traits were thus fixed at the value estimated for the Bioen-OSMOSE-NS configuration (see Chap. 2), except for the mean value of I_{\max} that was calibrated *de novo* for Ev-OSMOSE-NS (see next section “Model calibration”).

The initial additive genetic variance $\sigma_{A,z}^2(0)$ and the expression noise variance $\sigma_{e,z}^2$ were estimated according to the following procedure. Given additivity and independence of the genetic and micro-environmental effects on the phenotypic value of a trait (equation 17), phenotypic variance of a trait is the sum of additive genetic variance and expression noise variance $\sigma_z^2(0) = \sigma_{A,z}^2(0) + \sigma_{e,z}^2$. Heritability is defined as the proportion of phenotypic variance due to additive genetic variance, $h_z^2 = \sigma_{A,z}^2 / \sigma_z^2$, and is typically around 0.2 for life-history traits of vertebrates and ectotherms (Mousseau and Roff, 1987). Given a certain trait phenotypic variance $\sigma_z^2(0)$ (that can be estimated from field data see below), initial additive genetic variance and expression noise variance can then be estimated as $\sigma_{A,z}^2(0) = h_z^2 \sigma_z^2$ and $\sigma_{e,z}^2 = (1 - h_z^2) \sigma_z^2$.

The phenotypic variances $\sigma_{I_{\max}}^2(0)$, $\sigma_{m_0}^2(0)$ and $\sigma_r^2(0)$ were estimated from variability in length-at-age and maturation for each species using the same SMALK data as in Chapter 2 (see details in

Supporting Information S11). For the sake of simplicity, the phenotypic variance of the slope of the LMRN m_1 , $\sigma_{m_1}^2(0)$, was fixed to 0. This assumption implies that the slope of the LMRN m_1 cannot evolve (if there is no phenotypic variance, there is no additive genetic variance), all the maturation variance is explained by the population phenotypic variance of m_0 , $\sigma_{m_0}^2(0)$, and that the mean maturation length variance is constant at any age (see Supporting Information S11 section 2). This is justified by the fact that (i) the first order term in empirically documented evolutionary changes in maturation reaction norm is explained by a change of its intercept m_0 (e.g. Marty et al., (2014) for North Sea gadoids) so that evolution of the slope can be neglected in first approximation m_1 and (ii) population variance in maturation age and length can be correctly approximated by variance in the LMRN intercept only.

In the simulations presented in this chapter, the evolution of two out of the three traits with non-zero phenotypic variance was activated, i.e., the genotypic variance was set different from 0, with a heritability of 0.2, for these traits: the gonado-somatic index r and the intercept of the LMRN m_0 . The evolution of I_{\max} was not activated because the calibration of the coefficients k_1 and k_2 for the trade-off between I_{\max} and foraging mortality was not satisfying yet (see next section “Model calibration”) and the resulting evolutionary trends would have been subject to caution. However, the choice was made to keep phenotypic variance of I_{\max} included as it determines directly phenotypic variance in juvenile growth, which is one of the most variable traits in fish. In terms of sources of variance, this assumption means that all the phenotypic variance of I_{\max} is explained by the expression noise only, $\sigma_{I_{\max}}^2 = \sigma_{e,I_{\max}}^2$.

The final values of the expression noise variances and the additive genetic variances used for the simulations are given in Table 7.

The number of functional loci l_z and alleles per locus $n_{z,l}$ were fixed to 10 and 7, respectively, based on experience from previous monospecific eco-genetic models (Marty et al. 2015) and analogy with

the order of magnitude of the number of allelic values typically observed for neutral markers in fish such as microsatellites (e.g. Poulsen et al., 2006). These values also insured obtaining an initial normal distribution of the traits in the population.

Table 7: Micro-environmental noise and genotypic variances of process traits in Ev-OSOMOSE-NS. The sum of these variances is the total phenotypic variance of each trait.

Species	I_{\max}		r		m_0		m_1	
	$\sigma_{e,I_{\max}}^2$	$\sigma_{A,I_{\max}}^2(0)$	$\sigma_{e,r}^2$	$\sigma_{A,r}^2(0)$	σ_{e,m_0}^2	$\sigma_{A,m_0}^2(0)$	σ_{e,m_1}^2	$\sigma_{A,m_1}^2(0)$
Herring	0.09	0	0.02	4.85e-03	14.07	3.52	0	0
Mackerel	0.12	0	0.02	1.17e-02	9.24	2.31	0	0
Sandeel	0.12	0	0.02	6.00e-03	2.33	0.58	0	0
Sprat	0.03	0	0.01	6.38e-03	3.68	0.92	0	0
Norway pout	0.06	0	0.01	6.00e-03	30.33	7.58	0	0
Plaice	0.12	0	0.02	3.09e-03	45.87	11.47	0	0
Sole	0.28	0	0.06	1.07e-02	21.21	5.3	0	0
Saithe	0.08	0	0.02	3.66e-03	180.16	45.04	0	0
Cod	0.63	0	0.13	2.57e-03	283.56	70.89	0	0
Haddock	0.36	0	0.07	6.00e-03	36.22	9.05	0	0
Horse Mackerel	0.48	0	0.1	4.48e-03	6.26	1.57	0	0
Whiting	0.35	0	0.07	7.31e-03	11.54	2.89	0	0
Dab	0.12	0	0.02	6.00e-03	12.77	3.19	0	0
Grey gurnard	0.22	0	0.04	6.00e-03	12.24	3.06	0	0
Hake	0.4	0	0.08	6.00e-03	108.41	27.1	0	0

4.2.2.3 Model calibration

The Bioen-OSMOSE-NS configuration detailed in Morell et al. (submitted; Chap. 2) was calibrated to obtain estimates for unknown parameters, using maximum likelihood estimation based on an evolutionary optimization algorithm adapted to high-dimensional parameter space that is available in the calibraR R package (Oliveros-Ramos and Shin, 2016). The algorithm explores the space of unknown parameters so as to maximize the likelihood obtained by comparing model outputs to observed data.

The addition of a new evolutionary sub-model to the North Sea configuration modifies the simulation outputs of the model, notably by introducing interindividual variability through phenotypic variance, and thus the Ev-OSMOSE-NS model needed to be calibrated anew to re-estimate the same unknown parameters as in Bioen-OSMOSE-NS. The estimations of the parameters obtained from the

calibration of Bioen-OSMOSE-NS were used as initial guesses to speed up the calibration process. The calibration of the Ev-OSMOSE-NS model is an ‘ecological fit’ to ecological data using a model version with phenotypic variability but without genotypic transmission. The data used to calibrate Ev-OSMOSE-NS are fisheries landings (ICES, 2019a), length-at-age from scientific surveys from ICES database (NS-IBTS-Q1, ICES DATRAS 2022) and estimated biomasses for assessed species (ICES, 2016, 2018a, 2018b, 2018c, 2019b). The calibration is performed for an average state of the ecosystem for the period 2010-2019 by using observed data averaged over the period as target values (Supporting Information S12). For each species, the estimated parameters are the larval mortality, the mean maximum ingestion I_{\max} , the maximum fishing mortality rate, and the additional mortality rate. A parameter per LTL group named coefficient of accessibility to fish is also estimated. The new estimation of these parameters for the Ev-OSMOSE-NS model is given in Table 8 for species parameters and Table 9 for LTL parameters. Due to time constraints, the coefficients k_1 and k_2 for the trade-off between I_{\max} and foraging mortality were not calibrated rigorously through maximum likelihood estimation. For the simulations presented in this chapter, they were fixed so that foraging mortality for each species was on average (i.e. when accounting for phenotypic variance in I_{\max}) equal to 0.05 and the slope k_2 was manually tuned (and hence k_1 adjusted to maintain the average at 0.05) to obtain evolutionary trends in I_{\max} that were within reasonable ecological limits (results not shown obtained by activating evolution for I_{\max} contrary to the simulations presented here). Values of the two coefficients are also given in Table 8.

The calibrated configuration is run for 100 years. The first 70 years is the spin-up period, a period during which the system stabilizes. Mendelian transmission is activated on year 70. The results presented hereafter are the years after the Mendelian transmission activation. 28 replicates of the model are run with the same parameterization to account for Ev-OSMOSE-NS stochasticity.

Table 8: Calibrated species parameters for the 15 focus species in Ev-OSMOSE-NS.

Species	Calibrated parameters					
	I_{max}	Mortality				
		LARVAL μ_l	FISHING F_{max}	ADDITIONAL μ	FORAGING k_1	FORAGING k_2
$g \cdot g^{-6}$	y^{-1}	y^{-1}	y^{-1}	y^{-1}	cm^{-1}	
Herring (<i>Clupea harengus</i>)	13.96	7.12	0.59	0.14	0.054	0.95
Mackerel (<i>Scomber scombrus</i>)	16.69	4.23	1.09	0.52	0.055	0.7
Sandeel (<i>Ammodytes spp</i>)	9.3	2.06	0.95	0.45	0.052	0.95
Sprat (<i>Sprattus sprattus</i>)	12.25	1.00	0.20	0.16	0.057	1.1
Norway pout (<i>Trisopterus esmarkii</i>)	9.8	3.41	0.40	0.28	0.054	1.1
Plaice (<i>Pleuronectes platessa</i>)	10.39	5.79	0.09	0.16	0.05	1.1
Sole (<i>Solea solea</i>)	9.7	7.42	0.30	0.27	0.04	1.1
Saithe (<i>Pollachius virens</i>)	14.43	2.66	0.58	0.49	0.054	0.95
Cod (<i>Gadus morhua</i>)	20.38	8.85	0.32	0.53	0.031	0.95
Haddock (<i>Melanogrammus aeglefinus</i>)	15.99	5.1	0.07	0.58	0.04	0.95
Horse Mackerel (<i>Trachurus trachurus</i>)	13.59	0.15	0.04	0.27	0.036	0.95
Whiting (<i>Merlangius merlangus</i>)	17.85	8.66	0.45	0.13	0.041	0.95
Dab (<i>Limanda limanda</i>)	8.74	4.07	0.17	0.21	0.052	0.95
Grey gurnard (<i>Eutrigla gurnardus</i>)	13.8	5.28	0.32	0.08	0.047	0.95
Hake (<i>Merluccius merluccius</i>)	16.88	7.63	0.35	0.28	0.039	0.95

Table 9: Calibrated coefficients of accessibility to fish of low trophic level (LTL) groups in Ev-OSMOSE-NS.

LTL groups		Coefficient of accessibility to fish
Pelagic prey	Micro-phytoplankton	0.123
	Diatoms	0.042
	Hetero-trophic flagellates	0.349
	Micro-zooplankton	0.033
	Meso-zooplankton	0.088
Benthic prey	Suspension feeders	0.002
	Deposit feeders	7.96E-05
	Meio benthos	0.001
	Large benthos	0.012
	Very large benthos	0.014

4.3 Results

The NS configuration has already been calibrated and evaluated in a version without genotypic and phenotypic variance (Morell et al. submitted; Chap. 2). To avoid redundancy in this paper, the indicators used to evaluate the ecological validity of the configuration are in Supporting Information S12. Particular attention was paid to indicators showing the model's ability to reproduce realistic emergent variability (see Section 4.3.1). Considering Bioen-OSMOSE-NS as the reference configuration, we explored in which aspects Ev-OSMOSE improves the realism of model output. In consequence, we describe how the maturation and length-at-age outputs of Bioen-OSMOSE-NS (Morell et al. submitted; Chap. 2) differ from those produced by Ev-OSMOSE-NS and whether Ev-OSMOSE better fits observed data. The ability of the model to account for evolutionary responses that correctly respond to selective pressures is illustrated by the transmission of genotypic values between parental pools and newborn cohorts.

4.3.1 Emerging phenotypic variability

4.3.1.1 Maturation

The maturity ogive $o(a)$, the proportion of mature individuals at age a , from Ev-OSMOSE-NS and Bioen-OSMOSE-NS simulation outputs (Morell et al. submitted; Chap. 2) and observed data are compared to explore whether taking into account phenotypic variance in process traits improves model realism, especially as maturity ogives were not used as targets for calibration. The maturation process can be assessed with two types of Ev-OSMOSE outputs: (i) the mean maturation age or length and (ii) the variance of the maturation age or length. The mean maturation age is estimated as $\sum a(o(a) - o(a - 1))$. A better fit of the simulated variance to observations and of mean maturation length can be graphically evaluated with the slopes of the corresponding maturity ogives.

Compared to Bioen-OSMOSE-NS, Ev-OSMOSE-NS provides a better representation of mean age at maturity for haddock, hake, herring, plaice and sole (closer to observed mean ages at maturity), a similar one for saithe and whiting, but a worse one for cod, grey gurnard, Norway pout and sprat

(vertical lines, Figure 29A). Ev-OSMOSE-NS outputs reproduce better observed variance in mean age at maturity for all species except sprat and mackerel (curves, Figure 29A). The simulated mackerel ages at maturity fail to reproduce a credible shape for the age-based maturity ogive.

The evaluation of the model's maturation outputs is complemented with the length-based maturity ogives (Figure 29B). Those simulated with Ev-OSMOSE-NS show a much better visually fit to observed ones in terms of both mean and variance of lengths at maturity for all species except sprat. The fit to data is particularly good for haddock, herring and whiting length ogives.

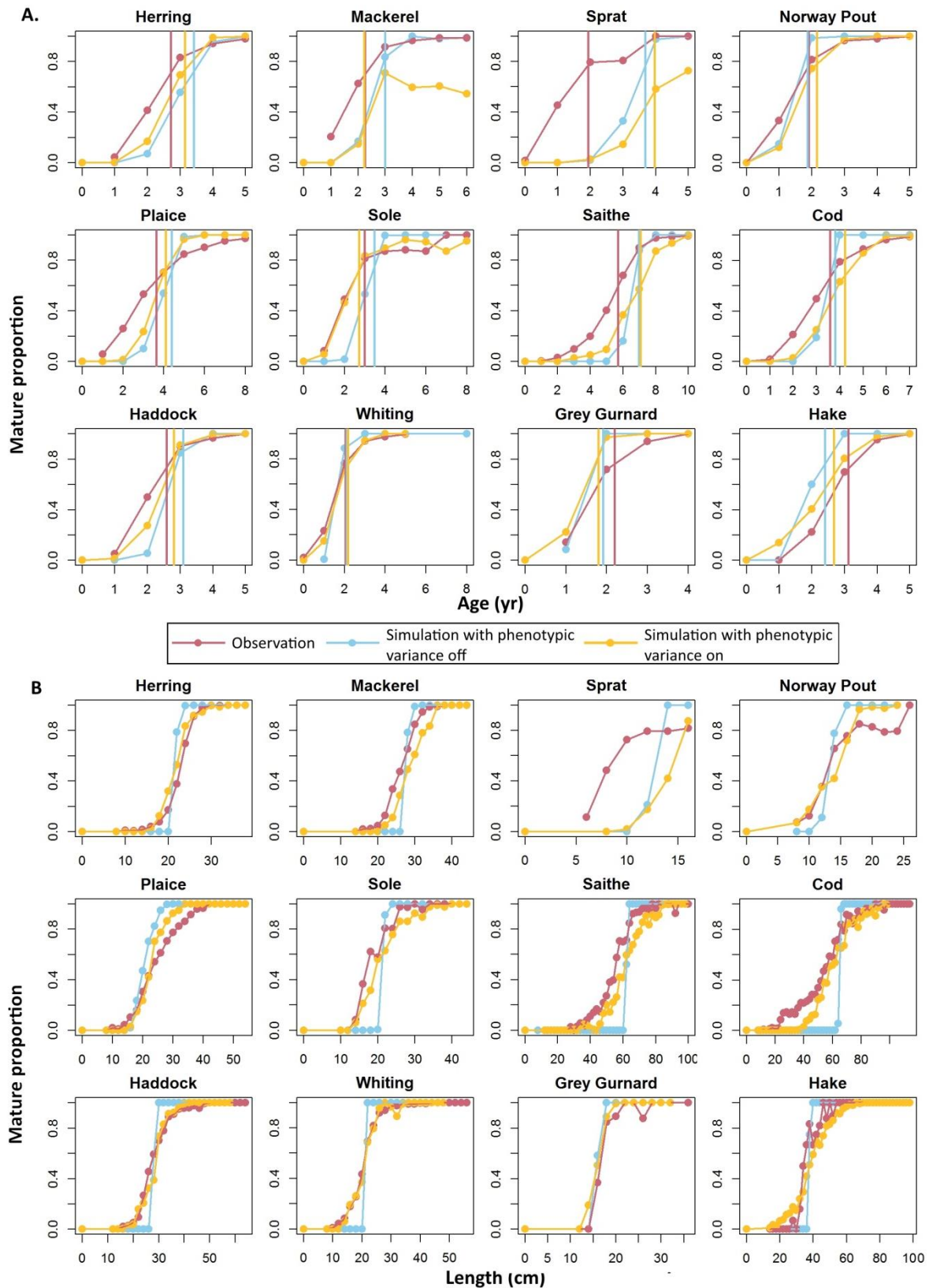


Figure 29: Age- (A) and length-based (B) maturity ogives per species for observed (red), simulated without (blue) and simulated with phenotypic variance (yellow) individual data for species for which empirical maturation data are available. Results are shown for the species for which there is enough data to estimate and plot the observed age and length maturity ogives. Age data are yearly grouped

and length data are grouped by 2- centimeter classes. The vertical lines are the mean ages at maturity (A). The mean length at maturity is not represented. Some observed length maturity ogives are not strictly increasing and do not allow a reliable estimation of the mean maturity length.

4.3.1.2 Length-at-age

The evaluation of the model on the simulated lengths-at-ages is performed in a similar way to the maturation indicators: we first inspect the shape of the length-at-age curves (Figure 30) and we also calculate the sum of squared errors (SSE) between the simulated and observed means and standard deviations of length at different ages (Figure 31). We chose the SSE of the standard deviations as an indicator of the goodness of fit for length variability at age, because the SSE of the variances would overly highlight outliers.

The length-at-age outputs from Ev-OSMOSE-NS correctly reproduce the shape of a von Bertalanffy-like growth curve and the length hierarchy between species. Figure 30 and Figure 31A highlight the degree of similarity in simulations of mean length-at-age between Bioen-OSMOSE-NS and Ev-OSMOSE-NS. Ev-OSMOSE produces better results in terms of mean for herring, haddock, and plaice and fits less well for mackerel, cod, Norway pout, saithe and whiting (Figure 31). A recurring trend is that the mean lengths-at-age simulated with Ev-OSMOSE fit poorly observed data for the older ages (cod, dab, grey gurnard, haddock, mackerel, sandeel, sole, sprat, whiting) while the Bioen-OSMOSE-NS results fit better at these ages.

We highlight three main trends in the fit of our models to the observed variability of length-at-age (Figure 30 and Figure 31B): (i) Ev-OSMOSE outputs generally fit better variance in observed data than Bioen-OSMOSE outputs for demersal species (in particular cod, haddock, saithe, whiting), except Norway pout, but (ii) not for pelagic species (herring, mackerel, sandeel, horse mackerel, sprat) and (iii) the fit is better at earlier ages than at older ages, i.e. the Ev-OSMOSE results tend to overestimate the variance of length at older ages.

Chapter 4 – Ev-OSMOSE description

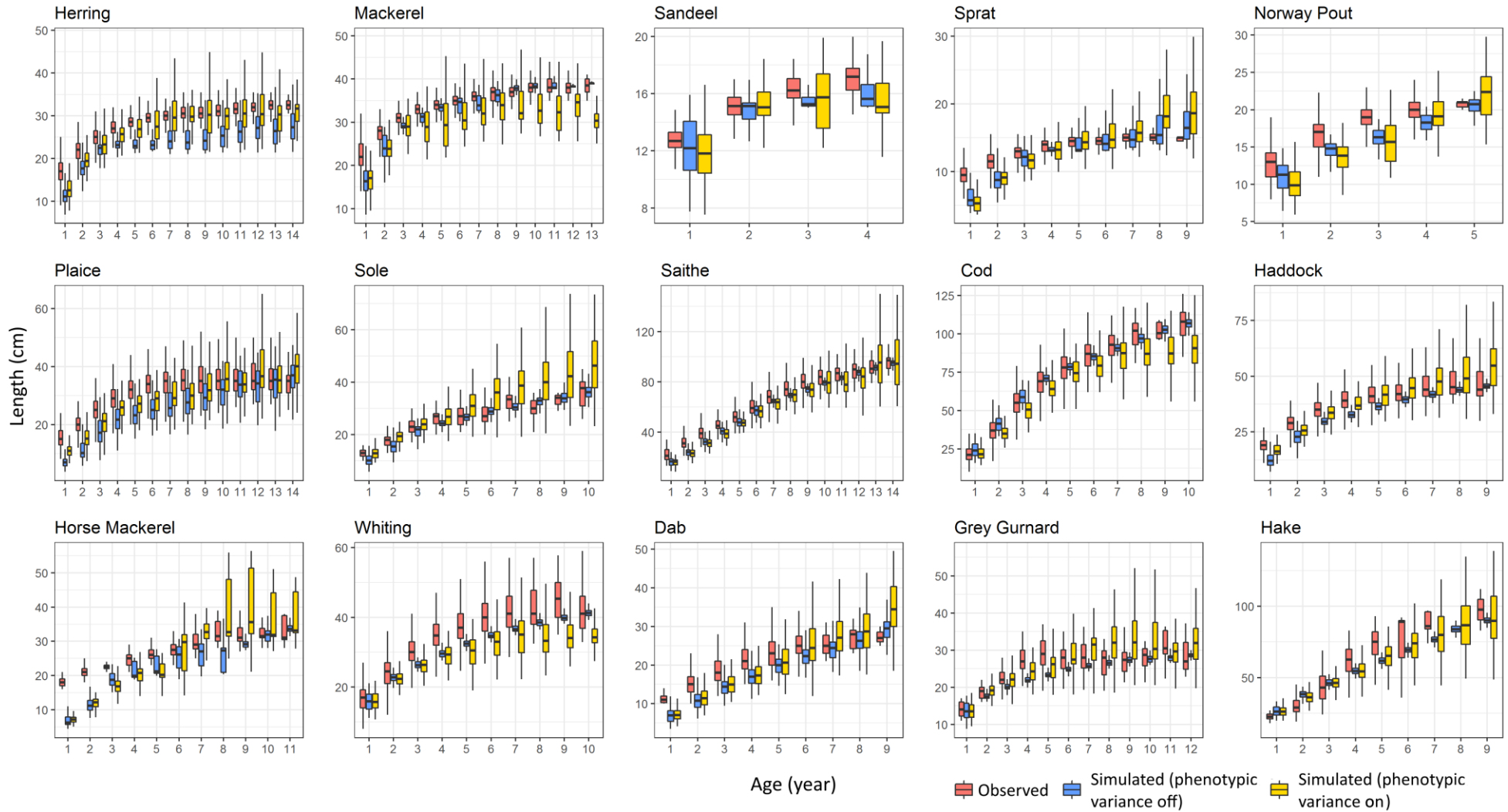


Figure 30: Boxplot of length-at-age per species for observed (red), simulated without (blue) and simulated with phenotypic variance (yellow) individual data. Horizontal bars represent the first, second and third quartiles of the data. The whiskers' extremities represent 1.5 times the interquartile space (the distance between the first and third quartile).

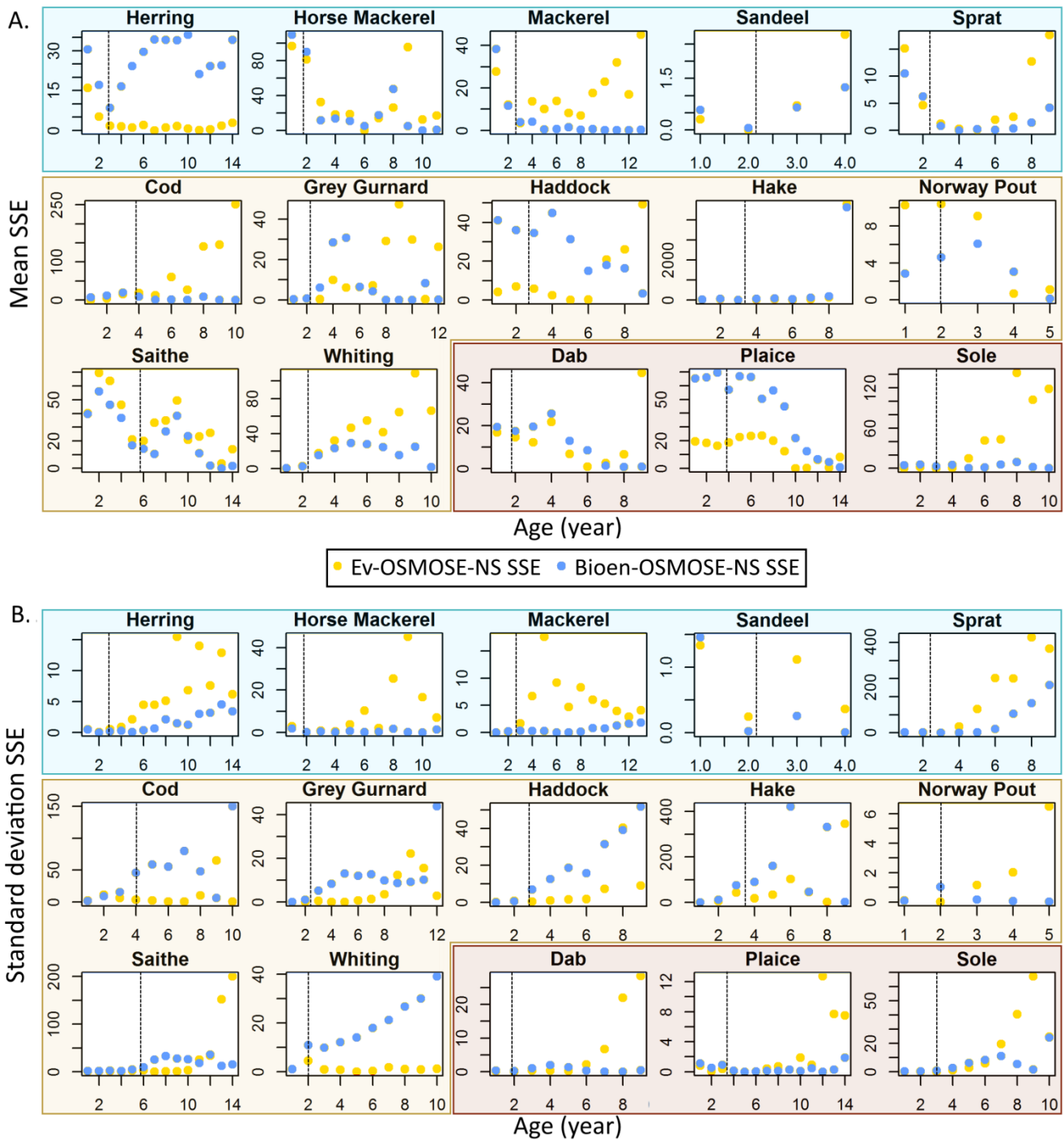


Figure 31: Sum of squared errors between observed and simulated mean (A) and standard deviation (B) of length-at-age from Ev-OSMOSE-NS (yellow dots) and Bioen-OSMOSE-NS (blue dots) per species. The vertical dotted lines represent the mean observed age at maturation. The species are grouped per position in the water column: pelagic (blue frame), demersal (beige frame) and benthic (brown frame) species (see Figure 28).

4.3.2 Genotypic value transmission

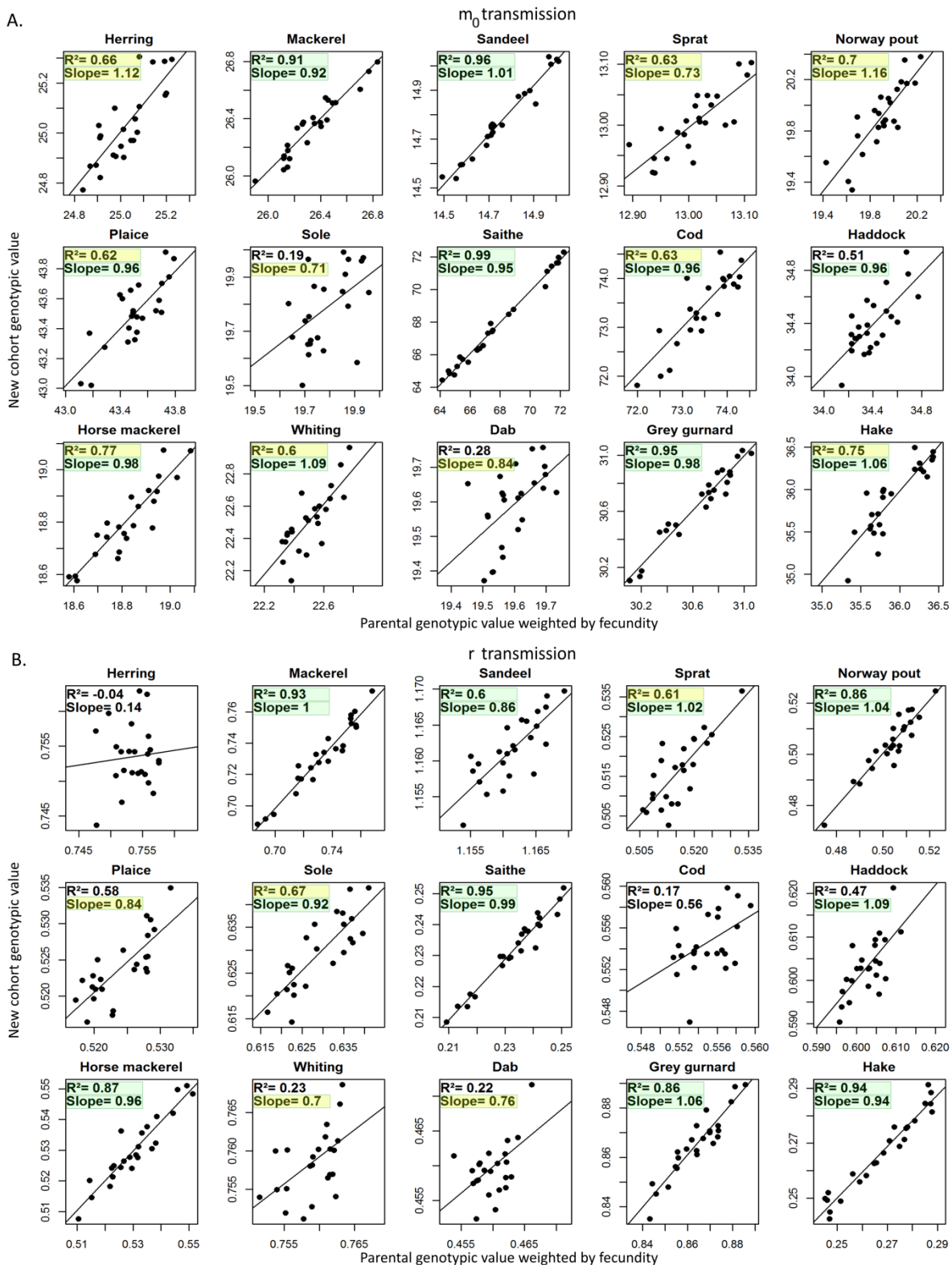


Figure 32: Transmission of genotypic values of the maturation reaction norm intercept m_0 (A) and of the gonado-somatic index r (B) from parental pools to the new spawned cohort. The mean parental genotypic value weighted by individual fecundity and averaged over the entire reproductive season is

compared to the mean genotypic value of the new spawned cohort during the same reproductive season. The slope and the R^2 of the regression are expected to be close to 1 in case of faithful transmission of genotypic values. The noise around the regression slope is a consequence of genetic drift due to stochasticity in the sampling of parental alleles. The slope and the R^2 highlighted in yellow and green are respectively the faithful and the very good faithful simulated transmission of genotypic values (green slope: between 0.9 and 1.1; yellow slope: between 0.7 and 0.9 or between 1.1 and 1.3; green R^2 : between 0.8 and 1; yellow R^2 : between 0.6 and 0.8).

To simulate evolution, part of the phenotypic variability needs to be transmitted from parents to offspring through mendelian inheritance. Phenotypic variability was described in part 3.1. Hereafter, we present results that validate the mendelian transmission process. The support of transmission of part of the phenotypic variability is the genotype and more precisely mean genotypic values are transmitted from parental pools to their offspring cohorts thanks to mendelian inheritance of alleles. Figure 32 illustrates the model capacity to transmit the parents' genotypic value to their offspring for the LMRN intercept m_0 (A) and for the gonado-somatic index r (B). This figure shows the linear regression between the fecundity-weighted mean parental genotypic value and the newborn genotypic value for each trait. A perfect transmission occurs when the regression slope is equal to 1 and the regression adjustment (R^2) is close to 1. Overall, for the two tested traits, we observe a good transmission of genotypic values. The regression slope is positive for all the species for both traits and between 0.5 and 1.2 for all species, except for herring for r . The transmission of m_0 is very faithful for 4 species (mackerel, sandeel, saithe and grey gurnard). The worst cases for m_0 are observed for sole, haddock and dab. The transmission of r is very faithful for 7 species (mackerel, sandeel, Norway pout, saithe, horse mackerel, grey gurnard and hake). The worst cases for r are observed for herring, cod, whiting, and dab. Unperfect transmission of genotypic values is probably due to genetic drift generated by the stochasticity in allele sampling, so-called stochastic sampling error; that could emerge from an insufficient diversity of genotypes in the population (i.e., an insufficient number of schools) or an insufficient number of new produced genotypes (i.e., insufficient number of newborn schools). The number of newborn schools per reproductive event is a model parameter (Morell et al. submitted; Chap. 2) from which depends the total number of schools

of a population. A simulation with 10 times more added schools per reproduction event than in the current configuration is presented in Supporting Information S13. The simulated transmission patterns in these additional simulations are less noisy and much closer to perfect transmission of genotypic values between parental populations and their offspring.

4.4 Discussion

4.4.1 Modeling phenotypic variance of life-history traits

4.4.1.1 Ev-OSMOSE-NS: A first step to model phenotypic variance

In this study, by applying the evolutionary model Ev-OSMOSE to the North Sea, we obtained a convincing average state of the ecosystem (Supporting Information S12, Figure 29, Figure 30 et Figure 31) and a good overall representation of the variance of life-history traits. The representation of the phenotypic variance is particularly good for the maturation process and encouraging for the growth process (Figure 29, Figure 30 et Figure 31).

The good representation of the length variance for juveniles to young adults for the majority of species is an indication of a good estimation of the phenotypic variance of the maximum ingestion rate $\sigma_{I_{\max}}^2(0)$ (Figure 31). Similarly, the good fit of the simulated slope of the age- and especially the length-based maturity ogives indicates the reaction norm maturation variance $\sigma_{m_0}^2(0)$ is correctly estimated (Figure 29). The overestimation of length variance at older ages indicates that (i) one or more aspects impacting these variances still need to be improved in the model, such as assumptions for variance parameter estimates or the reliability of some simulated mechanisms and/or (ii) the quality of length data at older ages is not good enough to be reliable.

4.4.1.2 Life history parameterization improvement

The mismatch between simulated and observed variance for length at older ages indicates that the simulation of the adult part of life history still needs improvement. The large SSE between simulated

and observed adult length-at-age variances is also partly due to the poor data quality at the oldest ages due to a small number of samples.

In other words, the poor data quality implies a poor estimate of the gonado-somatic ratio variance $\sigma_r^2(0)$ that results in a poor fit between simulated and observed data at older ages, as the observed length-at-age variance is probably lower than it should be. Another source of poor estimation of $\sigma_r^2(0)$ could come from the parameter estimation procedure where we assume that there is no co-variation between r and I_{max} . This hypothesis could be tested using individual growth curves from otolith back-calculation (Green et al., 2009) or data from experimentally raised individuals. Lastly, an incorrect modeling of the foraging-mortality tradeoff would impact the mean length and its variance at adult stage even without evolution: as predation is length-dependent, if the foraging-mortality trade-off does not counterbalance realistically the benefits to grow faster and toward higher lengths, then the simulated phenotypes with a higher I_{max} survive better and are more abundant at older age than in the wild, overestimating the mean and variance of length, as emerging in simulation from Ev-OSMOSE-NS (Figure 30, Figure 31).

4.4.1.3 Prey, predators and fishing impact emerging individual properties

Length-at-age depends on growth, maturation and reproductive parameters as well as size selective pressures such as fishing or predation. For example, an incorrect parameterization of fishing selectivity and a higher simulated exploitation rate than the actual one can lead to a smaller simulated than observed length at adult stage, a pattern that can become even more apparent in Ev-OSMOSE-NS when more phenotypic variability is added in the population. This case is observed for mackerel, sandeel and cod for example (Figure 30). The simulated lengths-at-age show a decrease at older ages. This pattern emerges from the truncation of the fast-growing fish part of the population: the fish that survive to these ages are small and slow-growing. If this pattern is not observed in the

data, it reflects overfishing in the simulation, either in terms of total fishing pressure or selectivity for larger lengths. The addition of growth process variability accentuates this pattern.

4.4.1.4 Limits from the model's life history description

The observed length-at-age variance is the sum of the variances due to additive genetic variability, the phenotypic expression noise and the phenotypic plasticity emerging from macro-environmental variations (Figure 26). In our method to estimate process-based-trait variance, we assumed that the emerging variance was the result of additive genetic and phenotypic expression noise variances only.

The variance of length-at-age in Bioen-OSMOSE-NS fully emerges from macro-environment (blue boxplots on Figure 30). When the additive genetic and phenotypic expression noise variances are included (i.e, on Ev-OSMOSE-NS), the model performs better on species for which phenotypic plasticity in response to macro-environmental variations in Bioen-OSMOSE-NS has few impacts on length-at-age variance such as cod, whiting, saithe or haddock for example (blue boxplots on Figure 30 and variance SSE on Figure 31). On the contrary, this implies that the simulated length-at-age variance is overestimated for species with a high phenotypic plasticity variance emerging from macro-environment variations in the wild. These species are mainly the small pelagic species (herring, sprat, and sandeel mainly) that feed on highly variable sources of food, mainly phyto- and zooplankton. Accounting for macro-environmental variations in variance parameter estimations would be a way to improve the simulated length-at-age variance.

The assumption of linearity for the maturation reaction norm does not allow to correctly represent the maturation patterns for some species such as mackerel (Figure 29A). By contrast to other species, the slope of the LMRN of mackerel is positive: fish that mature older are bigger. The species that empirically exhibit this maturation pattern also frequently exhibit a reaction norm that decreases at older ages (Heino et al., 2002; Marty et al., 2014) or a maximum length to mature (Nilsson-Örtman and Rowe, 2021). With a strictly increasing LMRN, some individuals never mature if their LMRN slope

is steeper than their growth rate. This case was not observed in Bioen-OSMOSE-NS (i.e. without phenotypic variance) but appears here in Ev-OSMOSE-NS with the modeling of phenotypic variance generating some individuals combining a steep positively sloped LMRN and slow growth.

4.4.1.5 Toward more evolving traits: technical improvement

In this study, we presented the simulated effects of phenotypic variance on three process-based traits, with activation of evolution on two of these traits, i.e., the reproductive investment trait r and a maturation process trait m_0 . Reproductive investment evolution (Wright et al., 2011a; Yoneda and Wright, 2004) and maturation evolution (de Roos et al., 2006; Marty et al., 2014; Mollet et al., 2007) are the two main known consequences of fisheries-induced evolution. Reported length-at-age evolution in the literature (Enberg et al., 2012) can be the consequence of evolutionary changes in the reproductive investment, the maturation process or juvenile growth. The evolution of juvenile growth was not modeled here in agreement with the fact that it has been seldom documented and remains weak compared to other traits' evolution (Enberg et al., 2012; Heino et al., 2015). Moreover, to correctly model juvenile growth evolution, which in our model translates into maximum mass-specific ingestion rate I_{max} evolution, the account of a trade-off between the foraging intensity, that should be positively related to I_{max} , and its associated mortality M_f is necessary (Enberg et al., 2009) but is difficult to parameterize in the absence of in situ or experimental data. A way to parameterize this trade-off in future studies would be to estimate the M_f unknown parameters k_1 and k_2 by using time series of trait values in an hindcast interannual calibration. Including the evolution of I_{max} would greatly increase the realism of the model as evolutionary pressures impact multiple traits including growth, especially in the context of length-selective fishing.

4.4.2 Genotypic value transmission

4.4.2.1 A faithful transmission of genotypic values implies a correct evolutionary trend

The genotypic value transmission between parental populations and new cohorts is essential in any eco-evolutionary model such as Ev-OSMOSE because it ensures that the advantageous alleles will be transmitted from parents to offspring: the effect of selection can then propagate through generations.

The transmission is validated from Figure 32 and Supplementary Information C, as we observed that the fecundity-weighted mean genotypic values of the parental pools are transferred to the newborn cohort. Furthermore, at the species level, a larger number of schools improves genotypic value transmission (see Supplementary Information C), decreasing the noise by reducing alleles' stochastic sampling error and thus genetic drift (see section 4.4.2.2).

Obtaining positive slopes and high R^2 for regressions of newborn genotypic values on parental ones indicates faithful transmission for both traits and for all the species. Then, the resulting evolutionary trends are reliable in terms of response to selection: a change in a parental trait's genotypic value due to selection during parent lifetime will be transmitted to offspring. The difference between a species with a faithful transmission and a species with a noisy one, as long as the slope is positive, will be in terms of the rate of the evolutionary response: the stochasticity in transmission will slow down the evolutionary response.

4.4.2.2 Genetic drift: a model sensitive to the number of super-individuals (schools)?

In the Ev-OSMOSE model, and more generally in the OSMOSE model, the biological individuals (fish) are grouped in super-individuals (groups of fish, called schools) to improve the calculation time. In the model, the number of schools added per reproductive event is empirically fixed to have at minimum a school of each age class per species per cell where the species is distributed. This minimum number of schools is a trade-off between reducing the stochasticity of the model and decreasing the computing needs (both in terms of required memory and calculation time). The use of

a genetic sub-model that explicitly describes the genetic diversity in the population implies another condition to determine the minimum number of schools, which is to limit stochasticity in allele sampling during reproductive events and then genetic drift. The genetic drift is related to the population size (in our case the number of schools per species) as it decreases with it (Masel, 2011) and more precisely with the associated effective population, defined as the size of an ideal population (random mating, equal sex ratio and no overlapping generations) that would have the same rate of genetic change than the actual population (Beissinger and McCullough, 2002). In Ev-OSMOSE, the structure in school limits the maximum effective population size at the number of schools and not the total abundance of individuals, which could artificially increase genetic drift.

These considerations are highlighted by comparing a simulation with a lower number of schools (Figure 32) that displays a stronger genetic drift than a simulation with 10 times more schools added per reproductive event (Supporting information S13). The increase of the number of schools in Ev-OSMOSE is limited due to problems in terms of calculation time: 50 years of the configuration presented in this paper runs in 20 minutes whereas 50 years of the configuration presented in Supporting Information S13 where the only difference is the number of schools runs in 15 hours on the same computer. Knowing that the model needs to be run thousands of times to be calibrated, this difference in calculation time cannot be neglected. It would be necessary to conduct a sensitivity analysis to identify an acceptable compromise between the faithfulness of genotypic value transmission, genetic drift and calculation time.

An interesting aspect is also the difference of genotypic value transmission between species. Some species exhibit an almost perfect transmission with a low number of schools (e.g., saithe, Figure 32) whereas others are still very noisy in the simulation with a high number of schools (e.g., whiting, Supporting Information S13). We hypothesize that differences at the interspecific level could arise from differences between species in terms of demography, selective pressures or genetic structure. Regarding the demography, the total size of the population, the total number of schools in the

population, the number of schools added per reproductive event and the total fecundity were not correlated with the faithfulness of the transmission (results not shown). The age structure of the mature part of the population could be an interesting feature to explore as overlapping reproductive generations partly explains differences between effective and real population sizes, and is the only source of differences between these included in Ev-OSMOSE, as otherwise mating is random and sex ratio is balanced. Regarding the genetic structure of the population, we observed that genotypic and phenotypic variances, heritability, allele frequencies and heterozygosity were not correlated with the faithfulness of transmission (results not shown). A next step would be to explore the relationship with effective population size and genetic drift. Lastly, as genetic drift impact is expected to be stronger for small populations or weak selection (Barton and Partridge, 2000), it would be interesting to explore the link between selective pressure intensity and genetic drift.

4.5 Conclusion

This first application of the eco-evolutionary multi-species model Ev-OSMOSE to the North Sea opens the field of eco-evolutionary studies to marine ecosystems models. This study underlines the parameterization feasibility in spite of the high data quality requirement to parameterize the phenotypic and genotypic variances of life-history traits. Ev-OSMOSE-NS is the first configuration to account for genotypic and phenotypic variances of several interacting species and succeeds to improve the simulated variances of life-history traits. It is an important step toward more realism notably in representing length-at-age distribution and the maturation process.

Ev-OSMOSE-NS is also, to our knowledge, the first multi-species model applied to a marine ecosystem that accounts for mendelian inheritance of traits from parents to their offspring for all the species of a food web simultaneously, thus allowing to account for the micro-evolution of exploited species in response to selective pressures such as fishing and climate change together with their co-evolution due to trophic interactions.

A next step is to use the Ev-OSMOSE model under climate change or fishing scenarios. We believe that the account of eco-evolutionary dynamics will improve future projections of marine biodiversity, at the interspecific and intraspecific levels, and fulfill a gap of knowledge on the evolution of interacting species in communities under multiple natural and anthropogenic selective pressures.

Chapter 5: Fisheries-induced evolution in an evolving community

Alaia Morell, Yunne-Jai Shin, Nicolas Barrier, Morgane Travers-Trolet, Bruno Ernande

ABSTRACT

Marine ecosystem models in fisheries research have been used to explore interspecific biodiversity impacts of climate change and fishing pressures considering only ecological dynamics. However, fish populations can also adapt to climate and fishing pressures, through evolutionary changes, resulting in changes in their life history that could mitigate or exacerbate the consequences of these pressures. Building on the individual ecosystem model OSMOSE, a multi-species eco-evolutionary model, Ev-OSMOSE, was developed to also account for plasticity and evolutionary dynamics in biodiversity responses to anthropic pressures.

The Ev-OSMOSE-NS model applied to the North Sea ecosystem is used in this study to explore the evolutionary response of maturation and reproductive investment of an evolving community to fishing and predation pressures. Our results highlight that the evolutionary trend of life history traits of a population mainly depends on the main pressure faced by the latter. Our result suggests also that fishing size-selectivity and trophic interactions may impact the direction of the evolutionary trend. The simultaneous evolution of interacting population results in an evolutionary equilibrium for the majority of the species, a phenomenon described as the Red Queen Hypothesis. One species on contrary exhibits lower and decreasing performances through on scenarios with evolution highlighting that evolution can also lead to evolutionary trap. Besides this species, our results highlight a global demographic stability of the community emerging from species coevolution.

Considerations of evolution in community models provide new understanding of evolving community changes and resilience. Furthermore, this study could have concrete management implications, as it

opens the research scope on the estimation of fishing pressure that counterbalance fisheries-induced evolution.

5.1 Introduction

Human activities can have evolutionary consequences on animal populations due to selective pressures such as climate change, harvesting or pollution (Bradshaw, 2006; Darimont et al., 2009; Fox, 1995; Parmesan, 2006). In marine ecosystems, fishing is one of the main anthropogenic selective pressures and resulting fisheries-induced evolution (FIE) is the main documented evolutionary impact of humans (Heino et al., 2015). FIE has been evidenced in empirical (Audzijonyte et al., 2013; Enberg et al., 2012), experimental (Audzijonyte et al., 2013; Conover and Baumann, 2009), and modeling studies (Audzijonyte et al., 2013; Dunlop et al., 2009). The numerous studies describing FIE are mainly monospecific and emphasize evolutionary changes of life-history traits (Heino et al., 2015), behavior (Sbragaglia et al., 2021; Uusi-Heikkilä et al., 2008) or physiology (Hollins et al., 2018). In addition, FIE can have cascading consequences on the evolving population dynamics and on species interacting with the evolving population. Consequences for interacting species can be ecological, when their population dynamics are affected, evolutionary, when FIE of the focal species induces co-evolutionary changes in the interacting species, or more generally eco-evolutionary, when both the ecological and the evolutionary dynamics of the community of interacting species are affected through a feedback loop (Brunner et al., 2019).

Predation is another selective pressure that can induce evolution (Edeline et al., 2007; Forestier et al., 2020b; Jusufovski and Kuparinen, 2020). In marine ecosystems, predation is generally size-selective (Ohlberger et al., 2019) as it decreases with body size. Since body size and related life-history traits have an heritable component, this predation-induced selective pressures can lead to evolution in prey life-history. Just as FIE, such predation-induced evolution (PIE) may have cascading ecological, co-evolutionary or eco-evolutionary repercussions on the predators and prey on the focal species.

Considering their potential ecological, co-evolutionary or eco-evolutionary implications, FIE and PIE should be considered at the multispecies level (Edeline and Loeuille, 2021). Several recent studies paved the way for a better understanding of such consequences in a multispecies context. First, the ecological effect of life-history trait changes on a marine fish community has recently been explored with a marine ecosystem model in which a slow body size change is imposed (as opposed to mechanistically emerging) at each generation for some exploited species (Audzijonyte et al., 2013; Audzijonyte et al., 2014). The results underline that phenotypic trait changes, whatever their nature and cause, cannot be ignored because they may modify the population and more generally community dynamics. Second, trait evolutionary changes in a single top predator embedded within an otherwise non-evolving aquatic food-web has been investigated (Jusufofski and Kuparinen, 2020). Focusing on the evolution of asymptotic size and reproductive investment, the results highlighted the cascading effect of predator trait evolutionary changes on the dynamics of lower trophic levels and the potential importance of trophic interactions for the evolutionary recovery of an exploited top predator. Third, a size-spectrum physiologically structured community model with evolving phenotypes has shown that predation and fishing can act as synergistic or antagonistic selective pressures on the evolution of maturation size depending on the body size of species (Forestier et al., 2020b).

These studies tackled in isolation different aspects of the eco-evolutionary effects of FIE and PIE in a multispecies context, by cutting the eco-evolutionary feedback loop into its evolution-to-ecology pathway and its ecology-to-evolution pathway (Brunner et al., 2019), by simplifying the system to single evolving species and/or trait or by stripping down mechanistic and genetic details. Yet, taken together they raise the necessity to understand multispecies multivariate trait evolutionary changes in a community through a holistic approach. In this chapter, we will use the Ev-OSMOSE model and the Ev-OSMOSE-NS configuration presented in the previous chapter to investigate the evolution of two life-history traits (maturation and reproductive effort) across fifteen teleost fish species and the

consequences for the community. Numerous cases of FIE have been reported in the North Sea, mainly in terms of maturation (Enberg and Heino, 2007; Grift et al., 2003; Marty et al., 2014; Mollet et al., 2007; van Walraven et al., 2010) and reproductive effort (van Walraven et al., 2010; Wright et al., 2011a; Yoneda and Wright, 2004). In this study, we focus on these two well-known life-history traits, and explore what their evolutionary trends are when exposed to two selective pressures: fishing and predation. The mechanisms underlying the simulated trends are investigated. Moreover, evolution is most often expected to improve the average fitness of the evolving population. Changes in species' average fitness are thus investigated to test whether, in an evolving community, the fitness of all species is improved or whether it is improved for some and impaired for others potentially due to frequency-dependent evolution as expected in ecological systems with multiple inter-specific interactions such as competition and predation (Heino et al., 1998; Meszena et al., 2002). Finally, the sum of the species' average fitness is used as an indicator of global community demographics.

5.2 Materials and methods

5.2.1 The multispecies Ev-OSMOSE model applied to the North Sea

5.2.1.1 General description

Ev-OSMOSE is a modeling tool developed to study eco-evolutionary dynamics in an evolving community in response to multiple pressures such as fishing, predation or climate change. The theoretical aspects of the model have been extensively described in Chapter 4 and are therefore not repeated here.

Ev-OSMOSE has been applied to the North Sea (NS) ecosystem by explicitly modelling the life cycle of 15 interacting species of fish and invertebrates. The validation of the Ev-OSMOSE-NS configuration was also presented in Chapter 4. The results displayed showed the similarity between observed and

modelled phenotypic variability of life-history traits and patterns of indicators emerging at a more integrated level such as size-at-ages or maturity ogives, thus allowing the validation of the modelling framework. The results from Chapter 4 also confirmed the model ability to describe correctly genotype transmission between a parental population and the new cohorts of offspring it produces.

Thanks to its representation of phenotypic variability, conferring variable fitness to individuals carrying different phenotypes and thus genotypes, and its ability to describe mendelian transmission of the latter across generations, Ev-OSMOSE is a suitable modeling framework to study the evolution of life-history traits in a multi-species context.

5.2.1.2 Predation and fishing mortalities

The size-selective fishing mortality rates are constant per size class across the year and between years (Figure 33). The selectivity curve is constrained between 0 and 1. The mortality rate of a size class is given by the product of the selectivity for this size class with the maximum fishing mortality rate F_{max} . The fishing rates faced by a population emerge from the size structure of the population.

Predation-induced mortality is an explicit stochastic size-dependent process that emerges from the spatial co-occurrence between predators and prey, and the predators' ingestion process. From the predation mortality applied to a prey school, emerges the sum of the biomass losses due to the ingestion of all predator schools for this prey which are simultaneously present in the same grid cell.

Fishing and predation mortalities are obtained in outputs of the model per life stage. We compare these mortalities at adult stage.

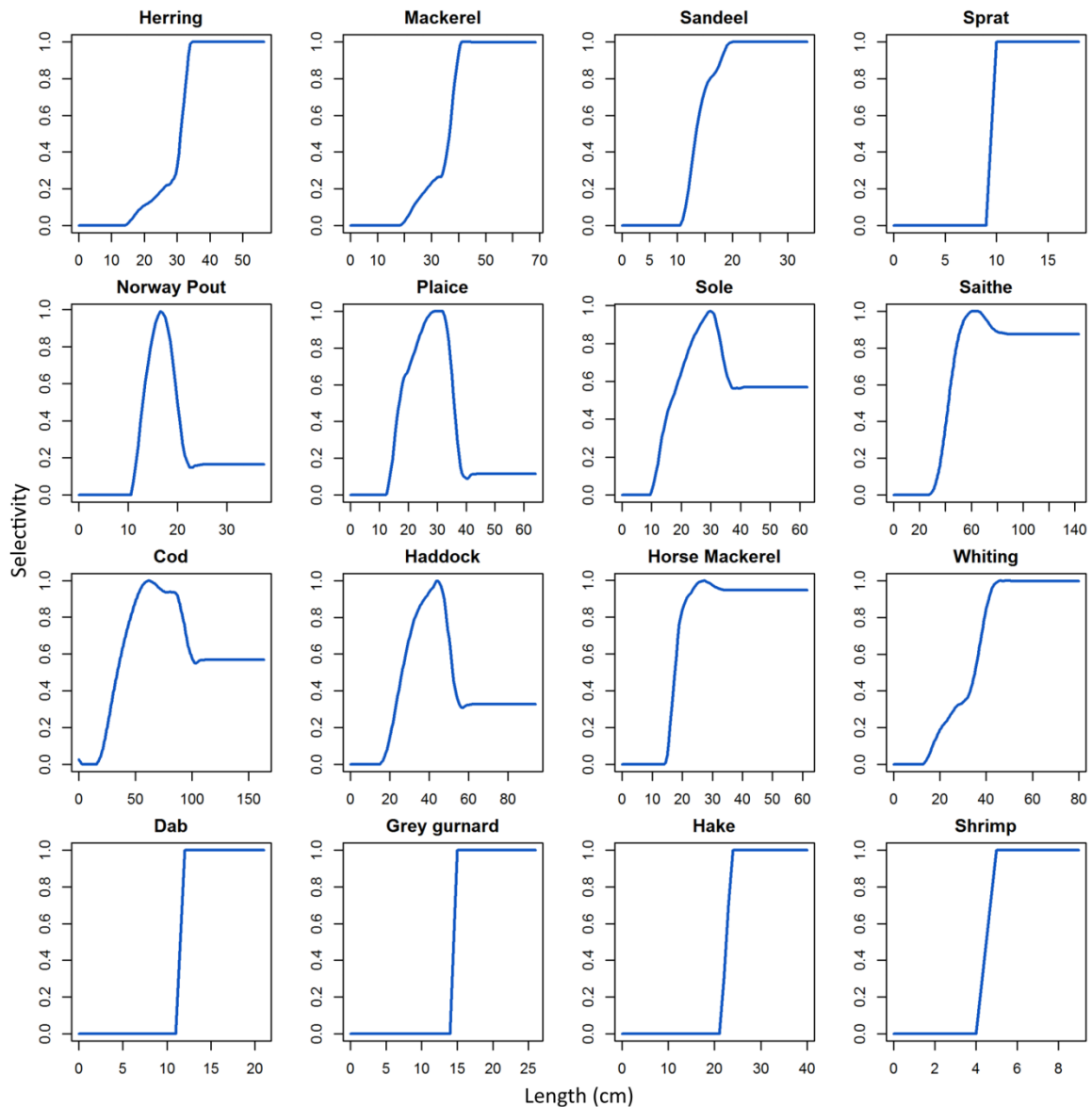


Figure 33: Fishing selectivity per species as parameterized in Ev-OSMOSE-NS.

5.2.2 Characteristics of the performed simulations

The configuration (set of parameters including calibrated ones) used in this study, Ev-OSMOSE-NS, is the same as the one presented in Chapter 4. Two sets of simulations, differing by the length of the time period simulated, were performed to obtain appropriate outputs allowing the exploration of two aspects of fisheries- and predation-induced evolution: on the one hand, trait evolution and, on the other hand, its impacts on species fitness.

To explore the trends of evolving traits, 100-year simulations are run. Trait mendelian transmission between parents and offspring is activated from year 70 onwards, which means that evolution start on this year of each simulation. The results are averaged over 28 simulation replicates to account for stochasticity of the model. The number of replicates was chosen for technical reasons. The simulations are run on the DATARMOR supercomputer. The DATARMOR nodes used for the simulations contain 28 cores. The replicates were thus parallelized and each was run on a single core. For each species, the mean genotypic values of the evolving traits are computed as the average of individual genotypic values. The two evolving traits are the intercept m_0 of the linear maturation reaction norm (LMRN) that describes all possible combinations of age and size at maturation for an individual and the reproductive effort r , which corresponds to individuals' gonado-somatic index.

Evolution of population traits is investigated over time and assessed through linear regression (with lm function) over the years 70 to 100, i.e., when evolution is activated. The evolutionary trends and corresponding linear regressions are represented in graphs of mean genotypic value (in both trait unit and in units of genotypic standard deviation of the trait σ_A) according to time (in years) for each trait and species. The y-axis of these graphs is standardized for each species and trait: it is centered on the trait's mean genotypic value averaged over 20 years prior to evolution activation (year 50 to 70) and its minimal and maximal limits are one trait genotypic standard deviation σ_A below and above the average, respectively. Due to this standardization, the evolutionary trend and the corresponding linear regression slope are visually comparable between species and traits as evolutionary changes are display on a scale determined by the trait's genotypic variability.

To explore how traits' evolution impacts species' average fitness and global community demographics, two sets of 28 simulation replicates lasting 300 years are run, one without and one with evolution enabled for comparison purpose. For the latter, trait mendelian transmission is activated from simulation year 70 onwards, meaning that evolution starts on this year. For each simulation set and species, fitness is calculated for each cohort born between year 70 and year 275

of the simulation, i.e., for 205 cohorts. The first 70 years are not considered as they constitute the spin-up period before evolution. Likewise, as the longest-lived species lives up to 25 years, cohorts born after year 275 are not considered to have fitness for the same number of complete cohorts for all species. For each cohort, outputs of total abundance and fecundity at each age are averaged over the 28 replicates and used to calculate the mean cohort fitness as its expected lifetime reproductive success R_0 as follows (Brommer, 2000; Stearns, 1992):

$$R_0 = \sum_{a=0}^{a=a_{\max}} s(a)N_{egg}(a) \quad (21)$$

where $s(a)$ is average survival from age 0 to a estimated as the ratio between total abundance at age a and at age 0 and $N_{egg}(a)$ is average fecundity, i.e., the average number of eggs produced per individual from age $a - 1$ to a . R_0 can simply be interpreted as the per generation ratio of multiplication of a population or the cohort replacement rate.

5.3 Results

5.3.1 Evolutionary trends in maturation and reproductive effort

As expected, the mean genotypic value of the intercept of the LMRN m_0 and the gonado-somatic index r was constant before evolution activation for both traits and all species (Figure 34). After the activation of evolution, traits' mean genotypic values exhibited either increasing, or constant or decreasing trends depending on species. Herring and plaice had the largest increase in m_0 mean genotypic value with a slope higher than $0.008 \sigma_A \cdot y^{-1}$ ($0.02 \text{ cm} \cdot y^{-1}$), indicating that they evolved towards maturation at older ages and larger sizes. In contrast, mackerel, sandeel, Norway pout, saithe and cod faced a strong decrease of m_0 mean genotypic value, with a slope steeper than -0.006 up to $-0.05 \sigma_A \cdot y^{-1}$ (-0.01 to $-0.334 \text{ cm} \cdot y^{-1}$), thus evolving towards earlier maturation at smaller sizes. Other species' m_0 mean genotypic values were roughly constant (haddock, sprat, horse mackerel; between 0.002 and $0.003 \sigma_A \cdot y^{-1}$), slowly increasing (sole, whiting, dab, grey gurnard between 0.004 and $0.006 \sigma_A \cdot y^{-1}$) or slowly decreasing (hake, $-0.004 \sigma_A \cdot y^{-1}$).

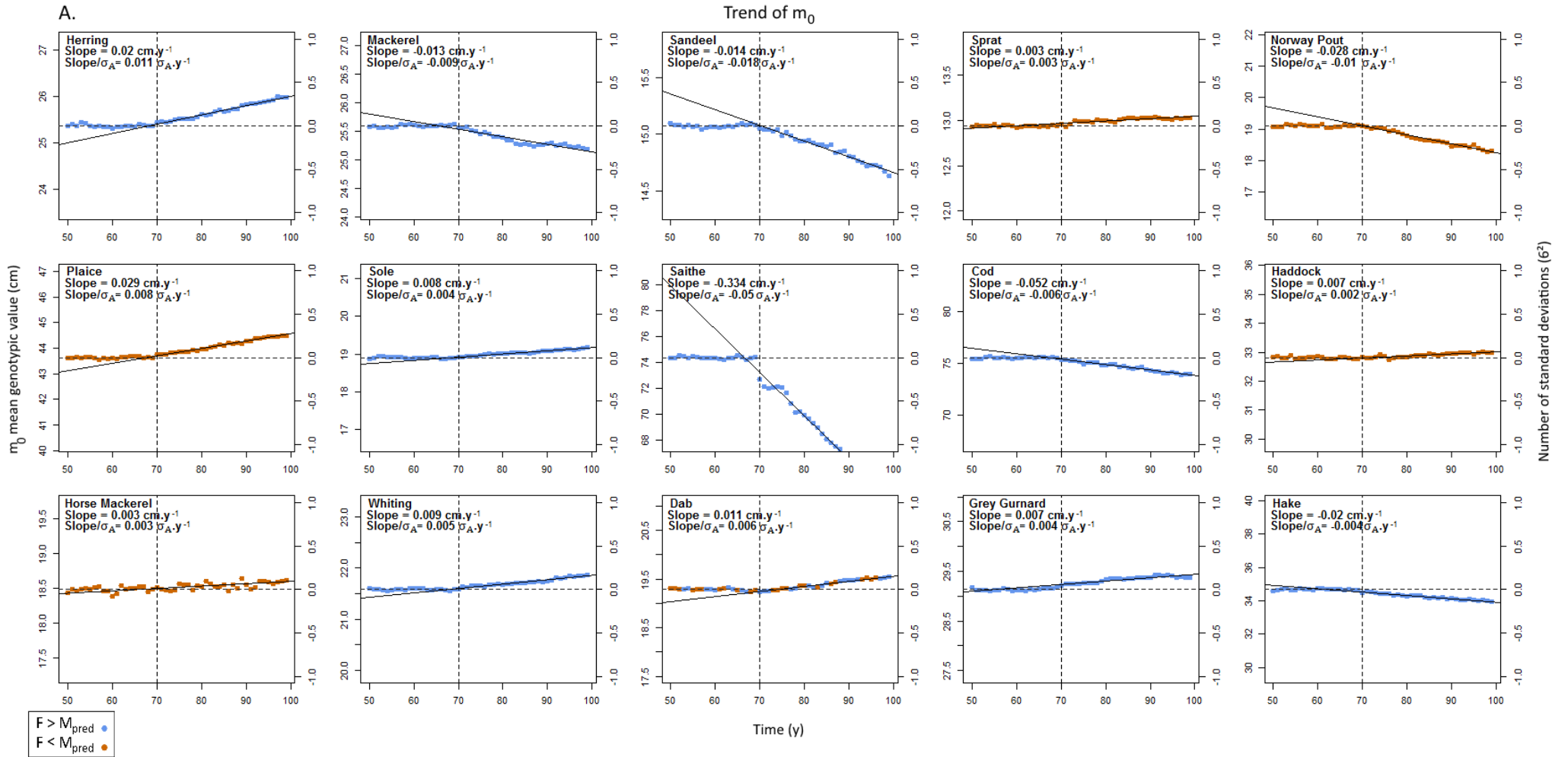
The r mean genotypic value of plaice, horse mackerel, and grey gurnard decreased markedly, with a slope between -0.009 and $-0.007 \sigma_A \cdot y^{-1}$ ($-0.0005 y^{-1}$; note that r is dimensionless as it is a ratio, hence the unit y^{-1} for the slope in trait unit per year), denoting evolution towards lower relative fecundity. In contrast, r mean genotypic value increased strongly for mackerel, saithe and hake with slopes steeper than 0.015 up to $0.025 \sigma_A \cdot y^{-1}$ (0.0015 to $0.0017 y^{-1}$), indicating evolution towards stronger reproductive investment. Other species' r mean genotypic values were roughly constant (sprat, haddock, and whiting; between 0.001 and $0.002 \sigma_A \cdot y^{-1}$), slowly decreasing (herring, sole, and dab; between -0.004 and $-0.003 \sigma_A \cdot y^{-1}$) or slowly increasing (sandeel, Norway pout, and cod; between 0.003 and $0.005 \sigma_A \cdot y^{-1}$).

Except for three species that exhibited a very weak or no trend (sprat, haddock, and whiting), the trends in m_0 and r mean genotypic values had opposite signs for all species, which materialized in strong negative correlations between times series of m_0 and r mean genotypic values (Table 10, last column).

The species with a decreasing m_0 mean genotypic value and an increasing r mean genotypic value were species that faced a fishing mortality higher than adult predation mortality (mackerel, sandeel, saithe, cod, and hake), except Norway pout (Table 10, first and second column). On the contrary, species with decreasing r mean genotypic value and increasing m_0 mean genotypic value were roughly equally split between species with higher predation mortality than fishing mortality (plaice, horse mackerel) and species with the opposite mortality pattern (grey gurnard, herring, sole). The majority of species with weak or no trend faced more predation mortality than fishing mortality (sprat, haddock, dab, whiting).

Table 10: Mean adult predation and fishing mortality rate per year per species (first and second columns respectively) and correlations of the times series trends of m_0 mean genotypic value and an r mean genotypic value per species (last column).

Species	Mean adult predation mortality rate per year (y^{-1})	Mean adult fishing mortality rate per year (y^{-1})	r- m_0 correlations
Herring	0.079	0.139	-0.96
Mackerel	0.047	0.265	-0.96
Sandeel	0.298	0.604	-0.91
Sprat	0.27	0.179	0.52
Norwat pout	2.045	0.116	-0.96
Plaice	0.079	0.073	-0.99
Sole	0.069	0.221	-0.96
Saithe	0.044	0.388	-0.99
Cod	0.024	0.289	-0.92
Haddock	0.135	0.049	0.54
Horse mackerel	0.08	0.034	-0.5
Whiting	0.104	0.161	0.54
Dab	0.143	0.143	-0.87
Grey gurnard	0.175	0.316	-0.91
Hake	0.175	0.327	-0.98



Chapter 5 – FIE in an evolving community

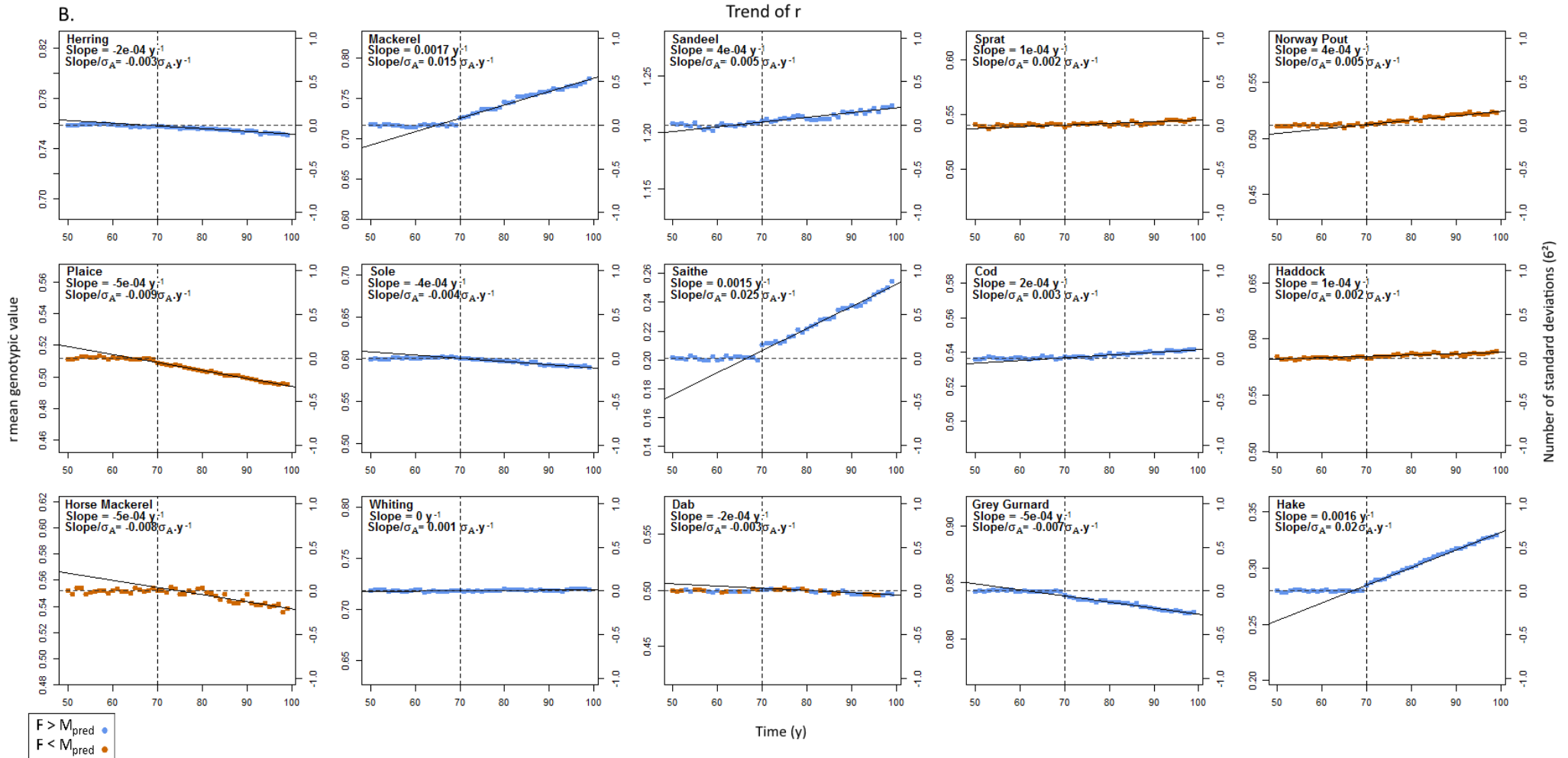


Figure 34: Evolution of the population mean genotypic values of m_0 (A) and r (B) over 50 years of simulation. The left y-axis gives the mean genotypic value in trait unit and the right y-axis in units of genotypic standard deviation of the trait σ_A , the latter allowing thus to compare trends' strength across species and traits. Evolution (trait mendelian transmission) is activated at year 70 (vertical dashed line). The horizontal dashed line is the mean genotypic value of the population averaged over the 20 years before the evolution activation (from year 50 to 70). Blue points are time steps for which fishing mortality is higher than predation mortality at adult stage and orange points are those for which fishing mortality is lower than predation mortality at adult stage. The

black line is the linear regression of the trait trend over time after the activation of evolution. The estimated slope of this regression is given on the plot in trait unit per year (slope) and in units of genotypic standard deviation of the trait per year (slope/ σ_A). All the slopes are significant (p-value < 0.05).

5.3.2 Implication for species' fitness and community demographics

The changes of mean cohort fitness throughout evolution at the species level (Figure 34) and their implications for community demographics (Figure 36) are investigated by comparing fitness time series without and with evolution. The mean fitness of a cohort R_0 can be interpreted as the expected (i.e., while accounting for survival probability) number of offspring of an individual in the cohort throughout its life and thus as the cohort replacement rate. As such it is a measure of the demographic growth rate of a population, values $R_0 > 1$ meaning an increase in abundance and values $R_0 < 1$ a decrease. The sum of species' mean cohort fitness at the community level can thus be used as an indicator of community growth in total abundance.

Figure 35 shows the species' mean fitness over cohorts and compares the trends with and without evolution. For half of the species (herring, mackerel, sandeel, sprat, horse mackerel and dab), R_0 remained on average stable over cohorts around a value of 1 in both scenarios, meaning that species abundance oscillated around a similar constant value with and without evolution. One exception was Norway pout, for which R_0 was stable but around an average value below 1 (around 0.98) suggesting a risk of collapse. However, the collapse was prevented by cohorts with R_0 values above 1 occurring regularly throughout the time series and thus replenishing the population. In contrast, two species, cod and sole, ended up collapsing after around 200 and 250 years respectively in both scenarios. This translated into R_0 values below 1 for all cohorts without and with evolution although the two species exhibited opposite fitness trends: a decreasing one for sole and an increasing one for cod. Yet, for both species, evolution increased R_0 compared to the scenario without evolution. However, fitness improvement through evolution was not enough for an "evolutionary rescue" to occur, as both species' R_0 remained under 1 even with evolution. Evolution improved fitness of plaice and grey

gurnard relative to the scenario without evolution with in both cases an almost constant value of R_0 above of 1. Fitness was also improved for saithe and hake in the evolution scenario but according to a very different pattern. There was a sharp increase of R_0 over the first 30 to 50 cohorts and then a slower decrease that seemed to stabilize around $R_0 = 1$, as expected through gradual evolutionary dynamics towards an evolutionary equilibrium under frequency-dependent selection. Finally, evolution impaired fitness in haddock and whiting as shown by the lower values of R_0 with evolution compared to those without. Moreover, for these two species R_0 values decreased over cohorts without and with evolution but evolution worsen the situation. For haddock, R_0 values with evolution fell below 1 on average at the end of the time series but did not for the scenario without evolution that stabilized around 1, suggesting a risk of collapse with evolution. Still, some cohorts had R_0 values above 1 which could prevent the population from collapsing just as for Norway pout. In contrast, for whiting R_0 values without evolution stabilized around 1 on average whereas those with evolution fell below 1 for every single cohort thus announcing population collapse with almost certainty.

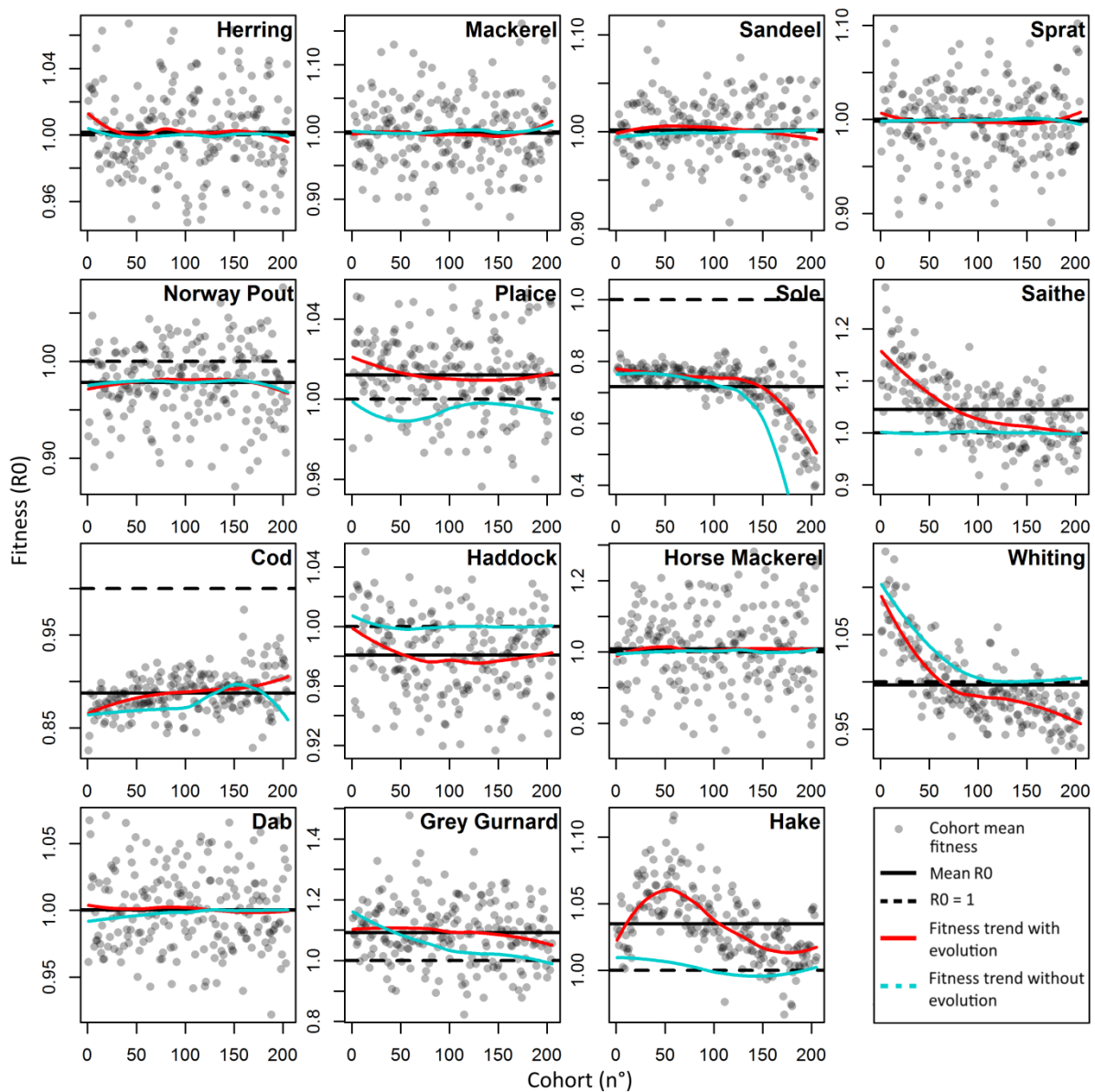


Figure 35: Fitness trends without and with evolution over 205 simulated cohorts by species, averaged over 28 replicates. The first cohort is born in year 70 (start of mendelian transmission in the scenario with evolution), the last in year 275. The horizontal black dashed line represents $R_0 = 1$, i.e., the fitness value below which population abundance decreases and above which it increases and for which an evolutionary equilibrium is reached under frequency-dependent selection. The gray dots are cohorts' mean fitness for the scenario with evolution. The horizontal black line is the average mean cohort fitness over the time series for the scenario with evolution. The red curve is the fitness trend with evolution represented by a loess smoother. For comparison purpose, the blue curve represents the fitness trend without evolution.

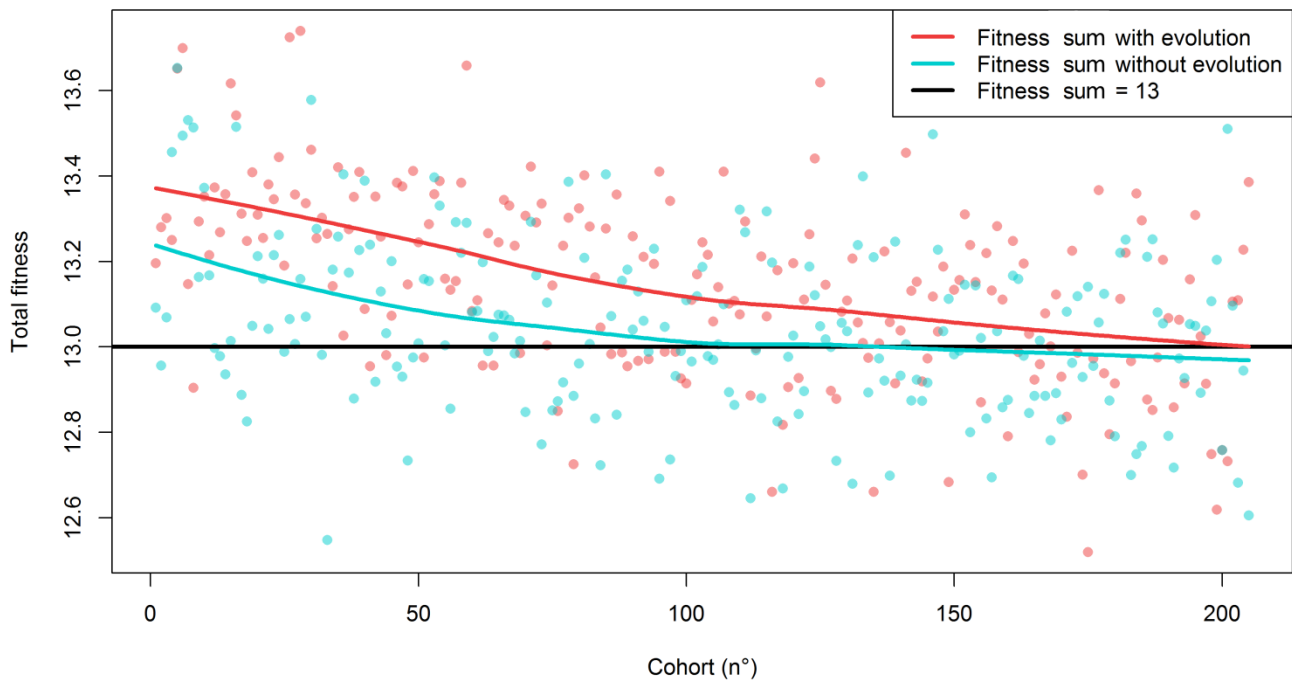


Figure 36: Trend in the sum of species' mean cohort fitness without (blue points and curve) and with evolution (red points and curve). As cod and sole collapsed during simulation, the sum of species' fitness is calculated excluding these two species, thus relying only on 13 species. A fitness sum above 13 implies an increase of the total community abundance and below 13 implies a decrease. Points are raw data and curves are loess smoothers.

The repercussion of evolution at the community level was an increase of total abundance relative to the scenario without evolution as testified by the fitness sum with evolution being on average larger than without (Figure 36 smoothing curves). The average advantage of the scenario with evolution relative to the scenario without was roughly stable over the first 50 cohorts and then decreased until the end of the time series. The average fitness sum without evolution decreased below 13 around cohort 140 meaning a potential decline in total abundance whereas with evolution seemed to stabilize around 13 suggesting global abundance and evolutionary equilibrium.

5.4 Discussion

5.4.1 Life-history evolutionary trends in a community

5.4.1.1 The main pressure at play drives the evolutionary trends

Empirical evidence of FIE has been first reported thirty years ago for the North Sea plaice (Rijnsdorp, 1993). Awareness of the phenomenon has been developing over the last 20 years (Browman et al., 2000; Heino, 1998; Law, 2000; Stokes and Law, 2000) and evidence from the wild regularly reported since then (Heino et al., 2015). Life-history trait evolution is the fisheries-induced evolutionary impact the most frequently described in literature. In most cases, fishing is a selective pressure in two respects: it increases the population's total mortality and it is often size-selective by targeting larger individuals mainly. These two selective pressures are expected to favor faster life histories, i.e., earlier maturation (Ernande et al., 2004; Marty et al., 2015; Olsen et al., 2004) and higher reproductive investment (Wright et al., 2011a; Yoneda and Wright, 2004), whereas consequences for growth may differ depending on their respective strength and the exact size-selectivity pattern of fishing mortality (Enberg et al., 2012). This is because elevated total mortality favors faster growth whereas size-selectivity targeting large individuals favors slower growth. Yet, most empirical evidence regarding growth so far pointed towards an evolutionary reduction of growth (Heino et al., 2015).

While all species experience fishing in our model, the expected pattern of life-history changes in response to fishing-induced selection was observed for only six out of the fifteen modeled species: mackerel, sandeel, Norway pout, saithe, cod and hake (Figure 34). Documented FIE of life-history traits concerns mainly the gadoids family across all ecosystems (Heino et al., 2015) and especially in the North Sea (Marty et al., 2014), which is concordant with our model as we observe the strongest tendencies in trait unit per year for cod, hake, Norway pout, and saithe. Most interestingly, except for Norway pout, these species were characterized by a fishing mortality rate that was higher than their experienced adult predation mortality rate (Table 10).

In contrast, some species faced a more intense predation pressure than fishing pressure (Figure 34, Table 10). Except for Norway pout, these species exhibited very weak, if any, evolving trends in their life-history traits (sprat, haddock, dab) or the opposite pattern than the one classically observed in

FIE studies: an increase in the intercept m_0 of the LMRN, meaning maturation at older ages and larger sizes, and a decreasing reproductive effort r (plaice, horse mackerel). Predation mortality is size-selective (Sogard, 1997) and decreases with size. It can thus generate a selective pressure (Fisk et al., 2007) opposed to fishing-induced selection. Our results suggest that predation can be the major selective force driving the evolutionary trends in life-history traits, as was documented in a freshwater prey-predator empirical study (Edeline et al., 2007), or can counterbalance fishing-induced selection thus resulting in almost no trend (haddock or sprat for example). To account for evolutionary impacts in an ecosystem approach to fisheries management (Laugen et al., 2014), appreciating that predation-induced selection can counterbalance or overcome fishing-induced selection is a necessary step. Further work is needed to better estimate fishing- and predation-induced selective pressures in a common framework, and identifying the fishing mortality that equilibrate with predation in terms of selective pressures may become an additional management objective in an evolutionarily enlightened management approach to fisheries.

5.4.1.2 Can the fishing selectivity pattern reverse trend?

The expected evolutionary response to fishing or predation as the main selective pressure (see previous Section) was not observed for all species. Norway pout showed increasing reproductive effort r and decreasing intercept m_0 of the LMRN while facing higher predation pressure than fishing. On the contrary, herring, sole and grey gurnard displayed decreasing r and increasing m_0 whereas they experienced higher fishing than predation mortality. Whiting is not considered here as the trends in its traits were very weak and we showed that mendelian trait transmission was not effective for this species (see Chapter 4).

Species with an unexpected evolutionary response (herring, Norway pout, sole, and grey gurnard) may experience a different selective pressure than hypothesized, which could arise from the fishing size-selectivity pattern (Boukal et al., 2008; Hutchings, 2009; Jørgensen et al., 2009; Kuparinen et al., 2009). In our model, it emerges from the combination of the size-selectivity of all the fishing gears

catching the species (Figure 33). Notably, sole and Norway pout fishing size-selectivity is partly bell-shaped, as is typical in fisheries including a significant part of gillnets. This selectivity pattern targets preferentially, although not exclusively, a small-range of intermediate size classes. In the case of sole, an increase in adult size-at-age implied by a decrease in r would thus lead to a decrease in fishing mortality. In the case of Norway pout, a small evolutionary change affecting adult size-at-age could result in a sharp decrease of fishing mortality in both directions (smaller or larger size), which introduces an evolutionary bistability, the end result depending on the specific context (Boukal et al., 2008). The adult mean size of Norway pout being lower than the size corresponding to the maximum of its fishing selectivity curve, we hypothesize that selection favors a shift towards smaller size, which occurred through evolution towards a higher r and a smaller m_0 . In addition, we hypothesize that the potential gain in size with a decrease of r would not be enough to escape predation. Norway pout is a main forage species (Cormon et al., 2016) with adult measuring between 10 and 25 cm in our simulations: if the larger phenotypes cannot escape from predators, then investing more into reproduction and escaping from fishing by reducing adult size-at-age is more advantageous.

For herring and grey gurnard, the fishing size-selectivity curve is a sigmoid, typical of fisheries dominated by trawls. The expected evolutionary response to a main selective pressure generated by a mortality that increases with size is an increase of reproductive investment r and a decrease of the maturity age and size through a decrease of the intercept m_0 of the LMRN. The opposite response was obtained for these two species. For these two species, fishing and predation mortality were low and of the same scale and the evolutionary trend of both traits was weak (see Figure 34). When fishing and predation are low and of the same scale of intensity, we hypothesize that other factors might influence the evolutionary trend. Trophic interactions, and more precisely resources acquisition, could be the selective pressure responsible for the evolutionary responses obtained. An increase in size, through a decrease in r and an increase in m_0 , could indeed be advantageous as it changes the trophic niche or the interspecific competition intensity (Edeline and Loeuille, 2021;

Loeuille and Loreau, 2005). A future step to better understand evolving marine fish communities would be to identify the conditions when trophic interactions drive evolutionary changes in life-history traits instead of fishing or predation.

5.4.1.3 Emergence of correlated evolutionary trends in life-history traits

In our model, maturation and reproductive effort are modeled as independent traits both genetically and environmentally (Chap. 4). Regarding genetics, the initial pools of alleles of the two traits are independent and, during the initialization, the alleles for each trait are independently randomly drawn within each pool. Regarding micro-environmental deviations, their distributions for each trait are independent and during the initialization, micro-environmental deviations for each trait are independently randomly drawn within each distribution. Despite initial trait independence, we observe an emerging negative correlation between the evolutionary trends of the two traits (Figure 34, Table 10) for 12 out of 15 species. Hence, the different species evolve towards a faster life history with earlier maturation and higher relative fecundity or a slower life history with later maturation and lower relative fecundity. The resulting correlation between life-history traits, called *pace-of-life syndrome*, implies the evolution of populations or species along a fast-slow life history continuum (Ricklefs and Wikelski, 2002). Empirical studies have shown that the *pace-of-life syndrome* is supported by underlying correlated behavior and physiology (Dammhahn et al., 2018). Here, our results suggest that evolutionary pressures can shape the correlation of life-history traits at the interspecific level despite their independence, that will involve coordinated changes in response to further evolutionary pressures (Forsman, 2015). It would be interesting to confirm our results with similar correlation emergence when more traits are allowed to evolve. Further work should also investigate whether the emergence of such correlations at interspecific level is a consequence of the emergence of trait correlations at intraspecific level, i.e., phenotypic or genetic correlations between individuals of a same species.

5.4.1.4 Rates of the evolution

The simulated rates of evolution (slopes in Figure 34) could be perceived as slower than observed ones from empirical studies: in our model, evolutionary rates of the intercept m_0 of the LMRN ranged from -0.334 to 0.029 cm.y^{-1} (from -0.05 to 0.011 $\sigma_A.\text{y}^{-1}$) and those of gonado-somatic index from -0.0005 to 0.0017 y^{-1} (-0.009 to 0.025 $\sigma_A.\text{y}^{-1}$). In the North Sea, the observed evolutionary changes are mainly described for the LMRN intercept for gadoids (for female: cod: -0.85 cm.y^{-1} , 1974-2006; haddock: -0.36 cm.y^{-1} , 1974-2006; whiting: -0.13 cm.y^{-1} , 1974-2006; Norway pout: -0.01 cm.y^{-1} , 1981-2006 (Marty et al., 2014)), herring (-0.05 cm.y^{-1} , 1990-2005 (Enberg and Heino, 2007)), sole (-0.1 cm.y^{-1} , 1966-1995 (Mollet et al., 2007)), and plaice (-0.1 cm.y^{-1} , 1955-1995 (Grift et al., 2003)).

The values from the literature were obtained for time series corresponding to earlier periods in the North Sea than the one simulated: here, we modeled evolutionary trends for the current state of the system from 2010 to 2019. Hence, the evolutionary trends may be lower in the current period due to the less intense fishing pressure observed for the majority of the species (ICES, 2019b, 2018c, 2018d, 2018e, 2016) but also potentially to genetic erosion due to earlier intense exploitation (Marty et al., 2015). Differences could also arise from our model itself due to (i) genetic drift related to stochastic sampling of alleles between parent and offspring that is increased as the parental population become smaller, which in our case was potentially amplified by the use of superindividuals, (ii) an underestimation of traits' heritability (initially fixed at 0.2) or (iii) an overestimation of population biomass in the model leading to an underestimation of fishing pressure.

5.4.2 Evolutionary changes' impact on fitness and demography

5.4.2.1 Constant species fitness: a case of co-evolution?

Using a multispecies model with a single evolving species, Jusufovski and Kuparinen, (2020) identified an advantage for the evolving species in terms of biomass when facing fishing relative to a non-evolutionary scenario. In our model with multiple evolving and interacting species, we would have expected a clear fitness gain for a majority of species, or a few winners and losers as a consequence of differential adaptation, especially since we model an average state of the ecosystem under average environmental and fishing conditions. Under such constant conditions, an evolutionary change in the life cycle is mostly expected to have a clear and unidirectional impact on the simulated fitness in contrast with varying environmental conditions that may render a phenotype adapted to the selective condition at one point in time maladapted to the conditions at another time. On the contrary, for the majority of species, we observed a constant average fitness around 1 that only allows the population to renew itself (Figure 35: herring, mackerel, sandeel and Norway pout) despite clear evolutionary trends in their life-history traits (Figure 34). This result highlights that evolution in multiple species context may lead to dampened evolutionary benefits from life history changes in terms of fitness and thus weakly impacts abundance dynamics. Such outcome exemplifies frequency-dependent selection that can typically emerge in ecological systems with multiple inter-specific interactions such as competition and predation (Heino et al., 1998; Meszena et al., 2002). In such case, evolution proceeds along a fitness landscape that is constantly moving as the focal species evolve and the other species co-evolve because fitness is conditional on the different species' trait value. As a result, evolutionary equilibrium is reached when attaining a conditional fitness maximum that has a value $R_0 = 1$. Most importantly here, the average fitness of the co-evolving species remains unchanged at $R_0 = 1$ despite continuous evolution due to unstable evolutionary equilibrium generated by the co-evolution of interacting species in constant "arms race", a phenomenon coined as the Red Queen Hypothesis (Brockhurst et al., 2014; Van Valen, 1973). Parallely, such demographic

compensatory effects between coevolving interacting species under human pressures has been reported in other ecosystems (Brans et al., 2022) and theorized as cryptic eco-evolutionary dynamics (Hendry et al., 2018; Kinnison et al., 2015). Kinnison et al. (2015) explains that cryptic eco-evolutionary dynamics pattern can be in appearance similar to ecological or even null expectations, and then named it cryptic. In our case, we hypothesize that the cryptic eco-evolutionary dynamics observed in fitness change and thus in abundance dynamics is explained by species coevolution and the Red Queen Hypothesis. This hypothesis could be explored in further work with simulations under different fishing scenario.

Despite the likely collapse of one species, withering, linked to evolution (the collapse of cod and sole occurring in scenarios without and with evolution), a global demographic stability of the community emerges from species coevolution and the Red Queen dynamics as shown by the stabilization of the sum of species' mean cohort fitness around 13 (Figure 36). This underscores the resilience potential of evolving interacting species in the face of exploitation, thanks to the adaptive potential of each species in the community. Given that the adaptive potential and the eco-evolutionary dynamics (Cortez, 2018) strongly depend on genetic variation, a genetic variance erosion, such as that caused by fishing (Marty et al., 2015), could disrupt the community stability observed in our results as a consequence of co-evolution. Our study thus highlights the critical need to measure and understand the dynamics of genetic variance and limit its erosion in order to promote management actions consistent with a demographically stable evolving fish community.

5.4.2.2 Gain for the community: the niche optimization

The sum of species' mean cohort fitness with evolution was larger than the without evolution (Figure 36) even though, in both scenarios, two species collapse (cod and sole). The decrease in fitness in the scenario without evolution while the species collapsed emphasizes that the vacant niche left by the collapse of cod and sole was not occupied by a new species. In contrast, in the scenario with evolution, hake fitness was higher indicating that hake has benefited from the collapse of sole and

cod, the latter being a competitor of hake. We hypothesize that the evolutionary potential of hake allowed it to achieve the gain in fitness necessary to "replace" the collapsed species. Therefore, the adaptive potential of species could be beneficial at the community level also for total community abundance considerations and not only stability. Consideration of evolution in community models provides a more realistic understanding of community changes and resilience. This result has also management implications, as it emphasizes that adaptive potential is beneficial at the community level, as it creates a community where species can more readily substitute each other.

Chapitre 6 : Discussion générale

Les modèles écosystémiques marins, dont parmi eux les modèles *end-to-end*, vont en se complexifiant. La qualité de l'ajout d'un processus dans un modèle peut être évaluée selon deux critères : l'amélioration de sa capacité à représenter la réalité et sa parcimonie (Fulton et al., 2003). Au regard de ces deux critères, l'ajout de nouveaux processus dans des modèles écosystémiques s'avère utile et nécessaire pour quatre aspects : (i) la compréhension nouvelle du fonctionnement des écosystèmes, (ii) le réalisme des nouveaux processus, (iii) l'existence de données pour les paramétrer ou les calibrer et (iv) l'implication de ceux-ci dans les changements écosystémiques observés.

Les travaux de thèse présentés dans ce manuscrit seront discutés au regard de ces quatre aspects. Tout d'abord, nous évaluerons le degré de compréhension des écosystèmes apporté par la description de la variabilité plastique et génétique des traits d'histoire de vie. Nous analyserons ensuite le réalisme apporté par les sous-modèles mécanistes ajoutés au modèle écosystémique OSMOSE dans le cadre de cette thèse ainsi que certaines pistes d'améliorations futures des processus représentés. Un inconvénient à l'augmentation du réalisme des modèles écosystémiques est la complexification de leur paramétrisation, de leur ajustement et de la compréhension des sorties simulées. Ce point sera discuté dans une troisième partie. Enfin, quantifier les impacts des nouveaux processus implémentés sur les changements écosystémiques est une étape cruciale pour déterminer la pertinence de la prise en compte de ces processus pour des raisons techniques et dans une optique de gestion des ressources. Cet aspect peut se traiter à l'aide de simulations sous scénarios climatiques et/ou scénarios de pêche. Ces questions ouvertes par le développement d'un modèle évolutionnaire d'écosystèmes marins seront traitées en dernière partie.

6.1 Variations intraspécifiques des traits d'histoire de vie dans un écosystème : une échelle nécessaire pour comprendre la diversité fonctionnelle et spécifique.

6.1.1 Déterminants environnementaux des flux physiologiques

Les préférences thermiques des espèces pour leurs capacités aérobies définissent en partie la biogéographie des espèces (Clarke et al., 2021). Cependant, les capacités aérobies ne sont pas les seules déterminants des températures auxquelles les organismes se trouvent : rencontrer des températures tolérées est une condition nécessaire mais pas suffisante au maintien d'une espèce et à la réalisation de ses flux physiologiques (Jutfelt et al., 2018).

Dans le chapitre 3, nous montrons qu'il existe un **écart**, parfois important, entre **les capacités d'acquisition d'énergie nette maximale** (*fundamental thermal performance curve*) et celles **réalisées** principalement en lien avec la **nourriture disponible** mais aussi **la concentration en oxygène**. Ce chapitre confirme que les capacités aérobies ne sont pas toujours de bons indicateurs des performances physiologiques réalisées, en tout cas pour l'acquisition nette d'énergie et les processus énergétiques en aval, et leur utilisation peut ainsi biaiser les projections des impacts du changement climatique.

Les résultats présentés au chapitre 3 peuvent aussi être interprétés sous l'angle de la variabilité intraspécifique des traits individuels qui émergent de la variabilité des flux physiologiques, comme les tailles-aux-âges par exemple. En l'absence de variabilité génétique, les variations des flux physiologiques sont uniquement liées à des variations environnementales.

Dans le modèle Bioen-OSMOSE, les variations des tailles-aux-âges peuvent être dues à la disponibilité en nourriture, à la température et à l'oxygène. La taille d'un individu dépend de son acquisition d'énergie nette réalisée sur l'ensemble de sa vie (l'acquisition d'énergie nette sera considérée comme un indicateur de performance dans la suite). La réponse réalisée de l'acquisition d'énergie

nette à la température nous renseigne sur les facteurs influençant la variation de l'acquisition nette d'énergie et en conséquence sur la variabilité des tailles-aux-âges émergentes.

Dans la Figure 37, trois réponses réalisées sont présentées. Quand l'oxygène et la nourriture ne sont pas limitants (cas A) ou sont limitants et constants (cas B), la variation physiologique et donc en tailles-aux-âges est uniquement liée à la température. Quand l'oxygène et la nourriture sont limitants mais non constants (cas C), la variation des flux physiologiques peut être influencée plus fortement par la nourriture et l'oxygène que par l'effet direct de la température sur les flux physiologiques.

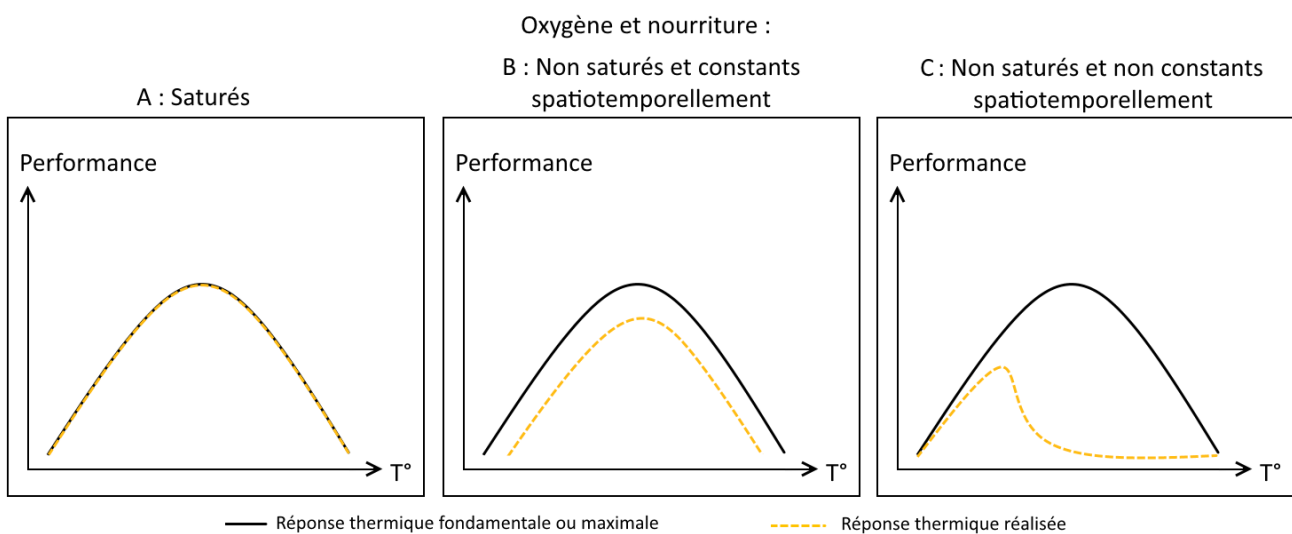


Figure 37: Illustration schématique d'une réponse fondamentale thermique d'une performance (pouvant être l'acquisition d'énergie nette par exemple) (courbes noires) et de trois exemples de réponses réalisées (courbes oranges en pointillés) : (A) un cas de nourriture et d'oxygène saturés, (B) un cas de nourriture et d'oxygène non saturés et constants spatiotemporellement, et (C) un cas de nourriture et d'oxygène non saturés et non constants spatiotemporellement de sorte à covarier avec la température.

Dans Bioen-OSMOSE-NS, une variabilité importante de la taille émerge dès l'âge 1 puis change peu aux âges suivants. Le chapitre 3 a également montré que durant la première année de vie, les courbes de performances réalisées sont principalement des cas de non-saturation en nourriture et de nourriture non constante (Figure 37C). Nous pouvons ainsi faire l'hypothèse que **la variation plastique des tailles-aux-âges** en mer du nord est actuellement principalement dominée par **l'impact de la variation en nourriture et ce potentiellement aux jeunes stades**. Cette lecture des courbes de performances thermiques réalisées permet de les interpréter à une échelle plus intégrée et de faire

un lien plus direct entre réponses physiologiques réalisées, variables biotiques et abiotiques et traits d'histoire de vie.

6.1.2 Variations génétiques des traits d'histoire de vie

La variation des traits d'histoire de vie est aussi déterminée par la **variation génétique** sous-jacente. Le chapitre 5 montre que la valeur moyenne et la variation des **traits d'histoire de vie** peut changer en évoluant face à deux forces sélectives majeures : la **pêche** et la **prédation**.

Ce chapitre montre que les tendances évolutives de traits d'histoire de vie sont un « **trade-off** » entre ces deux pressions sélectives qui peuvent s'équilibrer. Ces premiers résultats ouvrent une piste intéressante pour la **conservation** de la **diversité fonctionnelle, i.e., des traits** : la pêche peut avoir un impact nul sur la diversité fonctionnelle au niveau intra-spécifique si cette pression de sélection est en équilibre avec la prédation. L'étude doit maintenant être approfondie pour comprendre l'impact de cette situation d'équilibre au niveau de la **diversité génétique**. Est-ce que le point d'équilibre entre pêche et prédation pour la diversité fonctionnelle permet de préserver la diversité génétique ? Sur ce point, deux hypothèses sont possibles : (i) une faible pression de pêche permettant d'éviter des tendances évolutives des traits d'histoire de vie peut aussi permettre d'éviter l'érosion génétique ou (ii) cet état d'équilibre pourrait faire disparaître des allèles codant pour les génotypes les plus éloignés de la moyenne génotypique du trait du fait d'une pression de sélection globale stabilisante.

L'émergence de dynamiques **éco-évolutives cryptiques** dans une communauté qui évolue est l'autre résultat majeur du chapitre 5. Ces dynamiques cachées, a priori liées à des dynamiques évolutives de type « Reine Rouge » ou « course à l'armement » entre compétiteurs et/ou proies-prédateurs au sein de la communauté (Brockhurst et al., 2014; Van Valen, 1973), pourraient en partie expliquer la prise en compte tardive des dynamiques évolutives dans la gestion des ressources halieutiques. Le caractère cryptique des dynamiques éco-évolutives est une propriété ambivalente pour la

conservation. Au niveau écologique, les biomasses des populations peuvent se maintenir grâce aux réponses évolutives cachées : la communauté est ainsi résiliente et stable grâce aux dynamiques éco-évolutives cryptiques. Cependant, elles rendent plus difficile la détection de basculements du fonctionnement du système (Dakos et al., 2019) qui peuvent alors survenir en apparence de manière abrupte et inattendue (voir l'exemple de la morue de Terre-Neuve Hutchings and Myers, 1994; Olsen et al., 2005, 2004).

6.2 Réalisme & limites du cadre de modélisation Bioen-OSMOSE et Ev-OSMOSE

6.2.1 Apports d'un modèle bioénergétique pour modéliser le cycle de vie individuel

Le nouveau modèle bioénergétique décrit dans le chapitre 2 remplace un sous-modèle phénoménologique pour la croissance et la reproduction anciennement utilisé dans OSMOSE (Shin and Cury, 2004, 2001; Travers et al., 2009). Ce changement de modélisation du cycle de vie possède trois avantages majeurs : (i) la conservation de masse et d'énergie entre niveaux trophiques (mais pas au niveau de l'écosystème car la masse et l'énergie de l'égestion, de l'excrétion et de certaines mortalités sont perdues), (ii) une structure en taille et en âge réaliste, et (iii) une fécondité dynamique en réponse aux variations environnementales.

Grâce au premier point, le modèle Bioen-OSMOSE peut être utilisé pour étudier les flux de biomasses et d'énergie dans les réseaux trophiques et entre les niveaux trophiques en réponse au changement climatique (Brown et al., 2010; du Pontavice et al., 2021, 2020) ou à la pêche (Rochet and Benoît, 2012) en intégrant l'impact de changements de traits individuels.

L'amélioration de la structure en taille est un changement crucial pour le réalisme et la fiabilité du modèle. La description phénoménologique utilisée classiquement dans OSMOSE sans bioénergétique entraînait une surestimation des tailles-aux-âges dans la majorité des configurations du fait de

l'absence de calibration du processus de croissance (Travers-Trolet et Oliveros-Ramos pers. comm). Cette surestimation était problématique car une hypothèse de base du modèle est la prédation opportuniste basée sur la taille (Shin and Cury, 2004, 2001; Travers et al., 2009). Le biais était néanmoins constant entre espèces : la hiérarchie de taille entre espèces était de ce fait conservée. Cependant la surestimation de taille, et donc de poids, pouvait entraîner une sous-estimation de l'abondance pour une biomasse équivalente, ainsi qu'un problème d'accès trophique aux proies de bas niveau trophique et de petite taille modélisées par les modèles biogéochimiques. De plus, une mauvaise structure en taille peut propager une mauvaise représentation de l'effort de pêche et des captures par classe de taille et d'âge. La correction de ces biais par l'implémentation du modèle bioénergétique est en ce sens une grande amélioration pour l'utilisation du modèle pour tester des scénarios de gestion.

Enfin, la fécondité est maintenant dynamique en réponse aux variations environnementales de température, d'oxygène et de proies. Dans OSMOSE, elle était proportionnelle à la biomasse de femelles matures, sans conséquence possible de l'environnement. L'utilisation de Bioen-OSMOSE permet une variation de la fécondité relative selon l'amélioration ou la dégradation des conditions environnementales. Ceci implique des variations des abondances tailles initiales de cohortes pouvant impacter la dynamique de populations (Rickman et al., 2000). Cette amélioration peut avoir des conséquences importantes sous scénarios de changement climatique notamment dans lesquels le réchauffement et la désoxygénation des océans peuvent diminuer la fécondité (Crozier and Hutchings, 2014; Pörtner et al., 2001).

6.2.2 Comment affiner la description de la réponse à la température ?

6.2.2.1 La réponse à la température doit reposer sur des mécanismes valides

La réponse physiologique des organismes marins à la température est encore aujourd'hui débattue, notamment le mécanisme sur lequel cette réponse repose et ses conséquences sur les populations et les écosystèmes (Jutfelt et al., 2018; Lefevre, 2016; Lefevre et al., 2017, 2018; Pauly and Cheung, 2018a; Pörtner, 2001; Pörtner et al., 2017). Parmi les points discutés, Lefevre et al. (2018) insistent sur la nécessité de représenter des mécanismes valides pour faire des projections réalistes.

Dans le cas des modèles écosystèmes marins multispécifiques, l'ajout d'une réponse physiologique est une amélioration car elle permet de prendre en compte des processus nouveaux qui varient avec la température. La réponse croissante du taux métabolique de la maintenance selon une loi d'Arrhenius est un processus généralement accepté (Brown et al., 2004; Gillooly et al., 2002; Kooijman, 2010; Pörtner, 2001). L'apport en oxygène et en énergie augmente plus lentement que le flux de maintenance avec la température (Pörtner, 2001), voire peut diminuer. Le mécanisme régissant la réponse à la température de l'apport en oxygène et de l'énergie reste cependant débattue. La théorie GOLT (*Gill-Oxygen Limitation Theory*) associe cette réponse à une capacité limitée des branchies à extraire de l'oxygène du milieu (Cheung et al., 2013; Pauly and Cheung, 2018a, 2018b) mais est réfutée par une équipe d'éco-physiologistes (Lefevre, 2016; Lefevre et al., 2017). Dans Bioen-OSMOSE, le mécanisme régissant la réponse de l'apport d'oxygène et d'énergie quand la température augmente est la dénaturation des protéines (Angilletta, 2009; Clarke, 2019). Ce mécanisme n'est actuellement pas controversé à ma connaissance.

Cette première implémentation d'une réponse bioénergétique à la température dans un modèle d'écosystème marin multispécifique pourra être améliorée dans des travaux futurs. Les principales pistes sont l'ajout de réponses différentes par stade de vie (Killen et al., 2007; Neubauer and Andersen, 2019; Sampaio et al., 2021), l'évolution « darwinienne » de la plasticité thermique (Angilletta, 2009; Crozier and Hutchings, 2014), une réponse du taux d'ingestion à la température et l'ajout de *trade-offs* entre ingestion, maintenance et préférence thermique (Killen et al., 2010;

Metcalfé et al., 2016). Les deux dernières pistes et leurs implications au niveau des dynamiques de l'écosystème sont discutées dans les deux prochaines sous parties.

6.2.2.2 Réponse de l'ingestion à la température

La température impacte la fonction d'ingestion des poissons en lien avec des changements de locomotion et du comportement d'alimentation (Volkoff and Rønnestad, 2020). Au niveau mono-spécifique, une augmentation de température entraîne dans un premier temps une augmentation de l'ingestion jusqu'à un seuil après lequel elle diminue d'abord doucement puis brusquement. Ce seuil est inférieur à la température critique de l'espèce. Symétriquement, les organismes arrêtent brusquement d'ingérer en dessous d'un seuil inférieur de température (Volkoff and Rønnestad, 2020).

Les effets de la température sur l'ingestion n'ont pas été pris en compte dans le cadre de ces travaux. Pour les prendre en compte correctement, il serait nécessaire de considérer l'effet thermique sur les relations proies-prédateurs (Domenici et al., 2019) : l'ingestion des prédateurs peut potentiellement augmenter avec la température, tout comme la capacité de fuite des proies (Domenici et al., 2019; Wilson et al., 2010). Bien que potentiellement impactante, nous avons mis cette réponse de côté en raison du peu de données existant sur l'augmentation de l'ingestion d'une part, et sur l'augmentation de la vitesse de fuite des proies d'autre part, et donc de la difficulté à paramétrer la réponse résultante (mais voire Englund et al., 2011; Öhlund et al., 2015).

6.2.2.3 Modélisation des *trade-offs* entre traits d'histoire de vie et préférence thermique

Les taux métaboliques, notamment la maintenance, sont variables entre individus d'une même espèce, sont liés à la *fitness* et peuvent évoluer (Burton et al., 2011). Les variations des taux métaboliques peuvent influencer les préférences thermiques (Killen, 2014). Les variations intra-spécifiques de la maintenance sont également liées à des variations de croissance et de

comportements : les individus avec les plus hauts taux de maintenance sont des individus avec un comportement plus actif (dit *bold*) dans la recherche de nourriture (Hollins et al., 2018; Killen, 2014), donc une croissance potentiellement plus élevée et une exposition plus importante à la prédation. Les individus de ce type sont plus enclins à atteindre plus vite leur limite maximum de température à cause de leur allocation supérieure à la maintenance. Inclure le lien entre variations du taux métabolique de maintenance, variations de réponses à la température et variations des comportements alimentaires, le tout entraînant une variation transmissible de la *fitness* dans un modèle écosystémique serait un ambitieux développement qui permettrait l'étude réaliste de l'évolution des préférences thermiques en lien avec la physiologie (Crozier and Hutchings, 2014; Hollins et al., 2018).

6.2.3 Structure des génotypes

L'utilisation d'un modèle éco-génétique avec des traits codés par un nombre fini de loci et d'allèles est un premier pas vers une structure génétique réaliste par rapport à une description des traits par la génétique quantitative et son modèle infinitésimal qui fait l'hypothèse d'une infinité de loci à effets infinitésimaux codant pour un trait (Dunlop et al., 2009a, p. 2009; Enberg et al., 2009; Huisman and Tufto, 2012).

Il reste encore de nombreuses étapes à franchir pour améliorer le réalisme de la structure génétique codant pour les traits dans les modèles éco-génétiques. Les barrières principales viennent des connaissances existantes sur la structure même des génotypes qui restent limitées. Cependant, des études récentes d'association pangénomique ont tenté d'identifier les zones du génome associées à la croissance ou loci de caractères quantitatifs (quantitative trait loci, QTL) (Ali et al., 2020; McClelland et al., 2020) : une équipe a par exemple identifié 247 SNP (*single nucleotide polymorphisms*) associés à la masse somatique chez la truite arc-en-ciel (Ali et al., 2020). Elle a également identifié une partie du génome ayant un plus grand contrôle sur le poids du corps que les autres avec une concentration plus élevée de QTLs. Certains loci codants ayant plus d'importance

que les autres dans la valeur d'un trait ont également été détectés pour la maturation chez le saumon (Barson et al., 2015).

Au-delà du nombre de loci et de l'amplitude de leurs effets, les interactions entre gènes, un phénomène appelé épistasie, et les relations de dominance et de récessivité entre allèles d'un même locus vont également affecter la valeur des traits. En présence d'épistasie, les valeurs des loci ne sont plus additives mais peuvent être synergiques ou antagonistes par exemple. En cas de dominance et récessivité, certains allèles peuvent être portés mais non-exprimés en cas d'hétérozygotie. Ces caractéristiques de la structure du génome sont parfois mises en lumière pour une espèce et un trait en particulier comme par exemple la truite arc-en-ciel et la tolérance maximale à la température (Danzmann et al., 1999), le saumon d'Atlantique et un gène de régulation du métabolisme des sucres (Verspoor and Moyes, 2005) ou encore des cyclidés et la détermination du sexe (Ser et al., 2010).

Ainsi, une connaissance plus approfondie des gènes codants pour les traits d'histoire de vie ainsi que de leurs interactions est nécessaire pour les intégrer de façon réaliste dans des modèles éco-génétiques alléliques. Cette structure plus réaliste prenant en compte l'épistasie ou la dominance pourrait avoir un impact sur l'évolution des traits d'histoire de vie. Cette hypothèse pourrait être testée avec une version non-appliquée d'Ev-OSMOSE en l'utilisant comme un *toy model*.

Une analyse de sensibilité de la configuration Ev-OSMOSE-NS présentée au chapitre 4 pourrait être réalisée pour comprendre le lien entre variance génétique, taille de la population, taille des nouvelles cohortes, nombre d'allèles et de loci et dérive génétique. Dans la configuration présentée, le nombre de super-individus par cohorte a été fixé empiriquement de manière à éviter la dérive génétique. Pour certaines espèces, nous avons malgré tout identifié une dérive génétique importante démontrée par la différence marquée entre les valeurs génotypiques parentales (pondérées par la fécondité) et celles de leurs descendants au moment de la reproduction. Nous n'avons actuellement pas identifié de corrélation entre la dérive génétique chez ces espèces et la taille des populations et

des nouvelles cohortes en termes de super-individus. La taille efficace de population pourrait être une piste expliquant les niveaux de dérive génétique simulée (Husemann et al., 2016; Willi et al., 2006; Wright, 1938).

6.3 Des modèles écosystémiques se complexifiant : éclairage du fonctionnement des écosystèmes ou simulations de données aussi complexes que l'observé ?

Le développement de modèles comme Bioen-OSMOSE et Ev-OSMOSE pose plusieurs questions. Ce type de projets complexes est envisageable uniquement sur un temps long de plusieurs années. Le développement et l'application de ces modèles a été possible dans ce travail de thèse grâce à quatre ans de travail à plein temps. Explorer les nombreuses questions qui peuvent être traitées avec ces outils (dont seulement 2 exemples décrits dans les chapitres 3 et 5 principalement), perfectionner l'estimation de certains paramètres grâce aux données et à la calibration, faire des analyses de sensibilité de paramètres et de robustesse de processus sont autant d'activités qui nécessiteraient encore du temps. Ces explorations pourraient faire l'objet de projets doctoraux à part entière (voir l'analyse de sensibilité sur le modèle OSMOSE Humbolt, Luján Paredes, 2022). Ce temps en question est un investissement de long terme nécessaire qui permet la compréhension en profondeur d'une partie du fonctionnement des écosystèmes marins. Cette approche de temps long pour la compréhension de processus complexes est abordée plus fréquemment sous le nom de *slow science* (Owens, 2013). Le besoin de nouveaux développements dans les modèles écosystémiques marins (Rose et al., 2010) et l'attractivité de ces nouveaux développements peuvent entraîner une fuite en avant vers de nouveaux projets plus vendeurs et innovants. Cela pourrait entraîner la sous-exploitation du temps investi dans un projet de modèle écosystémique marin. Dans le cas de Bioen-OSMOSE et Ev-OSMOSE, il serait nécessaire d'explorer les possibilités permises par ces outils ainsi que de comprendre la complexité des résultats produits avant de les complexifier avec de nouveaux sous-modèles.

Du temps de recherche permet d'appréhender la complexité et la grande non-linéarité de nos objets et de nos outils d'étude. La question de la complexité des modèles écosystémiques a été soulevée assez rapidement avec l'avènement de leur développement (Fulton et al., 2003). Comment comprendre les résultats en sortie de modèles aussi complexes ? Comment les interpréter ? Comment les rendre utiles et applicables pour la gestion ? Est-ce que les signaux simulés ne deviennent pas aussi complexes que les données observées ? Des démarches permettent d'améliorer la fiabilité et la compréhension des modèles que nous utilisons. Ces démarches sont aussi cruciales pour valoriser le temps passé au développement de ses modèles, en les rendant fiables, réalistes et utiles pour la gestion.

Dans un objectif d'interpréter les résultats, de les rendre réalistes et utiles pour la gestion, la calibration est une étape clé (Oliveros-Ramos and Shin, 2016; Pethybridge et al., 2019). Plusieurs avantages résident dans le processus de calibration. La calibration d'un modèle est une démarche active qui permet de mieux comprendre les mécanismes et les éléments clés d'un écosystème. Par l'ajustement des paramètres pour reproduire les données observées, elle permet également d'augmenter la fiabilité des processus représentés. La compréhension des modèles d'écosystèmes complexes est également aidée par une analyse de sensibilité comme celles réalisées sur le modèle OSMOSE (Luján Paredes, 2022) ou sur le modèle Atlantis (Bracis et al., 2020).

Enfin, une façon de comprendre l'impact de processus sur l'écosystème est de faire des simulations sous scénarios comme les scénarios de gestion de pêche ou les scénarios climatiques. Ces questions sont explorées dans la partie suivante.

6.4 Perspectives

Les modèles Bioen-OSMOSE et Ev-OSMOSE et leur application à la mer du Nord permettent l'exploration de nouvelles problématiques de recherche sur les diversités génétique, fonctionnelle et spécifique, notamment leurs réponses au changement climatique et à la pêche.

6.4.1 Projections de biodiversité sous scénarios climatiques futurs

Nous avons présenté en introduction de ces travaux une diversité de modèles d'écosystèmes marins. Ces modèles sont des outils précieux pour réaliser des projections de la biodiversité marine sous scénarios de changement climatique à l'horizon 2050 et 2100 : il existe de très nombreux travaux traitant cette question par diverses approches de modélisation au niveau global (Cheung et al., 2009; du Pontavice et al., 2020; Fernandes et al., 2013; Jones and Cheung, 2015; Lefort et al., 2015) ou régional (Bossier et al., 2018; Bourdaud et al., 2021; Hoover et al., 2013; Moullec et al., 2019) et même une initiative de projections globales à l'aide d'ensembles de modèles (FISH-MIP, Lotze et al., 2019).

Au niveau régional, aucun de ces modèles ne représente à la fois les changements de distributions spatiales, les changements physiologiques et les changements de production primaire pour réaliser des projections futures de biodiversité. Aux échelles régionales comme globale, l'adaptation évolutive des traits d'histoire de vie n'a jamais été intégrée dans des scénarios futurs de biodiversité. Les modèles Bioen-OSMOSE et Ev-OSMOSE ont le potentiel d'intégrer ces processus dans des simulations sous scénarios. La configuration Bioen-OSMOSE-NS actuelle peut permettre la réalisation de travaux de projection dans un futur proche (voir partie 6.4.1.1).

L'utilisation d'Ev-OSMOSE-NS pour faire des projections de biodiversité sous scénarios climatiques et de pêche était un des objectifs initiaux de ces travaux de thèse. Cet objectif a été mis de côté pendant les travaux de thèse car il demande encore de développer une façon de prendre en compte le *trade-off* entre évolution et changements d'aire de distribution. Cette question est traitée dans la partie 6.4.1.2.

6.4.1.1 Comment les changements physiologiques en réponse au changement climatique impactent les écosystèmes ?

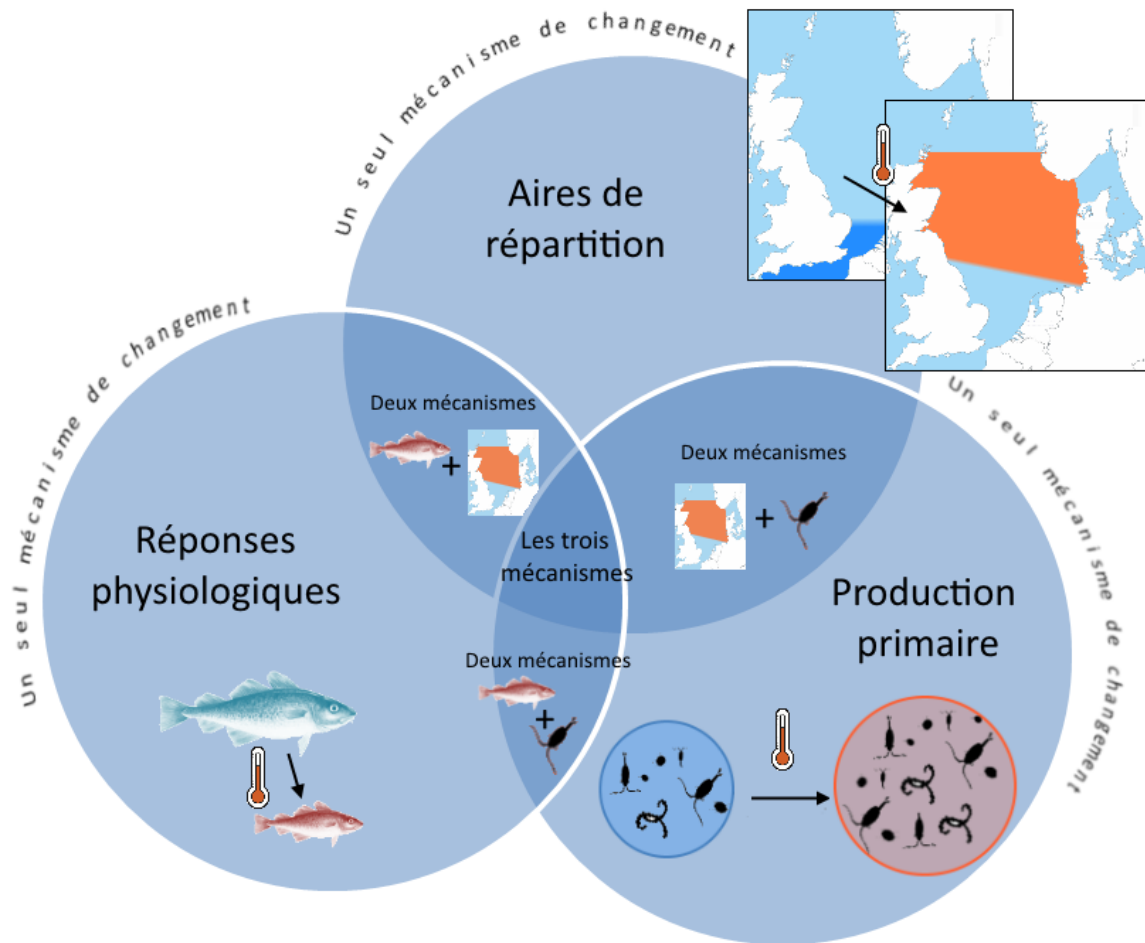


Figure 38: Plan de simulations avec sept scénarios testés en réponse au changement climatique en utilisant Bioen-OSMOSE-NS. Trois scénarios prennent en compte un seul mécanisme de réponse au changement climatique (réponses physiologiques, déplacements des aires de distributions des espèces, changements de la production primaire). Trois scénarios combinent deux à deux les mécanismes de réponse possible. Enfin, le dernier scénario combine les trois mécanismes.

La prise en compte des changements physiologiques en réponse au changement climatique a été identifiée comme un des six processus nécessaires à inclure dans les modèles (Urban et al., 2016).

Les modèles écosystémiques marins régionaux sont utilisés pour des scénarios futurs de biodiversité en prenant généralement en compte les changements de production primaire et les changements de distribution spatiale des espèces. L'apport principal du modèle Bioen-OSMOSE serait de réaliser des projections futures en explicitant l'impact des changements physiologiques des organismes sur l'écosystème. Pour démêler les changements issus des différents mécanismes de réponse au changement climatique, un plan de simulations a été conçu et est résumé dans la Figure 38. Si nous

considérons trois groupes de mécanismes principaux que sont les réponses à la production primaire, les réponses spatiales et les réponses physiologiques, une première étape consisterait à réaliser des simulations distinctes considérant chaque mécanisme de manière isolée. Cette étape nous permettrait d'identifier dans quelle mesure chaque mécanisme impacte les écosystèmes marins indépendamment des autres. Les simulations avec deux mécanismes explicites nous aideront à comprendre les interactions entre mécanismes. Enfin, une simulation avec les trois mécanismes de réponse au changement climatique sera considérée comme la simulation la plus réaliste de changement futur, dont les résultats pourront être mis en perspective par rapport aux premières simulations partielles. Par exemple, comparer cette simulation finale avec la simulation considérant uniquement changements des aires de répartition et de la production primaire permettra d'évaluer l'apport de la prise en compte des réponses physiologiques.

6.4.1.2 Quels sont les changements évolutifs des traits d'histoire de vie en réponse au changement climatique et leurs impacts écosystémiques ?

Les changements adaptatifs en réponse au changement climatique sont identifiés comme étant des mécanismes majeurs à prendre en compte pour réaliser des projections inter décennales plausibles des impacts du changement climatique (Urban et al., 2016). Dans Ev-OSMOSE, les populations peuvent répondre évolutivement au changement climatique par l'adaptation de leurs traits d'histoire de vie.

Sans évolution, seule la dispersion (qui permet le déplacement des aires de distribution) peut permettre le maintien de la biodiversité en contexte de changement climatique. En cas d'évolution, l'adaptation et la dispersion peuvent être des mécanismes de maintien (Thompson and Fronhofer, 2019). Ces mécanismes peuvent également entrer en conflit pour le maintien de la biodiversité (Thompson and Fronhofer, 2019; Urban et al., 2012) : des espèces peuvent s'établir en migrant dans des zones plus adaptées uniquement si la nouvelle niche climatique convoitée est libre. Si la niche

convoitée est occupée par une espèce résidente qui s'adapte plutôt que de migrer, il existe un conflit de compétition locale entre ces deux espèces pouvant résulter en une exclusion compétitive. Une modélisation de scénarios futurs réalistes devra prendre en compte la capacité de dispersion des espèces (Thompson and Fronhofer, 2019).

Un scénario avec des populations pouvant suivre parfaitement leur optimum thermique sous-estimera les impacts évolutifs du changement climatique. Au contraire, un scénario dans lequel les espèces ne peuvent pas suivre leur optimum surestimera l'évolution adaptative et/ou le déclin des espèces avec un potentiel adaptatif insuffisant.

En prenant en compte ces considérations, il semble que la première question qui pourrait être traitée à l'aide du modèle Ev-OSMOSE-NS serait : « Le potentiel adaptatif actuel des espèces est-il suffisant pour s'adapter au changement climatique en l'absence de dispersion ? ». Pour répondre à cette question, la configuration Ev-OSMOSE-NS pourrait être utilisée en ne modifiant pas les aires de distributions des espèces et en forçant le modèle avec des conditions futures de température, d'oxygène et de productions primaires et secondaires selon différents scénarios climatiques.

6.4.2 Scénarios de gestion de pêche qui optimisent la diversité génétique et minimisent le changement de diversité fonctionnelle

La gestion écosystémique des pêches (*Ecosystem-based fisheries management*) considère la santé globale de l'écosystème et non uniquement le maintien des espèces cibles (Pikitch et al., 2004). Les modèles d'écosystèmes marins régionaux sont des outils d'exploration et d'application de cette gestion écosystémique (Rose et al., 2010). De nombreuses applications de modèles existent déjà pour tester des scénarios de pêches (Espinoza-Tenorio et al., 2012; Perryman et al., 2021; Plagányi, 2007). Parmi les développements régulièrement discutés comme nécessaires à incorporer dans les modèles écosystémiques marins se trouve la prise en compte de la diversité génétique (Heymans et

al., 2020; Rose et al., 2010). Les scénarios de gestion de pêche testés dans les modèles écosystémiques marins en vue de la gestion écosystémique des pêches étudient principalement l'impact de la pêche sur la diversité spécifique alors que la compréhension de son impact sur tous les niveaux de biodiversité est nécessaire pour garantir un bon état des écosystèmes (E. Kenchington et al., 2003).

Le modèle Ev-OSMOSE prend en compte les processus nécessaires pour pouvoir tester l'impact des scénarios de différentes gestions de pêche sur la diversité génétique, fonctionnelle et spécifique.

Plusieurs mesures de gestion sont actuellement utilisées pour réduire l'impact de la pêche sur la diversité spécifique marine : la diminution de l'effort de pêche, l'augmentation du maillage des filets, l'utilisation d'engins de pêche plus sélectifs en taille et en espèces, la réduction des captures accidentelles et des rejets, et la mise en place d'aires marines protégées.

Différents scénarios de gestion pourront dans le futur être testés avec Ev-OSMOSE-NS pour explorer comment minimiser l'impact de la pêche sur les différents niveaux de biodiversité simultanément.

Une des premières utilisations futures d'Ev-OSMOSE-NS pourra permettre d'identifier les niveaux de mortalité par pêche qui permettent un point d'équilibre entre l'évolution induite par la pêche et la prédation, sans changer la sélectivité en taille des engins de pêche.

La diminution de la mortalité par pêche n'est pas le seul scénario de gestion qui peut permettre de trouver un point d'équilibre évolutif entre la pêche et la prédation. Le chapitre 5 montre que la sélectivité peut avoir son importance. Ainsi, il serait intéressant de chercher à optimiser les captures tout en minimisant les impacts évolutifs en modifiant la sélectivité en taille de la pêche.

Enfin, il a été montré que les aires marines protégées peuvent favoriser le maintien de la diversité génétique dans la zone protégée (R. Kenchington et al., 2003; Munguía-Vega et al., 2015). Ces réservoirs de diversité génétique pourraient servir à la préserver à l'échelle de l'ensemble de

l'écosystème. Il serait intéressant d'explorer la proportion d'une zone exploitée à protéger pour contrebalancer l'érosion génétique liée à la pêche (Marty et al., 2015; Pinsky and Palumbi, 2014).

6.5 Conclusion

Dans cette thèse, j'ai développé un modèle écosystémique marin décrivant l'évolution et la physiologie sous-jacentes aux traits d'histoire de vie. Ces travaux ont aussi permis de développer des méthodes d'estimation de paramètres cruciaux pour étudier la variation génétique et physiologique à partir de données relativement répandues : cette avancée rend possible la transposition de notre modèle à de nombreux autres écosystèmes pour étudier leurs dynamiques éco-évolutives.

L'utilisation du modèle développé dans le cadre de cette thèse a également permis d'étudier deux problématiques très différentes. La première problématique est l'étude des différences entre performances thermiques fondamentales et réalisées. Cette étude souligne notamment la nécessité de prendre en compte l'ensemble des facteurs influençant la physiologie pour faire des projections réalistes de traits d'histoire de vie futurs des organismes, et les conséquences potentielles de leurs changements sur les écosystèmes marins. Cette étude fait également le lien entre les études expérimentales d'écophysiologie et les conséquences des changements physiologiques sur les écosystèmes, un point souvent énoncé en perspectives des études d'écophysiologie.

La deuxième problématique traitée est l'étude de l'évolution des traits d'histoire de vie dans une communauté en réponse à la pêche et à la prédation. Les résultats obtenus dans cette thèse montrent qu'il est possible de gérer la pression de pêche de manière à limiter les impacts évolutifs sur les populations et les communautés.

Ces travaux sont une nouvelle pierre apportée à la compréhension des effets du changement climatique et de la pêche sur le fonctionnement des écosystèmes marins ainsi qu'à la gestion écosystémique des pêches grâce à l'exploration de différents niveaux de réponses et de biodiversité qui étaient jusqu'à présent encore peu étudiés à l'échelle écosystémique.

Références

- Albouy, C., Velez, L., Coll, M., Colloca, F., Le Loc'h, F., Mouillot, D., Gravel, D., 2014. From projected species distribution to food-web structure under climate change. *Global Change Biology* 20, 730–741. <https://doi.org/10.1111/gcb.12467>
- Ali, A., Al-Tobasei, R., Lourenco, D., Leeds, T., Kenney, B., Salem, M., 2020. Genome-wide identification of loci associated with growth in rainbow trout. *BMC Genomics* 21, 209. <https://doi.org/10.1186/s12864-020-6617-x>
- Altieri, A.H., Diaz, R.J., 2019. Chapter 24 - Dead Zones: Oxygen Depletion in Coastal Ecosystems, in: Sheppard, C. (Ed.), *World Seas: An Environmental Evaluation (Second Edition)*. Academic Press, pp. 453–473. <https://doi.org/10.1016/B978-0-12-805052-1.00021-8>
- Amara, R., Laffargue, P., Dewarumez, J.M., Maryniak, C., Lagardère, F., Luzac, C., 2001. Feeding ecology and growth of O-group flatfish (sole, dab and plaice) on a nursery ground (Southern Bight of the North Sea). *Journal of Fish Biology* 58, 788–803. <https://doi.org/10.1111/j.1095-8649.2001.tb00531.x>
- Andersen, K.H., 2019. *Fish Ecology, Evolution, and Exploitation: A New Theoretical Synthesis*. Princeton University Press.
- Angilletta, M.J., 2009. *Thermal Adaptation: A Theoretical and Empirical Synthesis*. OUP Oxford.
- Arcus, V.L., Prentice, E.J., Hobbs, J.K., Mulholland, A.J., Van der Kamp, M.W., Pudney, C.R., Parker, E.J., Schipper, L.A., 2016. On the Temperature Dependence of Enzyme-Catalyzed Rates. *Biochemistry*, 55(12), 1681–1688. <https://doi.org/10.1021/acs.biochem.5b01094>
- Ardichvili, A.N., Loeuille, N., Dakos, V., 2022. Evolutionary emergence of alternative stable states in shallow lakes. <https://doi.org/10.1101/2022.02.23.481597>
- Audzijonyte, A., Barneche, D.R., Baudron, A.R., Belmaker, J., Clark, T.D., Marshall, C.T., Morrongiello, J.R., van Rijn, I., 2018. Is oxygen limitation in warming waters a valid mechanism to explain decreased body sizes in aquatic ectotherms? *Global Ecology and Biogeography*. <https://doi.org/10.1111/geb.12847>
- Audzijonyte, A., Kuparinen, A., Fulton, E., 2014. Ecosystem effects of contemporary life-history changes are comparable to those of fishing. *Marine Ecology Progress Series* 495, 219–231. <https://doi.org/10.3354/meps10579>
- Audzijonyte, Asta, Kuparinen, A., Fulton, E.A., 2013. How fast is fisheries-induced evolution? Quantitative analysis of modelling and empirical studies. *Evolutionary Applications* 6, 585–595. <https://doi.org/10.1111/eva.12044>
- Audzijonyte, A., Kuparinen, A., Gorton, R., Fulton, E.A., 2013. Ecological consequences of body size decline in harvested fish species: positive feedback loops in trophic interactions amplify human impact. *Biology Letters* 9, 20121103–20121103. <https://doi.org/10.1098/rsbl.2012.1103>
- Audzijonyte, A., Pethybridge, H., Porobic, J., Gorton, R., Kaplan, I., Fulton, E.A., 2019. Atlantis: A spatially explicit end-to-end marine ecosystem model with dynamically integrated physics, ecology and socio-economic modules. *Methods in Ecology and Evolution* 10, 1814–1819. <https://doi.org/10.1111/2041-210X.13272>

- Audzijonyte, A., Richards, S.A., Stuart-Smith, R.D., Pecl, G., Edgar, G.J., Barrett, N.S., Payne, N., Blanchard, J.L., 2020. Fish body sizes change with temperature but not all species shrink with warming. *Nature Ecology & Evolution*. <https://doi.org/10.1038/s41559-020-1171-0>
- Barson, N.J., Aykanat, T., Hindar, K., Baranski, M., Bolstad, G.H., Fiske, P., Jacq, C., Jensen, A.J., Johnston, S.E., Karlsson, S., Kent, M., Moen, T., Niemelä, E., Nome, T., Næsje, T.F., Orell, P., Romakkaniemi, A., Sægvog, H., Urdal, K., Erkinaro, J., Lien, S., Primmer, C.R., 2015. Sex-dependent dominance at a single locus maintains variation in age at maturity in salmon. *Nature* 528, 405–408. <https://doi.org/10.1038/nature16062>
- Barton, N., Partridge, L., 2000. Limits to natural selection. *Bioessays* 22, 1075–1084. [https://doi.org/10.1002/1521-1878\(200012\)22:12<1075::AID-BIES5>3.0.CO;2-M](https://doi.org/10.1002/1521-1878(200012)22:12<1075::AID-BIES5>3.0.CO;2-M)
- Bastrikin, D.K., Gallego, A., Millar, C.P., Priede, I.G., Jones, E.G., 2014. Settlement length and temporal settlement patterns of juvenile cod (*Gadus morhua*), haddock (*Melanogrammus aeglefinus*), and whiting (*Merlangius merlangus*) in a northern North Sea coastal nursery area. *ICES Journal of Marine Science* 71, 2101–2113. <https://doi.org/10.1093/icesjms/fsu029>
- Baudron, A.R., Needle, C.L., Rijnsdorp, A.D., Marshall, C.T., 2014. Warming temperatures and smaller body sizes: synchronous changes in growth of North Sea fishes. *Global Change Biology* 20, 1023–1031. <https://doi.org/10.1111/gcb.12514>
- Beaugrand, G., 2004. The North Sea regime shift: Evidence, causes, mechanisms and consequences. *Progress in Oceanography, Regime shifts in the ocean. Reconciling observations and theory* 60, 245–262. <https://doi.org/10.1016/j.pocean.2004.02.018>
- Beaugrand, G., Brander, K.M., Alistair Lindley, J., Souissi, S., Reid, P.C., 2003. Plankton effect on cod recruitment in the North Sea. *Nature* 426, 661–664. <https://doi.org/10.1038/nature02164>
- Beaugrand, G., Kirby, R.R., 2018. How Do Marine Pelagic Species Respond to Climate Change? Theories and Observations. *Annual Review of Marine Science* 10, 169–197. <https://doi.org/10.1146/annurev-marine-121916-063304>
- Beissinger, S.R., McCullough, D.R., 2002. *Population Viability Analysis*. University of Chicago Press.
- Beukhof, E., Dencker, T.S., Palomares, M.L.D., Maureaud, A., 2019. A trait collection of marine fish species from North Atlantic and Northeast Pacific continental shelf seas. <https://doi.org/10.1594/PANGAEA.900866>
- Bianchi, D., Carozza, D.A., Galbraith, E.D., Guiet, J., DeVries, T., 2021. Estimating global biomass and biogeochemical cycling of marine fish with and without fishing. *Science Advances* 7, eabd7554. <https://doi.org/10.1126/sciadv.abd7554>
- Blanchard, J.L., Andersen, K.H., Scott, F., Hintzen, N.T., Piet, G., Jennings, S., 2014. Evaluating targets and trade-offs among fisheries and conservation objectives using a multispecies size spectrum model. *Journal of Applied Ecology* 51, 612–622. <https://doi.org/10.1111/1365-2664.12238>
- Boesch, Df., Brinsfield, Rb., 2000. Coastal Eutrophication and Agriculture: Contributions and Solutions, in: Balázs, E., Galante, E., Lynch, J.M., Schepers, J.S., Toutant, J.-P., Werner, D., Werry, P.A.Th.J. (Eds.), *Biological Resource Management Connecting Science and Policy*. Springer, Berlin, Heidelberg, pp. 93–115. https://doi.org/10.1007/978-3-662-04033-1_8

- Bolle, L.J., Dapper, R., Witte, J.I.J., Van Der Veer, H.W., 1994. Nursery grounds of dab (*Limanda limanda* L.) in the southern North Sea. *Netherlands Journal of Sea Research* 32, 299–307. [https://doi.org/10.1016/0077-7579\(94\)90007-8](https://doi.org/10.1016/0077-7579(94)90007-8)
- Bossier, S., Palacz, A.P., Nielsen, J.R., Christensen, A., Hoff, A., Maar, M., Gislason, H., Bastardie, F., Gorton, R., Fulton, E.A., 2018. The Baltic Sea Atlantis: An integrated end-to-end modelling framework evaluating ecosystem-wide effects of human-induced pressures. *PLOS ONE* 13, e0199168. <https://doi.org/10.1371/journal.pone.0199168>
- Bouffet-Halle, A., Mériguet, J., Carmignac, D., Agostini, S., Millot, A., Perret, S., Motard, E., Decenciere, B., Edeline, E., 2021. Density-dependent natural selection mediates harvest-induced trait changes. *Ecology Letters* 24, 648–657. <https://doi.org/10.1111/ele.13677>
- Boukal, D.S., Dieckmann, U., Enberg, K., Heino, M., Jørgensen, C., 2014. Life-history implications of the allometric scaling of growth. *Journal of Theoretical Biology* 359, 199–207. <https://doi.org/10.1016/j.jtbi.2014.05.022>
- Boukal, D.S., Dunlop, E.S., Heino, M., Dieckmann, U., 2008. Fisheries-induced evolution of body size and other life history traits: the impact of gear selectivity (Working paper), 7 s. ICES.
- Bourdaud, P., Ben Rais Lasram, F., Aраignous, E., Champagnat, J., Grusd, S., Halouani, G., Hattab, T., Leroy, B., Noguès, Q., Raoux, A., Safi, G., Niquil, N., 2021. Impacts of climate change on the Bay of Seine ecosystem: Forcing a spatio-temporal trophic model with predictions from an ecological niche model. *Fisheries Oceanography* 30, 471–489. <https://doi.org/10.1111/fog.12531>
- Bracis, C., Lehuta, S., Savina-Rolland, M., Travers-Trolet, M., Girardin, R., 2020. Improving confidence in complex ecosystem models: The sensitivity analysis of an Atlantis ecosystem model. *Ecological Modelling* 431, 109133. <https://doi.org/10.1016/j.ecolmodel.2020.109133>
- Bradshaw, A.D., 1965. Evolutionary Significance of Phenotypic Plasticity in Plants, in: Caspari, E.W., Thoday, J.M. (Eds.), *Advances in Genetics*. Academic Press, pp. 115–155. [https://doi.org/10.1016/S0065-2660\(08\)60048-6](https://doi.org/10.1016/S0065-2660(08)60048-6)
- Bradshaw, W.E., 2006. CLIMATE CHANGE: Evolutionary Response to Rapid Climate Change. *Science* 312, 1477–1478. <https://doi.org/10.1126/science.1127000>
- Brandl, S.J., Johansen, J.L., Casey, J.M., Tornabene, L., Morais, R.A., Burt, J.A., 2020. Extreme environmental conditions reduce coral reef fish biodiversity and productivity. *Nat Commun* 11, 3832. <https://doi.org/10.1038/s41467-020-17731-2>
- Brans, K.I., Tüzün, N., Sentis, A., De Meester, L., Stoks, R., 2022. Cryptic eco-evolutionary feedback in the city: Urban evolution of prey dampens the effect of urban evolution of the predator. *Journal of Animal Ecology* 91, 514–526. <https://doi.org/10.1111/1365-2656.13601>
- Breitburg, D., Levin, L.A., Oschlies, A., Grégoire, M., Chavez, F.P., Conley, D.J., Garçon, V., Gilbert, D., Gutiérrez, D., Isensee, K., Jacinto, G.S., Limburg, K.E., Montes, I., Naqvi, S.W.A., Pitcher, G.C., Rabalais, N.N., Roman, M.R., Rose, K.A., Seibel, B.A., Telszewski, M., Yasuhara, M., Zhang, J., 2018. Declining oxygen in the global ocean and coastal waters. *Science* 359, eaam7240. <https://doi.org/10.1126/science.aam7240>
- Brockhurst, M.A., Chapman, T., King, K.C., Mank, J.E., Paterson, S., Hurst, G.D.D., 2014. Running with the Red Queen: the role of biotic conflicts in evolution. *Proc Biol Sci* 281, 20141382. <https://doi.org/10.1098/rspb.2014.1382>

- Brommer, J.E., 2000. The evolution of fitness in life-history theory. *Biol Rev Camb Philos Soc* 75, 377–404. <https://doi.org/10.1017/s000632310000551x>
- Brosset, P., Le Bourg, B., Costalago, D., Bănar, D., Van Beveren, E., Bourdeix, J., Fromentin, J., Ménard, F., Sarau, C., 2016. Linking small pelagic dietary shifts with ecosystem changes in the Gulf of Lions. *Marine Ecology Progress Series* 554, 157–171. <https://doi.org/10.3354/meps11796>
- Browman, H., Hutchings, J., Conover, D., Stokes, K., Law, R., Walters, C., 2000. Evolution of fisheries science. *Mar. Ecol. Prog. Ser.* 208, 299–313. <https://doi.org/10.3354/meps208299>
- Brown, C.J., Fulton, E.A., Hobday, A.J., Matear, R.J., Possingham, H.P., Bulman, C., Christensen, V., Forrest, R.E., Gehrke, P.C., Gribble, N.A., Griffiths, S.P., Lozano-Montes, H., Martin, J.M., Metcalf, S., Okey, T.A., Watson, R., Richardson, A.J., 2010. Effects of climate-driven primary production change on marine food webs: implications for fisheries and conservation. *Global Change Biology* 16, 1194–1212. <https://doi.org/10.1111/j.1365-2486.2009.02046.x>
- Brown, J.H., Gillooly, J.F., Allen, A.P., Savage, V.M., West, G.B., 2004. TOWARD A METABOLIC THEORY OF ECOLOGY. *Ecology* 85, 1771–1789. <https://doi.org/10.1890/03-9000>
- Brunner, F.S., Deere, J.A., Egas, M., Eizaguirre, C., Raeymaekers, J.A.M., 2019. The diversity of eco-evolutionary dynamics: Comparing the feedbacks between ecology and evolution across scales. *Functional Ecology* 33, 7–12. <https://doi.org/10.1111/1365-2435.13268>
- Bull, A.T., Goodfellow, M., Slater, J.H., 1992. Biodiversity as a Source of Innovation in Biotechnology. *Annual Review of Microbiology* 46, 219–246. <https://doi.org/10.1146/annurev.mi.46.100192.001251>
- Burton, T., Killen, S.S., Armstrong, J.D., Metcalfe, N.B., 2011. What causes intraspecific variation in resting metabolic rate and what are its ecological consequences? *Proceedings of the Royal Society B: Biological Sciences* 278, 3465–3473. <https://doi.org/10.1098/rspb.2011.1778>
- Butenschön, M., Clark, J., Aldridge, J.N., Allen, J.I., Artioli, Y., Blackford, J., Bruggeman, J., Cazenave, P., Ciavatta, S., Kay, S., Lessin, G., van Leeuwen, S., van der Molen, J., de Mora, L., Polimene, L., Saille, S., Stephens, N., Torres, R., 2016. ERSEM 15.06: a generic model for marine biogeochemistry and the ecosystem dynamics of the lower trophic levels. *Geoscientific Model Development* 9, 1293–1339. <https://doi.org/10.5194/gmd-9-1293-2016>
- Cariou, T., Dubroca, L., Vogel, C., Bez, N., 2021. Comparison of the spatiotemporal distribution of three flatfish species in the Seine estuary nursery grounds. *Estuarine, Coastal and Shelf Science* 259, 107471. <https://doi.org/10.1016/j.ecss.2021.107471>
- Catalán, I.A., Auch, D., Kamermans, P., Morales-Nin, B., Angelopoulos, N.V., Reglero, P., Sandersfeld, T., Peck, M.A., 2019. Critically examining the knowledge base required to mechanistically project climate impacts: A case study of Europe’s fish and shellfish. *Fish and Fisheries* 20, 501–517. <https://doi.org/10.1111/faf.12359>
- Chaparro-Pedraza, P.C., de Roos, A.M., 2020. Ecological changes with minor effect initiate evolution to delayed regime shifts. *Nature Ecology & Evolution*. <https://doi.org/10.1038/s41559-020-1110-0>
- Charnov, E.L., Turner, T.F., Winemiller, K.O., 2001. Reproductive constraints and the evolution of life histories with indeterminate growth. *Proceedings of the National Academy of Sciences* 98, 9460–9464. <https://doi.org/10.1073/pnas.161294498>

- Chen, W., Staneva, J., Grayek, S., Schulz-Stellenfleth, J., Greinert, J., 2022. The role of heat wave events in the occurrence and persistence of thermal stratification in the southern North Sea. *Natural Hazards and Earth System Sciences* 22, 1683–1698. <https://doi.org/10.5194/nhess-22-1683-2022>
- Cheung, W.W.L., Lam, V.W.Y., Sarmiento, J.L., Kearney, K., Watson, R., Pauly, D., 2009. Projecting global marine biodiversity impacts under climate change scenarios. *Fish and Fisheries* 10, 235–251. <https://doi.org/10.1111/j.1467-2979.2008.00315.x>
- Cheung, W.W.L., Sarmiento, J.L., Dunne, J., Frölicher, T.L., Lam, V.W.Y., Deng Palomares, M.L., Watson, R., Pauly, D., 2013. Shrinking of fishes exacerbates impacts of global ocean changes on marine ecosystems. *Nature Clim Change* 3, 254–258. <https://doi.org/10.1038/nclimate1691>
- Christensen, V., Pauly, D., 1992. ECOPATH II — a software for balancing steady-state ecosystem models and calculating network characteristics. *Ecological Modelling* 61, 169–185. [https://doi.org/10.1016/0304-3800\(92\)90016-8](https://doi.org/10.1016/0304-3800(92)90016-8)
- Christensen, V., Walters, C.J., 2004. Ecopath with Ecosim: methods, capabilities and limitations. *Ecological Modelling, Placing Fisheries in their Ecosystem Context* 172, 109–139. <https://doi.org/10.1016/j.ecolmodel.2003.09.003>
- Claireaux, M., dos Santos Schmidt, T.C., Olsen, E.M., Slotte, A., Varpe, Ø., Heino, M., Enberg, K., 2021. Eight decades of adaptive changes in herring reproductive investment: the joint effect of environment and exploitation. *ICES Journal of Marine Science* 78, 631–639. <https://doi.org/10.1093/icesjms/fsaa123>
- Clark, N.E., Lovell, R., Wheeler, B.W., Higgins, S.L., Depledge, M.H., Norris, K., 2014. Biodiversity, cultural pathways, and human health: a framework. *Trends in Ecology & Evolution* 29, 198–204. <https://doi.org/10.1016/j.tree.2014.01.009>
- Clark, T.D., Sandblom, E., Jutfelt, F., 2013. Aerobic scope measurements of fishes in an era of climate change: respirometry, relevance and recommendations. *Journal of Experimental Biology* 216, 2771–2782. <https://doi.org/10.1242/jeb.084251>
- Clarke, A., 2019. Energy Flow in Growth and Production. *Trends in Ecology & Evolution* 34, 502–509. <https://doi.org/10.1016/j.tree.2019.02.003>
- Clarke, A., 2017. *Principles of Thermal Ecology: Temperature, Energy and Life*. Oxford University Press, Oxford, New York.
- Clarke, T.M., Wabnitz, C.C.C., Striegel, S., Frölicher, T.L., Reygondeau, G., Cheung, W.W.L., 2021. Aerobic growth index (AGI): An index to understand the impacts of ocean warming and deoxygenation on global marine fisheries resources. *Progress in Oceanography* 195, 102588. <https://doi.org/10.1016/j.pocean.2021.102588>
- Cohen, D.M., Inada, T., Iwamoto, T., Scialabba, N., 1990. Gadiform fishes of the world (Order Gadiformes). An annotated and illustrated catalogue of cods, hakes, grenadiers and other gadiform fishes known to date. *FAO Fish. Synop.* 125(10). Rome: FAO. Vol. 10., 442 p.
- Colebrook, J.M., 1985. Sea surface temperature and zooplankton, North Sea, 1948 to 1983. *ICES Journal of Marine Science* 42, 179–185. <https://doi.org/10.1093/icesjms/42.2.179>
- Coll, M., Shannon, L.J., Kleisner, K.M., Juan-Jordá, M.J., Bundy, A., Akoglu, A.G., Banaru, D., Boldt, J.L., Borges, M.F., Cook, A., Diallo, I., Fu, C., Fox, C., Gascuel, D., Gurney, L.J., Hattab, T., Heymans,

- J.J., Jouffre, D., Knight, B.R., Kucukavsar, S., Large, S.I., Lynam, C., Machias, A., Marshall, K.N., Masski, H., Ojaveer, H., Piroddi, C., Tam, J., Thiao, D., Thiaw, M., Torres, M.A., Travers-Trolet, M., Tsagarakis, K., Tuck, I., van der Meeren, G.I., Yemane, D., Zador, S.G., Shin, Y.-J., 2016. Ecological indicators to capture the effects of fishing on biodiversity and conservation status of marine ecosystems. *Ecological Indicators* 60, 947–962. <https://doi.org/10.1016/j.ecolind.2015.08.048>
- Colléter, M., Valls, A., Guitton, J., Gascuel, D., Pauly, D., Christensen, V., 2015. Global overview of the applications of the Ecopath with Ecosim modeling approach using the EcoBase models repository. *Ecological Modelling* 302, 42–53. <https://doi.org/10.1016/j.ecolmodel.2015.01.025>
- Conover, D.O., Baumann, H., 2009. PERSPECTIVE: The role of experiments in understanding fishery-induced evolution. *Evolutionary Applications* 2, 276–290. <https://doi.org/10.1111/j.1752-4571.2009.00079.x>
- Cook, R.M., Sinclair, A., Stefánsson, G., 1997. Potential collapse of North Sea cod stocks. *Nature* 385, 521–522. <https://doi.org/10.1038/385521a0>
- Corcoran, A.A., Boeing, W.J., 2012. Biodiversity Increases the Productivity and Stability of Phytoplankton Communities. *PLOS ONE* 7, e49397. <https://doi.org/10.1371/journal.pone.0049397>
- Cormon, X., Kempf, A., Vermard, Y., Vinther, M., Marchal, P., 2016. Emergence of a new predator in the North Sea: evaluation of potential trophic impacts focused on hake, saithe, and Norway pout. *ICES Journal of Marine Science* 73, 1370–1381. <https://doi.org/10.1093/icesjms/fsw050>
- Cortez, M.H., 2018. Genetic variation determines which feedbacks drive and alter predator–prey eco-evolutionary cycles. *Ecological Monographs* 88, 353–371. <https://doi.org/10.1002/ecm.1304>
- Crozier, L.G., Hutchings, J.A., 2014. Plastic and evolutionary responses to climate change in fish. *Evolutionary Applications* 7, 68–87. <https://doi.org/10.1111/eva.12135>
- Cushing, D.H., 1990. , in: *Plankton Production and Year-Class Strength in Fish Populations: An Update of the Match/Mismatch Hypothesis*. In *Advances in Marine Biology*, J.H.S.B. and A.J. Southward, Ed. (Academic Press),. pp. 249–293.
- Daan, N., 1973. A quantitative analysis of the food intake of North Sea cod, *Gadus Morhua*. *Netherlands Journal of Sea Research* 6, 479–517. [https://doi.org/10.1016/0077-7579\(73\)90002-1](https://doi.org/10.1016/0077-7579(73)90002-1)
- Dahlke, F.T., Wohlrab, S., Butzin, M., Pörtner, H.-O., 2020. Thermal bottlenecks in the life cycle define climate vulnerability of fish. *Science* 369, 65–70. <https://doi.org/10.1126/science.aaz3658>
- Dakos, V., Matthews, B., Hendry, A.P., Levine, J., Loeuille, N., Norberg, J., Nosil, P., Scheffer, M., De Meester, L., 2019. Ecosystem tipping points in an evolving world. *Nat Ecol Evol* 3, 355–362. <https://doi.org/10.1038/s41559-019-0797-2>
- Dammhahn, M., Dingemanse, N.J., Niemelä, P.T., Réale, D., 2018. Pace-of-life syndromes: a framework for the adaptive integration of behaviour, physiology and life history. *Behav Ecol Sociobiol* 72, 62. <https://doi.org/10.1007/s00265-018-2473-y>
- Danzmann, R.G., Jackson, T.R., M. Ferguson, M., 1999. Epistasis in allelic expression at upper temperature tolerance QTL in rainbow trout. *Aquaculture* 173, 45–58. [https://doi.org/10.1016/S0044-8486\(98\)00465-7](https://doi.org/10.1016/S0044-8486(98)00465-7)

- Darimont, C.T., Carlson, S.M., Kinnison, M.T., Paquet, P.C., Reimchen, T.E., Wilmers, C.C., 2009. Human predators outpace other agents of trait change in the wild. *Proc Natl Acad Sci U S A* 106, 952–954. <https://doi.org/10.1073/pnas.0809235106>
- Darwin, C., 1859. *On the Origin of Species*.
- DATRAS, 2010. ICES Database of Trawl Surveys (DATRAS), Extraction 21 JANUARY 2019 Q1 North Sea International Bottom Trawl Survey (IBTS) data 2010-2019; <http://datras.ices.dk>. ICES, Copenhagen.
- Daufresne, M., Lengfellner, K., Sommer, U., 2009. Global warming benefits the small in aquatic ecosystems. *Proceedings of the National Academy of Sciences* 106, 12788–12793. <https://doi.org/10.1073/pnas.0902080106>
- de Groot, S.J., 1986. Marine sand and gravel extraction in the North Atlantic and its potential environmental impact, with emphasis on the North Sea. *Ocean Management* 10, 21–36. [https://doi.org/10.1016/0302-184X\(86\)90004-1](https://doi.org/10.1016/0302-184X(86)90004-1)
- de Roos, A.M., Boukal, D.S., Persson, L., 2006. Evolutionary regime shifts in age and size at maturation of exploited fish stocks. *Proceedings of the Royal Society B: Biological Sciences* 273, 1873–1880. <https://doi.org/10.1098/rspb.2006.3518>
- De Silva, S.S., 1973. Food and feeding habits of the herring *Clupea harengus* and the sprat *C. sprattus* in inshore waters of the west coast of Scotland. *Marine Biology* 20, 282–290. <https://doi.org/10.1007/BF00354272>
- Dencker, T.S., Pecuchet, L., Beukhof, E., Richardson, K., Payne, M.R., Lindegren, M., 2017. Temporal and spatial differences between taxonomic and trait biodiversity in a large marine ecosystem: Causes and consequences. *PLOS ONE* 12, e0189731. <https://doi.org/10.1371/journal.pone.0189731>
- Deutsch, C., Penn, J.L., Seibel, B., 2020. Metabolic trait diversity shapes marine biogeography. *Nature* 585, 557–562. <https://doi.org/10.1038/s41586-020-2721-y>
- Di Pane, J., Joly, L., Koubbi, P., Giraldo, C., Monchy, S., Tavernier, E., Marchal, P., Loots, C., 2019. Ontogenetic shift in the energy allocation strategy and physiological condition of larval plaice (*Pleuronectes platessa*). *PLOS ONE* 14, e0222261. <https://doi.org/10.1371/journal.pone.0222261>
- Di Pane, J., Koubbi, P., Giraldo, C., Lefebvre, V., Caboche, J., Marchal, P., Loots, C., 2020. Recent changes in ichthyoplanktonic assemblages of the eastern English Channel. *Journal of Sea Research* 157, 101848. <https://doi.org/10.1016/j.seares.2020.101848>
- Diaz, F., Bănaru, D., Verley, P., Shin, Y.-J., 2019. Implementation of an end-to-end model of the Gulf of Lions ecosystem (NW Mediterranean Sea). II. Investigating the effects of high trophic levels on nutrients and plankton dynamics and associated feedbacks. *Ecological Modelling* 405, 51–68. <https://doi.org/10.1016/j.ecolmodel.2019.05.004>
- Dickey-Collas, M., Nash, R.D.M., Brunel, T., van Damme, C.J.G., Marshall, C.T., Payne, M.R., Corten, A., Geffen, A.J., Peck, M.A., Hatfield, E.M.C., Hintzen, N.T., Enberg, K., Kell, L.T., Simmonds, E.J., 2010. Lessons learned from stock collapse and recovery of North Sea herring: a review. *ICES Journal of Marine Science* 67, 1875–1886. <https://doi.org/10.1093/icesjms/fsq033>

- Discours de Axel Kahn au colloque “Ensemble, protéger la biodiversité marine : connaître pour agir”
<https://youtu.be/DQz8Hyfra-Q?t=5878>, 2020.
- Domenici, P., Allan, B.J.M., Lefrançois, C., McCormick, M.I., 2019. The effect of climate change on the escape kinematics and performance of fishes: implications for future predator–prey interactions. *Conservation Physiology* 7, coz078. <https://doi.org/10.1093/conphys/coz078>
- Doney, S.C., Ruckelshaus, M., Emmett Duffy, J., Barry, J.P., Chan, F., English, C.A., Galindo, H.M., Grebmeier, J.M., Hollowed, A.B., Knowlton, N., Polovina, J., Rabalais, N.N., Sydeman, W.J., Talley, L.D., 2012. Climate Change Impacts on Marine Ecosystems. *Annual Review of Marine Science* 4, 11–37. <https://doi.org/10.1146/annurev-marine-041911-111611>
- du Pontavice, H., Gascuel, D., Reygondeau, G., Maureaud, A., Cheung, W.W.L., 2020. Climate change undermines the global functioning of marine food webs. *Global Change Biology* 26, 1306–1318. <https://doi.org/10.1111/gcb.14944>
- du Pontavice, H., Gascuel, D., Reygondeau, G., Stock, C., Cheung, W.W.L., 2021. Climate-induced decrease in biomass flow in marine food webs may severely affect predators and ecosystem production. *Global Change Biology* 27, 2608–2622. <https://doi.org/10.1111/gcb.15576>
- Du Pontavice, H., Gascuel, D., Reygondeau, G., Stock, C., Cheung, W.W.L., 2020. Climate-induced decrease in biomass flow in marine food webs may severely affect predators and ecosystem production. *Global Change Biology* n/a. <https://doi.org/10.1111/gcb.15576>
- Dulvy, N.K., Rogers, S.I., Jennings, S., Stelzenmiller, V., Dye, S.R., Skjoldal, H.R., 2008. Climate change and deepening of the North Sea fish assemblage: a biotic indicator of warming seas. *Journal of Applied Ecology* 45, 1029–1039. <https://doi.org/10.1111/j.1365-2664.2008.01488.x>
- Dunlop, E.S., Baskett, M.L., Heino, M., Dieckmann, U., 2009a. ORIGINAL ARTICLE: Propensity of marine reserves to reduce the evolutionary effects of fishing in a migratory species: Reserves and fisheries-induced evolution. *Evolutionary Applications* 2, 371–393. <https://doi.org/10.1111/j.1752-4571.2009.00089.x>
- Dunlop, E.S., Eikeset, A.M., Stenseth, N.C., 2015. From genes to populations: how fisheries-induced evolution alters stock productivity. *Ecological Applications* 25, 1860–1868. <https://doi.org/10.1890/14-1862.1>
- Dunlop, E.S., Heino, M., Dieckmann, U., 2009b. Eco-genetic modeling of contemporary life-history evolution. *Ecological Applications* 19, 1815–1834. <https://doi.org/10.1890/08-1404.1>
- Edeline, E., Carlson, S.M., Stige, L.C., Winfield, I.J., Fletcher, J.M., James, J.B., Haugen, T.O., Vøllestad, L.A., Stenseth, N.C., 2007. Trait changes in a harvested population are driven by a dynamic tug-of-war between natural and harvest selection. *Proceedings of the National Academy of Sciences* 104, 15799–15804. <https://doi.org/10.1073/pnas.0705908104>
- Edeline, E., Loeuille, N., 2021. Size-dependent eco-evolutionary feedbacks in harvested systems. *Oikos* 130, 1636–1649.
- Eikeset, A.M., Richter, A., Dunlop, E.S., Dieckmann, U., Stenseth, N.C., 2013. Economic repercussions of fisheries-induced evolution. *Proceedings of the National Academy of Sciences* 110, 12259–12264. <https://doi.org/10.1073/pnas.1212593110>
- Enberg, K., Heino, M., 2007. Fisheries-induced Life History Changes in Herring (*Clupea harengus*) [WWW Document]. URL <https://iiasa.dev.local/> (accessed 9.19.22).

- Enberg, K., Jørgensen, C., Dunlop, E.S., Heino, M., Dieckmann, U., 2009. ORIGINAL ARTICLE: Implications of fisheries-induced evolution for stock rebuilding and recovery: Fisheries-induced evolution and stock recovery. *Evolutionary Applications* 2, 394–414. <https://doi.org/10.1111/j.1752-4571.2009.00077.x>
- Enberg, K., Jørgensen, C., Dunlop, E.S., Varpe, Ø., Boukal, D.S., Baulier, L., Eliassen, S., Heino, M., 2012. Fishing-induced evolution of growth: concepts, mechanisms and the empirical evidence: Fishing-induced evolution of growth. *Marine Ecology* 33, 1–25. <https://doi.org/10.1111/j.1439-0485.2011.00460.x>
- Engelhard, G.H., Heino, M., 2004. Maturity changes in Norwegian spring-spawning herring *Clupea harengus*: compensatory or evolutionary responses? *Marine Ecology Progress Series* 272, 245–256. <https://doi.org/10.3354/meps272245>
- Engelhard, G.H., Peck, M.A., Rindorf, A., C. Smout, S., van Deurs, M., Raab, K., Andersen, K.H., Garthe, S., Lauerburg, R.A.M., Scott, F., Brunel, T., Aarts, G., van Kooten, T., Dickey-Collas, M., 2014. Forage fish, their fisheries, and their predators: who drives whom? *ICES Journal of Marine Science* 71, 90–104. <https://doi.org/10.1093/icesjms/fst087>
- Englund, G., Öhlund, G., Hein, C.L., Diehl, S., 2011. Temperature dependence of the functional response. *Ecology Letters* 14, 914–921. <https://doi.org/10.1111/j.1461-0248.2011.01661.x>
- Ernande, B., Dieckmann, U., Heino, M., 2004. Adaptive changes in harvested populations: plasticity and evolution of age and size at maturation. *Proceedings of the Royal Society B: Biological Sciences* 271, 415–423. <https://doi.org/10.1098/rspb.2003.2519>
- Espinoza-Tenorio, A., Wolff, M., Taylor, M.H., Espejel, I., 2012. What model suits ecosystem-based fisheries management? A plea for a structured modeling process. *Rev Fish Biol Fisheries* 22, 81–94. <https://doi.org/10.1007/s11160-011-9224-8>
- Exposito-Alonso, M., Booker, T.R., Czech, L., Gillespie, L., Hateley, S., Kyriazis, C.C., Lang, P.L.M., Leventhal, L., Nogues-Bravo, D., Pagowski, V., Ruffley, M., Spence, J.P., Toro Arana, S.E., Weiß, C.L., Zess, E., 2022. Genetic diversity loss in the Anthropocene. *Science* 377, 1431–1435. <https://doi.org/10.1126/science.abn5642>
- Favro, L.D., Kuo, P.K., McDonald, J.F., 1979. Population-Genetic Study of the Effects of Selective Fishing on the Growth Rate of Trout. *J. Fish. Res. Bd. Can.* 36, 552–561. <https://doi.org/10.1139/f79-079>
- Fernandes, J.A., Cheung, W.W.L., Jennings, S., Butenschön, M., de Mora, L., Frölicher, T.L., Barange, M., Grant, A., 2013. Modelling the effects of climate change on the distribution and production of marine fishes: accounting for trophic interactions in a dynamic bioclimate envelope model. *Global Change Biology* 19, 2596–2607. <https://doi.org/10.1111/gcb.12231>
- Fisk, D.L., Latta, L.C., Knapp, R.A., Pfrender, M.E., 2007. Rapid evolution in response to introduced predators I: rates and patterns of morphological and life-history trait divergence. *BMC Evolutionary Biology* 7, 22. <https://doi.org/10.1186/1471-2148-7-22>
- Forestier, R., Blanchard, J., Nash, K., Fulton, B., Johnson, C., Audzijonyte, A., 2020a. Interacting forces of predation and fishing affect species' maturation size (preprint). Preprints. <https://doi.org/10.22541/au.159863315.53329984>

- Forestier, R., Blanchard, J.L., Nash, K.L., Fulton, E.A., Johnson, C., Audzijonyte, A., 2020b. Interacting forces of predation and fishing affect species' maturation size. *Ecology and Evolution* 10, 14033–14051. <https://doi.org/10.1002/ece3.6995>
- Forsman, A., 2015. Rethinking phenotypic plasticity and its consequences for individuals, populations and species. *Heredity* 115, 276–284. <https://doi.org/10.1038/hdy.2014.92>
- Fox, G.A., 1995. Tinkering with the tinkerer: pollution versus evolution. *Environ Health Perspect* 103, 93–100.
- Frid, C.L.J., Harwood, K.G., Hall, S.J., Hall, J.A., 2000. Long-term changes in the benthic communities on North Sea fishing grounds. *ICES Journal of Marine Science* 57, 1303–1309. <https://doi.org/10.1006/jmsc.2000.0900>
- Fujii, T., 2015. Temporal variation in environmental conditions and the structure of fish assemblages around an offshore oil platform in the North Sea. *Marine Environmental Research* 108, 69–82. <https://doi.org/10.1016/j.marenvres.2015.03.013>
- Fulton, E., Smith, A., Johnson, C., 2003. Effect of complexity on marine ecosystem models. *Mar. Ecol. Prog. Ser.* 253, 1–16. <https://doi.org/10.3354/meps253001>
- Gascuel, D., 2019. Pour une révolution dans la mer: De la surpêche à la résilience. Actes Sud Nature.
- Geary, W.L., Bode, M., Doherty, T.S., Fulton, E.A., Nimmo, D.G., Tulloch, A.I.T., Tulloch, V.J.D., Ritchie, E.G., 2020. A guide to ecosystem models and their environmental applications. *Nature Ecology & Evolution*. <https://doi.org/10.1038/s41559-020-01298-8>
- Giacomini, H.C., De Marco, P., Petrere, M., 2009. Exploring community assembly through an individual-based model for trophic interactions. *Ecological Modelling* 220, 23–39. <https://doi.org/10.1016/j.ecolmodel.2008.09.005>
- Gienapp, P., Teplitsky, C., Alho, J.S., Mills, J.A., Merilä, J., 2008. Climate change and evolution: disentangling environmental and genetic responses. *Mol. Ecol.* 17, 167–178. <https://doi.org/10.1111/j.1365-294X.2007.03413.x>
- Gillooly, James.F., Charnov, E.L., West, G.B., Savage, V.M., Brown, J.H., 2002. Effects of size and temperature on developmental time. *Nature* 417, 70–73. <https://doi.org/10.1038/417070a>
- Giraldo, C., Ernande, B., Cresson, P., Kopp, D., Cachera, M., Travers-Trolet, M., Lefebvre, S., 2017. Depth gradient in the resource use of a fish community from a semi-enclosed sea: Benthic-pelagic coupling in fish diet. *Limnology and Oceanography* 62, 2213–2226. <https://doi.org/10.1002/lno.10561>
- Girardin, R., Fulton, E.A., Lehuta, S., Rolland, M., Thébaud, O., Travers-Trolet, M., Vermard, Y., Marchal, P., 2018. Identification of the main processes underlying ecosystem functioning in the Eastern English Channel, with a focus on flatfish species, as revealed through the application of the Atlantis end-to-end model. *Estuarine, Coastal and Shelf Science, Vectors of change in the marine environment* 201, 208–222. <https://doi.org/10.1016/j.ecss.2016.10.016>
- Gislason, H., 1994. Ecosystem effects of fishing activities in the North Sea. *Marine Pollution Bulletin, Environmental Perspective for the Northern Seas* 29, 520–527. [https://doi.org/10.1016/0025-326X\(94\)90680-7](https://doi.org/10.1016/0025-326X(94)90680-7)

- Gislason, H., Daan, N., Rice, J.C., Pope, J.G., 2010. Size, growth, temperature and the natural mortality of marine fish. *Fish and Fisheries* 11, 149–158. <https://doi.org/10.1111/j.1467-2979.2009.00350.x>
- Glamann, J., Hanspach, J., Abson, D.J., Collier, N., Fischer, J., 2017. The intersection of food security and biodiversity conservation: a review. *Reg Environ Change* 17, 1303–1313. <https://doi.org/10.1007/s10113-015-0873-3>
- Gobin, J., Lester, N.P., Fox, M.G., Dunlop, E.S., 2018. Ecological change alters the evolutionary response to harvest in a freshwater fish. *Ecological Applications* 28, 2175–2186. <https://doi.org/10.1002/eap.1805>
- Green, B.S., Mapstone, B.D., Carlos, G., Begg, G.A., 2009. *Tropical Fish Otoliths: Assessment, Management, and Ecology*.
- Grift, R.E., Rijnsdorp, A.D., Barot, S., Heino, M., Dieckmann, U., 2003. Fisheries-induced trends in reaction norms for maturation in North Sea plaice. *Marine Ecology Progress Series* 257, 247–257. <https://doi.org/10.3354/meps257247>
- Grimm, V., Ayllón, D., Railsback, S.F., 2017. Next-Generation Individual-Based Models Integrate Biodiversity and Ecosystems: Yes We Can, and Yes We Must. *Ecosystems* 20, 229–236. <https://doi.org/10.1007/s10021-016-0071-2>
- Halouani, G., Ben Rais Lasram, -->Frida, Shin, Y.-J., Velez, L., Verley, P., Hattab, T., Oliveros-Ramos, R., Diaz, F., Ménard, F., Baklouti, M., Guyennon, A., Romdhane, M.S., -->Le Loc h, F., 2016. Modelling food web structure using an end-to-end approach in the coastal ecosystem of the Gulf of Gabes (Tunisia). *Ecological Modelling* 339, 45–57. <https://doi.org/10.1016/j.ecolmodel.2016.08.008>
- Halpern, B.S., Frazier, M., Potapenko, J., Casey, K.S., Koenig, K., Longo, C., Lowndes, J.S., Rockwood, R.C., Selig, E.R., Selkoe, K.A., Walbridge, S., 2015. Spatial and temporal changes in cumulative human impacts on the world's ocean. *Nat Commun* 6, 7615. <https://doi.org/10.1038/ncomms8615>
- Halpern, B.S., Selkoe, K.A., Micheli, F., Kappel, C.V., 2007. Evaluating and Ranking the Vulnerability of Global Marine Ecosystems to Anthropogenic Threats. *Conservation Biology* 21, 1301–1315. <https://doi.org/10.1111/j.1523-1739.2007.00752.x>
- Halpern, B.S., Walbridge, S., Selkoe, K.A., Kappel, C.V., Micheli, F., D'Agrosa, C., Bruno, J.F., Casey, K.S., Ebert, C., Fox, H.E., Fujita, R., Heinemann, D., Lenihan, H.S., Madin, E.M.P., Perry, M.T., Selig, E.R., Spalding, M., Steneck, R., Watson, R., 2008. A global map of human impact on marine ecosystems. *Science* 319, 948–952. <https://doi.org/10.1126/science.1149345>
- Handford, P., Bell, G., Reimchen, T., 1977. A Gillnet Fishery Considered as an Experiment in Artificial Selection. *J. Fish. Res. Bd. Can.* 34, 954–961. <https://doi.org/10.1139/f77-148>
- Harrald, M., Wright, P.J., Neat, F.C., 2010. Substock variation in reproductive traits in North Sea cod (*Gadus morhua*). *Can. J. Fish. Aquat. Sci.* 67, 866–876. <https://doi.org/10.1139/F10-030>
- Hazel, J.R., Eugene Williams, E., 1990. The role of alterations in membrane lipid composition in enabling physiological adaptation of organisms to their physical environment. *Progress in Lipid Research* 29, 167–227. [https://doi.org/10.1016/0163-7827\(90\)90002-3](https://doi.org/10.1016/0163-7827(90)90002-3)

- Heath, M.R., 2012. Ecosystem limits to food web fluxes and fisheries yields in the North Sea simulated with an end-to-end food web model. *Progress in Oceanography, End-to-End Modeling: Toward Comparative Analysis of Marine Ecosystem Organization* 102, 42–66. <https://doi.org/10.1016/j.pocean.2012.03.004>
- Heino, M., 1998. Management of evolving fish stocks 55, 12.
- Heino, M., Baulier, L., Boukal, D.S., Ernande, B., Johnston, F.D., Mollet, F.M., Pardoe, H., Therkildsen, N.O., Uusi-Heikkilä, S., Vainikka, A., Arlinghaus, R., Dankel, D.J., Dunlop, E.S., Eikeset, A.M., Enberg, K., Engelhard, G.H., Jorgensen, C., Laugen, A.T., Matsumura, S., Nussle, S., Urbach, D., Whitlock, R., Rijnsdorp, A.D., Dieckmann, U., 2013. Can fisheries-induced evolution shift reference points for fisheries management? *ICES Journal of Marine Science* 70, 707–721. <https://doi.org/10.1093/icesjms/fst077>
- Heino, M., Díaz Pauli, B., Dieckmann, U., 2015. Fisheries-Induced Evolution. *Annual Review of Ecology, Evolution, and Systematics* 46, 461–480. <https://doi.org/10.1146/annurev-ecolsys-112414-054339>
- Heino, M., Dieckmann, U., Godø, O.R., 2002. Measuring probabilistic reaction norms for age and size at maturation. *Evolution* 56, 669–678.
- Heino, M., Metz, J.A., Kaitala, V., 1998. The enigma of frequency-dependent selection. *Trends Ecol Evol* 13, 367–370. [https://doi.org/10.1016/s0169-5347\(98\)01380-9](https://doi.org/10.1016/s0169-5347(98)01380-9)
- Hendriks, I.E., Duarte, C.M., Álvarez, M., 2010. Vulnerability of marine biodiversity to ocean acidification: A meta-analysis. *Estuarine, Coastal and Shelf Science* 86, 157–164. <https://doi.org/10.1016/j.ecss.2009.11.022>
- Hendry, A.P., 2016. *Eco-evolutionary Dynamics*. Princeton University Press. <https://doi.org/10.1515/9781400883080>
- Hendry, A.P., Schoen, D.J., Wolak, M.E., Reid, J.M., 2018. The Contemporary Evolution of Fitness. *Annu. Rev. Ecol. Evol. Syst.* 49, 457–476. <https://doi.org/10.1146/annurev-ecolsys-110617-062358>
- Henriksen, O., Rindorf, A., Mosegaard, H., Payne, M.R., van Deurs, M., 2021. Get up early: Revealing behavioral responses of sandeel to ocean warming using commercial catch data. *Ecology and Evolution* n/a. <https://doi.org/10.1002/ece3.8310>
- Heuer, R.M., Grosell, M., 2014. Physiological impacts of elevated carbon dioxide and ocean acidification on fish. *American Journal of Physiology-Regulatory, Integrative and Comparative Physiology* 307, R1061–R1084. <https://doi.org/10.1152/ajpregu.00064.2014>
- Heymans, J.J., Bundy, A., Christensen, V., Coll, M., de Mutsert, K., Fulton, E.A., Piroddi, C., Shin, Y.-J., Steenbeek, J., Travers-Trolet, M., 2020. The Ocean Decade: A True Ecosystem Modeling Challenge. *Frontiers in Marine Science* 7. <https://doi.org/10.3389/fmars.2020.554573>
- Hildebrand, J.A., 2009. Anthropogenic and natural sources of ambient noise in the ocean. *Marine Ecology Progress Series* 395, 5–20. <https://doi.org/10.3354/meps08353>
- Hill Cruz, M., Frenger, I., Getzlaff, J., Kriest, I., Xue, T., Shin, Y.-J., 2022. Understanding the drivers of fish variability in an end-to-end model of the Northern Humboldt Current System. *Ecological Modelling* 472, 110097. <https://doi.org/10.1016/j.ecolmodel.2022.110097>

- Hislop, J.R.G., Robb, A.P., Bell, M.A., Armstrong, D.W., 1991. The diet and food consumption of whiting (*Merlangius merlangus*) in the North Sea. *ICES J Mar Sci* 48, 139–156.
<https://doi.org/10.1093/icesjms/48.2.139>
- Hjelset, A.M., 2014. Fishery-induced changes in Norwegian red king crab (*Paralithodes camtschaticus*) reproductive potential. *ICES Journal of Marine Science* 71, 365–373.
<https://doi.org/10.1093/icesjms/fst126>
- Hjort, J., 1914. Fluctuations in the great fisheries of northern Europe viewed in the light of biological research. *Rapp. P.-V. Reun. Cons. Int. Explo. Mer*, 20: 1–228.
- Hobday, A.J., Pecl, G.T., 2014. Identification of global marine hotspots: sentinels for change and vanguards for adaptation action. *Rev Fish Biol Fisheries* 24, 415–425.
<https://doi.org/10.1007/s11160-013-9326-6>
- Hochachka, P.W., Somero, G.N., 2002. *Biochemical Adaptation: Mechanism and Process in Physiological Evolution*. Oxford University Press.
- Hoegh-Guldberg, O., Poloczanska, E.S., Skirving, W., Dove, S., 2017. Coral Reef Ecosystems under Climate Change and Ocean Acidification. *Frontiers in Marine Science* 4.
- Holling, C.S., 1959. The Components of Predation as Revealed by a Study of Small-Mammal Predation of the European Pine Sawfly¹. *The Canadian Entomologist* 91, 293–320.
<https://doi.org/10.4039/Ent91293-5>
- Hollins, J., Thambithurai, D., Koeck, B., Crespel, A., Bailey, D.M., Cooke, S.J., Lindström, J., Parsons, K.J., Killen, S.S., 2018. A physiological perspective on fisheries-induced evolution. *Evolutionary Applications* 11, 561–576. <https://doi.org/10.1111/eva.12597>
- Holt, J., Butenschön, M., Wakelin, S.L., Artioli, Y., Allen, J.I., 2012. Oceanic controls on the primary production of the northwest European continental shelf: model experiments under recent past conditions and a potential future scenario. *Biogeosciences* 9, 97–117.
<https://doi.org/10.5194/bg-9-97-2012>
- Holt, R.E., Jorgensen, C., 2015. Climate change in fish: effects of respiratory constraints on optimal life history and behaviour. *Biology Letters* 11, 20141032–20141032.
<https://doi.org/10.1098/rsbl.2014.1032>
- Holt, R.E., Jorgensen, C., 2014. Climate warming causes life-history evolution in a model for Atlantic cod (*Gadus morhua*). *Conservation Physiology* 2, cou050–cou050.
<https://doi.org/10.1093/conphys/cou050>
- Hoover, C., Pitcher, T., Christensen, V., 2013. Effects of hunting, fishing and climate change on the Hudson Bay marine ecosystem: II. Ecosystem model future projections. *Ecological Modelling, Global Climate Change and Marine Ecosystems* 264, 143–156.
<https://doi.org/10.1016/j.ecolmodel.2013.01.010>
- Houde, E.D., 2008. Emerging from Hjort's Shadow. *J. Northw. Atl. Fish. Sci.* 41, 53–70.
<https://doi.org/10.2960/J.v41.m634>
- Houle, D., 1992. Comparing evolvability and variability of quantitative traits. *Genetics* 130, 195–204.
<https://doi.org/10.1093/genetics/130.1.195>

- Howes, M.-J.R., Quave, C.L., Collemare, J., Tatsis, E.C., Twilley, D., Lulekal, E., Farlow, A., Li, L., Cazar, M.-E., Leaman, D.J., Prescott, T.A.K., Milliken, W., Martin, C., De Canha, M.N., Lall, N., Qin, H., Walker, B.E., Vásquez-Londoño, C., Allkin, B., Rivers, M., Simmonds, M.S.J., Bell, E., Battison, A., Felix, J., Forest, F., Leon, C., Williams, C., Nic Lughadha, E., 2020. Molecules from nature: Reconciling biodiversity conservation and global healthcare imperatives for sustainable use of medicinal plants and fungi. *PLANTS, PEOPLE, PLANET* 2, 463–481. <https://doi.org/10.1002/ppp3.10138>
- Hrycik, A.R., Collingsworth, P.D., Sesterhenn, T.M., Goto, D., Höök, T.O., 2019. Movement rule selection through eco-genetic modeling: Application to diurnal vertical movement. *Journal of Theoretical Biology* 478, 128–138. <https://doi.org/10.1016/j.jtbi.2019.06.019>
- Huey, R.B., Stevenson, R.D., 1979. Integrating Thermal Physiology and Ecology of Ectotherms: A Discussion of Approaches. *American Zoologist* 19, 357–366. <https://doi.org/10.1093/icb/19.1.357>
- Huisman, J., Tufto, J., 2012. Comparison of Non-Gaussian Quantitative Genetic Models for Migration and Stabilizing Selection. *Evolution* 66, 3444–3461. <https://doi.org/10.1111/j.1558-5646.2012.01707.x>
- Husemann, M., Zachos, F.E., Paxton, R.J., Habel, J.C., 2016. Effective population size in ecology and evolution. *Heredity (Edinb)* 117, 191–192. <https://doi.org/10.1038/hdy.2016.75>
- Hutchings, J.A., 2009. ORIGINAL ARTICLE: Avoidance of fisheries-induced evolution: management implications for catch selectivity and limit reference points. *Evolutionary Applications* 2, 324–334. <https://doi.org/10.1111/j.1752-4571.2009.00085.x>
- Hutchings, J.A., Kuparinen, A., 2019. Implications of fisheries-induced evolution for population recovery: Refocusing the science and refining its communication. *Fish and Fisheries* n/a. <https://doi.org/10.1111/faf.12424>
- Hutchings, J.A., Myers, R.A., 1994. What Can Be Learned from the Collapse of a Renewable Resource? Atlantic Cod, *Gadus morhua*, of Newfoundland and Labrador. *Can. J. Fish. Aquat. Sci.* 51, 2126–2146. <https://doi.org/10.1139/f94-214>
- ICES, 2021. Working Group for the Assessment of Demersal Stocks in the North Sea and Skagerrak (WGNSSK) (report). ICES Scientific Reports. <https://doi.org/10.17895/ices.pub.8211>
- ICES, 2019a. Catches in FAO area 27 by country, species, area and year as provided by the national authorities. Source: Eurostat/ICES data compilation of catch statistics - ICES 2019, Copenhagen. Format: Archived dataset in .xlsx and .csv formats. Version: 16-09-2019.
- ICES, 2019b. Working group on widely distributed stocks (WGWIDE). ICES Scientific Reports. 1:36. 948 pp. <http://doi.org/10.17895/ices.pub.5574>.
- ICES, 2018a. Greater North Sea Ecoregion ? Ecosystem overview. ICES. <https://doi.org/10.17895/ices.pub.4670>
- ICES, 2018b. Greater North Sea Ecoregion ? Fisheries overview. ICES. <https://doi.org/10.17895/ices.pub.4647>
- ICES, 2018c. Report of the Herring Assessment Working Group for the Area South of 62°N (HAWG) (29-31 January 2018 and 12-20 March 2018) (No. ICES CM 2018/ACOM:07).

- ICES, 2018d. Report of the Working Group for the Bay of Biscay and the Iberian Waters Ecoregion (WGBIE) (3-10 May 2018. No. ICES CM 2018/ACOM:12).
- ICES, 2018e. Report of the Working Group on the Assessment of Demersal Stocks in the North Sea and Skagerrak (WGNSSK) (24 April - 3 May 2018) (No. ICES CM 2018/ACOM:22).
- ICES, 2016. Report of the Benchmark Workshop on Sandeel (WKSand 2016). (31 October - 4 November. No. ICES CM 2016/ACOM:33).
- IPBES, 2019a. IPBES (2019), Global assessment report of the Intergovernmental Science-Policy Platform on Biodiversity and Ecosystem Services, Brondízio, E. S., Settele, J., Díaz, S., Ngo, H. T. (eds). IPBES secretariat, Bonn, Germany. 1144 pages. ISBN: 978-3-947851-20-1 1148.
- IPBES, 2019b. Summary for policymakers of the global assessment report on biodiversity and ecosystem services of the Intergovernmental Science-Policy Platform on Biodiversity and Ecosystem Services. S. Díaz, J. Settele, E. S. Brondízio E.S., H. T. Ngo, M. Guèze, J. Agard, A. Arneeth, P. Balvanera, K. A. Brauman, S. H. M. Butchart, K. M. A. Chan, L. A. Garibaldi, K. Ichii, J. Liu, S. M. Subramanian, G. F. Midgley, P. Miloslavich, Z. Molnár, D. Obura, A. Pfaff, S. Polasky, A. Purvis, J. Razaque, B. Reyers, R. Roy Chowdhury, Y. J. Shin, I. J. Visseren-Hamakers, K. J. Willis, and C. N. Zayas (eds.). IPBES secretariat, Bonn, Germany. 56 pages.
- Janssen, F., Schrum, C., Backhaus, J.O., 1999. A climatological data set of temperature and salinity for the Baltic Sea and the North Sea. *Deutsche Hydrographische Zeitschrift* 51, 5–245. <https://doi.org/10.1007/BF02933676>
- Jennings, S, Alvsvåg, J., Cotter, A.J.R., Ehrich, S., Greenstreet, S.P.R., Jarre-Teichmann, A., Mergardt, N., Rijnsdorp, A.D., Smedstad, O., 1999. Fishing effects in northeast Atlantic shelf seas: patterns in fishing effort, diversity and community structure. III. International trawling effort in the North Sea: an analysis of spatial and temporal trends. *Fisheries Research* 40, 125–134. [https://doi.org/10.1016/S0165-7836\(98\)00208-2](https://doi.org/10.1016/S0165-7836(98)00208-2)
- Jennings, Simon, Greenstreet, Simon.P.R., Reynolds, John.D., 1999. Structural change in an exploited fish community: a consequence of differential fishing effects on species with contrasting life histories. *Journal of Animal Ecology* 68, 617–627. <https://doi.org/10.1046/j.1365-2656.1999.00312.x>
- Johansen, W., 1909. *Elemente der exakten Erblichkeitslehre*. G. Fisher, Jena.
- Johnson, F.H., Lewin, I., 1946. The growth rate of *E. coli* in relation to temperature, quinine and coenzyme. *Journal of Cellular and Comparative. Physiology*, 28(1), 47–75. <https://doi.org/10.1002/jcp.1030280104>
- Joly, L.J., Loots, C., Meunier, C.L., Boersma, M., Collet, S., Lefebvre, V., Zambonino-Infante, J.-L., Giraldo, C., 2021. Maturation of the digestive system of Downs herring larvae (*Clupea harengus*, Linnaeus, 1758): identification of critical periods through ontogeny. *Mar Biol* 168, 82. <https://doi.org/10.1007/s00227-021-03894-z>
- Jones, J.E., Howarth, M.J., 1995. Salinity models of the southern North Sea. *Continental Shelf Research* 15, 705–727. [https://doi.org/10.1016/0278-4343\(94\)E0028-K](https://doi.org/10.1016/0278-4343(94)E0028-K)
- Jones, M.C., Cheung, W.W.L., 2015. Multi-model ensemble projections of climate change effects on global marine biodiversity. *ICES Journal of Marine Science* 72, 741–752. <https://doi.org/10.1093/icesjms/fsu172>

- Jørgensen, C., Ernande, B., Fiksen, Ø., 2009. ORIGINAL ARTICLE: Size-selective fishing gear and life history evolution in the Northeast Arctic cod: Size-selective fishing and life history evolution. *Evolutionary Applications* 2, 356–370. <https://doi.org/10.1111/j.1752-4571.2009.00075.x>
- Jørgensen, C., Fiksen, Ø., 2010. Modelling fishing-induced adaptations and consequences for natural mortality. *Can. J. Fish. Aquat. Sci.* 67, 1086–1097. <https://doi.org/10.1139/F10-049>
- Jusufovski, D., Kuparinen, A., 2020. Exploring individual and population eco-evolutionary feedbacks under the coupled effects of fishing and predation. *Fisheries Research* 231, 105713. <https://doi.org/10.1016/j.fishres.2020.105713>
- Jutfelt, F., Norin, T., Ern, R., Overgaard, J., Wang, T., McKenzie, D.J., Lefevre, S., Nilsson, G.E., Metcalfe, N.B., Hickey, A.J.R., Brijs, J., Speers-Roesch, B., Roche, D.G., Gamperl, A.K., Raby, G.D., Morgan, R., Esbaugh, A.J., Gräns, A., Axelsson, M., Ekström, A., Sandblom, E., Binning, S.A., Hicks, J.W., Seebacher, F., Jørgensen, C., Killen, S.S., Schulte, P.M., Clark, T.D., 2018. Oxygen- and capacity-limited thermal tolerance: blurring ecology and physiology. *Journal of Experimental Biology* 221, jeb169615. <https://doi.org/10.1242/jeb.169615>
- Kakuschke, A., Prange, A., 2007. The Influence of Metal Pollution on the Immune System A Potential Stressor for Marine Mammals in the North Sea. *International Journal of Comparative Psychology* 20.
- Kenchington, E., Heino, M., Nielsen, E.E., 2003. Managing marine genetic diversity: time for action? *ICES Journal of Marine Science* 60, 1172–1176. [https://doi.org/10.1016/S1054-3139\(03\)00136-X](https://doi.org/10.1016/S1054-3139(03)00136-X)
- Kenchington, R., Ward, T., Hegerl, E., 2003. The Benefits of Marine Protected Areas.
- Killen, S.S., 2014. Growth trajectory influences temperature preference in fish through an effect on metabolic rate. *Journal of Animal Ecology* 83, 1513–1522. <https://doi.org/10.1111/1365-2656.12244>
- Killen, S.S., Atkinson, D., Glazier, D.S., 2010. The intraspecific scaling of metabolic rate with body mass in fishes depends on lifestyle and temperature. *Ecology Letters* 13, 184–193. <https://doi.org/10.1111/j.1461-0248.2009.01415.x>
- Killen, S.S., Costa, I., Brown, J.A., Gamperl, A.K., 2007. Little left in the tank: metabolic scaling in marine teleosts and its implications for aerobic scope. *Proceedings of the Royal Society B: Biological Sciences* 274, 431–438. <https://doi.org/10.1098/rspb.2006.3741>
- Kinnison, M.T., Hairston, N.G., Hendry, A.P., 2015. Cryptic eco-evolutionary dynamics. *Ann N Y Acad Sci* 1360, 120–144. <https://doi.org/10.1111/nyas.12974>
- Koch, R.E., Buchanan, K.L., Casagrande, S., Crino, O., Dowling, D.K., Hill, G.E., Hood, W.R., McKenzie, M., Mariette, M.M., Noble, D.W.A., Pavlova, A., Seebacher, F., Sunnucks, P., Udino, E., White, C.R., Salin, K., Stier, A., 2021. Integrating Mitochondrial Aerobic Metabolism into Ecology and Evolution. *Trends in Ecology & Evolution* 36, 321–332. <https://doi.org/10.1016/j.tree.2020.12.006>
- Kooijman, S.A.L.M., 2010. *Dynamic Energy Budget Theory for Metabolic Organisation*. Cambridge University Press.
- Krause, M., Fock, H., Greve, W., Winkler, G., 2003. North sea zooplankton: a review. *Senckenbergiana maritima* 33, 71–204. <https://doi.org/10.1007/BF03043048>

- Kuparinen, A., Cano, J.M., Loehr, J., Herczeg, G., Gonda, A., Merilä, J., 2011. Fish age at maturation is influenced by temperature independently of growth. *Oecologia* 167, 435–443. <https://doi.org/10.1007/s00442-011-1989-x>
- Kuparinen, A., Kuikka, S., Merilä, J., 2009. Estimating fisheries-induced selection: traditional gear selectivity research meets fisheries-induced evolution. *Evolutionary Applications* 2, 234–243. <https://doi.org/10.1111/j.1752-4571.2009.00070.x>
- Kuparinen, A., Uusi-Heikkilä, S., 2019. Atlantic cod recovery from the Allee effect zone: contrasting ecological and evolutionary rescue. *Fish and Fisheries* n/a. <https://doi.org/10.1111/faf.12470>
- Laffoley, D., Baxter, J.M., 2019. Ocean deoxygenation : everyone’s problem. IUCN. <https://doi.org/10.2305/IUCN.CH.2019.13.en>
- Last, J.M., 1989. The food of herring, *Clupea harengus*, in the North Sea, 1983–1986. *Journal of Fish Biology* 34, 489–501. <https://doi.org/10.1111/j.1095-8649.1989.tb03330.x>
- Laugen, A.T., Engelhard, G.H., Whitlock, R., Arlinghaus, R., Dankel, D.J., Dunlop, E.S., Eikeset, A.M., Enberg, K., Jørgensen, C., Matsumura, S., Nusslé, S., Urbach, D., Baulier, L., Boukal, D.S., Ernande, B., Johnston, F.D., Mollet, F., Pardoe, H., Therkildsen, N.O., Uusi-Heikkilä, S., Vainikka, A., Heino, M., Rijnsdorp, A.D., Dieckmann, U., 2014. Evolutionary impact assessment: accounting for evolutionary consequences of fishing in an ecosystem approach to fisheries management. *Fish and Fisheries* 15, 65–96. <https://doi.org/10.1111/faf.12007>
- Lavaud, R., Thomas, Y., Pecquerie, L., Benoît, H.P., Guyondet, T., Flye-Sainte-Marie, J., Chabot, D., 2019. Modeling the impact of hypoxia on the energy budget of Atlantic cod in two populations of the Gulf of Saint-Lawrence, Canada. *Journal of Sea Research* 143, 243–253. <https://doi.org/10.1016/j.seares.2018.07.001>
- Law, R., 2000. Fishing, selection, and phenotypic evolution. *ICES J Mar Sci* 57, 659–668. <https://doi.org/10.1006/jmsc.2000.0731>
- Law, R., Grey, D.R., 1989. Evolution of yields from populations with age-specific cropping. *Evol Ecol* 3, 343–359. <https://doi.org/10.1007/BF02285264>
- Le Pape, O., Bonhommeau, S., 2015. The food limitation hypothesis for juvenile marine fish. *Fish and Fisheries* 16, 373–398. <https://doi.org/10.1111/faf.12063>
- Le Pape, O., Gilliers, C., Riou, P., Morin, J., Amara, R., Désaunay, Y., 2007. Convergent signs of degradation in both the capacity and the quality of an essential fish habitat: state of the Seine estuary (France) flatfish nurseries. *Hydrobiologia* 588, 225–229. <https://doi.org/10.1007/s10750-007-0665-y>
- Lefevre, S., 2016. Are global warming and ocean acidification conspiring against marine ectotherms? A meta-analysis of the respiratory effects of elevated temperature, high CO₂ and their interaction. *Conserv Physiol* 4, cow009. <https://doi.org/10.1093/conphys/cow009>
- Lefevre, S., McKenzie, D.J., Nilsson, G.E., 2018. In modelling effects of global warming, invalid assumptions lead to unrealistic projections. *Global Change Biology* 24, 553–556. <https://doi.org/10.1111/gcb.13978>
- Lefevre, S., McKenzie, D.J., Nilsson, G.E., 2017. Models projecting the fate of fish populations under climate change need to be based on valid physiological mechanisms. *Global Change Biology* 23, 3449–3459. <https://doi.org/10.1111/gcb.13652>

- Lefevre, S., Wang, T., McKenzie, D.J., 2021. The role of mechanistic physiology in investigating impacts of global warming on fishes. *J Exp Biol* 224, jeb238840. <https://doi.org/10.1242/jeb.238840>
- Lefort, S., Aumont, O., Bopp, L., Arsouze, T., Gehlen, M., Maury, O., 2015. Spatial and body-size dependent response of marine pelagic communities to projected global climate change. *Global Change Biology* 21, 154–164. <https://doi.org/10.1111/gcb.12679>
- Leroy, G., Carroll, E.L., Bruford, M.W., DeWoody, J.A., Strand, A., Waits, L., Wang, J., 2018. Next-generation metrics for monitoring genetic erosion within populations of conservation concern. *Evolutionary Applications* 11, 1066–1083. <https://doi.org/10.1111/eva.12564>
- Lester, N.P., Shuter, B.J., Abrams, P.A., 2004. Interpreting the von Bertalanffy model of somatic growth in fishes: the cost of reproduction. *Proceedings of the Royal Society of London B: Biological Sciences* 271, 1625–1631. <https://doi.org/10.1098/rspb.2004.2778>
- Lewy, P., 2004. A stochastic age-length-structured multispecies model applied to North Sea stocks 33.
- Lindgren, M., Van Deurs, M., MacKenzie, B.R., Worsoe Clausen, L., Christensen, A., Rindorf, A., 2018. Productivity and recovery of forage fish under climate change and fishing: North Sea sandeel as a case study. *Fisheries Oceanography* 27, 212–221. <https://doi.org/10.1111/fog.12246>
- Lindmark, M., Audzijonyte, A., Blanchard, J.L., Gårdmark, A., 2022. Temperature impacts on fish physiology and resource abundance lead to faster growth but smaller fish sizes and yields under warming. *Global Change Biology* n/a. <https://doi.org/10.1111/gcb.16341>
- Loeuille, N., 2019. Eco-evolutionary dynamics in a disturbed world: implications for the maintenance of ecological networks. *F1000Research* 8, 97. <https://doi.org/10.12688/f1000research.15629.1>
- Loeuille, N., Loreau, M., 2005. Evolutionary emergence of size-structured food webs. *PNAS* 102, 5761–5766. <https://doi.org/10.1073/pnas.0408424102>
- Lotze, H.K., 2007. Rise and fall of fishing and marine resource use in the Wadden Sea, southern North Sea. *Fisheries Research, History of marine animal populations and their exploitation in northern Europe* 87, 208–218. <https://doi.org/10.1016/j.fishres.2006.12.009>
- Lotze, H.K., Tittensor, D.P., Bryndum-Buchholz, A., Eddy, T.D., Cheung, W.W.L., Galbraith, E.D., Barange, M., Barrier, N., Bianchi, D., Blanchard, J.L., Bopp, L., Büchner, M., Bulman, C.M., Carozza, D.A., Christensen, V., Coll, M., Dunne, J.P., Fulton, E.A., Jennings, S., Jones, M.C., Mackinson, S., Maury, O., Niiranen, S., Oliveros-Ramos, R., Roy, T., Fernandes, J.A., Schewe, J., Shin, Y.-J., Silva, T.A.M., Steenbeek, J., Stock, C.A., Verley, P., Volkholz, J., Walker, N.D., Worm, B., 2019. Global ensemble projections reveal trophic amplification of ocean biomass declines with climate change. *Proceedings of the National Academy of Sciences* 116, 12907–12912. <https://doi.org/10.1073/pnas.1900194116>
- Luján Paredes, D.C., 2022. Dealing with uncertainty in complex models : an application to the OSMOSE ecosystem model of the northern Humboldt current system (These de doctorat). université Paris-Saclay.
- Lynch, M., Walsh, B., 1998. *Genetics and Analysis of Quantitative Traits*, Sinauer Associates, Inc, Sunderland. ed.

- MacKenzie, K., 1985. The use of parasites as biological tags in population studies of herring (*Clupea harengus* L.) in the North Sea and to the north and west of Scotland. *ICES Journal of Marine Science* 42, 33–64. <https://doi.org/10.1093/icesjms/42.1.33>
- Mackinson, S., Daskalov, G., 2007. An ecosystem model of the North Sea to support an ecosystem approach to fisheries management: description and parameterisation 200.
- Mangel, M., 2003. *Environment and Longevity: The Demography of the Growth Rate* 15.
- Marty, L., Dieckmann, U., Ernande, B., 2015. Fisheries-induced neutral and adaptive evolution in exploited fish populations and consequences for their adaptive potential. *Evolutionary Applications* 8, 47–63. <https://doi.org/10.1111/eva.12220>
- Marty, L., Dieckmann, U., Rochet, M.-J., Ernande, B., 2011. Impact of Environmental Covariation in Growth and Mortality on Evolving Maturation Reaction Norms. *The American Naturalist* 177, E98–E118. <https://doi.org/10.1086/658988>
- Marty, L., Rochet, M., Ernande, B., 2014. Temporal trends in age and size at maturation of four North Sea gadid species: cod, haddock, whiting and Norway pout. *Marine Ecology Progress Series* 497, 179–197. <https://doi.org/10.3354/meps10580>
- Masel, J., 2011. Genetic drift. *Current Biology* 21, R837–R838. <https://doi.org/10.1016/j.cub.2011.08.007>
- Maury, O., 2010. An overview of APECOSM, a spatialized mass balanced “Apex Predators ECOSystem Model” to study physiologically structured tuna population dynamics in their ecosystem. *Progress in Oceanography, Special Issue: Parameterisation of Trophic Interactions in Ecosystem Modelling* 84, 113–117. <https://doi.org/10.1016/j.pocean.2009.09.013>
- McClelland, E.K., Chan, M.T.T., Lin, X., Sakhrani, D., Vincelli, F., Kim, J.-H., Heath, D.D., Devlin, R.H., 2020. Loci associated with variation in gene expression and growth in juvenile salmon are influenced by the presence of a growth hormone transgene. *BMC Genomics* 21, 185. <https://doi.org/10.1186/s12864-020-6586-0>
- McLean, M., Auber, A., Graham, N.A.J., Houk, P., Villéger, S., Violle, C., Thuiller, W., Wilson, S.K., Mouillot, D., 2019a. Trait structure and redundancy determine sensitivity to disturbance in marine fish communities. *Global Change Biology* 25, 3424–3437. <https://doi.org/10.1111/gcb.14662>
- McLean, M., Mouillot, D., Auber, A., 2018a. Ecological and life history traits explain a climate-induced shift in a temperate marine fish community. *Marine Ecology Progress Series* 606, 175–186. <https://doi.org/10.3354/meps12766>
- McLean, M., Mouillot, D., Goascoz, N., Schlaich, I., Auber, A., 2019b. Functional reorganization of marine fish nurseries under climate warming. *Glob Chang Biol* 25, 660–674. <https://doi.org/10.1111/gcb.14501>
- McLean, M., Mouillot, D., Lindegren, M., Engelhard, G., Villéger, S., Marchal, P., Brind’Amour, A., Auber, A., 2018b. A Climate-Driven Functional Inversion of Connected Marine Ecosystems. *Current Biology* 28, 3654-3660.e3. <https://doi.org/10.1016/j.cub.2018.09.050>
- McLean, M., Mouillot, D., Lindegren, M., Villéger, S., Engelhard, G., Murgier, J., Auber, A., 2019c. Fish communities diverge in species but converge in traits over three decades of warming. *Global Change Biology* 25, 3972–3984. <https://doi.org/10.1111/gcb.14785>

- Mendel, G., 1866. Versuche über Pflanzen-hybriden. Verhandlungen des naturforschenden Vereines in Brünn, Bd. IV für das Jahr 1865, Abhandlungen, :3-45.
- Merilä, J., Hendry, A.P., 2014. Climate change, adaptation, and phenotypic plasticity: the problem and the evidence. *Evolutionary Applications* 7, 1–14. <https://doi.org/10.1111/eva.12137>
- Merilä, J., Sheldon, B.C., 1999. Genetic architecture of fitness and nonfitness traits: empirical patterns and development of ideas. *Heredity* 83, 103–109. <https://doi.org/10.1046/j.1365-2540.1999.00585.x>
- Meszéna, G., Kisdi, É., Dieckmann, U., Geritz, S.A.H., Metz, J.A.J., 2002. Evolutionary Optimisation Models and Matrix Games in the Unified Perspective of Adaptive Dynamics. *Selection* 2, 193–220. <https://doi.org/10.1556/Select.2.2001.1-2.14>
- Metcalfe, N.B., Van Leeuwen, T.E., Killen, S.S., 2016. Does individual variation in metabolic phenotype predict fish behaviour and performance? *Journal of Fish Biology* 88, 298–321. <https://doi.org/10.1111/jfb.12699>
- Metz, J.A.J., Nisbet, R.M., Geritz, S.A.H., 1992. How should we define ‘fitness’ for general ecological scenarios? *Trends in Ecology & Evolution* 7, 198–202. [https://doi.org/10.1016/0169-5347\(92\)90073-K](https://doi.org/10.1016/0169-5347(92)90073-K)
- Middel, H., Verones, F., 2017. Making Marine Noise Pollution Impacts Heard: The Case of Cetaceans in the North Sea within Life Cycle Impact Assessment. *Sustainability* 9, 1138. <https://doi.org/10.3390/su9071138>
- Mollet, F.M., Kraak, S.B.M., Rijnsdorp, A.D., 2007. Fisheries-induced evolutionary changes in maturation reaction norms in North Sea sole *Solea solea*. *Marine Ecology Progress Series* 351, 189–199. <https://doi.org/10.3354/meps07138>
- Moullec, F., Barrier, N., Guilhaumon, F., Marsaleix, P., Somot, S., Shin, Y.-J., 2019. An End-to-End model reveals losers and winners in a warming Mediterranean Sea. *Front. Mar. Sci.* 6. <https://doi.org/10.3389/fmars.2019.00345>
- Mousseau, T., Roff, D., 1987. Mousseau TA, Roff DA. Natural selection and the heritability of fitness components. *Heredity* 59: 181-197. *Heredity* 59 (Pt 2), 181–97. <https://doi.org/10.1038/hdy.1987.113>
- Munguía-Vega, A., Sáenz-Arroyo, A., Greenley, A.P., Espinoza-Montes, J.A., Palumbi, S.R., Rossetto, M., Micheli, F., 2015. Marine reserves help preserve genetic diversity after impacts derived from climate variability: Lessons from the pink abalone in Baja California. *Global Ecology and Conservation* 4, 264–276. <https://doi.org/10.1016/j.gecco.2015.07.005>
- Murgier, J., McLean, M., Maire, A., Mouillot, D., Loiseau, N., Munoz, F., Violle, C., Auber, A., 2021. Rebound in functional distinctiveness following warming and reduced fishing in the North Sea. *Proceedings of the Royal Society B: Biological Sciences* 288, 20201600. <https://doi.org/10.1098/rspb.2020.1600>
- Murren, C.J., Auld, J.R., Callahan, H., Ghalambor, C.K., Handelsman, C.A., Heskell, M.A., Kingsolver, J.G., Maclean, H.J., Masel, J., Maughan, H., Pfennig, D.W., Relyea, R.A., Seiter, S., Snell-Rood, E., Steiner, U.K., Schlichting, C.D., 2015. Constraints on the evolution of phenotypic plasticity: limits and costs of phenotype and plasticity. *Heredity* 115, 293–301. <https://doi.org/10.1038/hdy.2015.8>

- Naish, K.A., Hard, J.J., 2008. Bridging the gap between the genotype and the phenotype: linking genetic variation, selection and adaptation in fishes. *Fish and Fisheries* 9, 396–422. <https://doi.org/10.1111/j.1467-2979.2008.00302.x>
- Neubauer, P., Andersen, K.H., 2019. Thermal performance of fish is explained by an interplay between physiology, behaviour and ecology. *Conservation Physiology* 7. <https://doi.org/10.1093/conphys/coz025>
- Neuheimer, A.B., Grønkjær, P., 2012. Climate effects on size-at-age: growth in warming waters compensates for earlier maturity in an exploited marine fish. *Global Change Biology* 18, 1812–1822. <https://doi.org/10.1111/j.1365-2486.2012.02673.x>
- Nilsson-Örtman, V., Rowe, L., 2021. The evolution of developmental thresholds and reaction norms for age and size at maturity. *PNAS* 118. <https://doi.org/10.1073/pnas.2017185118>
- Nogues, Q., Araignous, E., Bourdaud, P., Halouani, G., Raoux, A., Foucher, É., Loc'h, F.L., Loew-Turbout, F., Ben Rais Lasram, F., Dauvin, J.-C., Niquil, N., 2022. Spatialized ecological network analysis for ecosystem-based management: effects of climate change, marine renewable energy, and fishing on ecosystem functioning in the Bay of Seine. *ICES Journal of Marine Science* 79, 1098–1112. <https://doi.org/10.1093/icesjms/fsac026>
- Norberg, J., Urban, M.C., Vellend, M., Klausmeier, C.A., Loeuille, N., 2012. Eco-evolutionary responses of biodiversity to climate change. *Nature Climate Change* 2, 747–751. <https://doi.org/10.1038/nclimate1588>
- Ohlberger, J., Schindler, D.E., Ward, E.J., Walsworth, T.E., Essington, T.E., 2019. Resurgence of an apex marine predator and the decline in prey body size. *PNAS* 116, 26682–26689. <https://doi.org/10.1073/pnas.1910930116>
- Öhlund, G., Hedström, P., Norman, S., Hein, C.L., Englund, G., 2015. Temperature dependence of predation depends on the relative performance of predators and prey. *Proceedings of the Royal Society B: Biological Sciences* 282, 20142254. <https://doi.org/10.1098/rspb.2014.2254>
- Ojaveer, E., Aps, R., 2003. Sprat, *Sprattus sprattus balticus* (Schn.). p. 79-87. In E. Ojaveer, E. Pihu and T. Saat (eds). *Fishes of Estonia*. Estonian Academy Publishers, Tallinn. 416 p.
- Oliveros-Ramos, R., Shin, Y.-J., 2016. *calibrar*: an R package for fitting complex ecological models 25. <https://doi.org/10.48550/arXiv.1603.03141>
- Oliveros-Ramos, R., Verley, P., Echevin, V., Shin, Y.-J., 2017. A sequential approach to calibrate ecosystem models with multiple time series data. *Progress in Oceanography* 151, 227–244. <https://doi.org/10.1016/j.pcean.2017.01.002>
- Olsen, E.M., Heino, M., Lilly, G.R., Morgan, M.J., Brattey, J., Ernande, B., Dieckmann, U., 2004. Maturation trends indicative of rapid evolution preceded the collapse of northern cod. *Nature* 428, 932–935. <https://doi.org/10.1038/nature02430>
- Olsen, E.M., Lilly, G.R., Heino, M., Morgan, M.J., Brattey, J., Dieckmann, U., 2005. Assessing changes in age and size at maturation in collapsing populations of Atlantic cod (*Gadus morhua*). *Can. J. Fish. Aquat. Sci.* 62, 811–823. <https://doi.org/10.1139/f05-065>
- Olsen, E.M., Ottersen, G., Llope, M., Chan, K.-S., Beaugrand, G., Stenseth, N.Ch., 2011. Spawning stock and recruitment in North Sea cod shaped by food and climate. *Proceedings of the Royal Society B: Biological Sciences* 278, 504–510. <https://doi.org/10.1098/rspb.2010.1465>

- Owens, B., 2013. Long-term research: Slow science. *Nature* 495, 300–303.
<https://doi.org/10.1038/495300a>
- Pankhurst, N.W., Munday, P.L., Pankhurst, N.W., Munday, P.L., 2011. Effects of climate change on fish reproduction and early life history stages. *Mar. Freshwater Res.* 62, 1015–1026.
<https://doi.org/10.1071/MF10269>
- Pardoe, H., Dunlop, E., Marteinsdóttir, G., Dieckmann, U., 2019. Eco-genetic modelling of stock structure and the evolutionary effects of fishing: the case of Icelandic cod 48.
- Parmesan, C., 2006. Ecological and Evolutionary Responses to Recent Climate Change. *Annual Review of Ecology, Evolution, and Systematics* 37, 637–669.
<https://doi.org/10.1146/annurev.ecolsys.37.091305.110100>
- Pauls, S.U., Nowak, C., Bálint, M., Pfenninger, M., 2013. The impact of global climate change on genetic diversity within populations and species. *Molecular Ecology* 22, 925–946.
<https://doi.org/10.1111/mec.12152>
- Pauly, D., 1998. Fishing Down Marine Food Webs. *Science* 279, 860–863.
<https://doi.org/10.1126/science.279.5352.860>
- Pauly, D., 1994. A framework for latitudinal comparisons of flatfish recruitment. *Netherlands Journal of Sea Research* 32, 107–118. [https://doi.org/10.1016/0077-7579\(94\)90035-3](https://doi.org/10.1016/0077-7579(94)90035-3)
- Pauly, D., Cheung, W.W.L., 2018a. On confusing cause and effect in the oxygen limitation of fish. *Global Change Biology* 24, e743–e744. <https://doi.org/10.1111/gcb.14383>
- Pauly, D., Cheung, W.W.L., 2018b. Sound physiological knowledge and principles in modeling shrinking of fishes under climate change. *Glob Chang Biol* 24, e15–e26.
<https://doi.org/10.1111/gcb.13831>
- Pawar, S., Dell, A.I., Savage, V.M., 2015. From Metabolic Constraints on Individuals to the Dynamics of Ecosystems, in: *Aquatic Functional Biodiversity*. Elsevier, pp. 3–36.
<https://doi.org/10.1016/B978-0-12-417015-5.00001-3>
- Payne, M.R., Hatfield, E.M.C., Dickey-Collas, M., Falkenhaus, T., Gallego, A., Gröger, J., Licandro, P., Llope, M., Munk, P., Röckmann, C., Schmidt, J.O., Nash, R.D.M., 2009. Recruitment in a changing environment: the 2000s North Sea herring recruitment failure. *ICES Journal of Marine Science* 66, 272–277. <https://doi.org/10.1093/icesjms/fsn211>
- Payne, N.L., Morley, S.A., Halsey, L.G., Smith, J.A., Stuart-Smith, R., Waldock, C., Bates, A.E., 2021. Fish heating tolerance scales similarly across individual physiology and populations. *Commun Biol* 4, 1–5. <https://doi.org/10.1038/s42003-021-01773-3>
- Pelletier, F., Garant, D., Hendry, A.P., 2009. Eco-evolutionary dynamics. *Philosophical Transactions of the Royal Society B: Biological Sciences* 364, 1483–1489.
<https://doi.org/10.1098/rstb.2009.0027>
- Perälä, T., Kuparinen, A., 2020. Eco-evolutionary dynamics driven by fishing: From single species models to dynamic evolution within complex food webs. *Evolutionary Applications* n/a.
<https://doi.org/10.1111/eva.13058>
- Perry, A.L., Low, P.J., Ellis, J.R., Reynolds, J.D., 2005. Climate Change and Distribution Shifts in Marine Fishes. *Science* 308, 1912–1915. <https://doi.org/10.1126/science.1111322>

- Perryman, H.A., Hansen, C., Howell, D., Olsen, E., 2021. A Review of Applications Evaluating Fisheries Management Scenarios through Marine Ecosystem Models. *Reviews in Fisheries Science & Aquaculture* 1–36. <https://doi.org/10.1080/23308249.2021.1884642>
- Pethybridge, H.R., Weijerman, M., Perryman, H., Audzijonyte, A., Porobic, J., McGregor, V., Girardin, R., Bulman, C., Ortega-Cisneros, K., Sinerchia, M., Hutton, T., Lozano-Montes, H., Mori, M., Novaglio, C., Fay, G., Gorton, R., Fulton, E., 2019. Calibrating process-based marine ecosystem models: An example case using Atlantis. *Ecological Modelling* 412, 108822. <https://doi.org/10.1016/j.ecolmodel.2019.108822>
- Piet, G.J., Pfisterer, A.B., Rijnsdorp, A.D., 1998. On factors structuring the flatfish assemblage in the southern North Sea. *Journal of Sea Research* 40, 143–152. [https://doi.org/10.1016/S1385-1101\(98\)00008-2](https://doi.org/10.1016/S1385-1101(98)00008-2)
- Pigliucci, M., Murren, C.J., Schlichting, C.D., 2006. Phenotypic plasticity and evolution by genetic assimilation. *Journal of Experimental Biology* 209, 2362–2367. <https://doi.org/10.1242/jeb.02070>
- Pikitch, E.K., Santora, C., Babcock, E.A., Bakun, A., Bonfil, R., Conover, D.O., Dayton, P., Doukakis, P., Fluharty, D., Heneman, B., Houde, E.D., Link, J., Livingston, P.A., Mangel, M., McAllister, M.K., Pope, J., Sainsbury, K.J., 2004. Ecosystem-Based Fishery Management. *Science* 305, 346–347. <https://doi.org/10.1126/science.1098222>
- Pimm, S.L., Jenkins, C.N., Abell, R., Brooks, T.M., Gittleman, J.L., Joppa, L.N., Raven, P.H., Roberts, C.M., Sexton, J.O., 2014. The biodiversity of species and their rates of extinction, distribution, and protection. *Science* 344, 1246752. <https://doi.org/10.1126/science.1246752>
- Pinnegar, J.K., 2014. DAPSTOM - An Integrated Database & Portal for Fish Stomach Records. Version 4.7. Centre for Environment, Fisheries & Aquaculture Science, Lowestoft, UK. February 2014, 39pp.
- Pinsky, M.L., Palumbi, S.R., 2014. Meta-analysis reveals lower genetic diversity in overfished populations. *Molecular Ecology* 23, 29–39. <https://doi.org/10.1111/mec.12509>
- Plagányi, É.E., 2007. Models for an Ecosystem Approach to Fisheries. Food & Agriculture Org.
- Planque, B., Mullon, C., 2020. Modelling chance and necessity in natural systems. *ICES Journal of Marine Science* 77, 1573–1588. <https://doi.org/10.1093/icesjms/fsz173>
- Pörtner, H.-O., 2021. Climate impacts on organisms, ecosystems and human societies: integrating OCLTT into a wider context. *Journal of Experimental Biology* 224, jeb238360. <https://doi.org/10.1242/jeb.238360>
- Pörtner, H.O., 2001. Climate change and temperature-dependent biogeography: oxygen limitation of thermal tolerance in animals. *Naturwissenschaften* 88, 137–146. <https://doi.org/10.1007/s001140100216>
- Pörtner, H.O., Berdal, B., Blust, R., Brix, O., Colosimo, A., De Wachter, B., Giuliani, A., Johansen, T., Fischer, T., Knust, R., Lannig, G., Naevdal, G., Nedenes, A., Nyhammer, G., Sartoris, F.J., Serendero, I., Sirabella, P., Thorkildsen, S., Zakhartsev, M., 2001. Climate induced temperature effects on growth performance, fecundity and recruitment in marine fish: developing a hypothesis for cause and effect relationships in Atlantic cod (*Gadus morhua*) and common eelpout (*Zoarces viviparus*). *Continental Shelf Research, European Land-Ocean Interaction* 21, 1975–1997. [https://doi.org/10.1016/S0278-4343\(01\)00038-3](https://doi.org/10.1016/S0278-4343(01)00038-3)

- Pörtner, H.-O., Bock, C., Mark, F.C., 2017. Oxygen- and capacity-limited thermal tolerance: bridging ecology and physiology. *J Exp Biol* 220, 2685–2696. <https://doi.org/10.1242/jeb.134585>
- Pörtner, H.O., Farrell, A.P., 2008. Physiology and Climate Change. *Science, New Series* 322, 690–692.
- Pörtner, H.O., Peck, M.A., 2010. Climate change effects on fishes and fisheries: towards a cause-and-effect understanding. *Journal of Fish Biology* 77, 1745–1779. <https://doi.org/10.1111/j.1095-8649.2010.02783.x>
- Pörtner, H.O., Schulte, P.M., Wood, C.M., Schiemer, F., 2010. Niche dimensions in fishes: an integrative view. *Physiol Biochem Zool* 83, 808–826. <https://doi.org/10.1086/655977>
- Poulsen, N.A., Nielsen, E.E., Schierup, M.H., Loeschcke, V., GrønkJær, P., 2006. Long-term stability and effective population size in North Sea and Baltic Sea cod (*Gadus morhua*). *Molecular Ecology* 15, 321–331. <https://doi.org/10.1111/j.1365-294X.2005.02777.x>
- Price, T., Schluter, D., 1991. On the Low Heritability of Life-History Traits. *Evolution* 45, 853–861. <https://doi.org/10.1111/j.1558-5646.1991.tb04354.x>
- Prosnier, L., Médoc, V., Loeuille, N., 2020. Evolution of predator foraging in response to prey infection favors species coexistence. *bioRxiv*.
- Quince, C., Abrams, P.A., Shuter, B.J., Lester, N.P., 2008. Biphase growth in fish I: Theoretical foundations. *Journal of Theoretical Biology* 254, 197–206. <https://doi.org/10.1016/j.jtbi.2008.05.029>
- Raab, K., Nagelkerke, L. a. J., Boérée, C., Rijnsdorp, A.D., Temming, A., Dickey-Collas, M., 2012. Dietary overlap between the potential competitors herring, sprat and anchovy in the North Sea. *Marine Ecology Progress Series* 470, 101–111. <https://doi.org/10.3354/meps09919>
- Reise, K., Gollasch, S., Wolff, W.J., 1998. Introduced marine species of the North Sea coasts. *Helgolander Meeresunters* 52, 219–234. <https://doi.org/10.1007/BF02908898>
- Ricker, W.E., 1981. Changes in the Average Size and Average Age of Pacific Salmon. *Can. J. Fish. Aquat. Sci.* 38, 1636–1656. <https://doi.org/10.1139/f81-213>
- Ricklefs, R.E., Wikelski, M., 2002. The physiology/life-history nexus. *Trends in Ecology & Evolution* 17, 462–468. [https://doi.org/10.1016/S0169-5347\(02\)02578-8](https://doi.org/10.1016/S0169-5347(02)02578-8)
- Rickman, S.J., Dulvy, N.K., Jennings, S., Reynolds, J.D., 2000. Recruitment variation related to fecundity in marine fishes. *Can. J. Fish. Aquat. Sci.* 57, 116–124. <https://doi.org/10.1139/f99-205>
- Rijnsdorp, A.D., 1993. Fisheries as a large-scale experiment on life-history evolution: disentangling phenotypic and genetic effects in changes in maturation and reproduction of North Sea plaice, *Pleuronectes platessa* L. *Oecologia* 96, 391–401. <https://doi.org/10.1007/BF00317510>
- Rijnsdorp, A.D., Grift, R.E., Kraak, S.B., 2005. Fisheries-induced adaptive change in reproductive investment in North Sea plaice (*Pleuronectes platessa*)? *Can. J. Fish. Aquat. Sci.* 62, 833–843. <https://doi.org/10.1139/f05-039>
- Rijnsdorp, A.D., Vingerhoed, B., 2001. Feeding of plaice *Pleuronectes platessa* L. and sole *Solea solea* (L.) in relation to the effects of bottom trawling. *Journal of Sea Research* 45, 219–229. [https://doi.org/10.1016/S1385-1101\(01\)00047-8](https://doi.org/10.1016/S1385-1101(01)00047-8)

- Ripple, W.J., Estes, J.A., Schmitz, O.J., Constant, V., Kaylor, M.J., Lenz, A., Motley, J.L., Self, K.E., Taylor, D.S., Wolf, C., 2016. What is a Trophic Cascade? *Trends in Ecology & Evolution* 31, 842–849. <https://doi.org/10.1016/j.tree.2016.08.010>
- Robb, A.P., Hislop, J.R.G., 1980. The food of five gadoid species during the pelagic O-group phase in the northern North Sea. *Journal of Fish Biology* 16, 199–217. <https://doi.org/10.1111/j.1095-8649.1980.tb03699.x>
- Rochet, M.-J., Benoît, E., 2012. Fishing destabilizes the biomass flow in the marine size spectrum. *Proceedings of the Royal Society B: Biological Sciences* 279, 284–292. <https://doi.org/10.1098/rspb.2011.0893>
- Roff, D., 1993. *Evolution Of Life Histories: Theory and Analysis*. Springer Science & Business Media.
- Roff, D.A., 1992. *The evolution of life histories: theory and analysis*. Chapman and Hall, New York.
- Romero-Mujalli, D., Jeltsch, F., Tiedemann, R., 2019. Individual-based modeling of eco-evolutionary dynamics: state of the art and future directions. *Regional Environmental Change* 19, 1–12. <https://doi.org/10.1007/s10113-018-1406-7>
- Rose, K.A., Allen, J.I., Artioli, Y., Barange, M., Blackford, J., Carlotti, F., Cropp, R., Daewel, U., Edwards, K., Flynn, K., Hill, S.L., HilleRisLambers, R., Huse, G., Mackinson, S., Megrey, B., Moll, A., Rivkin, R., Salihoglu, B., Schrum, C., Shannon, L., Shin, Y.-J., Smith, S.L., Smith, C., Solidoro, C., St. John, M., Zhou, M., 2010. End-To-End Models for the Analysis of Marine Ecosystems: Challenges, Issues, and Next Steps. *Marine and Coastal Fisheries* 2, 115–130. <https://doi.org/10.1577/C09-059.1>
- Rubalcaba, J.G., Verberk, W.C.E.P., Hendriks, A.J., Saris, B., Woods, H.A., 2020. Oxygen limitation may affect the temperature and size dependence of metabolism in aquatic ectotherms. *Proceedings of the National Academy of Sciences* 117, 31963–31968. <https://doi.org/10.1073/pnas.2003292117>
- Ruegg, K., Turbek, S., 2022. Estimating global genetic diversity loss. *Science* 377, 1384–1385. <https://doi.org/10.1126/science.add0007>
- Rummel, C., 2014. Occurrence and potential effects of plastic ingestion by pelagic and demersal fish from the North Sea and Baltic Sea (diplom). EPIC3. Johannes Gutenberg-Universität Mainz.
- Rutterford, L.A., Simpson, S.D., Jennings, S., Johnson, M.P., Blanchard, J.L., Schön, P.-J., Sims, D.W., Tinker, J., Genner, M.J., 2015. Future fish distributions constrained by depth in warming seas. *Nature Clim Change* 5, 569–573. <https://doi.org/10.1038/nclimate2607>
- Sampaio, E., Santos, C., Rosa, I.C., Ferreira, V., Pörtner, H.-O., Duarte, C.M., Levin, L.A., Rosa, R., 2021. Impacts of hypoxic events surpass those of future ocean warming and acidification. *Nature Ecology & Evolution* 1–11. <https://doi.org/10.1038/s41559-020-01370-3>
- Sbragaglia, V., Jolles, J.W., Coll, M., Arlinghaus, R., 2021. Fisheries-induced changes of shoaling behaviour: mechanisms and potential consequences. *Trends in Ecology & Evolution* 36, 885–888. <https://doi.org/10.1016/j.tree.2021.06.015>
- Ser, J.R., Roberts, R.B., Kocher, T.D., 2010. Multiple Interacting Loci Control Sex Determination in Lake Malawi Cichlid Fish. *Evolution* 64, 486–501. <https://doi.org/10.1111/j.1558-5646.2009.00871.x>

- Serpetti, N., Baudron, A.R., Burrows, M.T., Payne, B.L., Helaouët, P., Fernandes, P.G., Heymans, J.J., 2017. Impact of ocean warming on sustainable fisheries management informs the Ecosystem Approach to Fisheries. *Sci Rep* 7, 13438. <https://doi.org/10.1038/s41598-017-13220-7>
- Sherman, K., Belkin, I.M., Friedland, K.D., O'Reilly, J., Hyde, K., 2009. Accelerated Warming and Emergent Trends in Fisheries Biomass Yields of the World's Large Marine Ecosystems. *AMBIO: A Journal of the Human Environment* 38, 215–224. <https://doi.org/10.1579/0044-7447-38.4.215>
- Shin, Y.-J., Cury, P., 2004. Using an individual-based model of fish assemblages to study the response of size spectra to changes in fishing. *Canadian Journal of Fisheries and Aquatic Sciences* 61, 414–431. <https://doi.org/10.1139/f03-154>
- Shin, Y.-J., Cury, P., 2001. Exploring fish community dynamics through size-dependent trophic interactions using a spatialized individual-based model. *Aquatic Living Resources* 14, 65–80. [https://doi.org/10.1016/S0990-7440\(01\)01106-8](https://doi.org/10.1016/S0990-7440(01)01106-8)
- Shin, Y.-J., Shannon, L., Cury, P., 2004. Simulations of fishing effect on the southern benguela fish community using an individual-based model : learning from a comparison with ecosim. *African Journal of Marine Science* 26, 95–114.
- Skogen, M.D., Eilola, K., Hansen, J.L.S., Meier, H.E.M., Molchanov, M.S., Ryabchenko, V.A., 2014. Eutrophication status of the North Sea, Skagerrak, Kattegat and the Baltic Sea in present and future climates: A model study. *Journal of Marine Systems* 132, 174–184. <https://doi.org/10.1016/j.jmarsys.2014.02.004>
- Sogard, S.M., 1997. Size-Selective Mortality in the Juvenile Stage of Teleost Fishes: A Review. *Bulletin of Marine Science* 60, 1129–1157.
- Soularue, J.P., Kremer, A., 2012. Assortative mating and gene flow generate clinal phenological variation in trees. *BMC Evolutionary Biology*, 12, 79.
- Stäbler, M., Kempf, A., Mackinson, S., Poos, J.J., Garcia, C., Temming, A., 2016. Combining efforts to make maximum sustainable yields and good environmental status match in a food-web model of the southern North Sea. *Ecological Modelling, Ecopath 30 years – Modelling ecosystem dynamics: beyond boundaries with EwE* 331, 17–30. <https://doi.org/10.1016/j.ecolmodel.2016.01.020>
- Stearns, S.C., 1992. *The Evolution of Life Histories*. OUP Oxford.
- Stearns, S.C., Koella, J.C., 1986. The Evolution of Phenotypic Plasticity in Life-History Traits: Predictions of Reaction Norms for Age and Size at Maturity. *Evolution* 40, 893–913. <https://doi.org/10.2307/2408752>
- Steenbeek, J., Buszowski, J., Chagaris, D., Christensen, V., Coll, M., Fulton, E.A., Katsanevakis, S., Lewis, K.A., Mazaris, A.D., Macias, D., de Mutsert, K., Oldford, G., Pennino, M.G., Piroddi, C., Romagnoni, G., Serpetti, N., Shin, Y.-J., Spence, M.A., Stelzenmüller, V., 2021. Making spatial-temporal marine ecosystem modelling better – A perspective. *Environmental Modelling & Software* 145, 105209. <https://doi.org/10.1016/j.envsoft.2021.105209>
- Stenberg, C., Støttrup, J.G., Deurs, M. van, Berg, C.W., Dinesen, G.E., Mosegaard, H., Grome, T.M., Leonhard, S.B., 2015. Long-term effects of an offshore wind farm in the North Sea on fish communities. *Marine Ecology Progress Series* 528, 257–265. <https://doi.org/10.3354/meps11261>

- Stokes, K., Law, R., 2000. Fishing as an evolutionary force. *Marine Ecology Progress Series* 208, 307–309.
- Talluto, M.V., Boulangeat, I., Ameztegui, A., Aubin, I., Berteaux, D., Butler, A., Doyon, F., Drever, C.R., Fortin, M.-J., Franceschini, T., Liénard, J., McKenney, D., Solarik, K.A., Strigul, N., Thuiller, W., Gravel, D., 2016. Cross-scale integration of knowledge for predicting species ranges: a metamodeling framework. *Global Ecology and Biogeography* 25, 238–249. <https://doi.org/10.1111/geb.12395>
- Taylor, A.D., 1990. Metapopulations, Dispersal, and Predator-Prey Dynamics: An Overview. *Ecology* 71, 429–433. <https://doi.org/10.2307/1940297>
- Teal, L.R., Hal, R. van, Kooten, T. van, Ruardij, P., Rijnsdorp, A.D., 2012. Bio-energetics underpins the spatial response of North Sea plaice (*Pleuronectes platessa* L.) and sole (*Solea solea* L.) to climate change. *Global Change Biology* 18, 3291–3305. <https://doi.org/10.1111/j.1365-2486.2012.02795.x>
- Thomas, Y., Flye-Sainte-Marie, J., Chabot, D., Aguirre-Velarde, A., Marques, G.M., Pecquerie, L., 2019. Effects of hypoxia on metabolic functions in marine organisms: Observed patterns and modelling assumptions within the context of Dynamic Energy Budget (DEB) theory. *Journal of Sea Research* 143, 231–242. <https://doi.org/10.1016/j.seares.2018.05.001>
- Thompson, P.L., Fronhofer, E.A., 2019. The conflict between adaptation and dispersal for maintaining biodiversity in changing environments. *Proceedings of the National Academy of Sciences* 116, 21061–21067. <https://doi.org/10.1073/pnas.1911796116>
- Timmerman, C.-A., Giraldo, C., Cresson, P., Ernande, B., Travers-Trolet, M., Rouquette, M., Denamiel, M., Lefebvre, S., 2021. Plasticity of trophic interactions in fish assemblages results in temporal stability of benthic-pelagic couplings. *Marine Environmental Research* 170, 105412. <https://doi.org/10.1016/j.marenvres.2021.105412>
- Timmerman, C.-A., Marchal, P., Denamiel, M., Couvreur, C., Cresson, P., 2020. Seasonal and ontogenetic variation of whiting diet in the Eastern English Channel and the Southern North Sea. *PLOS ONE* 15, e0239436. <https://doi.org/10.1371/journal.pone.0239436>
- Tittensor, D.P., Novaglio, C., Harrison, C.S., Heneghan, R.F., Barrier, N., Bianchi, D., Bopp, L., Bryndum-Buchholz, A., Britten, G.L., Büchner, M., 2021. Next-generation ensemble projections reveal higher climate risks for marine ecosystems. *Nature climate change* 11, 973–981.
- Tobin, D., Wright, P.J., 2011. Temperature effects on female maturation in a temperate marine fish. *Journal of Experimental Marine Biology and Ecology* 403, 9–13. <https://doi.org/10.1016/j.jembe.2011.03.018>
- Travers, M., Shin, Y.-J., Jennings, S., Cury, P., 2007. Towards end-to-end models for investigating the effects of climate and fishing in marine ecosystems. *Progress in Oceanography* 75, 751–770. <https://doi.org/10.1016/j.pocean.2007.08.001>
- Travers, M., Shin, Y.-J., Jennings, S., Machu, E., Huggett, J.A., Field, J.G., Cury, P.M., 2009. Two-way coupling versus one-way forcing of plankton and fish models to predict ecosystem changes in the Benguela. *Ecological Modelling, Selected Papers from the Sixth European Conference on Ecological Modelling - ECEM '07, on Challenges for ecological modelling in a changing world:*

- Global Changes, Sustainability and Ecosystem Based Management, November 27-30, 2007, Trieste, Italy 220, 3089–3099. <https://doi.org/10.1016/j.ecolmodel.2009.08.016>
- Travers-Trolet, M., Bourdaud, P., Genu, M., Velez, L., Vermard, Y., 2020. The Risky Decrease of Fishing Reference Points Under Climate Change. *Front. Mar. Sci.* 7. <https://doi.org/10.3389/fmars.2020.568232>
- Travers-Trolet, M., Coppin, F., Cresson, P., Cugier, P., Oliveros-Ramos, R., Verley, P., 2019. Emergence of negative trophic level-size relationships from a size-based, individual-based multispecies fish model. *Ecological Modelling* 410, 108800. <https://doi.org/10.1016/j.ecolmodel.2019.108800>
- Tromeur, E., Loeuille, N., 2022. Effects of adaptive harvesting on fishing down processes and resilience changes in predator-prey systems. <https://doi.org/10.1101/290460>
- Tscharntke, T., Clough, Y., Wanger, T.C., Jackson, L., Motzke, I., Perfecto, I., Vandermeer, J., Whitbread, A., 2012. Global food security, biodiversity conservation and the future of agricultural intensification. *Biological Conservation, ADVANCING ENVIRONMENTAL CONSERVATION: ESSAYS IN HONOR OF NAVJOT SODHI* 151, 53–59. <https://doi.org/10.1016/j.biocon.2012.01.068>
- Urban, M.C., Bocedi, G., Hendry, A.P., Mihoub, J.-B., Pe'er, G., Singer, A., Bridle, J.R., Crozier, L.G., De Meester, L., Godsoe, W., Gonzalez, A., Hellmann, J.J., Holt, R.D., Huth, A., Johst, K., Krug, C.B., Leadley, P.W., Palmer, S.C.F., Pantel, J.H., Schmitz, A., Zollner, P.A., Travis, J.M.J., 2016. Improving the forecast for biodiversity under climate change. *Science* 353, aad8466. <https://doi.org/10.1126/science.aad8466>
- Urban, M.C., De Meester, L., Vellend, M., Stoks, R., Vanoverbeke, J., 2012. A crucial step toward realism: responses to climate change from an evolving metacommunity perspective. *Evol Appl* 5, 154–167. <https://doi.org/10.1111/j.1752-4571.2011.00208.x>
- Uszko, W., Huss, M., Gårdmark, A., 2022. Smaller species but larger stages: Warming effects on inter- and intraspecific community size structure. *Ecology* 103. <https://doi.org/10.1002/ecy.3699>
- Uusi-Heikkilä, S., Wolter, C., Klefoth, T., Arlinghaus, R., 2008. A behavioral perspective on fishing-induced evolution. *Trends in Ecology & Evolution* 23, 419–421. <https://doi.org/10.1016/j.tree.2008.04.006>
- Van Alsenoy, V., Bernard, P., Van Grieken, R., 1993. Elemental concentrations and heavy metal pollution in sediments and suspended matter from the Belgian North Sea and the Scheldt estuary. *Science of The Total Environment* 133, 153–181. [https://doi.org/10.1016/0048-9697\(93\)90119-Q](https://doi.org/10.1016/0048-9697(93)90119-Q)
- van Dalfsen, J.A., Essink, K., Madsen, H.T., Birklund, J., Romero, J., Manzanera, M., 2000. Differential response of macrozoobenthos to marine sand extraction in the North Sea and the Western Mediterranean. *ICES Journal of Marine Science* 57, 1439–1445. <https://doi.org/10.1006/jmsc.2000.0919>
- van de Wolfshaar, K.E. van de, Daewel, U., Hjøllø, S.S., Troost, T.A., Kreuz, M., Pätsch, J., Ji, R., Maar, M., 2021. Sensitivity of the fish community to different prey fields and importance of spatial-seasonal patterns. *Marine Ecology Progress Series* 680, 79–95. <https://doi.org/10.3354/meps13885>

- van Rijn, I., Buba, Y., DeLong, J., Kiflawi, M., Belmaker, J., 2017. Large but uneven reduction in fish size across species in relation to changing sea temperatures. *Global Change Biology* 23, 3667–3674. <https://doi.org/10.1111/gcb.13688>
- Van Valen, L., 1973. A new evolutionary law. *Evol. Theory* 1, 1–30.
- van Walraven, L., Mollet, F.M., van Damme, C.J.G., Rijnsdorp, A.D., 2010. Fisheries-induced evolution in growth, maturation and reproductive investment of the sexually dimorphic North Sea plaice (*Pleuronectes platessa* L.). *Journal of Sea Research, Proceedings of the Seventh International Symposium on Flatfish Ecology, Part I* 64, 85–93. <https://doi.org/10.1016/j.seares.2009.07.003>
- van Wijk, S.J., Taylor, M.I., Creer, S., Dreyer, C., Rodrigues, F.M., Ramnarine, I.W., van Oosterhout, C., Carvalho, G.R., 2013. Experimental harvesting of fish populations drives genetically based shifts in body size and maturation. *Frontiers in Ecology and the Environment* 11, 181–187. <https://doi.org/10.1890/120229>
- Vaquer-Sunyer, R., Duarte, C.M., 2008. Thresholds of hypoxia for marine biodiversity. *Proceedings of the National Academy of Sciences* 105, 15452–15457. <https://doi.org/10.1073/pnas.0803833105>
- Verhulst, P.F., 1838. Notice sur la loi que la population suit dans son accroissement. *Corresp. Mathématique Phys.*, 10, 113–121.
- Verspoor, E., Moyes, C.D., 2005. Evidence for co-dominant allelic expression of a phosphoglucosyltransferase regulatory locus polymorphism in the Atlantic salmon. *Journal of Fish Biology* 67, 213–218. <https://doi.org/10.1111/j.0022-1112.2005.00850.x>
- Villéger, S., Miranda, J.R., Hernández, D.F., Mouillot, D., 2010. Contrasting changes in taxonomic vs. functional diversity of tropical fish communities after habitat degradation. *Ecological Applications* 20, 1512–1522. <https://doi.org/10.1890/09-1310.1>
- Volkoff, H., Rønnestad, I., 2020. Effects of temperature on feeding and digestive processes in fish. *Temperature* 7, 307–320. <https://doi.org/10.1080/23328940.2020.1765950>
- Wakelin, S.L., Artioli, Y., Holt, J.T., Butenschön, M., Blackford, J., 2020. Controls on near-bed oxygen concentration on the Northwest European Continental Shelf under a potential future climate scenario. *Progress in Oceanography* 187, 102400. <https://doi.org/10.1016/j.pocean.2020.102400>
- Walters, C., Christensen, V., Pauly, D., 1997. Structuring dynamic models of exploited ecosystems from trophic mass-balance assessments. *Reviews in Fish Biology and Fisheries* 7, 139–172. <https://doi.org/10.1023/A:1018479526149>
- Waples, R.S., Audzijonyte, A., 2016. Fishery-induced evolution provides insights into adaptive responses of marine species to climate change. *Frontiers in Ecology and the Environment* 14, 217–224. <https://doi.org/10.1002/fee.1264>
- Watson, J.D., Crick, F.H.C., 1953. Molecular Structure of Nucleic Acids: A Structure for Deoxyribose Nucleic Acid. *Nature* 171, 737–738. <https://doi.org/10.1038/171737a0>
- West, G.H., Brown, J.H., Enquist, B.J., 2001. A general model for ontogenetic growth. *Nature*.

- Willi, Y., Van Buskirk, J., Hoffmann, A.A., 2006. Limits to the Adaptive Potential of Small Populations. *Annual Review of Ecology, Evolution, and Systematics* 37, 433–458.
<https://doi.org/10.1146/annurev.ecolsys.37.091305.110145>
- Wilson, R.S., Lefrançois, C., Domenici, P., Johnston, I.A., 2010. Environmental influences on unsteady swimming behaviour: consequences for predator-prey and mating encounters in teleosts. CRC Press. <https://doi.org/10.1201/b10190>
- Wright, P.J., Gibb, F.M., Gibb, I.M., Millar, C.P., 2011a. Reproductive investment in the North Sea haddock: temporal and spatial variation. *Marine Ecology Progress Series* 432, 149–160.
<https://doi.org/10.3354/meps09168>
- Wright, P.J., Millar, C.P., Gibb, F.M., 2011b. Intra-stock differences in maturation schedules of Atlantic cod, *Gadus morhua*. *ICES Journal of Marine Science* 68, 1918–1927.
<https://doi.org/10.1093/icesjms/fsr111>
- Wright, S., 1938. Size of population and breeding structure in relation to evolution. *Science* 87, 430–431.
- Xu, W., Liu, Yongxue, Wu, W., Dong, Y., Lu, W., Liu, Yongchao, Zhao, B., Li, H., Yang, R., 2020. Proliferation of offshore wind farms in the North Sea and surrounding waters revealed by satellite image time series. *Renewable and Sustainable Energy Reviews* 133, 110167.
<https://doi.org/10.1016/j.rser.2020.110167>
- Yacine, Y., Allhoff, K.T., Weinbach, A., Loeuille, N., 2021. Collapse and rescue of evolutionary food webs under global warming. *Journal of Animal Ecology* 90, 710–722.
<https://doi.org/10.1111/1365-2656.13405>
- Yoneda, M., Wright, P.J., 2004. Temporal and spatial variation in reproductive investment of Atlantic cod *Gadus morhua* in the northern North Sea and Scottish west coast. *Mar. Ecol. Prog. Ser.* 276:237-248.
- Young, K.A., Cluney, V.A., Weir, L.K., 2020. Fisheries-induced evolution of alternative male life history tactics in Coho salmon. *Evolutionary Applications* n/a. <https://doi.org/10.1111/eva.12970>

Annexes

8.1 Annexes du chapitre 2

8.1.1 Supporting Information S1: Process overview

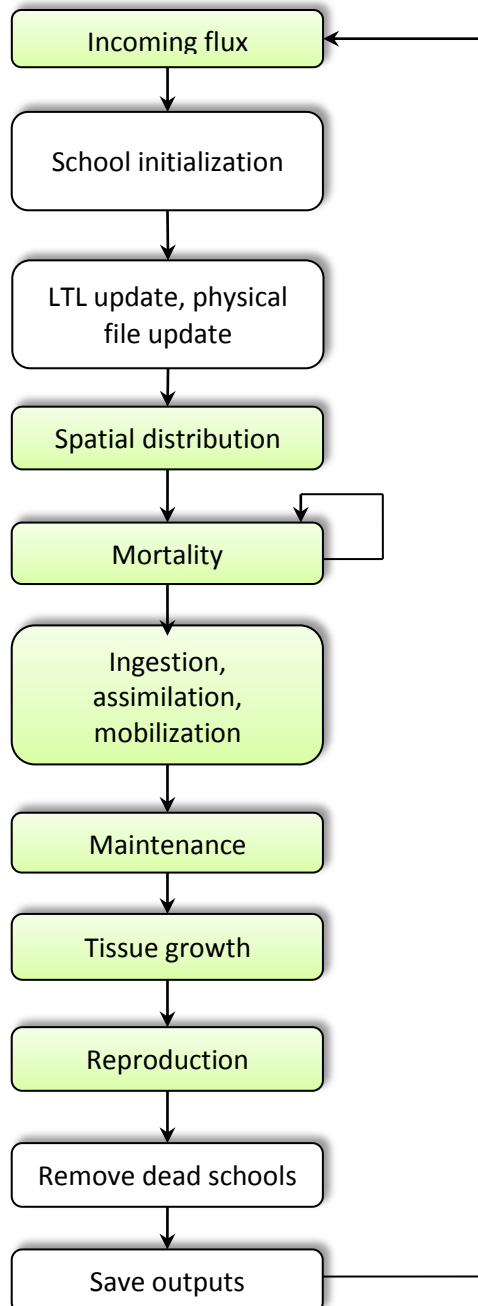


Figure S1: Process execution order during a Bioen-OSMOSE time step, green processes are the biological process; white processes are the IT processes. (LTL: low trophic level)

Within each time step t , the following processes take place in the order described in Fig. S1. Mortality is divided into sub-time steps to take into account the simultaneity of mortality processes (see details of mortality sub-time steps within each time step at <http://documentation.osmose-model.org/>).

1. Income flux of biomass

Some species might realize only part of their life cycle in the model area (e.g., ontogenetic migration in the area) or might immigrate into the model area (e.g., invasive species, climate-induced range extension), which is described by an influx of schools over time.

2. School initialization

All schools are initialized for the new time step, i.e., state or emerging individual variables are reset to their initial value (e.g., number of dead individuals, ingested food) or updated (e.g., age $a(i, t)$) as required.

3. Environment and resource update

The value of physico-chemical factors $pc_k(c, t, z)$ and the biomass of low trophic level (LTL) organisms $B_{LTL}(c, j, t)$ are updated for each cell c of the spatial grid, using data from forcing files.

4. Spatial distribution

The model is forced with maps of species distribution (either presence/absence or densities, resulting directly from survey data or from climate niche models). Ontogenic and/or seasonal migration can be parameterized, by specifying as input of the model distinct distribution maps depending on stage, age and/or season. At each time step, schools move to an adjacent grid cell

according to a random walk within their distribution map. For species that do not spend their entire lifecycle in the simulated area (due to, e.g., seasonal reproduction migration or ontogenic habitat shift), schools can emigrate from or immigrate to the model area during specified time steps, generating an outgoing or incoming flux of biomass.

5. Mortality

Schools experience mortality (modeled as a decrease of school abundance) related to predation, starvation, foraging, fishing and background causes (non-explicit additional predation, senescence and diseases) whose value differs between larvae stage (larval mortality) and older stages (additional mortality). Starvation mortality is directly linked to the maintenance process (see below) and relies thus on the amount of net energy at the previous time step (t-1).

6. Ingestion, assimilation and mobilization

Food ingestion based on the predation process on other schools and/or LTL groups, assimilation and mobilization for metabolic processes take place for each school. The school order is randomly selected.

7. Maintenance

Part of schools' mobilized energy is used for the maintenance of existing tissues and basal activities such as foraging. If maintenance needs cannot be covered, the gonadic compartment is used as an energy reserve to cover them and no further metabolic process takes place. If the gonadic compartment cannot cover the maintenance costs, schools are in a state of "energetic" starvation which results in starvation mortality applied at the next time step.

8. New tissue production: somatic and gonadic growth

When maintenance costs are covered from mobilized energy, the remaining net energy of a school is used for new tissue production. Sexually immature individuals allocate all energy to somatic growth whereas mature ones share energy between somatic and gonadic growth.

9. Reproduction

During time steps corresponding to the species' breeding period, sexually mature schools reproduce panmictically. Eggs are produced from adult gonad mass and are released in new schools distributed randomly across the larval area at the beginning of the next time step.

Schools go through these processes depending on their life-history stage. During the egg stage and the endogenous-feeding larval stage (typically the first time step of a school life), no food ingestion occurs so processes 6 to 9 do not apply and mortality of process 5 is restricted to predation and background causes. After transition to exogenous feeding, no energy is allocated to reproduction during the larval, post-larval and juvenile stages; therefore, only processes 1 to 8 are prosecuted. Schools at the adult stage go through all processes.

Processes 1 to 3 are strictly similar to those in the existing OSMOSE model and the reader is referred to its description (<http://documentation.osmose-model.org/>) for more details. Process 5 includes a new mortality term linked to foraging —and processes 6 to 10 are new and described in the main text of this article.

8.1.2 Supporting Information S2: Parametrization of the new sub-model

1 - Estimation of the bioenergetic sub-model parameters from Size Maturity Age Length Key

(SMALK) data

The bioenergetic sub-model implemented in Bioen-OSMOSE requires ten parameters per species in input (without the oxygen and temperature parameter responses) plus three two intermediate parameters: there are two parameters for the length-somatic mass allometric relationship, nine parameters for the processes of growth and reproduction, and two parameters for the linear maturation reaction norm. Intermediate parameters are parameter that are not input parameters of Bioen-OSMOSE but that are used to estimated directly (see Supporting Information S2) or indirectly through calibration process (see Section 2.2.2.3 in main text) input parameters of Bioen-OSMOSE. Most of these parameters can be estimated from a common set of individual-level data classically referred to as Sex Maturity Age Length Key (SMALK) data. Sex data are used to test for sexual dimorphism in the species. If sexual dimorphism is present, only female data are retained for all parameter estimates.

To estimate the parameters k and α of the allometric relationship between length and somatic mass, a nonlinear regression was fitted to the length-mass data.

The estimation of growth and reproduction parameters uses the reformulation by Boukal et al. (2014) of the general biphasic growth model proposed by Quince et al. (2008) and formerly derived by Lester et al. (2004) for the specific case of a constant gonado-somatic index.

This model predicts individuals' size as a function of their age and maturity status based on the average age at maturation a_{mat} in the population and their initial size w_1 estimated from the SMALK data.

Under the assumption of a constant net energy mass-specific per year during the individual lifespan and across the population spatial distribution, our model is equivalent to the model of Boukal et al. (2014). We note the annual mean mass-specific net energy acquisition rate \bar{e}_p : this parameter is equivalent to c of the Boukal model. The individual's lifetime growth trajectory is described according to the following set of equations:

$$w(a) = \begin{cases} \left(w_{a_0}^{1-\beta} + (1-\beta)\bar{e}_p (a - a_0) \right)^{\frac{1}{1-\beta}} & \text{if } m(a) = 0 \\ \left(\frac{\eta\bar{e}_p}{r} - \left(\frac{\eta\bar{e}_p}{r} - (w_{a_0}^{1-\beta} + (1-\beta)\bar{e}_p(a_m - a_0)) \right) \left(\frac{1}{1+(1-\beta)\frac{r}{\eta}} \right)^{a-a_m} \right)^{\frac{1}{1-\beta}} & \text{if } m(a) = 1 \end{cases} \quad (S1)$$

where a is individual's age, a_0 the age for which initial mass is observed and all other parameters are as in the main text.

In our case, the initial mass observed is for age 1 for all the species. The mean age at maturity a_{mat} was determined from the age maturity ogive estimated by fitting a logistic regression to age and maturity data. For all species, the scaling exponent of maximum ingestion rate and maintenance rate with body mass β was set to 0.75 following the classical power law for metabolic rates (West et al., 1997) and the ratio η of gonad energy density to soma energy density was assumed to be 1 by default: the gonado-somatic index (GSI) r was then the energetic GSI. Alternative values of β and q can be used for other applications whenever necessary data to estimate them are available. To estimate r and the annual mass-specific net energy acquisition rate \bar{e}_p , the biphasic growth model was fitted on mass-at-age or length-at-age data (thanks to the allometric length-somatic mass relationship), using a nonlinear regression. The same statistical weight was attributed to all age classes by weighting each data point of a given age class by the inverse of its abundance. To estimate the multiplicative factor of maximum mass-specific net energy acquisition rate for the larval stage θ' , the model was fitted between age 0 and 1 using the mass at age 0 (w_{egg}) and the mass at age 1 w_1 as data points (see section 2 in Supporting information S2 for w_{egg} estimation). θ' is an intermediate

parameter to estimate θ the multiplicative factor of the maximum ingestion rate per mass unit for the first year of life (see Eq. 3, main text). θ is calculated as follow:

$$\theta = \frac{I_{max} + (\theta' - 1)\bar{e}_p}{I_{max}} \quad (S2)$$

with I_{max} the maximum ingestion rate mass-specific.

The parameterization of the maturation process is based on the probabilistic maturation reaction norm (PMRN), estimated from size, age and maturity data following the method described in Barot et al. (2004) and summarized hereafter. The first step is to estimate an age and size maturity ogive, i.e., the proportion of mature individuals as a function of age and size, with or without interactions, through logistic regression on age, size and maturity data. The second step is to estimate the length increment at each age using size and age data. The third step is to build the PMRN by estimating the probability of becoming mature for each possible age-length combination using the two previous ingredients (see Barot et al. (2004) for further details).

To obtain a linear deterministic maturation reaction norm (LMRN) from the PMRN, a logistic regression is fitted to the estimates of the probabilities of becoming mature as a linear function of age and length. The resulting age-length iso-probability line for which there is a 50% probability of maturing is then taken as the estimate of the LMRN and its intercept and slope are used as estimates of m_0 and m_1 , respectively. The LMRN is considered deterministic in the sense that when an individual reaches an age-length combination located on the reaction norm, it becomes mature with probability 1 (Eq. 13 in Main Text).

2 - Estimating the egg mass

There is not much reliable data on the wet mass of the eggs of marine fish species in the literature. In contrast, relative fecundity, i.e., the number of eggs laid per gram of mature female φ_S is a much more common data. With r , the GSI estimated from the SMALK data (see Supporting Information

S2.1), we estimate the mass of an egg needed to obtain a relative fecundity that emerges from the model similar to that observed:

$$w_{egg} = \frac{r}{\varphi_S} \quad (S3)$$

The number of eggs laid per gram of mature female φ_S values for the North Sea species are in Supporting Information S4, Table S4 and the reference are in Supporting Information S6 in the column fecundity.

3 - Physiological thermal response curves parameters estimation

The thermal response curves in Bioen-OSMOSE are detailed in the eq. 6, 7, 8 and 9 in the main text. The mobilization and maintenance response parameter estimation uses the properties of the resulting net energy available for new tissues E_P (Eq. 9 in the main text). E_P has the classic bell-shaped response to temperature consistent with the OCLTT theory. Under the assumption of maximum oxygen saturation and combining Eq. 4, 7, and 9 in the main text, mass-specific net energy available for new tissue production $E_P(i, t)/w(i, t)^\beta = e_P(i, t)$ can be written

$$e_P(i, t) = \xi \iota(i, t) \varphi_M(T(i, t)) - c_m \varphi_m(T(i, t)). \quad (S4)$$

with $\iota(i, t)$ denoting mass-specific ingestion rate $I(i, t)/w(i, t)^\beta$. Averaging over an individual's lifetime and under the assumption of a constant inter annual ingestion, we obtain the average mass-specific net energy over an individual's lifespan \bar{e}_p as:

$$\bar{e}_p = \frac{1}{\tau} \int_0^\tau e_P(i, t) dt = \frac{\xi}{\tau} \bar{\iota} \int_0^\tau \varphi_M(T(i, t)) dt - \frac{c_m}{\tau} \int_0^\tau \varphi_m(T(i, t)) dt. \quad (S5)$$

with τ the individual's lifespan in years and $\bar{\iota}$ the annual mass-specific ingestion rate.

Under the additional assumption of a constant temperature T throughout an individual's lifetime, the equation simplifies to

$$\bar{e}_p(T) = \xi \bar{l} \varphi_M(T) - c_m \varphi_m(T) \quad (S6)$$

with $\bar{l} = \frac{1}{\tau} \int_0^\tau l(i, t) dt$ the lifetime-mean annual mass-specific ingestion rate. In these conditions, i.e. maximum oxygen saturation and constant temperature over an individual's lifetime, our bioenergetic model is strictly equivalent to the biphasic growth model of Boukal et al. (2014).

There are five unknown parameters for the thermal response of mobilization and maintenance, namely ε_M , ε_D , and T_p for $\varphi_M(\cdot)$ and ε_m and c_m for $\varphi_m(\cdot)$ (see Table S1). These can be (owing to the various assumptions underlying Eq. S6) estimated together with the mean annual mass-specific ingestion rate \bar{l} as a by-product from the numerical resolution of a system of six nonlinear equations resulting from six particular data points. Four data points correspond to remarkable points of the function $\bar{e}_p(T)$. The first and second point, are related to the physiological minimum (T_{min}), and maximum (T_{max}) temperatures that are respectively defined as the lower and upper temperature thresholds at which \bar{e}_p becomes null, $\bar{e}_p(T_{min}) = \bar{e}_p(T_{max}) = 0$. The third point relates to the optimum temperature (T_{opt}) that corresponds to the temperature at which \bar{e}_p is maximum and thus its derivative according to temperature is null, $\frac{\partial \bar{e}_p(T)}{\partial T} |_{T=T_{opt}} = 0$. The fourth data point is estimated from observations: at the mean temperature in the distribution area over the year, T_a , the population of the area acquires energy at the rate per unit of body mass (see S2.1 for estimation procedure for \bar{e}_p). T_{min} , T_{opt} , T_{max} and T_a are species dependent. The mobilization is a physiological temperature-dependent flux: hypothetically, the value of the flux reaches 0 at a temperature of absolute zero. This fifth data point is species independent. The sixth data point is the value of the maintenance rate c_{SMR} at T_{ref} from the literature. The six data points are used to estimate six parameters with the numerical resolution of a mathematical nonlinear system.

$$\left\{ \begin{array}{l} \overline{E}_p(T_{min}) = 0 \\ \overline{E}_p(T_{max}) = 0 \\ \overline{E}_p'(T_{opt}) = 0 \\ \overline{E}_p(T_a) = c \\ \varphi_M(0) = 0 \\ C_m = c_{SMR} \cdot e^{\frac{\varepsilon_m}{k_B} \left(\frac{1}{T_{ref}} \right)} \end{array} \right. \quad (S7)$$

Table S1: Description of the parameters of the physiological thermal response curves and the data required to estimate them.

	Parameter	Description	Source
Mobilization response	T_p	The temperature at which the mobilization reaches its maximum	Estimated
	ε_M	The activation energy for the Arrhenius-like increase with temperature before T_p	Estimated
	ε_D	The activation energy for the energy mobilization decline with temperature after T_p	Estimated
	k_B	The Boltzmann constant	1.38064852
	\underline{l}	Mean annual mass-specific ingestion rate	Estimated
Maintenance response	C_m	The absolute mass-specific maintenance rate	Estimated
	ε_m	The activation energy for maintenance rate increase with temperature	Estimated
	c_{smr}	The mass-specific maintenance rate at the temperature T_{ref}	Literature
	T_{ref}	The temperature at which c_{smr} is measured	Literature
Net energy response	T_{min}	Temperature at which the net energy reaches 0 for a temperature under T_{opt}	Literature, experimental or from climatic niche
	T_{opt}	Temperature at which E_p is maximum	
	T_{max}	Temperature at which the net energy reaches 0 for a temperature above T_{opt}	

	T_a	Mean temperature in the distribution area over the year	Calculated from forcing files
	\bar{e}_p	Mass-specific net energy acquisition rate. Given the T_a definition, is the value at T_a .	Estimated (Supporting Information S2.1)

A nonlinear equation solver available in R within the package “nleqslv” was used to solve the system (4). To parameterize temperature preference, the use of physiological preference data is advised. In NS-Bioen-OSMOSE, T_{min} and T_{max} are parameterized with Dahlke et al. (2020) database. In parallel, an estimation of T_{min} and T_{max} is done from thermal niches derived from specific global distribution occurrences from databases: the Ocean Biogeographic Information System (<http://www.iobis.org/>), the Global Biodiversity Information Facility (<https://www.gbif.org/>), the Vertebrate biodiversity Networks, <http://vertnet.org/>, and the UC Berkeley's Natural History Data, (<https://bnhm.berkeley.edu/informatics/ecoengine/>). The spatial distribution model method used to obtain the thermal niches is from Ben Rais Lasram et al., (2020). A linear relationship is fitted between the physiological T_{min} and T_{max} and the thermal niches-derived T_{min} and T_{max} respectively, for the species with available data. This linear relationship is used to estimate the physiological T_{min} and T_{max} for the species without data (shrimp, grey gurnard, whiting, mackerel, norway pout and dab) in the database from Dahlke et al. (2020). T_{opt} is estimated from thermal niches estimated with global distribution occurrences and temperature at the occurrences, similarly to T_{min} and T_{max} .

4 - Parameter estimation of the mobilization response curve to oxygen

To estimate the parameters $c_{O,1}$ and $c_{O,2}$ of the mobilization response to oxygen, a nonlinear least square regression (nls function in R) of the response function (Eq. 5 in the main text) was fitted on the respiration rate relative to oxygen concentration or saturation. The data were extracted from the

literature (Supporting Information S6). The parameters for species without data were filled by the parameter of the closest species in the phylogenetic tree.

5 - Parameterization of the reproduction seasonality

In Bioen-OSMOSE, the spawning seasonality is represented by a set of parameters $sp(t)$ indicating the proportion of the current energy available in the gonad used to produce and release eggs at the time step t .

The proportion of the gonad energy used at a time step t , $sp(t)$, is calculated from the proportion of eggs $p_{e;t}$ released at time step t compared to the annual total released eggs. The seasonality of eggs' release can be found in the literature and was classically used in previous versions of OSMOSE. The proportion of gonad energy used to release eggs $sp(t)$ at the time step t is linked with $p_{e;t}$ and with the cumulative proportion of the eggs already released within this reproductive season (released at the time steps anterior to the time step t in the reproductive season):

$$sp(t) = \begin{cases} n_r \cdot p_{e;t} & \text{if } t = 1 \\ \frac{n_r \cdot p_{e;t}}{\prod_{j=1}^{t-1} 1 - p_{g;j}} & \text{if } t > 1 \end{cases} \quad (S8)$$

with j the number of time steps in the reproductive season before the time step t and n_r the number of reproductive seasons in the year.

8.1.3 Supporting Information S3: Mortality process description

At each time step, a school experiences several mortality sources. The total mortality of a school i is the sum of predation mortality caused by other schools, foraging mortality, starvation mortality, fishing mortality, larval mortality and additional mortalities (i.e. senescence, diseases, and non-explicitly modeled predators). Within each time step t , the different mortality sources impact a school i in a random order (across both sources of mortality and schools) and are implemented through iterations over sub-time steps (here 10 sub-time steps occur within a time step) so as to simulate the simultaneous nature of these processes (see <http://documentation.osmose-model.org/> for more details).

The mortality induced by predation emerges from the ingestion process previously described (see section 2.2.1.2.1 *Ingestion, assimilation and mobilization* in main text) and thus is an explicit stochastic size-dependent process depending on the spatial co-occurrence between predators and prey. The predation-induced loss of biomass experienced by school i is simply the sum of biomass losses due to the ingestion of all predator schools j present in the same grid cell $c(i, t)$ at time step t and with adequate minimum R_{min} and maximum R_{max} predator to prey size ratios,

$$\frac{dB(i,t)}{dt} = \sum_j \frac{\gamma(j,i)B(i,t)}{P(j,t)} I(j, t)$$

$$\text{with } j \in \left\{ j \mid (c(i, t) = c(j, t)) \cap \left(\frac{L(j,t)}{R_{max}} \leq L(i, t) \leq \frac{L(j,t)}{R_{min}} \right) \right\}, \quad (S9)$$

where $B(i, t)$ is the biomass of school i , $P(j, t)$ is the prey biomass for school j , R_{min} and R_{max} the minimum and maximum predator to prey size ratio based on individual total length, $c(i, t)$ the cell of the school i and $\gamma(j, i)$ is the accessibility coefficient of potential prey school i to school j (see Eq. 1 and Table 2 in the main text). Then, the ratio $\frac{\gamma(j,i)B(i,t)}{P(j,t)}$ is a proportion of school i in the predator j 's ingestion $I(j, t)$. Change in the number of individuals of school i due to predation during a sub-time step dt is then given by:

$$N(i, t + dt) = N(i, t) \left(1 - \frac{\sum_j \frac{\gamma(j,i)B(i,t)}{P(j,t)} I(j,t)}{w(i,t)}\right)$$

$$\text{with } j \in \left\{j \mid (c(i, t) = c(j, t)) \cap \left(\frac{L(j,t)}{R_{max}} \leq L(i, t) \leq \frac{L(j,t)}{R_{min}}\right)\right\}. \quad (S10)$$

Starvation occurs when an individual cannot cover its maintenance needs, i.e., when net energy is negative $E_p(i, t) < 0$, even by drawing energy from its gonadic reserves, i.e., when $\eta E_p(i, t) < -g(i, t)$ (see sub-section 2.2.1.2.4 “New tissue production: somatic and gonadic growth” for details in main text). In this case, schools undergo a decrease in biomass equaling the energetic deficit that remains after accounting for the energy reserves contained in the gonadic compartment:

$$B(i, t + \Delta t) = B(i, t) - N(i, t)(|E_p(i, t)| - g(i, t)/\eta) \text{ if } \eta E_p(i, t) < -g(i, t), \quad (S11)$$

The energetic debt of time step $t+\Delta t$ is equally shared between the sub time step dt , so that change in the number of individuals of school i during the sub-time step dt due to energetic starvation during time step dt is given by:

$$N(i, t + dt) = \frac{N(i, t).dt}{\Delta t} \left(1 - \frac{|E_p(i, t)| - g(i, t)/\eta}{w(i, t)}\right) \text{ if } \eta E_p(i, t) < -g(i, t). \quad (S12)$$

As the mortality process is implemented before ingestion (see Supporting Information 1), starvation mortality at time step t relies on the net energy amount obtained at the previous time step. During the first time step of a school, i.e., at the egg life stage, the school does not feed to model the yolk reserve. Therefore, starvation does not occur at the first time step nor at the second time step as starvation relies on the energy acquired at the previous time step.

Schools experience size-selective fishing that generates an instantaneous fishing mortality rate $F(i, t)$ for a school i at time step t defined as follows:

$$F(i, t) = F_{max} q(L(i, t)) \quad (S13)$$

with $q(L(i, t))$ the size-selectivity of the fishery that varies between 0 and 1 with individual length, and F_{max} is the maximum instantaneous fishing mortality rate. Change in the number of individuals in school i due to fishing during time sub time step dt is then obtained as follows:

$$N(i, t + dt) = N(i, t) e^{-F(i, t) dt} \quad (S14)$$

Finally, in order to account for the additional mortality sources that are not represented by the previous mortality terms (e.g. senescence, diseases, or non-explicitly modeled predators), an instantaneous life-stage specific additional mortality rate $M(i, t)$ is defined as follows:

$$M(i, t) = \begin{cases} \mu_l' & \text{if } a(i, t) < a_l' \\ \mu & \text{otherwise} \end{cases} \quad (S15)$$

with μ_l' the instantaneous larval additional mortality rate and μ its counterpart after a_l' , the first feeding age, and for the rest of the life cycle. Change in the number of individuals in school i due to additional mortality during sub-time step dt is given by:

$$N(i, t + dt) = N(i, t) e^{-M(i, t) dt} \quad (S16)$$

Table S2: Description of the parameters of the mortality sub-model

Symbol	Description	Units	Equations	Source
Δt	Time step	y		-
dt	Sub-time step			
F_{max}	Maximum instantaneous fishing mortality rate	y ⁻¹	S13	Calibrated
a_l'	First feeding age	y	S15	Literature
μ_l'	Instantaneous larval additional mortality rate	y ⁻¹	S15	Calibrated
μ	Instantaneous additional mortality rate for individuals older than first-feeding age	y ⁻¹	S15	Calibrated

8.1.4 Supporting Information S4: Input parameters and intermediate parameters of Bioen-OSMOSE-NS for the 16 species modeled explicitly.

1 – Species specific input parameters

Table S3: Input parameters parameters of Bioen-OSMOSE-NS for the 16 species modeled explicitly. $\alpha, k, r, m_0, m_1, w_{egg}$ and θ are estimated (see Supporting Information S2.1). a_{max} drawn from the literature (see Supporting Information S6). When R_{min} and R_{max} shift with ontogeny, the size threshold of the shift is provided in the predation threshold column. R_{min}, R_{max} and their threshold are from literature. Mobilization and maintenance parameters are estimated (see Supporting Information S2.3). I_{max} and mortality parameters are calibrated (see 2.2.2.3 in main text for details about the calibration process). Some parameters are assumed equal for all the species: η is set to 1, ξ is set to 0.8, a_l is set to 1, and β is set to 0.75. The references of parameters from literature are in Supporting information S6.

Species	GROWTH, REPRODUCTION AND CONDITION										PREDATION		
	α	k	r	I_{max}	m_1	m_0	w_{egg}	a_{max}	θ	$n_{S(i)}$	R_{min}	R_{max}	Threshold
	-	$g.cm^{-\alpha}$	-	$g.g^{-\theta}\Delta t^{-1}$	$cm.y^{-1}$	cm	g	$year$	-	-	-	-	cm
Herring (<i>Clupea harengus</i>)	3.41	0.002	0.77	14	-0.9	25.36	6.67e-04	17	1.56	25	250	5	-
Mackerel (<i>Scomber scombrus</i>)	3.06	0.007	0.75	16.4	0.78	25.76	5.86e-04	17	1.66	38	150	2.5	-
Sandeel (<i>Ammodytes spp</i>)	3.44	0.001	1.2	9.5	0	15	9.97e-04	10	1.66	38	1000	8	-
Sprat (<i>Sprattus sprattus</i>)	3.15	0.005	0.56	12.1	0	12.96	2.80e-04	10	1.56	38	1000	8	-
Norway pout (<i>Trisopterus esmarkii</i>)	3.1	0.006	0.5	9.9	-3.54	19.22	1.57e-04	7	1.92	30	500	1.5	-
Plaice (<i>Pleuronectes platessa</i>)	3.02	0.009	0.52	10.9	-4.99	43.51	2.04e-03	25	1.85	50	100/50	5	8
Sole (<i>Solea solea</i>)	3.26	0.004	0.6	9.9	0.69	19.17	5.81e-04	17	1.6	50	100/50	10	8
Saithe (<i>Pollachius virens</i>)	3.24	0.003	0.21	14.5	-1.75	74.1	3.30e-04	21	1.82	30	50/15	2	20
Cod (<i>Gadus morhua</i>)	3.21	0.005	0.54	21.6	-2.74	75.26	4.55e-04	17	1.38	25	50/15	2/1.3	12
Haddock (<i>Melanogrammus aeglefinus</i>)	3.24	0.004	0.59	15.8	-1.62	32.85	1.36e-03	18	1.56	38	50/15	1.7	12

Annexes

Horse Mackerel (<i>Trachurus trachurus</i>)	2.7	0.027	0.55	13.4	0	18.5	7.35e-04	15	1.51	38	150	2.5	-
Whiting (<i>Merlangius merlangus</i>)	3.26	0.003	0.73	17.8	-0.33	21.72	4.29e-04	16	1.39	38	100/20/10	1.5/1.1	10/40
Dab (<i>Limanda limanda</i>)	3.21	0.006	0.5	8.8	-2.47	19.03	1.72e-04	10	1.68	50	100/50	5	30
Grey gurnard (<i>Eutrigla gurnardus</i>)	3.15	0.005	0.87	13.6	-6.81	28.89	9.92e-04	15	1.48	30	100/30	2	12
Hake (<i>Merluccius merluccius</i>)	3.16	0.004	0.29	17.3	1.47	34.15	6.72e-04	15	1.84	20	50/15	2/1.1	12
Shrimp	2.81	0.01	1.65	8.9	0	5.37	2.03e-03	3	1.07	25	1000	8	-

MAINTENANCE		MOBILIZATION					MORTALITY		
TEMPERATURE		TEMPERATURE			OXYGEN		FISHING	LARVAL	ADDITIONAL
ε_m	c_m	ε_M	$\varepsilon_D - \varepsilon_M$	T_p	$c_{O,1}$	$c_{O,2}$	F_{max}	μ_L	μ
eV	$g \cdot \Delta t^{-1}$	eV	eV	$^{\circ}C$	-	%	y^{-1}	y^{-1}	y^{-1}
0.6	1.49E+11	1.93	1.01E-04	43.1	1	8.1	0.8	6.1	0.17
0.33	5.03E+06	1.67	1.02E-04	46.85	1	8.1	2.86	4.65	0.3
0.47	5.40E+08	1.96	1.01E-04	43.29	1	7.3	1.79	2.26	0.19
0.27	2.57E+05	1.15	1.06E-04	68.31	1	8.1	0.33	0.94	0.12
0.17	5.82E+03	3.21	9.43E-05	23.8	1.48	54.6	0.58	3.76	0.31
0.38	1.54E+07	1.8	1.02E-04	46.59	2	99	0.13	5.22	0.07
0.42	5.28E+07	2.54	9.87E-05	35.12	2.6	179.4	0.26	7.01	0.34
0.26	2.74E+05	2.64	9.59E-05	27.87	1.48	54.6	0.53	2.73	0.6
0.48	2.07E+09	2.27	9.84E-05	34.77	1.48	54.6	0.31	9.34	0.58
0.31	1.96E+06	2.43	9.69E-05	30.67	1.48	54.6	0.08	2.82	0.8
0.25	1.04E+05	2.28	9.89E-05	39.39	1	8.1	0.1	1.2	0.27
0.3	1.36E+06	1.93	1.01E-04	41.91	1.48	54.6	0.61	8.56	0.16
0.46	2.86E+08	2.55	9.86E-05	34.92	2.3095	139.189	0.18	4.63	0.25
0.31	1.47E+06	1.98	1.00E-04	41.49	1.48	54.6	0.36	5.15	0.07
0.25	1.74E+05	2.92	9.60E-05	30.06	1.48	54.6	0.42	7.72	0.32
0.4	3.10E+07	2.25	9.97E-05	38.54	1.475	47	0.02	0.06	0.21

2 – Species specific intermediate parameters

Table S4: Species specific intermediate parameters. Intermediate parameters are parameter that are not input parameters of Bioen-OSMOSE-NS but that are used to estimated directly (see Supporting Information S2) or indirectly through calibration process (see Section 2.2.2.3 in main text) input parameters of Bioen-OSMOSE-NS.

	Fecundity	Larval growth	Maintenance		Temperature preference		
	φ_s $g.(g\ female)^{-1}.y^{-1}$	θ'	T_{ref} °C	c_{smr} $g.g^{-\alpha}.y^{-1}$	T_{min} °C	T_{opt} °C	T_{max} °C
Species		-					
Herring	1159	3.36	9.6	5.51	-1.3	10.3	20.1
Mackerel	1275	3.93	1	5.20	-0.5	10.7	24.3
Sandeel	1202	3.2	10	2.84	-0.7	12.5	27.1
Sprat	1993	5.52	9.6	5.51	-0.1	12.1	24.8
Norway pout	3199	5.66	10	2.70	1.4	7.7	25.1
Plaice	255	4.46	14	3.95	1	12.6	26.5
Sole	1040	2.85	10	1.07	1.6	12.9	31.3
Saithe	630	4.47	10	2.79	-0.2	7.2	21.8
Cod	1188	2.1	10	2.22	-2	9.1	23
Haddock	430	2.91	10	2.70	-0.9	7.9	23.3
Horse Mackerel	1655	3.36	14	6.25	4.8	14.5	33.5
Whiting	1700	2.48	10	3.09	1.1	11.6	27
Dab	2931	3.2	14	3.95	1.8	12.1	27
Grey gurnard	873	2.79	10	2.70	1.5	12	27.7
Hake	426	4.11	10	2.70	3.7	11.3	28.9
Shrimp	815	1.28	8	1.85	1.5	12.5	28.1

3 – Predator-prey accessibility matrix.

Annexes

Table S5: Accessibility coefficients γ (Eq. 1) between potential predators and prey depend on their water-column position and represent the proportion of prey biomass accessible to a predator. The vertical position of individuals depends on their life stage, which is indicated in the last column. Shrimp (>0.25 year) and sandeels are exceptions due to their day/night migrations.

		Predator					
		Pelagic	Demersal	Benthic	Sandeel (>0.25 year)	Shrimp	
Focus Prey	Pelagic	0.8	0.4	0	0.8	0	Norway pout (<0.25 year), Sandeel (<0.25 year), Cod (<0.25 year), Saithe (<0.25 year), Grey gurnard (<0.25 year), Whiting (<0.25 year), Haddock (<0.25 year), Dab (<0.25 year), Sole (<0.25 year), Plaice (<0.25 year), Hake (<0.25 year), Sprat, Horse mackerel, Mackerel, Herring
	Demersal	0.4	0.8	0	0.4	0	Norway pout (>0.25 year), Cod (>0.25 year), Saithe (>0.25 year), Grey gurnard (>0.25 year), Whiting (>0.25 year), Haddock (>0.25 year), Hake (>0.25 year)
	Benthic	0	0.4	0.8	0	0.8	Dab (>0.25 year), Sole (>0.25 year), Plaice (>0.25 year)
	Sandeels (>0.25 year)	0.4	0.8	0.4	0.8	0.4	Sandeels (>0.25 year)
	Shrimp	0.2	0.4	0.8	0.2	0.8	Shrimp
Resource prey	Pelagic LTL	1	0.5	0	1	0.5	Dinoflagellates, Diatoms, Micro zooplankton, Meso zooplankton, Macro zooplankton
	Benthic LTL	0.04	0.5	1	0.04	0.5	Suspension Feeders, Deposit Feeders, Meiobenthos

8.1.5 Supporting Information S5: Parameters of the low trophic level (LTL) groups.

The trophic levels are set based on expert knowledge, except for the meso-zooplankton, the suspension feeder, the large and very large benthos for which trophic levels are taken from Kopp et al. (2015). The accessibility coefficients to fish are estimated through the calibration process (see 2.2.2.3 Calibration).

	LTL groups	Size range (cm)	Trophic level	Accessibility coefficient to fish
PELAGIC PREY	Micro-phytoplankton	0.0002 – 0.002	1	0.133
	Diatoms	0.001 – 0.02	1	0.028
	Hetero-trophic flagellates	0.0002 – 0.002	2	0.187
	Micro-zooplankton	0.002 – 0.02	2	0.032
	Meso-zooplankton	0.02 – 0.5	2.3	0.073
BENTHIC PREY	Suspension feeders	2 - 5	2.2 (bivalves)	0.002
	Deposit feeders	0.1 - 2	2	5.7e-5
	Meio benthos	0.0045 - 0.5	3	0.001
	Large benthos	5-10	2.6 (Small Crab)	0.018
	Very large benthos	10-15	3.6 (Large Crab)	0.014

8.1.6 Supporting Information S6: References for the life cycle parameters used in the North Sea model.

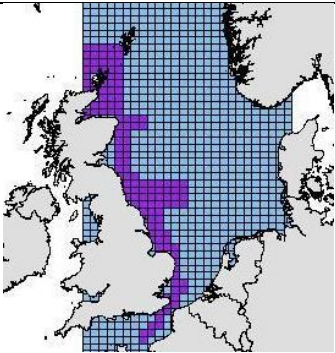
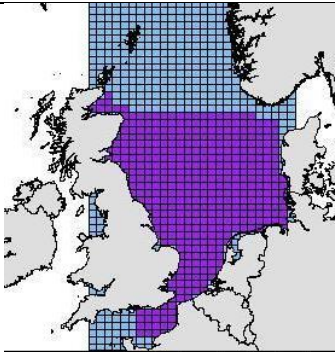
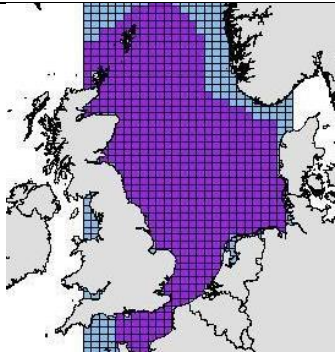
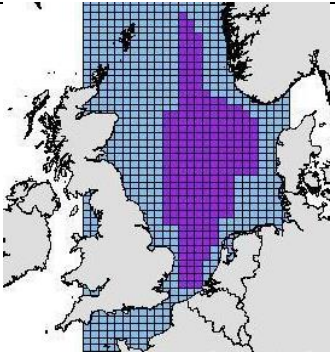
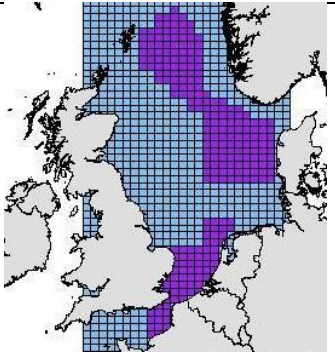
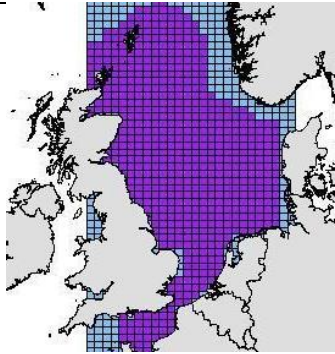
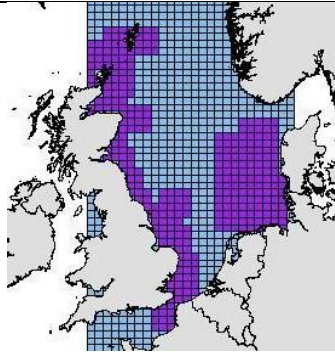
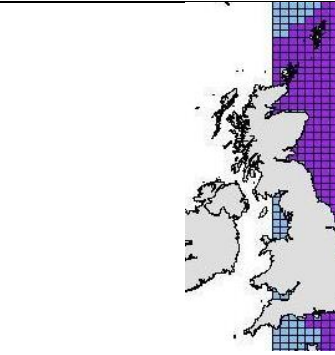
The length-mass parameters were estimated from SMALK data, except for shrimp (Oh et al., 2001).

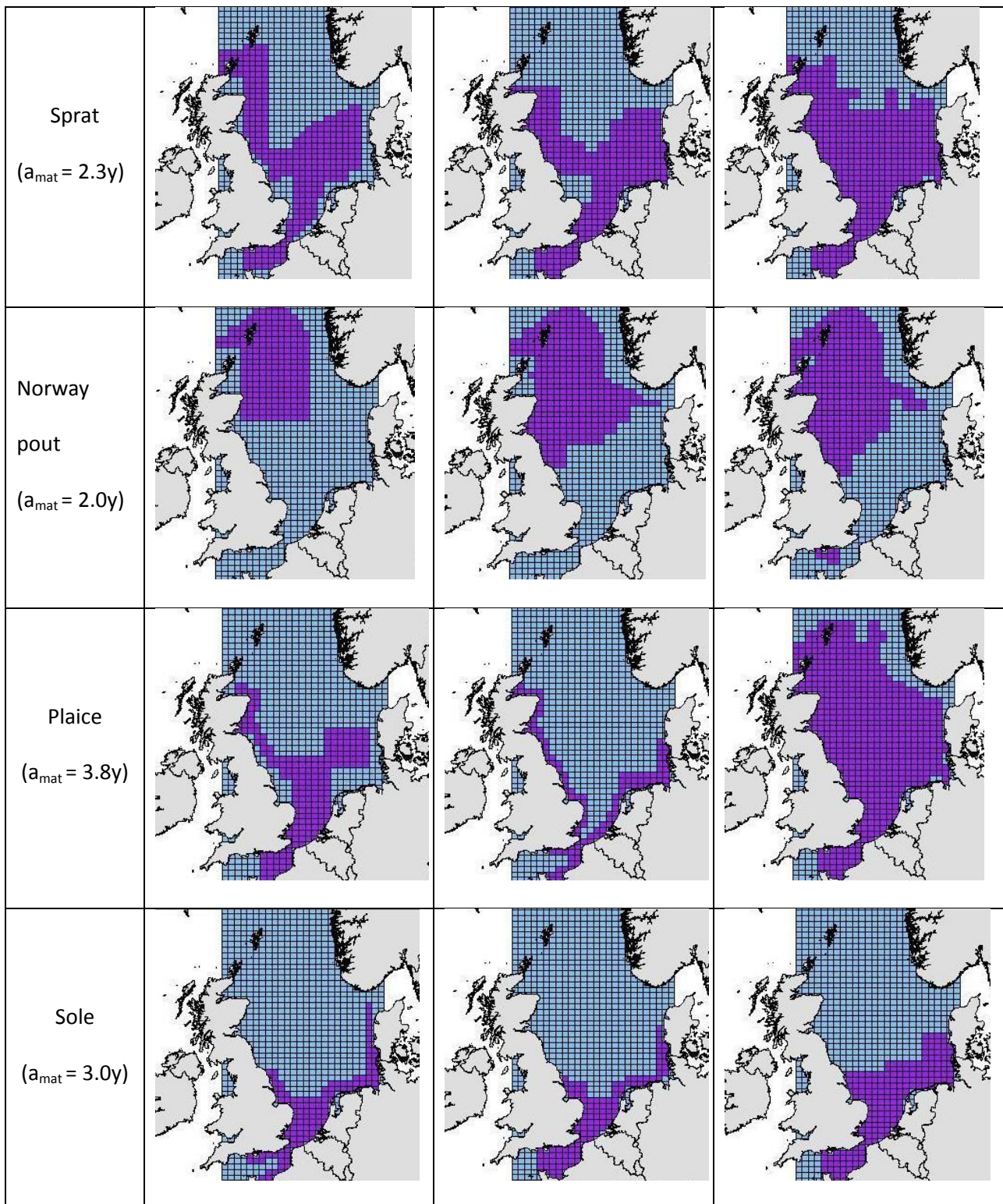
R_{min} and R_{max} based on Pinnegar (2014) and manually adjusted on diet.

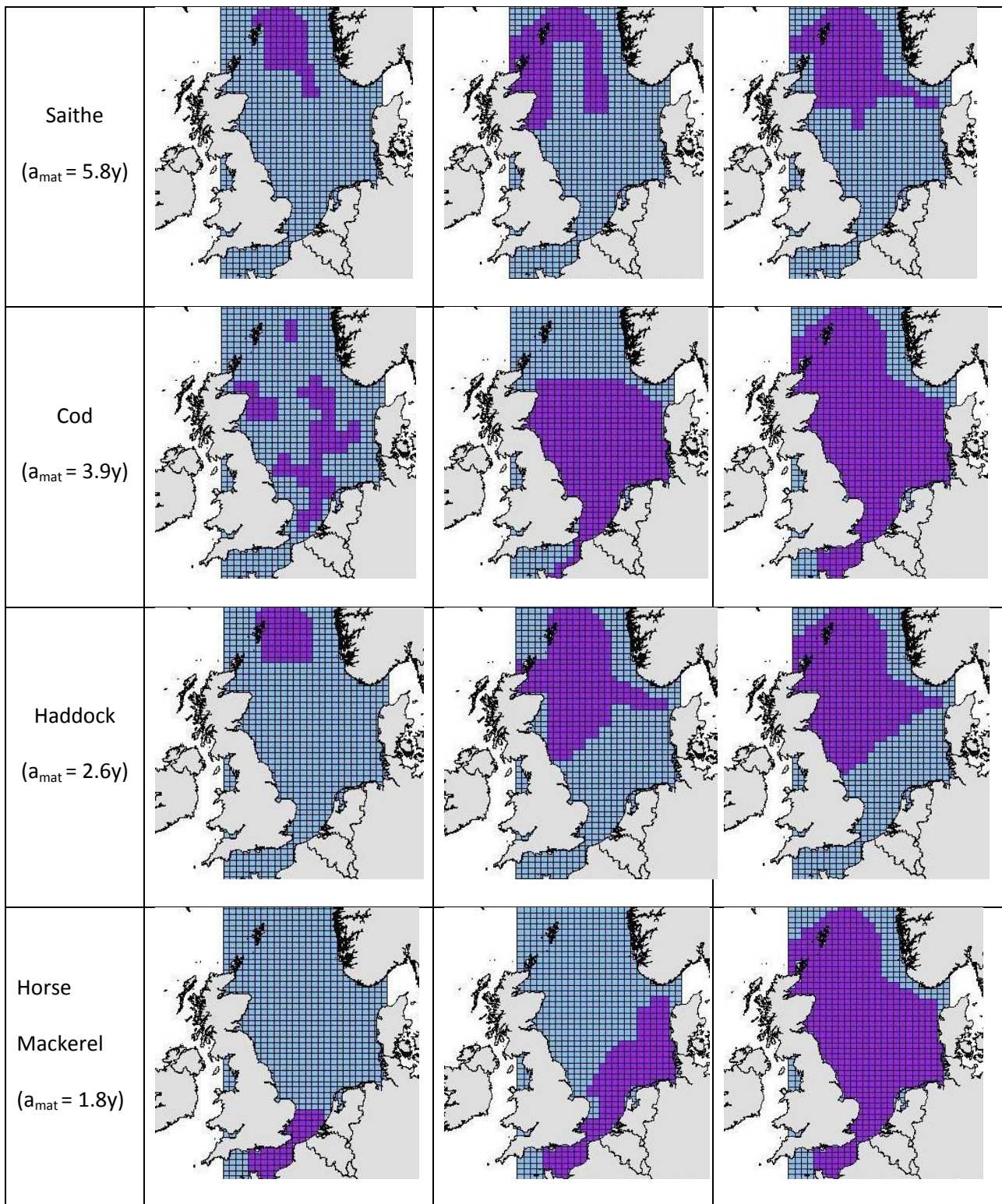
Species	Fecundity	Spawning season	Maintenance	Oxygen response
Herring	Muus & Nielsen, 1999	Muus & Nielsen, 1999, Baxter, 1958	Same as sprat	Same as mackerel
Mackerel	Macer, 1976	Muus & Nielsen, 1999	Dickson, 2002	(Dickson, 2002)
Sandeel	Bergstad et al., 2001	Muus & Nielsen, 1999	Behrens & Steffensen, 2007	Behrens & Steffensen, 2007
Sprat	De Silva, 1973	Koli, 1990; MacKenzie & Köster, 2004	Meskendahl, 2013	Same as mackerel
Norway pout	Christiansen et al., 1997	Muus & Nielsen, 1999	Teleost value, Clarke & Johnston, 1999	Same as cod
Plaice	van Damme et al., 2009	Fox et al., 2000	Clarke & Johnston, 1999	Steffensen et al., 1982
Sole	Witthames et al., 1995	Quéro et al., 1986	Lefrançois & Claireaux, 2003	Lefrançois & Claireaux, 2003
Saithe	Cohen et al., 1990	ICES, 2012	Steinhausen et al., 2005	Same as cod
Cod	Yoneda & Wright, 2004	Narberhaus et al., 2012; Cohen et al., 1990	Claireaux et al., 2000	Claireaux et al., 2000
Haddock	Sonina, 1971	Muus & Nielsen, 1999	Average of cod, saithe and whiting rate	Same as cod
Horse Mackerel	Eltink & Vingerhoed, 1989	Muus & Nielsen, 1999	Geist et al., 2013	Same as mackerel
Whiting	Hislop, 1966	Hehir, 2003; Cohen et al., 1990	Steinhausen et al., 2005	Same as cod
Dab	Bohl, 1956	Muus & Nielsen, 1999	Same as sole	Average of sole and plaice response
Grey gurnard	Muus & Nielsen, 1999	Muus & Nielsen, 1999	Teleost value, Clarke & Johnston, 1999	Same as cod
Hake	Mehault et al., 2010	Mehault et al., 2010	Average of cod, saithe and whiting rate	Same as cod
Shrimp	Bilgin & Samsun, 2006	WGCRAN, 2015	Dupont-Prinet et al., 2013	Dupont-Prinet et al., 2013

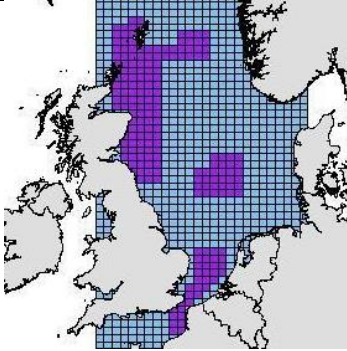
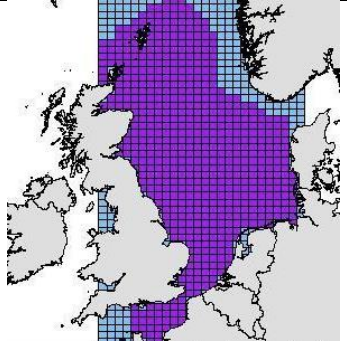
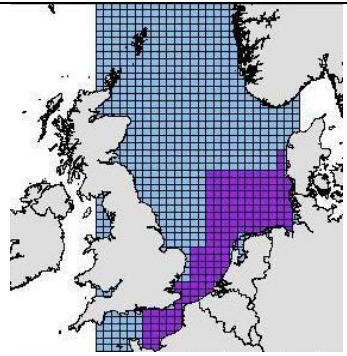
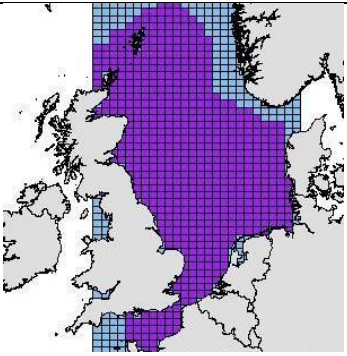
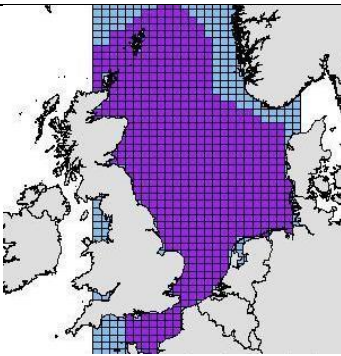
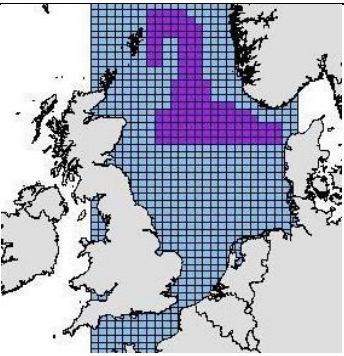
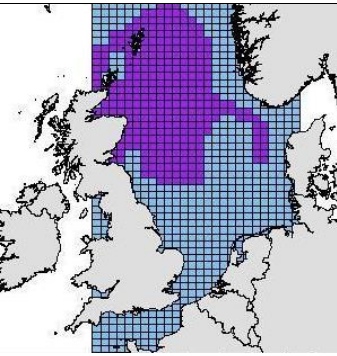
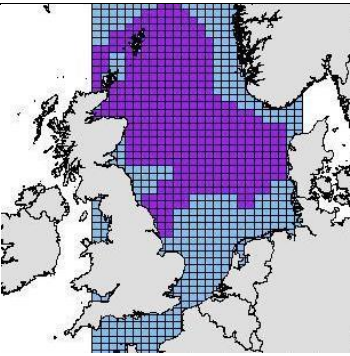
8.1.7 Supporting Information S7: Species distribution relative to ontogenetic stages.

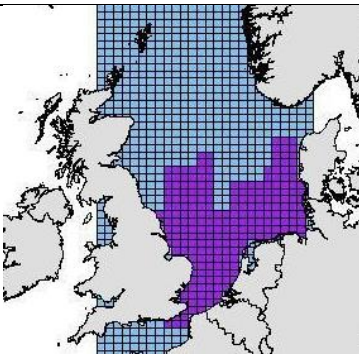
The threshold between larvae and juvenile stage is set to 0.25 year for all the species. The threshold between juvenile and adult stage is species dependent and corresponds to the mean age at maturation (a_{mat}). The distribution was obtained from IBTS data for period 2010-2019, Coull et al. (1998), Sundbly et al. (2017), Van der Land (1991) and Mackinson & Daskalov (2007).

Stage \ Species	Egg and larvae (<0.25y)	Juvenile (0.25y < - < a_{mat})	Adult (> a_{mat})
Herring ($a_{mat} = 2.9y$)			
Mackerel ($a_{mat} = 2.5y$)			
Sandeel ($a_{mat} = 2.2y$)			



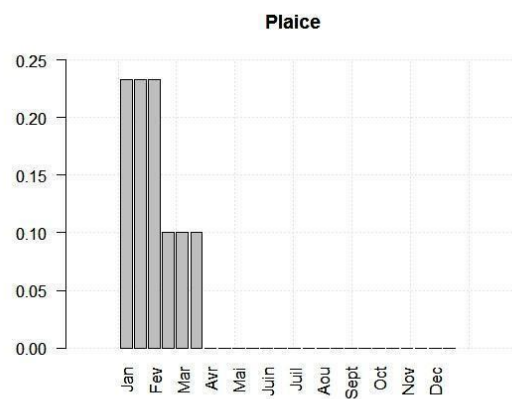
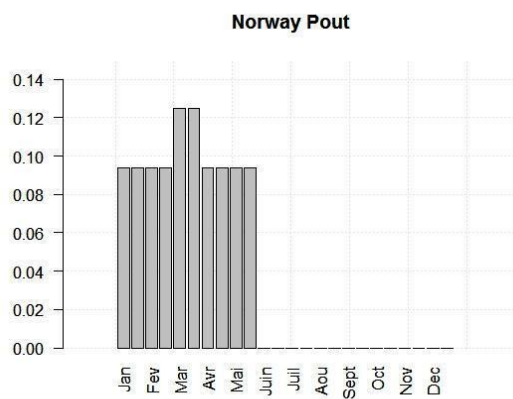
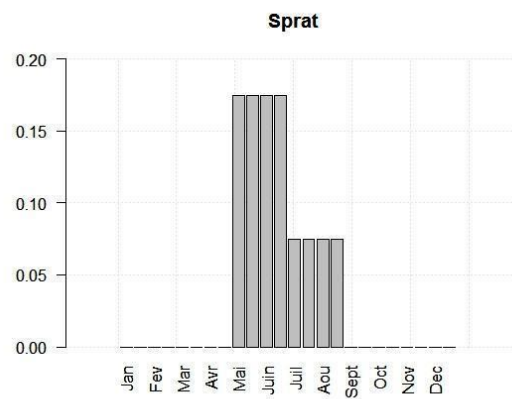
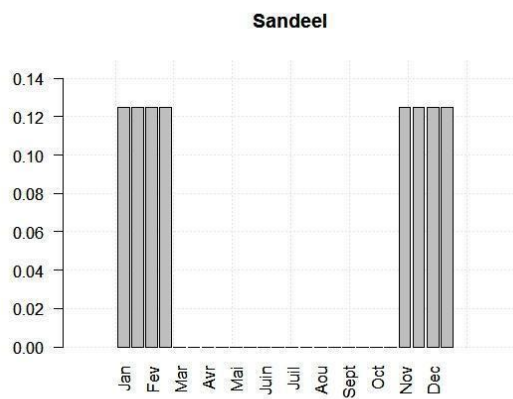
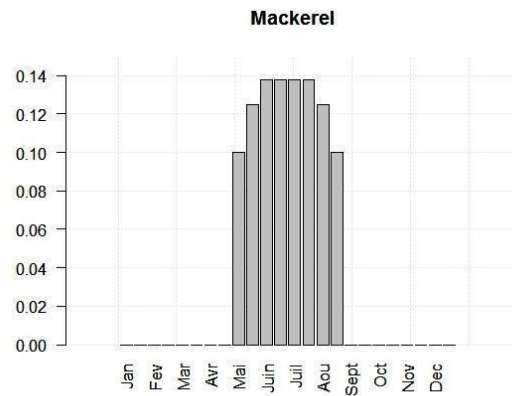
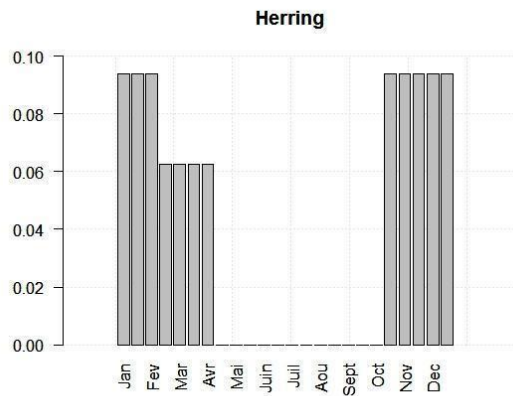


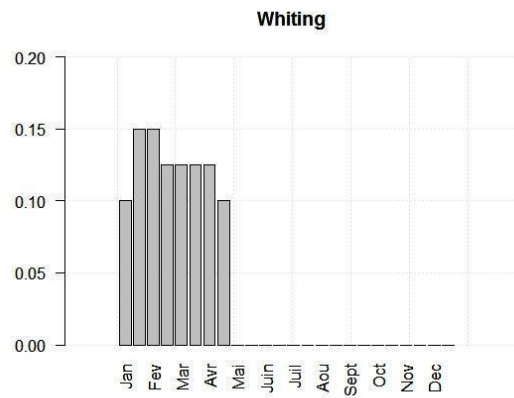
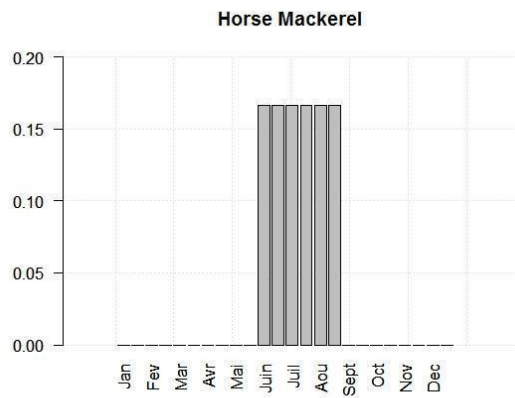
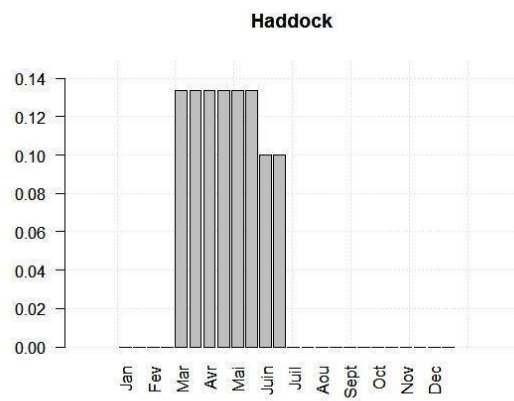
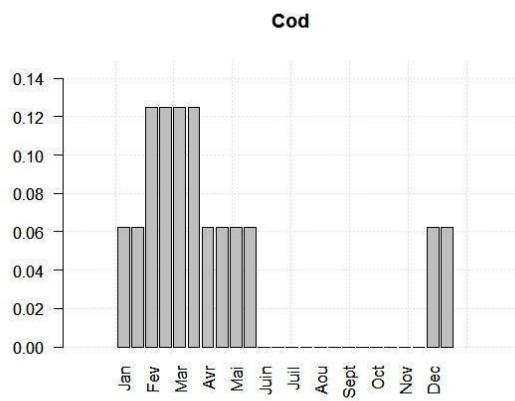
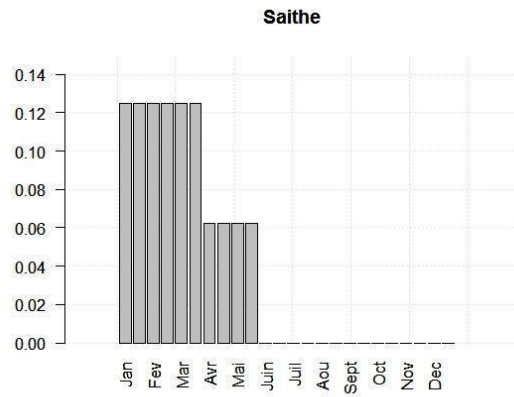
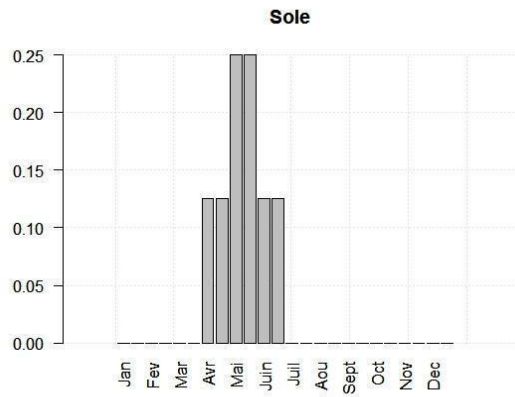
<p>Whiting ($a_{mat} = 2.2y$)</p>			
<p>Dab ($a_{mat} = 1.7y$)</p>			
<p>Grey gurnard ($a_{mat} = 2.2y$)</p>			
<p>Hake ($a_{mat} = 3.4y$)</p>			

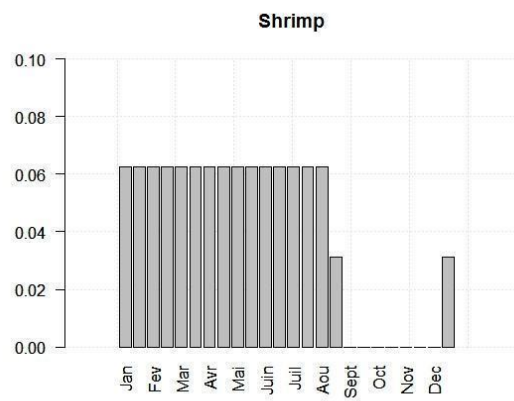
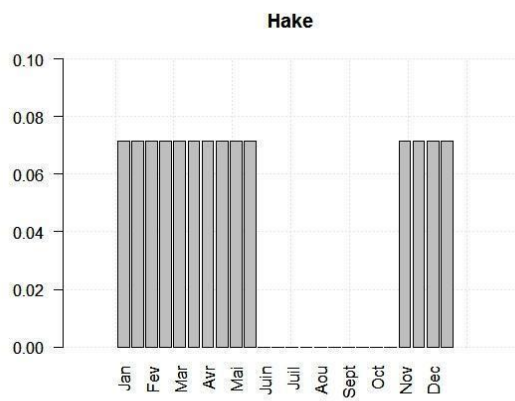
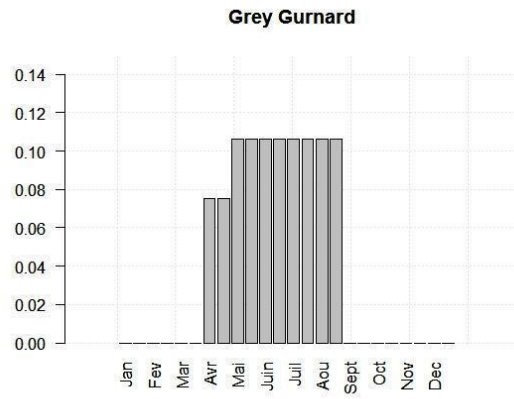
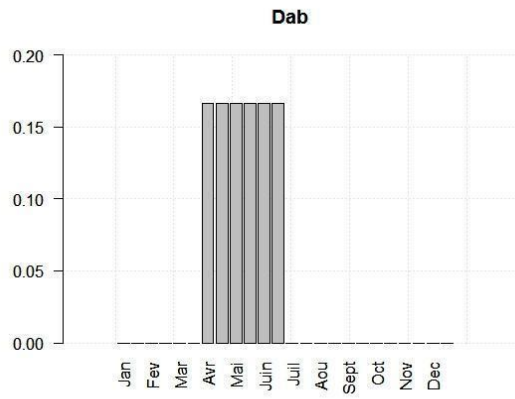
<p>Shrimp ($a_{mat} = 1y$)</p>	 A map of the North Atlantic region, including parts of North America, Europe, and Greenland. A blue grid pattern covers a large area in the upper right quadrant, extending from the coast of North America towards Europe. A purple shaded area is located in the lower right quadrant, covering parts of the North Atlantic and the western coast of Europe. The rest of the map is white with black outlines for landmasses.
---	--

8.1.8 Supporting Information S8: Reproductive season.

The diagram is the proportion of released eggs per time step t $p_{e,t}$ relative to the annual total released eggs (see Eq. S8). The references are given in Supporting information S6.







8.1.9 Supporting Information S9: Monthly maps of LTL and temperature and oxygen variables from POLCOMS-ERSEM averaged on the 2010-2019 period.

The LTL biomasses are vertically integrated and provided as tons per cell. Temperature and oxygen variables are available in the entire water column (vertically integrated) and at the sea bottom.

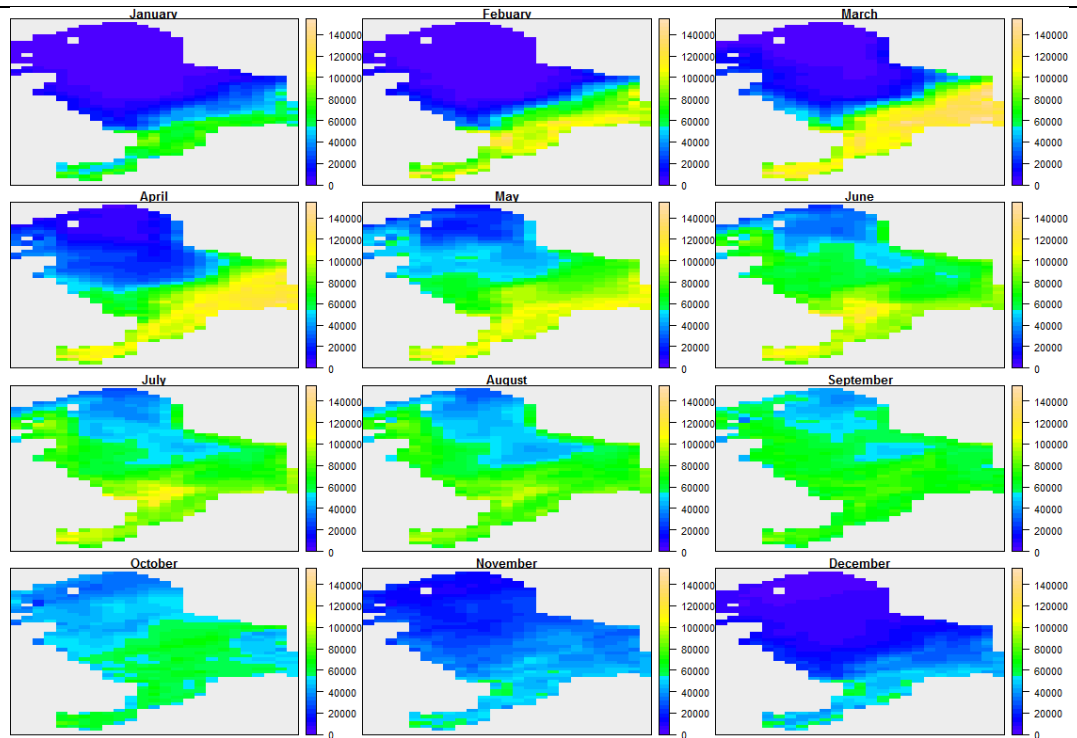
Temperature is in Celsius, Oxygen is in % of saturation.

LTL

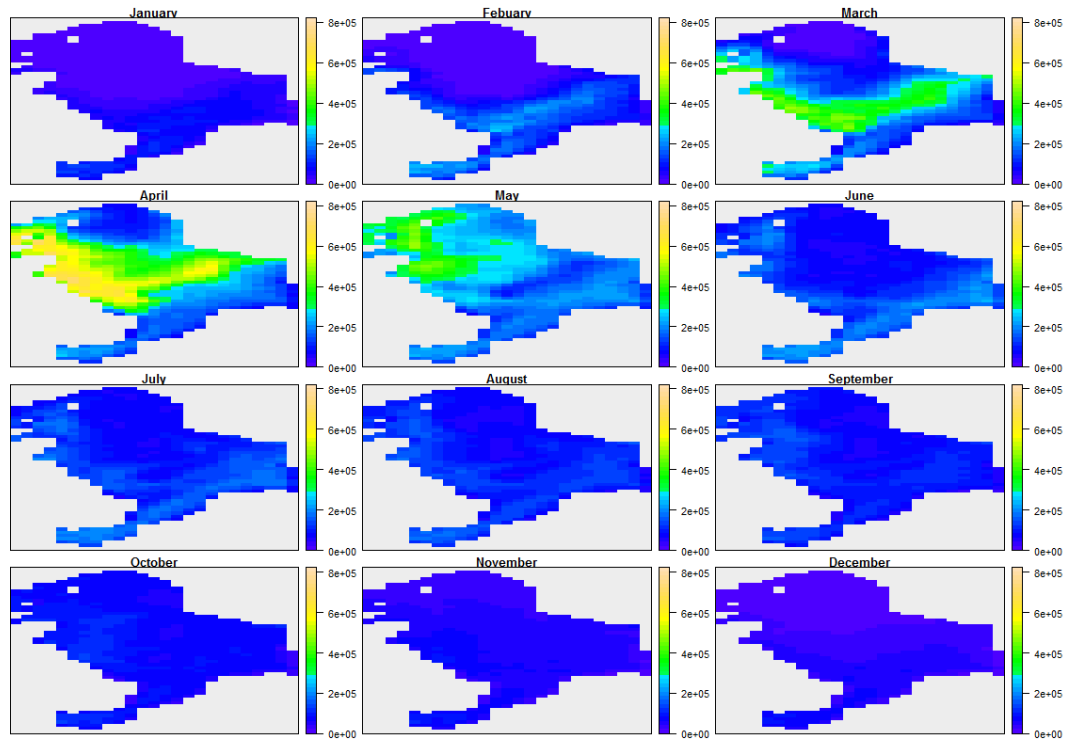
Maps

groups

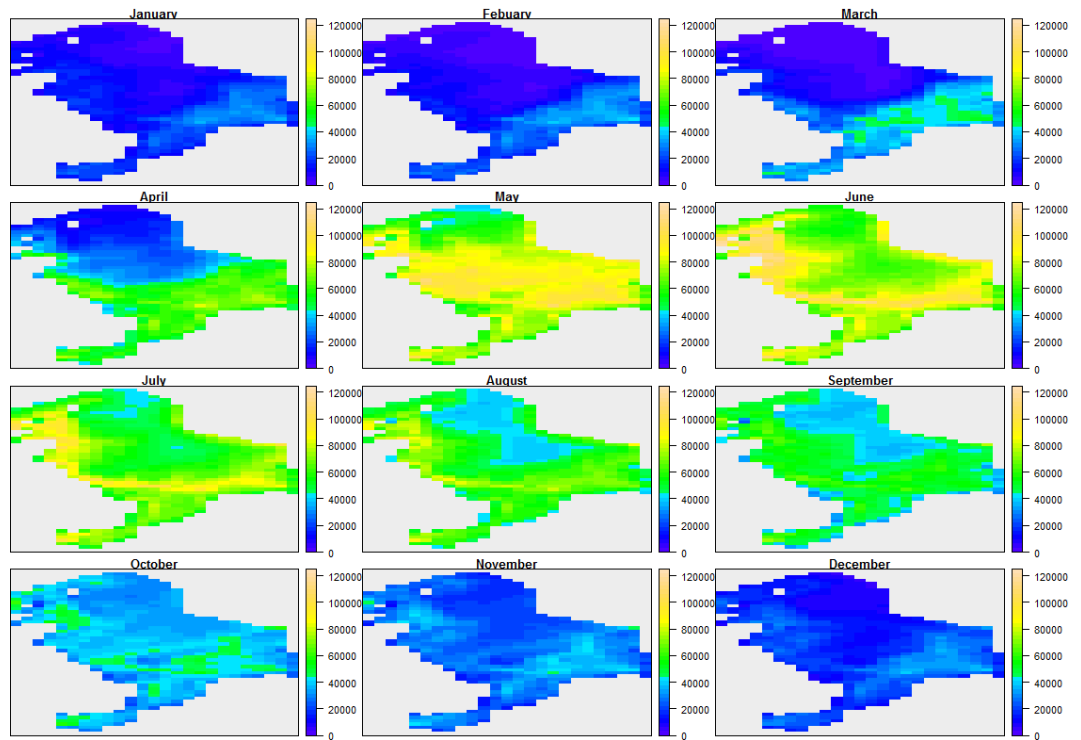
Micro-phytoplankton



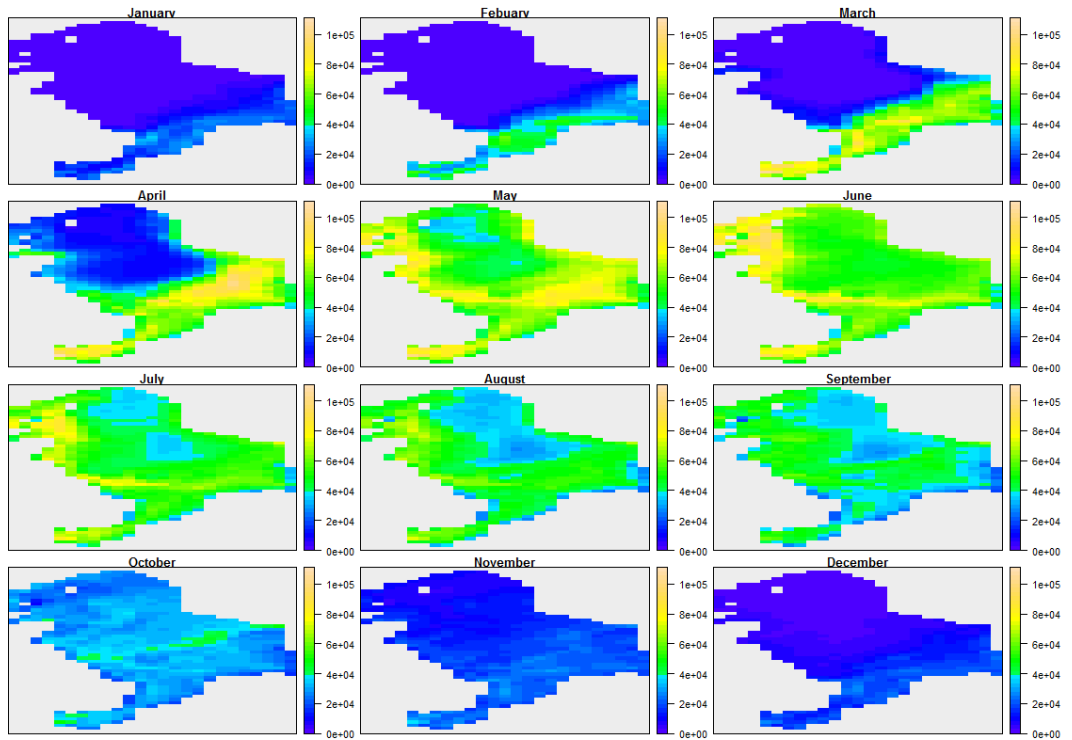
Diatoms



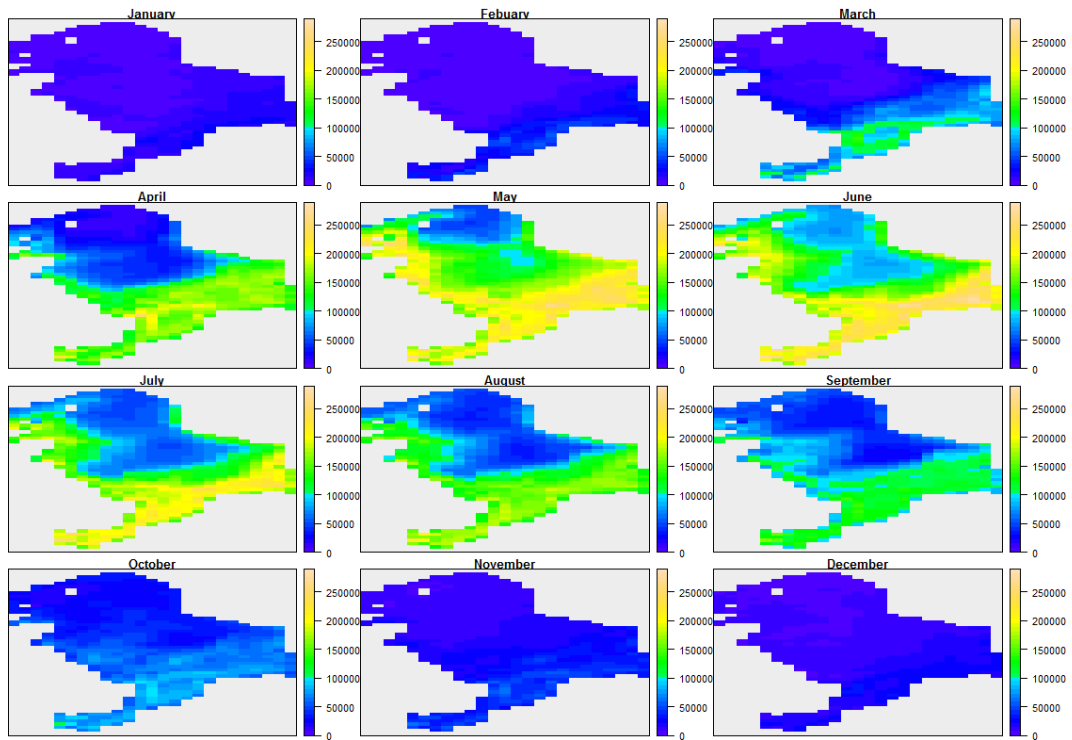
Hetero-trophic flagellates



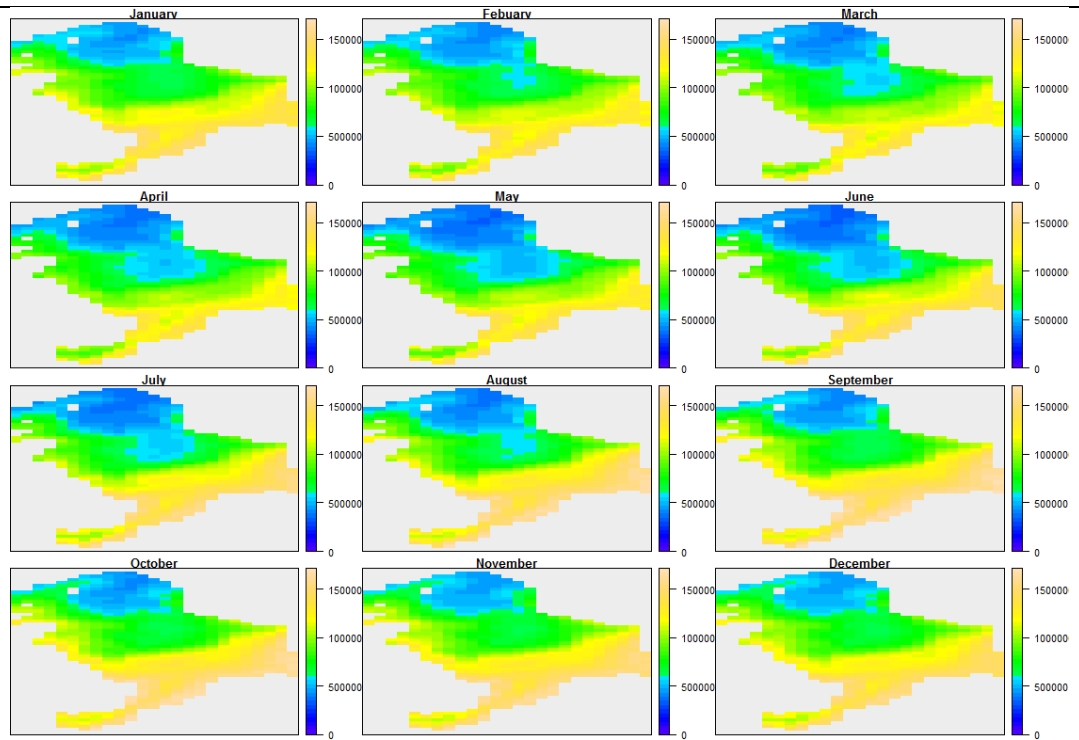
Micro-zooplankton



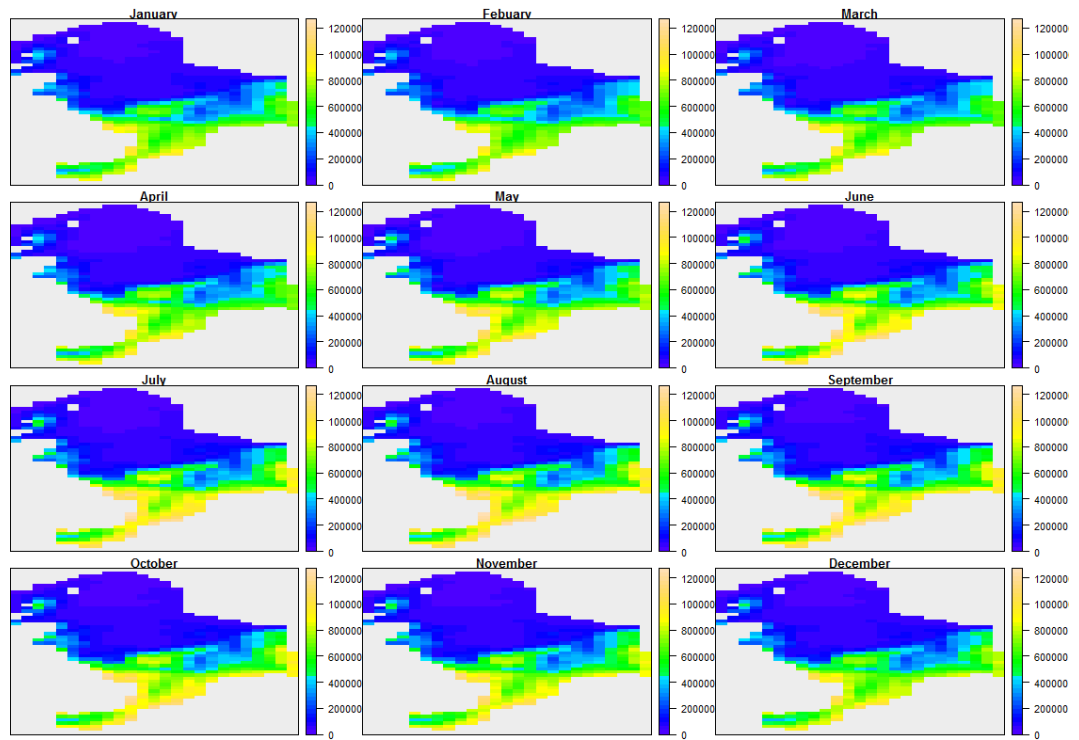
Meso-zooplankton



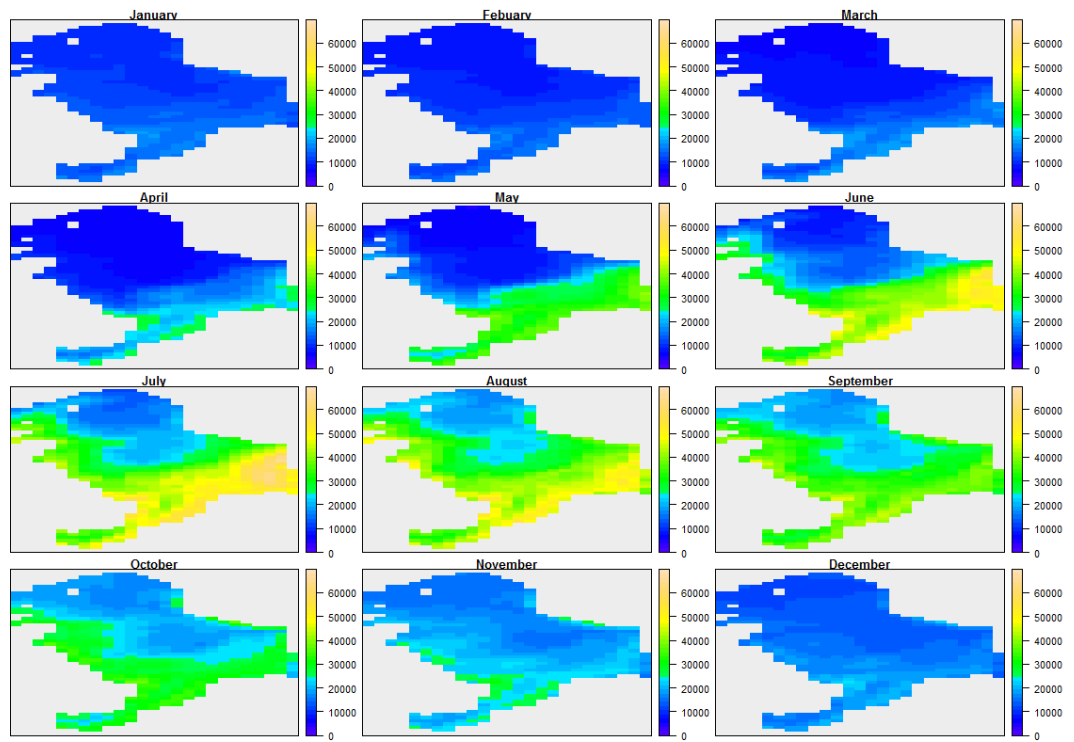
SuspensionFeeders



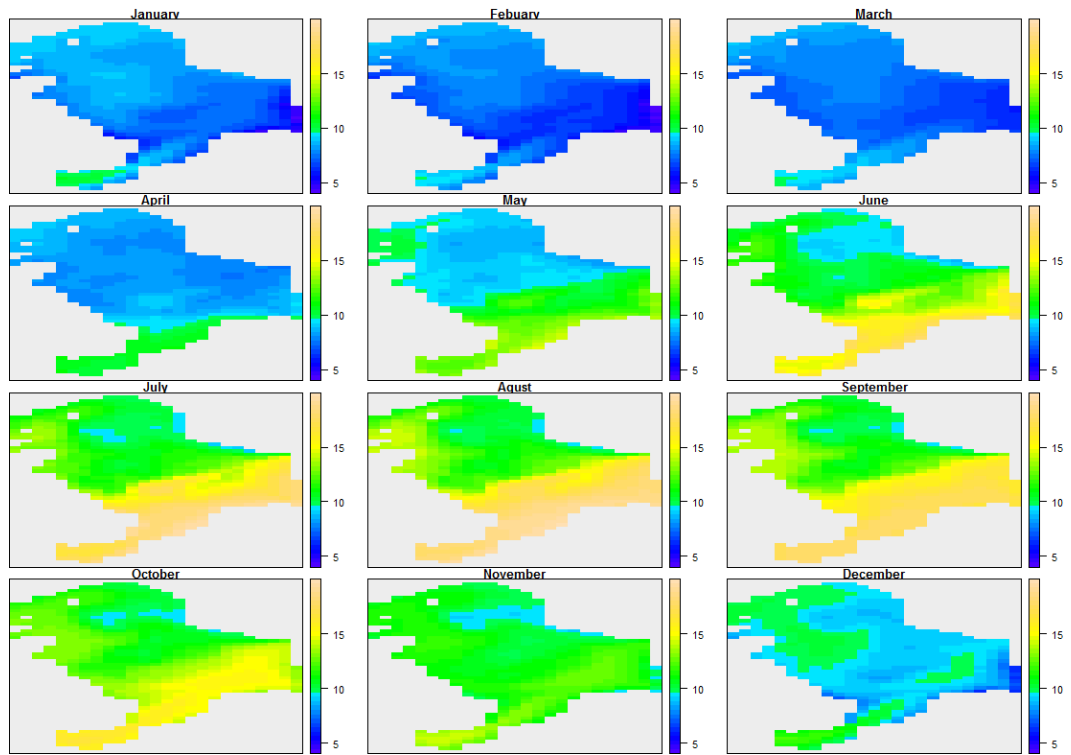
DepositFeeders



Meiobenthos

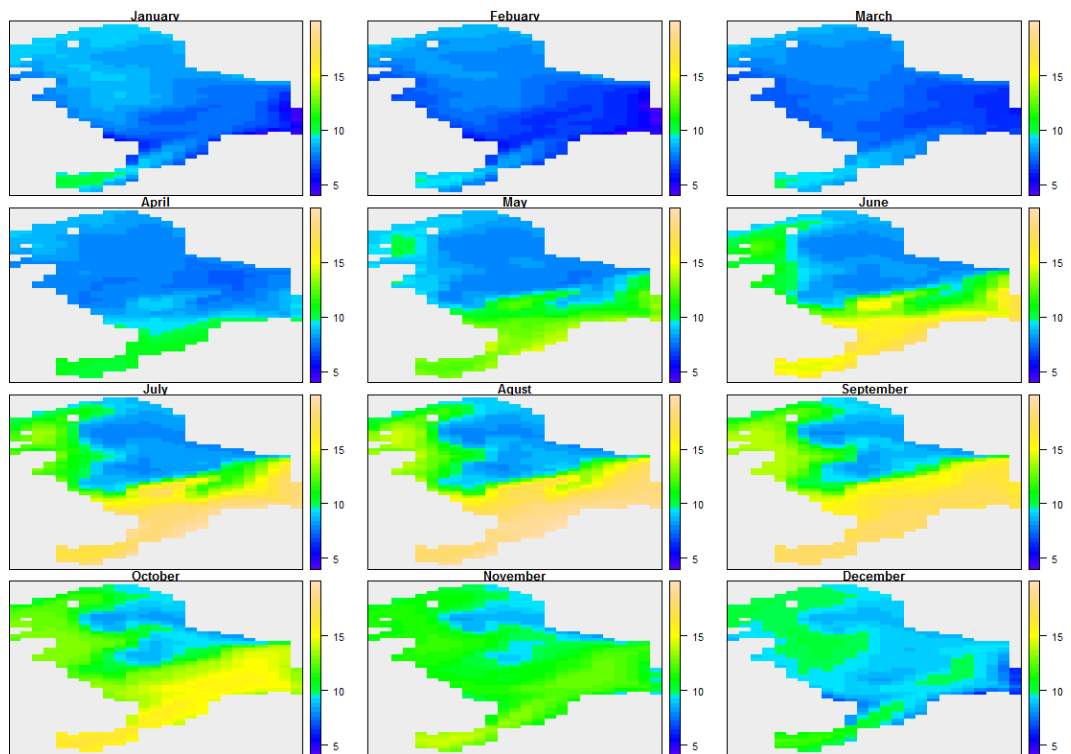


Column integration

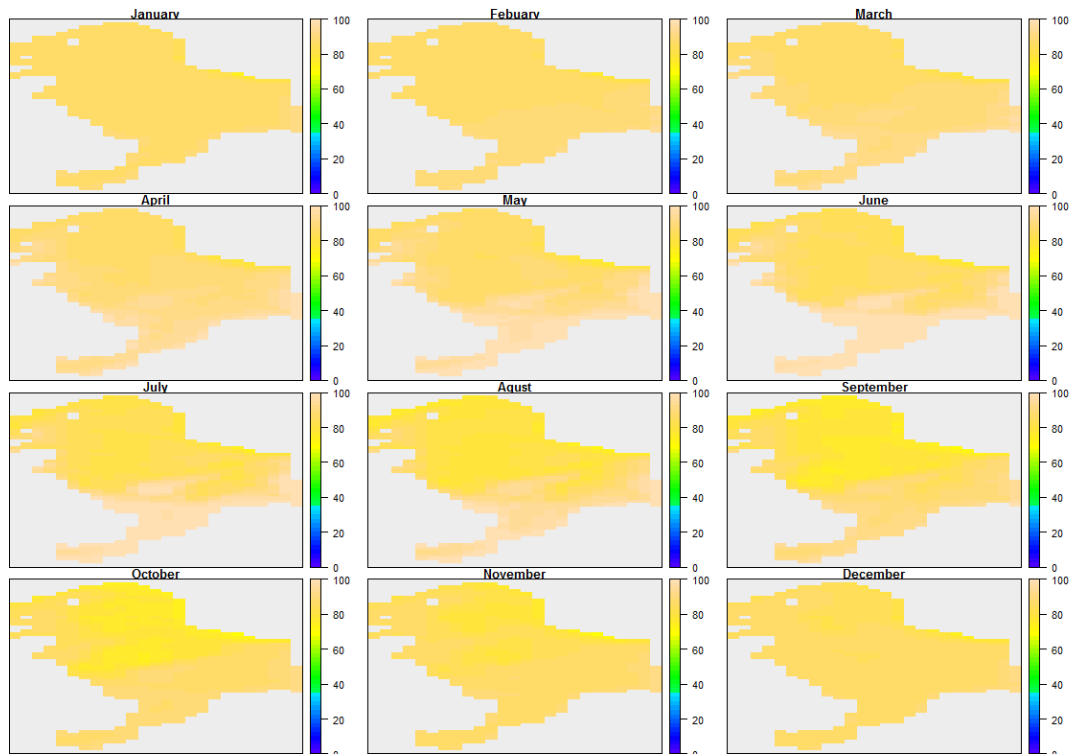


Temperature

Bottom

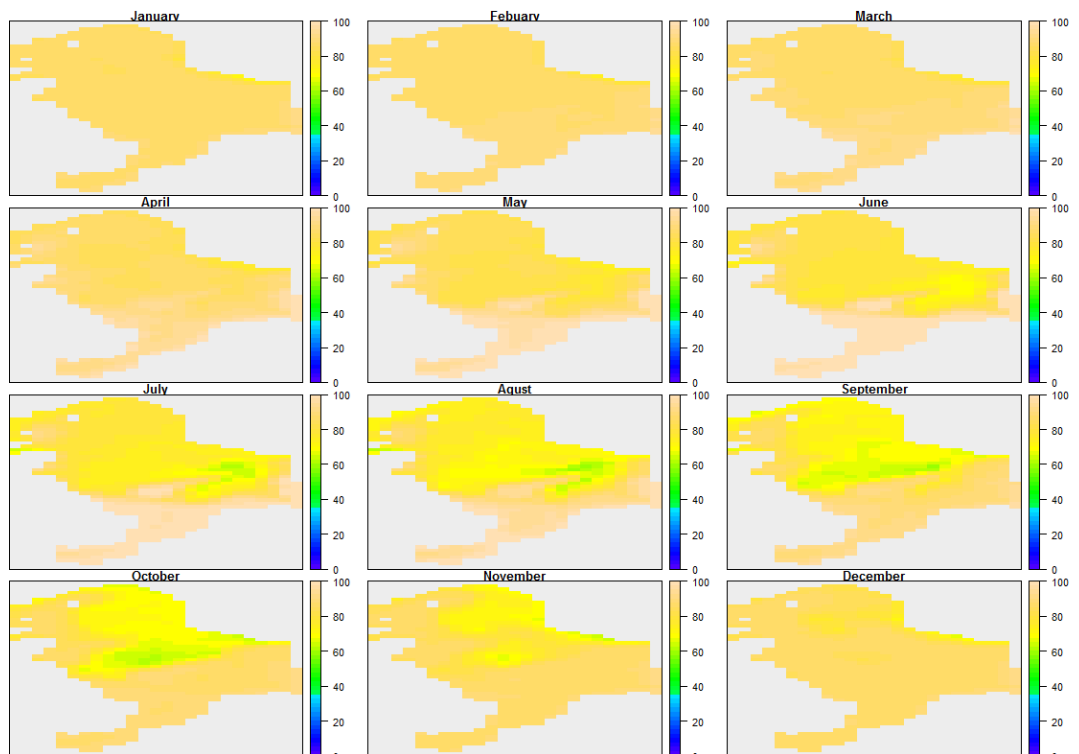


Column integration



Oxygen

Bottom



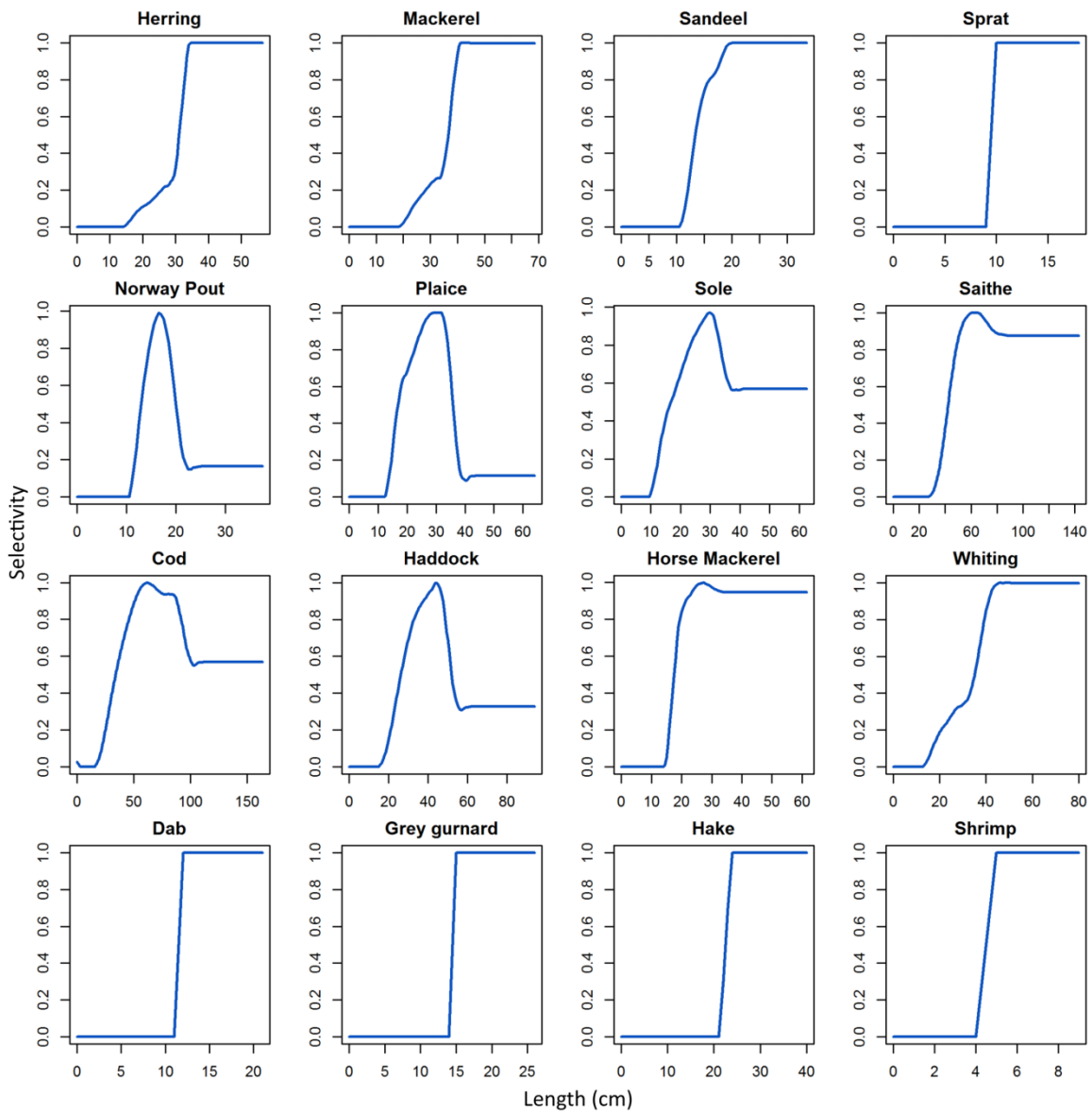
8.1.10 Supporting Information S10: Target values for the calibration.

The target values were average on the period 2010 to 2019. Data used to calibrate Bioen-OSMOSE-NS are fisheries landings (ICES, 2019a), size-at-age from scientific surveys (NS-IBTS-Q1, ICES. North Sea International Bottom Trawl Survey (2010-2019). Available online at <http://datras.ices.dk>) and estimated biomasses for assessed species (ICES, 2019b, 2018c, 2018d, 2018e, 2016) (see section 2.2.2.3 Calibration in main text for more details).

	Herring	Mackerel	Sandeel	Sprat	N. Pout	Plaice	Sole	Saithe	Cod	Haddock	H. Mackerel	Whiting	Dab	G. Gurnard	Hake	Shrimp	
Biomass (10 ³ tonnes)	4 252	1 719	1 735	1 309	393	969	78	354	206	379		363	201		62		
Catches (10 ³ tonnes)	443	285	292	161	57	119	16	76	41	36	21	31	49	7	18	37	
Size-at-age (cm)	1	16.4	22.9		9.3	13	15.7	13	22.9	23.9	22.1	11.4	18.5	11.4	13.6	33.3	
	2	21.9	28.1	15.9	11.4	16.4	20.2	18.2	34.4	39.1	30	20	24.9	14.8	18.3	44.2	
	3	25.2	31.4	17.5	12.8	18.4	24.4	23.2	41.7	55.8	35.3	20	30.2	18.8	22.4	58.6	
	4	27.2	33.3	17.4	13.7	19.9	27.9	26.7	48	69	38.7	26	34.2	22	27	68.4	
	5	28.5	34.3	17.8	14.3	20.6	30.2	27.7	54.5	77.9	40.2	34	36.6	23.5	28.7	75.8	
	6	29.5	35	18.3	14.5		31.6	27.6	61.8	85.5	41.4	33	37.9	25.2	27.5	77.5	
	7	30.1	36.1		14.8		32.4	30.6	69.7	90.2	43.4	33.9	38.8	25.7	27.8	87.3	
	8	30.6	36.6		15		32.9	28.8	75.8	96.1	44.5	35.6	38.9	27.1	26.7	85.1	
	9	30.7	37.4		15		32.9	28.8	80.8	97.4	45.4	36.4	38.3	27.3	27.7	88.7	
	10	31.1	38		15		33	33.2	85.2	105.1		36.7	38.4		27.8		
	11	31.5	38.7				33.3	30.7	87.1	103		37			31		
	12	31.9	38.8				32.9	32.8	89.8			37			29		
	13	32.3	38.7				34.1	31	93.3								
	14	32.5	40.1				33.4		97.4								
	15						33.6		94.8								
	16						35.7		98.9								

8.1.11 Supporting Information S11: Fishing selectivity per species.

Fishing size-selectivity per species. We used fishing mortality rates estimated from stock assessments (ICES, 2019b, 2018c, 2018d, 2018e, 2016). When available, fishing mortality rates per age class were converted to fishing mortality rates per size class using species specific von Bertalanffy growth models. When the only data available is a constant fishing mortality rate for a species and a size at recruitment, a knife-edge selectivity curve is used (sprat, dab, grey gurnard, hake and shrimp).



8.2 Annexes du chapitre 4

8.2.1 Supporting Information S11 - Estimation procedure for the coefficient of variations of the traits under selection

1. Estimation of phenotypic variance of the juvenile growth coefficient c and the gonado-somatic index r

The growth in length of an individual i can be described as:

$$l_i(c_i, a_{m,i}, r_i, a) = \begin{cases} \left(l_0^{\alpha(1-\beta)} + \frac{c_i(1-\beta)}{k(1-\beta)} (a - 1 + \theta) \right)^{\frac{1}{\alpha(1-\beta)}} & \text{for } a \leq a_{m,i} \\ \left(\frac{qc_i}{r_i k^{1-\beta}} - \left(\frac{qc_i}{r_i k^{1-\beta}} - \left(l_0^{\alpha(1-\beta)} + \frac{c_i(1-\beta)}{k(1-\beta)} (a_{m,i} - 1 + \theta) \right) \right) \left(\frac{1}{1+(1-\beta)\frac{r_i}{q}} \right)^{a-a_{m,i}} \right)^{\frac{1}{\alpha(1-\beta)}} & \text{otherwise} \end{cases} \quad (S17)$$

We denote $\lambda_i(c_i, a_{m,i}, r_i, a) = l_i(c_i, a_{m,i}, r_i, a)^{\alpha(1-\beta)}$ the transformed length at age, which gives:

$$\lambda_i(c_i, a_{m,i}, r_i, a) = \begin{cases} \lambda_0 + \frac{c_i(1-\beta)}{k(1-\beta)} (a - 1 + \theta) & \text{for } a \leq a_{m,i} \\ \frac{qc_i}{r_i k^{1-\beta}} - \left(\frac{qc_i}{r_i k^{1-\beta}} - \left(\lambda_0 + \frac{c_i(1-\beta)}{k(1-\beta)} (a_{m,i} - 1 + \theta) \right) \right) \left(\frac{1}{1+(1-\beta)\frac{r_i}{q}} \right)^{a-a_{m,i}} & \text{otherwise} \end{cases} \quad (S18)$$

with $\lambda_0 = l_0^{\alpha(1-\beta)}$.

Applying the Delta method to the growth equation (S18) and neglecting second order terms in the Taylor expansion, we obtain:

$$\sigma_\lambda^2(a) = \left(\frac{(1-\beta)}{k(1-\beta)} a \right)^2 \sigma_c^2 \quad (S19a)$$

$$\sigma_c = \sigma_\lambda(a) \cdot \frac{k^{(1-\beta)}}{(1-\beta) \cdot (a-1+\theta)}$$

for any age $a \leq a_m$ and:

$$\begin{aligned}
\sigma_\lambda^2(a) &\approx \left(\frac{\partial \lambda(c, \bar{a}_m, \bar{r}, a)}{\partial c} \Big|_{c=\bar{c}} \right)^2 \sigma_c^2 + \left(\frac{\partial \lambda(\bar{c}, a_m, \bar{r}, a)}{\partial a_m} \Big|_{a_m=\bar{a}_m} \right)^2 \sigma_{a_m}^2 + \left(\frac{\partial \lambda(\bar{c}, \bar{a}_m, r, a)}{\partial r} \Big|_{r=\bar{r}} \right)^2 \sigma_r^2 + \\
&2 \frac{\partial \lambda(c, \bar{a}_m, \bar{r}, a)}{\partial c} \Big|_{c=\bar{c}} \frac{\partial \lambda(\bar{c}, a_m, \bar{r}, a)}{\partial a_m} \Big|_{a_m=\bar{a}_m} \sigma_{c, a_m} + 2 \frac{\partial \lambda(\bar{c}, a_m, \bar{r}, a)}{\partial a_m} \Big|_{a_m=\bar{a}_m} \frac{\partial \lambda(\bar{c}, \bar{a}_m, r, a)}{\partial r} \Big|_{r=\bar{r}} \sigma_{a_m, r} + \\
&2 \frac{\partial \lambda(c, \bar{a}_m, \bar{r}, a)}{\partial c} \Big|_{c=\bar{c}} \frac{\partial \lambda(\bar{c}, \bar{a}_m, r, a)}{\partial r} \Big|_{r=\bar{r}} \sigma_{c, r}
\end{aligned} \tag{S19b}$$

for any age $a > a_m$ where σ_x^2 and $\sigma_{x,y}$ denote variance of x and covariance of x and y , respectively.

Under the assumption of negligible covariances between c , a_m , and r we obtain further:

$$\begin{aligned}
\sigma_\lambda^2(a) &\approx \left(\frac{\partial \lambda(c, \bar{a}_m, \bar{r}, a)}{\partial c} \Big|_{c=\bar{c}} \right)^2 \sigma_c^2 + \left(\frac{\partial \lambda(\bar{c}, a_m, \bar{r}, a)}{\partial a_m} \Big|_{a_m=\bar{a}_m} \right)^2 \sigma_{a_m}^2 + \left(\frac{\partial \lambda(\bar{c}, \bar{a}_m, r, a)}{\partial r} \Big|_{r=\bar{r}} \right)^2 \sigma_r^2 + \\
&2 \frac{\partial \lambda(c, \bar{a}_m, \bar{r}, a)}{\partial c} \Big|_{c=\bar{c}} \frac{\partial \lambda(\bar{c}, a_m, \bar{r}, a)}{\partial a_m} \Big|_{a_m=\bar{a}_m} \sigma_{c, a_m} \text{ for } a > a_m
\end{aligned} \tag{S20}$$

Denoting the age-dependent maturity ogive $o(a)$, the maturation probability at age is obtained as:

$$m(a) = \frac{o(a) - o(a-1)}{1 - o(a-1)}.$$

Mean maturation can thus be obtained as:

$$\bar{a}_m = \frac{\sum_{a=0}^{+\infty} a m(a)}{\sum_{a=0}^{+\infty} m(a)}$$

and its variance as:

$$\sigma_{a_m}^2 = \frac{\sum_{a=0}^{+\infty} (a - \bar{a}_m)^2 m(a)}{\sum_{a=0}^{+\infty} m(a)} \tag{S21}$$

Given that we know σ_c^2 from equation (S19a) and $\sigma_{a_m}^2$ from equation (S21), then we can deduce an approximation of σ_r^2 from equation (S20):

$$\begin{aligned}
\sigma_r^2 &\approx \\
&\left(\sigma_\lambda^2(a) - \left(\frac{\partial \lambda(c, \bar{a}_m, \bar{r}, a)}{\partial c} \Big|_{c=\bar{c}} \right)^2 \sigma_c^2 - \left(\frac{\partial \lambda(\bar{c}, a_m, \bar{r}, a)}{\partial a_m} \Big|_{a_m=\bar{a}_m} \right)^2 \sigma_{a_m}^2 - \right. \\
&2 \frac{\partial \lambda(c, \bar{a}_m, \bar{r}, a)}{\partial c} \Big|_{c=\bar{c}} \frac{\partial \lambda(\bar{c}, a_m, \bar{r}, a)}{\partial a_m} \Big|_{a_m=\bar{a}_m} \sigma_{c, a_m} \left. \right) \left(\frac{\partial \lambda(\bar{c}, \bar{a}_m, r, a)}{\partial r} \Big|_{r=\bar{r}} \right)^{-2}
\end{aligned} \tag{S22}$$

Equations (S19a) and (S22) allow estimating σ_c^2 and σ_r^2 from length-at-age data for fully immature individuals, i.e., for any age a so that $o(a) = 0$ for the former, and for fully mature individuals, i.e., for any age a so that $o(a) = 1$ for the latter.

One way to combine these equations for an estimation across all ages is to look for the values of σ_c^2 and σ_r^2 minimizing the sum of squared differences between $\sigma_\lambda^2(a)$, the variance of transformed length at age, and the right handside of equations (S19a) and (S20) respectively weighted by the probability of being immature $(1 - o(a))$ and being mature $o(a)$:

$$\begin{aligned} (\hat{\sigma}_c^2, \hat{\sigma}_r^2) = \operatorname{argmin}_{\sigma_c^2, \sigma_r^2} \sum_{a=0}^{+\infty} & \left[(1 - o(a)) \left(\sigma_\lambda^2(a) - \left(\frac{(1-\beta)}{k^{(1-\beta)}} a \right)^2 \sigma_c^2 \right)^2 + o(a) \left(\sigma_\lambda^2(a) - \right. \right. \\ & \left. \left(\frac{\partial \lambda(c, \bar{a}_m, \bar{r}, a)}{\partial c} \Big|_{c=\bar{c}} \right)^2 \sigma_c^2 - \left(\frac{\partial \lambda(\bar{c}, a_m, \bar{r}, a)}{\partial a_m} \Big|_{a_m=\bar{a}_m} \right)^2 \sigma_{a_m}^2 - \left(\frac{\partial \lambda(\bar{c}, \bar{a}_m, r, a)}{\partial r} \Big|_{r=\bar{r}} \right)^2 \sigma_r^2 - \right. \\ & \left. \left. 2 \frac{\partial \lambda(c, \bar{a}_m, \bar{r}, a)}{\partial c} \Big|_{c=\bar{c}} \frac{\partial \lambda(\bar{c}, a_m, \bar{r}, a)}{\partial a_m} \Big|_{a_m=\bar{a}_m} \sigma_{c, a_m} \right)^2 \right] \end{aligned} \quad (\text{S23a})$$

with $\sigma_{a_m}^2$ estimated using equation (S21) and with:

$$\frac{\partial \lambda(c, \bar{a}_m, \bar{r}, a)}{\partial c} \Big|_{c=\bar{c}} = \frac{q}{\bar{r} k^{1-\beta}} - \left(\frac{q}{\bar{r} k^{1-\beta}} - (1-\beta) \frac{\bar{a}_m}{k^{1-\beta}} \right) \left(\frac{1}{1+(1-\beta)\frac{\bar{r}}{q}} \right)^{a-\bar{a}_m} \quad (\text{S23b})$$

$$\begin{aligned} \frac{\partial \lambda(\bar{c}, a_m, \bar{r}, a)}{\partial a_m} \Big|_{a_m=\bar{a}_m} = \\ (1-\beta) \frac{\bar{c}}{k^{1-\beta}} \left(\frac{1}{1+(1-\beta)\frac{\bar{r}}{q}} \right)^{a-\bar{a}_m} + \log \left(\frac{1}{1+(1-\beta)\frac{\bar{r}}{q}} \right) \left(\frac{q\bar{c}}{\bar{r} k^{1-\beta}} - \left(\lambda_0 + \frac{\bar{c}(1-\beta)}{k^{(1-\beta)}} \bar{a}_m \right) \right) \left(\frac{1}{1+(1-\beta)\frac{\bar{r}}{q}} \right)^{a-\bar{a}_m} \end{aligned} \quad (\text{S23c})$$

$$\begin{aligned} \frac{\partial \lambda(\bar{c}, \bar{a}_m, r, a)}{\partial r} \Big|_{r=\bar{r}} = \\ \frac{q\bar{c}}{\bar{r}^2 k^{1-\beta}} \left(\left(\frac{1}{1+(1-\beta)\frac{\bar{r}}{q}} \right)^{a-\bar{a}_m} - 1 \right) + \frac{(1-\beta)}{q} (a - \bar{a}_m) \left(\frac{q\bar{c}}{\bar{r} k^{1-\beta}} - \left(\lambda_0 + \frac{\bar{c}(1-\beta)}{k^{(1-\beta)}} \bar{a}_m \right) \right) \left(\frac{1}{1+(1-\beta)\frac{\bar{r}}{q}} \right)^{1+a-\bar{a}_m} \end{aligned} \quad (\text{S23d})$$

where \bar{c} , \bar{a}_m , and \bar{r} are the mean parameter values that can were estimated from the input parameter estimation procedure.

2. Estimation of phenotypic variance of the linear probabilistic maturation reaction norm parameters

The maturation probability of an individual i of age a and length l conditional on being alive and still immature can be described by a Heaviside step function:

$$H(l - l_{m,i}(a)) \quad (S24)$$

where $l_{m,i}(a)$ is the individual's maturation length at age a . Equation (8) thus describes an individual's maturation reaction norm. Phenotypic variation in maturation length across individuals aged a is described by the probability density function $f_a(l_m)$ with mean $\bar{l}_m(a)$ and standard deviation $\sigma_{l_m}(a)$. The population-level PMRN $p(l, a)$ is then obtained as:

$$p(l, a) = \int_{-\infty}^{+\infty} H(l - l_m) f_a(l_m) dl_m = \int_{-\infty}^l f_a(l_m) dl_m \quad (S25)$$

which is the cumulative distribution function of maturation lengths at age a .

The derivative of the population-level PMRN according to length allows thus to empirically estimate the probability density function of maturation length:

$$\frac{\partial p(l, a)}{\partial l} = f_a(l) \quad (S26)$$

The mean and variance of maturation length at any age a can thus be estimated from the empirical PMRN $\hat{p}(l, a)$ as:

$$\hat{l}_m(a) = \int_{-\infty}^{+\infty} l \frac{\partial \hat{p}(l, a)}{\partial l} dl \quad (S27a)$$

and:

$$\hat{\sigma}_{l_m}^2(a) = \int_{-\infty}^{+\infty} (l - \bar{l}_m(a))^2 \frac{\partial \hat{p}(l, a)}{\partial l} dl \quad (S27b)$$

Under the assumption of a linear maturation reaction norm with a fix envelop, the maturation length of an individual i is described at any age a by:

$$\sigma_{l_m}^2(a) = \sigma_{l_m,0}^2$$

3. Estimation of covariance between the juvenile growth coefficient c and age at maturation a_m

To compute the covariance between age at maturation a_m and growth potential c , we need to estimate the joint probability density of these two random variables that we will denote as $g(a_m, c)$.

Under the assumptions of our model, i.e. that survival only depends on length, the number of newly maturing individuals between age a and $a + 1$ and between transformed length $\lambda = l^{\alpha(1-\beta)}$ and $\lambda + \Delta\lambda$ is given by:

$$N_i(a, \lambda)s(a, \lambda)p(a, \lambda) \tag{S28}$$

where $N_i(a, \lambda)$ is the number of immature individuals aged a with transformed length λ , $s(a, \lambda)$ is survival from age a to $a + 1$ and transformed length λ to $\lambda + \Delta\lambda$ (which results from the combination of natural and fishing mortality) and $p(a, \lambda)$ is the prospective version of the PMRN.

As immature growth in transformed length λ is linear with age according to $\lambda = \frac{c(1-\beta)}{k^{(1-\beta)}} a$, all dependencies on λ can be turned into dependencies on c by a simple change of variable:

$$c = \frac{k^{(1-\beta)} \lambda}{(1-\beta) a} \tag{S29}$$

so that the number of newly maturing individuals between age a and $a + 1$ for a growth potential c is given by:

$$N_i(a, c)s(a, c)p(a, c) \tag{S30}$$

If the age and length distribution of sampled individuals n_i is representative of that of the population N_i , the joint probability distribution of maturation age and growth potential is then obtained as:

$$g(a, c) = n_i(a, c)s(a, c)p(a, c)/G \tag{S31}$$

with $G = \sum_{a=0}^{a_{max}} \int_{-\infty}^{+\infty} n_i(a, c) s(a, c) p(a, c) dc$ a normalization constant insuring that the joint probability density function sums to 1.

An estimate of the covariance between age at maturation a_m and growth potential c is then obtained as:

$$\sigma_{c, a_m} = \sum_{a'_m=0}^{a_{max}} \int_{-\infty}^{+\infty} (a_m - \bar{a}_m)(c - \bar{c}) g(a_m, c) dc \tag{S32}$$

with $\bar{a}_m = \sum_{a_m=0}^{a_{max}} a_m \int_{-\infty}^{+\infty} g(a_m, c) dc$ and $\bar{c} = \int_{-\infty}^{+\infty} c \sum_{a_m=0}^{a_{max}} g(a_m, c) dc$

8.2.2 Supporting Information S12 – Ecological validation of Ev-OSMOSE-NS: Simulated biomass and catches.

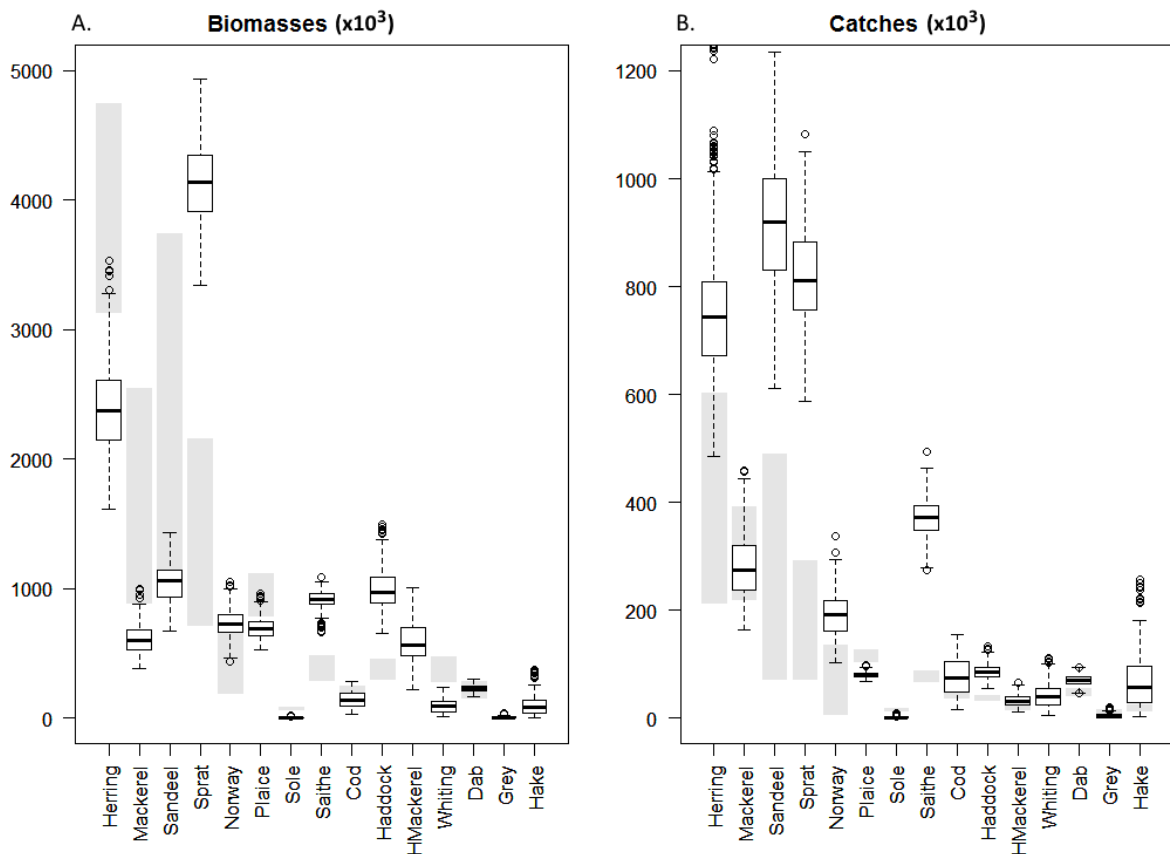


Figure S2: Fisheries catches (A) and biomasses (B), in thousand tons, per species for stock assessment estimates and simulated data averaged over 28 replicates (boxplots). The boxplots represent the simulated data for 28 replicated simulations (stochastic model) for the catches and biomasses per species, with the first, second and third quartiles represented horizontally in each plot. The averaged

simulated are from year 50 to 70, before the evolution activated at the year 70. The gray bars show the minimal and maximum values observed for catch and biomass estimates from stock assessment for the 2010-2019 period. The species without gray bars for biomasses are not assessed in the area.

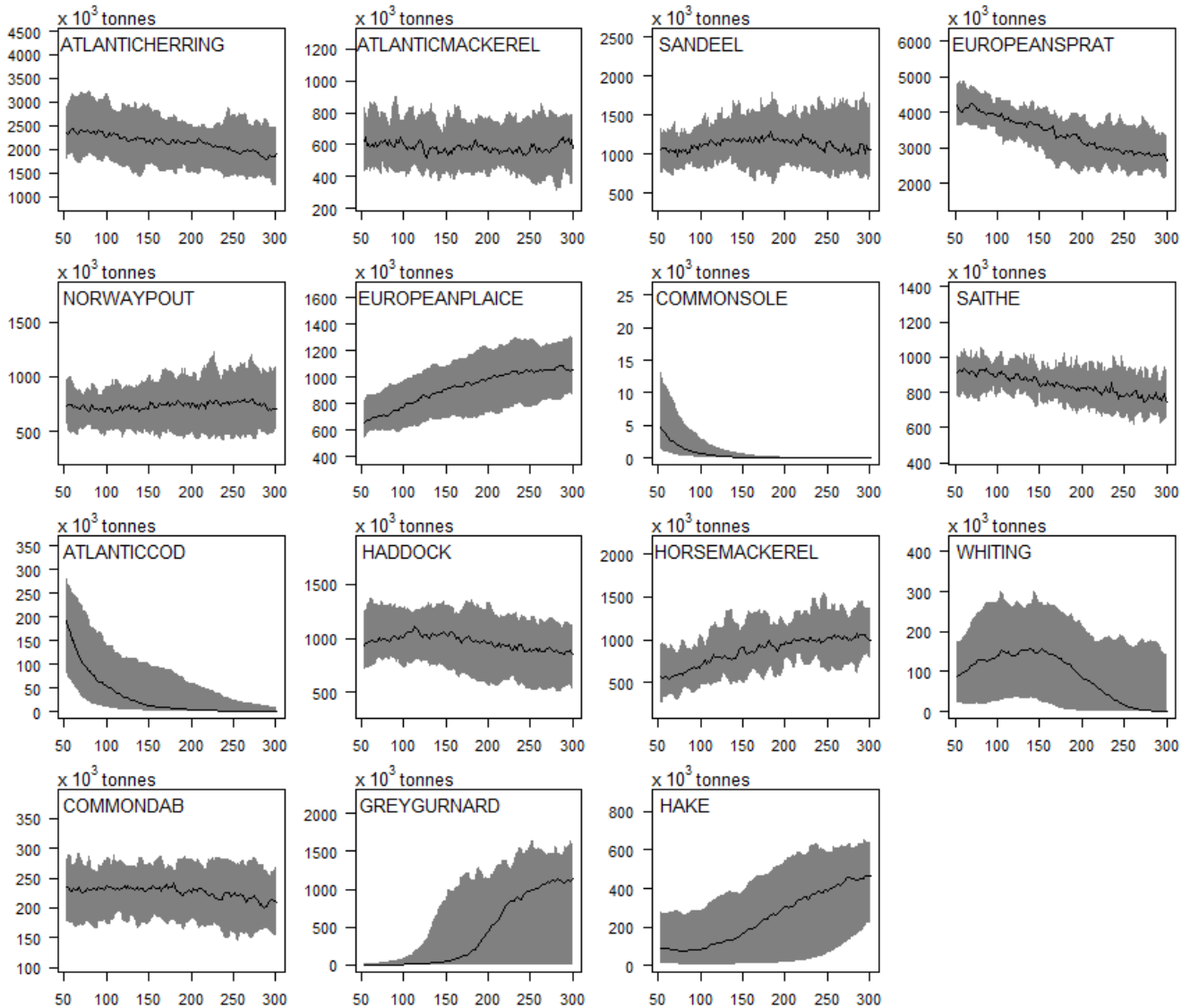


Figure S3: Simulated time series of biomasses. Data averaged over 28 replicates (black line) and replicates variability due to stochasticity (grey area). The configuration is considered stable between year 50 and 70, except for cod and sole. The genotype transmission is activated after year 70.

8.2.3 Supporting Information S13 – Genotype transmission validation

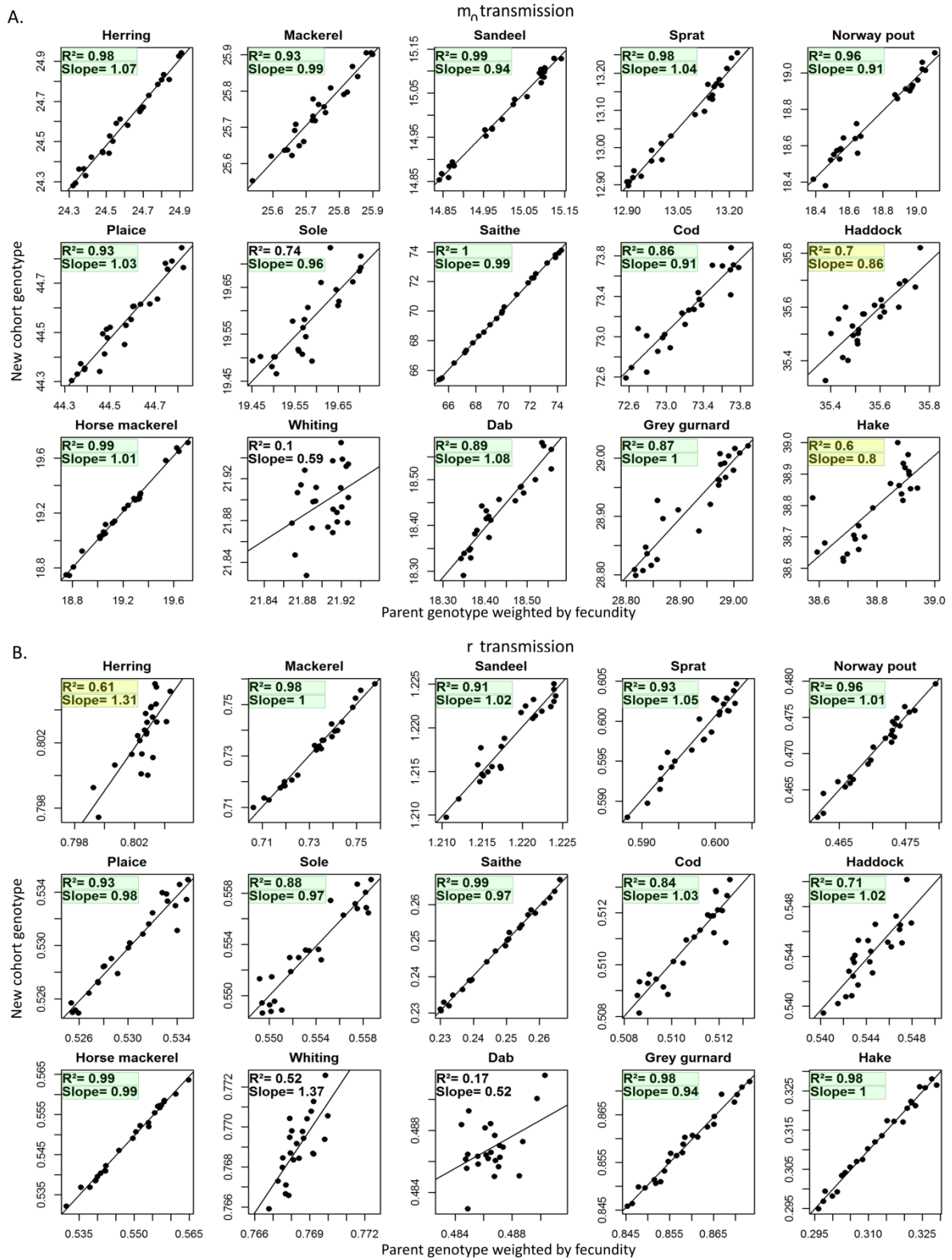


Figure S4: Transmission of genotypic value of the maturation reaction norm origin m_0 (A) and of the gonado-somatic index r (B) from parent to the new spawned cohort in a simulation where the number of schools created per reproductive event is 10 times higher than in the configuration presented in the main text. The mean parent genotypic value weighted by individual fecundity average over the entire reproductive season time step is compared to the mean genotypic value of the new spawned cohort during the same reproductive season. The slope and the regression adjustment are expected to be close to 1. The noise around the regression slope is a consequence of drift due random parental allele selection and random mating. As in Figure 32 in chapter 4 in main text, the slope and the R^2 highlighted in yellow and green are respectively the good and the very good fit of simulated data to expected pattern (green slope: between 0.9 and 1.1; yellow slope: between 0.7 and 0.9 or between 1.1 and 1.3; green R^2 : between 0.8 and 1; yellow R^2 : between 0.6 and 0.8).

8.3 Références des annexes

- Barot, S., Heino, M., O'Brien, L., Dieckmann, U., 2003. Estimating reaction norms for age and size at maturation when age at first reproduction is unknown 38.
- Baxter, I.G., 1958. Fecundities of winter-spring and summer-autumn herring spawners. ICES: C.M. 42:9.
- Behrens, J.W., Steffensen, J.F., 2007. The effect of hypoxia on behavioural and physiological aspects of lesser sandeel, *Ammodytes tobianus* (Linnaeus, 1785). *Mar Biol* 150, 1365–1377.
<https://doi.org/10.1007/s00227-006-0456-4>
- Ben Rais Lasram, F., Hattab, T., Nogues, Q., Beaugrand, G., Dauvin, J.C., Halouani, G., Le Loc'h, F., Niquil, N., Leroy, B., 2020. An open-source framework to model present and future marine species distributions at local scale. *Ecological Informatics* 59, 101130.
<https://doi.org/10.1016/j.ecoinf.2020.101130>
- Bergstad, O.A., Høines, A.S., Krüger-Johnsen, E.M., 2001. Spawning time, age and size at maturity, and fecundity of sandeel, *Ammodytes marinus*, in the northeastern North Sea and in unfished coastal waters off Norway. *Aquat. Living Resour.* 14:293-301.
- Bilgin, S., Samsun, O., 2006. Fecundity and Egg Size of Three Shrimp Species, *Crangon crangon*, *Palaemon adspersus*, and *Palaemon elegans* (Crustacea: Decapoda: Caridea), off Sinop Peninsula (Turkey) in the Black Sea 10.
- Bohl, H., 1956. On the biology of the dab in the North Sea. ICES: C.M. 5pp.
- Boukal, D.S., Dieckmann, U., Enberg, K., Heino, M., Jørgensen, C., 2014. Life-history implications of the allometric scaling of growth. *Journal of Theoretical Biology* 359, 199–207.
<https://doi.org/10.1016/j.jtbi.2014.05.022>
- Christiansen, J.S., Fevolden, S.E., Karamushlo, O.V., Karamushko, L.I., 1997. Reproductive traits of marine fish in relation to their mode of oviposition and zoogeographic distribution. ICES CM 1997/CC. 14 p.
- Claireaux, G., Webber, D.M., Lagardère, J.-P., Kerr, S.R., 2000. Influence of water temperature and oxygenation on the aerobic metabolic scope of Atlantic cod (*Gadus morhua*). *Journal of Sea Research* 44, 257–265. [https://doi.org/10.1016/S1385-1101\(00\)00053-8](https://doi.org/10.1016/S1385-1101(00)00053-8)
- Clarke, A., Johnston, N.M., 1999. Scaling of metabolic rate with body mass and temperature in teleost fish. *Journal of Animal Ecology* 13.
- Cohen, D.M., Inada, T., Iwamoto, T., Scialabba, N., 1990. Gadiform fishes of the world (Order Gadiformes). An annotated and illustrated catalogue of cods, hakes, grenadiers and other gadiform fishes known to date. *FAO Fish. Synop.* 125(10). Rome: FAO. Vol. 10., 442 p.
- Coull, K.A., Johnston, R., Rogers, S.I., 1998. Fisheries Sensitivity Maps in British Waters 63.
- Dahlke, F., Wohlrab, S., Butzin, M., Pörtner, H.-O., 2020. Experimental data compilation, thermal tolerance and thermal responsiveness of fish species and life stages.
<https://doi.org/10.1594/PANGAEA.917796>

De Silva, S.S., 1973. Food and feeding habits of the herring *Clupea harengus* and the sprat *C. sprattus* in inshore waters of the west coast of Scotland. *Marine Biology* 20, 282–290. <https://doi.org/10.1007/BF00354272>

Dickson, K.A., 2002. Temperature effects on sustained swimming in mackerel 12.

Dupont-Prinet, A., Pillet, M., Chabot, D., Hansen, T., Tremblay, R., Audet, C., 2013. Northern shrimp (*Pandalus borealis*) oxygen consumption and metabolic enzyme activities are severely constrained by hypoxia in the Estuary and Gulf of St. Lawrence. *Journal of Experimental Marine Biology and Ecology* 448, 298–307. <https://doi.org/10.1016/j.jembe.2013.07.019>

Eltink, A., Vingerhoed, B., 1989. The total fecundity of Western horse mackerel (*Trachurus trachurus* L.). *ICES:C.M. H(44):11p.*

Fox, C.J., Planque, B., Darby, C.D., 2000. Synchrony in the recruitment time-series of plaice (*Pleuronectes platessa* L) around the United Kingdom and the influence of sea temperature. *J. Sea Res.* 44:159-168.

Geist, S.J., Ekau, W., Kunzmann, A., 2013. Energy demand of larval and juvenile Cape horse mackerels, *Trachurus capensis*, and indications of hypoxia tolerance as benefit in a changing environment. *Mar Biol* 160, 3221–3232. <https://doi.org/10.1007/s00227-013-2309-2>

Hehir, I., 2003. Age, growth and reproductive biology of whiting *Merlangius merlangus* in the Celtic Sea. Galway-Mayo Institute of Technology. Master thesis. 210p.

Hislop, J.R.G., 1966. A note on the fecundity of whiting in the North Sea. *ICES C.M.* 19:9.

ICES, 2019a. Catches in FAO area 27 by country, species, area and year as provided by the national authorities. Source: Eurostat/ICES data compilation of catch statistics - ICES 2019, Copenhagen. Format: Archived dataset in .xlsx and .csv formats. Version: 16-09-2019.

ICES, 2019b. Working group on widely distributed stocks (WGWIDE). *ICES Scientific Reports.* 1:36. 948 pp. <http://doi.org/10.17895/ices.pub.5574>.

ICES, 2018a. Report of the Herring Assessment Working Group for the Area South of 62°N (HAWG) (29-31 January 2018 and 12-20 March 2018) (No. ICES CM 2018/ACOM:07).

ICES, 2018b. Report of the Working Group for the Bay of Biscay and the Iberian Waters Ecoregion (WGBIE) (3-10 May 2018. No. ICES CM 2018/ACOM:12).

ICES, 2018c. Report of the Working Group on the Assessment of Demersal Stocks in the North Sea and Skagerrak (WGNSSK) (24 April - 3 May 2018) (No. ICES CM 2018/ACOM:22).

ICES, 2016. Report of the Benchmark Workshop on Sandeel (WKSand 2016). (31 October - 4 November. No. ICES CM 2016/ACOM:33).

ICES, 2012. Report of the Working Group on the Assessment of Demersal Stocks in the North Sea and Skagerrak (WGNSSK), 27 April - 03 May 2012, ICES Headquarters, Copenhagen. *ICES CM 2012/ACON:13.* 1346 p.

Koli, L., 1990. Suomen kalat. [Fishes of Finland]. Werner Söderström Osakeyhtiö. Helsinki. 357 p. (in Finnish).

Kopp, D., Lefebvre, S., Cachera, M., Villanueva, M.C., Ernande, B., 2015. Reorganization of a marine trophic network along an inshore–offshore gradient due to stronger pelagic–benthic coupling in

coastal areas. *Progress in Oceanography* 130, 157–171.
<https://doi.org/10.1016/j.pocean.2014.11.001>

Lefrançois, C., Claireaux, G., 2003. Influence of ambient oxygenation and temperature on metabolic scope and scope for heart rate in the common sole *Solea solea*. *Marine Ecology Progress Series* 259, 273–284. <https://doi.org/10.3354/meps259273>

Lester, N.P., Shuter, B.J., Abrams, P.A., 2004. Interpreting the von Bertalanffy model of somatic growth in fishes: the cost of reproduction. *Proceedings of the Royal Society of London B: Biological Sciences* 271, 1625–1631. <https://doi.org/10.1098/rspb.2004.2778>

Macer, C.T., 1976. Observations on the maturity and fecundity of mackerel (*Scomber scombrus* L.). ICES: C.M. H:6(mineo).

MacKenzie, B.R., Köster, F.W., 2004. Fish Production and Climate: Sprat in the Baltic Sea. *Ecology* 85, 784–794.

Mackinson, S., Daskalov, G., 2007. An ecosystem model of the North Sea to support an ecosystem approach to fisheries management: description and parameterisation 200.

Mehault, S., Dominguez-Petit, R., Cervino, S., Saborido-Rey, F., 2010. Variability in total egg production and implications for management of the southern stock of European hake. *Fish. Res.* 104(1-3):111-122.

Meskendahl, L., 2013. Metabolic rates and feeding behaviour of sprat, *Sprattus sprattus* L. (PhD). University of Hamburg, Hamburg, Germany.

Muus, B.J., Nielsen, J.G., 1999. Sea fish. *Scandinavian Fishing Year Book*, Hedehusene, Denmark. 340 p.

Narberhaus, I., Krause, J., Bernitt, U., 2012. Threatened biodiversity in the German North and Baltic seas. *Naturschutz und Biologische Vielfalt*, Heft 117. Federal Agency for Nature Conservation, Bonn, Germany.

Oh, C.-W., Hartnoll, R.G., Nash, R.D.M., 2001. Feeding ecology of the common shrimp Crangon crangon in Port Erin Bay, Isle of Man, Irish Sea. *Marine Ecology Progress Series* 214, 211–223.
<https://doi.org/10.3354/meps214211>

Pinnegar, J.K., 2014. DAPSTOM - An Integrated Database & Portal for Fish Stomach Records. Version 4.7. Centre for Environment, Fisheries & Aquaculture Science, Lowestoft, UK. February 2014, 39pp.

Quéro, J.C., Desoutter, M., Lagardère, F., 1986. Soleidae. p. 1308-1324. In P.J.P. Whitehead, M.-L. Bauchot, J.-C. Hureau, J. Nielsen and E. Tortonese (eds.) *Fishes of the North-eastern Atlantic and the Mediterranean*. UNESCO, Paris. Vol. 3.

Quince, C., Abrams, P.A., Shuter, B.J., Lester, N.P., 2008. Biphasic growth in fish I: Theoretical foundations. *Journal of Theoretical Biology* 254, 197–206. <https://doi.org/10.1016/j.jtbi.2008.05.029>

Report of the Working Group on Crangon Fisheries and Life History (WGCRAN), 2015. 60.

Sonina, M.A., 1971. La fécondité de l'églefin arcto-norvégien (*Melanogrammus aeglefinus* L.). ICES: C.M. F(16):11.

Steinhausen, M.F., Steffensen, J.F., Andersen, N.G., 2005. Tail beat frequency as a predictor of swimming speed and oxygen consumption of saithe (*Pollachius virens*) and whiting (*Merlangius*

merlangus) during forced swimming. *Marine Biology* 148, 197–204. <https://doi.org/10.1007/s00227-005-0055-9>

Sundbly, S., Kristiansen, T., Nash, R., Johannessen, T., 2017. Dynamic Mapping of North Sea Spawning – Report of the KINO Project - Semantic Scholar.

van Damme, C.J.G., Bolle, L.J., Fox, C.J., Fossum, P., Kraus, G., Munk, P., Rohlf, N., Witthames, P.R., Dickey-Collas, M., 2009. A reanalysis of North Sea plaice spawning-stock biomass using the annual egg production method. *ICES J. Mar. Sci.* 66:1999-2011.

Van der Land, M.A., 1991. Distribution of flatfish eggs in the 1989 egg surveys in the southeastern North Sea, and mortality of plaice and sole eggs. *Netherlands Journal of Sea Research* 27, 277–286. [https://doi.org/10.1016/0077-7579\(91\)90030-5](https://doi.org/10.1016/0077-7579(91)90030-5)

West, G.B., Brown, J.H., Enquist, B.J., 1997. A General Model for the Origin of Allometric Scaling Laws in Biology. *Science* 276, 122–126. <https://doi.org/10.1126/science.276.5309.122>

Witthames, P.R., Greer Walker, M., Dinis, M.T., Whiting, C.L., 1995. The geographical variation in the potential annual fecundity of dover sole *Solea solea* (L.) from European shelf waters during 1991. *Netherlands Journal of Sea Research* 34, 45–58. [https://doi.org/10.1016/0077-7579\(95\)90013-6](https://doi.org/10.1016/0077-7579(95)90013-6)

Yoneda, M., Wright, P.J., 2004. Temporal and spatial variation in reproductive investment of Atlantic cod *Gadus morhua* in the northern North Sea and Scottish west coast. *Mar. Ecol. Prog. Ser.* 276:237-248.

Résumé : Les scénarios de changements globaux sont précieux pour guider les stratégies de gestion et de gouvernance, inciter à la prise de décision et augmenter la prise de conscience collective des tendances futures de la biodiversité. Le degré de réalisme et d'intégration des modèles écosystémiques utilisés à cet effet est en constante progression, mais ils négligent encore souvent l'évolution des populations marines dans les projections futures. Or, celles-ci s'adaptent aux changements globaux, que ce soit par la plasticité phénotypique ou l'évolution, au travers de modifications de leurs caractéristiques biologiques telles que les traits d'histoire de vie, physiologiques et bioénergétiques. L'enjeu de cette thèse est de développer un modèle écosystémique qui permette d'explorer des scénarios de biodiversité aux échelles intra- et inter-spécifiques en représentant explicitement la plasticité phénotypique des traits d'histoire de vie, leur variabilité génétique, leur sélection et leur évolution sous l'influence combinée de la pêche et du changement climatique, ainsi que la dérive génétique et la perte de diversité génétique qui en résultent. Appliqué à la mer du Nord, ce nouveau modèle est utilisé pour comprendre les processus responsables des changements de traits d'histoire de vie qu'ils soient d'origine plastique ou d'origine évolutive. D'une part, les processus bioénergétiques sous-jacents aux changements plastiques sont étudiés par une approche originale comparant les différences entre les courbes de réponses thermiques fondamentales et réalisées pour différentes espèces et stades du cycle de vie. D'autre part, les changements des traits d'histoire de vie sont explorés à travers le prisme de l'évolution grâce à la prise en compte de pressions de sélection multiples telles que la pêche, les interactions proie-prédateurs et le changement climatique. L'intégration des processus plastiques et évolutifs dans les modèles écosystémiques permet de décrire la variabilité interindividuelle des traits biologiques et de comprendre leurs tendances temporelles observées dans le milieu marin. En cela, elle répond à l'enjeu crucial de crédibilité des projections de la biodiversité intra- et inter-spécifique sous scénarios combinant climat et pêche. L'intégration de ces processus permettra également de quantifier plus précisément les effets synergiques et antagonistes de ces deux pressions et de prendre en compte la capacité d'adaptation des populations aux changements globaux pour estimer de manière plus fiable leur résilience.

Mots clés : Traits d'histoire de vie, Modèle écosystémique, Réponses physiologiques thermiques, Evolution induite par la pêche, Hypoxie

Abstract: Global change scenarios are valuable for guiding management and governance strategies, stimulating decision making, and increasing collective awareness of future biodiversity trends. The degree of realism and integration of ecosystem models used for this purpose is constantly improving, but they still often neglect the evolution of marine populations in future projections. However, marine populations adapt to global changes, either through phenotypic plasticity or evolution, through modifications of their biological characteristics such as life history traits, physiological and bioenergetic traits. The challenge of this thesis is to develop an ecosystem model that allows the exploration of biodiversity scenarios at intra- and inter-specific scales by explicitly representing the phenotypic plasticity of life history traits, their genetic variability, selection and evolution under the combined influence of fisheries and climate change, and the resulting genetic drift and loss of genetic diversity. Applied to the North Sea, this new model is used to understand the processes responsible for changes in life history traits, whether they are of plastic or evolutionary origin. On the one hand, the bioenergetic processes underlying plastic changes are studied by an original approach comparing the differences between the fundamental and realized thermal response curves for different species and life history stages. On the other hand, changes in life history traits are explored through an evolutionary lens by taking into account multiple selection pressures such as fishing, prey-predator interactions and climate change. The integration of plastic and evolutionary processes in ecosystem models allows to describe the inter-individual variability of biological traits and to understand their temporal trends observed in the marine environment. In this way, it responds to the crucial issue of credibility of intra- and inter-specific biodiversity projections under scenarios combining climate and fisheries. The integration of these processes will also allow to quantify more precisely the synergistic and antagonistic effects of these two pressures and to take into account the capacity of populations to adapt to global changes in order to estimate more reliably their resilience.

Keyword: Life history traits, Ecosystem modeling, Thermal physiological responses, Fisheries-induced evolution, Hypoxia